DIAGENESIS OF MIDDLE DEVONIAN PRESQU'ILE DOLOMITE PINE POINT NWT AND ADJACENT SUBSURFACE

by

HAIRUO QING

Department of Geological Sciences McGill University Montreal, Quebec, Canada

A thesis submitted to the Faculty of Graduate Studies and Research in partial fulfilment of the requirements for the degree of Doctor of Philosophy

(c) June 1991

TABLE OF CONTENTS

	page
PREFACE	6
Contribution to original knowledge	6
Acknowledgements	8
ABSTRACT	10
RESUME	11
Chapter 1.	
INTRODUCTION	12
1.1 Objectives	12
1.2 Methods	13
1.3 Previous studies	18
1.4 Organization of the thesis	21
Chapter 2.	
GEOLOGIC SETTING AND STRATIGRAPHY	24
2.1 Geologic setting	24
2.1.1 Regional geological history	24
2.1.2 Structural geology	29
2.1.3 Paleolatitude and paleoclimate	30
2.1.4 Sea-level variation during Middle Devonian	32
2.2 Stratigraphy associated with the Presqu'ile barrier	34
2.2.1 Keg River Formation	36
2.2.2 Pine Point Formation	37
2.2.3 Sulphur Point Formation	37
2.2.4 Muskeg Formation	38
2.2.5 Buffalo River and Windy Point formations	38

2.2.6 Watt Mountain Formation	. 39
2.3.7 Slave Point Formation	. 39
2.3 Conclusions	. 40
Chapter 3.	
DIAGENETIC PARAGENESIS	. 42
3.1 Submarine diagenesis	11
3.2 Subaerial diagenesis	
3.3 Subsurface diagenesis	
3.4 Conclusions	, 39
Chapter 4.	
BURIAL AND GEOTHERMAL HISTORY	. 60
4.1 Burial history reconstruction based on stratigraphic records	60
4.2 Organic geochemistry	67
4.3 Apatite fission-track analyses	68
4.4 Conodont colour-alteration index	69
4.5 Conclusions	. 70
Chapter 5.	
ORIGIN OF MIDDLE DEVONIAN PRESQU'ILE DOLOMITE:	
EVIDENCE FROM PETROGRAPHY, GEOCHEMISTRY, AND FLUID INCLUSIONS	. 71
5.1 Introduction	. 71
5.2 Petrography and spatial distribution of dolomites	
5.2 Todography and spatial distribution of doloninos	73

5.3 Oxygen and carbon isotopes	92
5.3.1 Results	93
5.3.2 Discussion	98
5.4 Sr isotopes	112
5.4.1 Results	114
5.4.2 Discussion	119
5.5.3 Sources of radiogenic Sr	123
5.5 Fluid inclusions	126
5.5.1 Results	128
5.5.2 Discussion	144
5.6 Trace elements	151
5.6.1 Results	153
5.6.2 Discussion	154
5.6.3 Fluid-flow direction during dolomitization	163
5.7 Discussion and conclusions	170
5.7.1 Fine-crystalline dolomite	172
5.7.2 Medium-crystalline dolomite	173
5.7.2 Coarse-crystalline and saddle dolomites	175
Chapter 6. RARE-EARTH ELEMENT GEOCHEMISTRY OF DOLOMITES IN THE	
PRESQU'ILE BARRIER: IMPLICATIONS FOR WATER/ROCK RATIOS DURING DOLOMITIZATION	184
6.1 Introduction	184
6.2 Results	185
6.3 Discussion	191
6.4 Conclusions	201

Chapter 7.

HYDROTHERMAL ORIGIN OF DISSOLUTION VUGS AND BRECCIAS IN PRESQU'ILE BARRIER, HOST OF PINE POINT MVT DEPOSITS	
7.1 Introduction	203
7.2 Dissolution features at Pine Point and adjacent subsurface	205
7.3 Discussion	213
7.4 Conclusions	221
Chapter 8.	
TIMING OF MINERALIZATION AT PINE POINT INFERRED FROM DIAGENESIS OF HOST DOLOMITES	224
8.1 Previous dating for Pine Point deposits	224
8.2 Discussion	226
8.3 Conclusions	228
Chapter 9.	
SUMMARY AND CONCLUSIONS	230
9.1 Diagenetic paragenesis	230
9.2 Dolomitization	230
9.3 Origin of dissolution vugs and breccias	237
9.4 Timing of mineralization	239
9.5 Closing remarks	
DECEDENCES	041

AP	PENDICES	260
1.	List of wells studied	260
2.	$\delta^{18}O$ and $\delta^{13}C$ values of the Presqu'ile barrier carbonates	265
3.	87 Sr/86 Sr ratio of the Presqu'ile barrier carbonates	271
4.	Fluid inclusion measurements	273
5.	Major and trace element concentrations of the Presqu'ile barrier carbonates	277
6	Rare earth element concentrations of the Presqu'ile barrier carbonates	285
7.	List of figures	288
8.	List of tables	292

PREFACE

The following statements are made in fulfilment of the "Guidelines Concerning Thesis Preparation" of McGill University.

CONTRIBUTIONS TO ORIGINAL KNOWLEDGE

Prior to this research project, studies of diagenesis of the Presqu'ile carbonates were concentrated at the Pine Point area and interpretations were based mainly on petrographic observations. This is the first regional project that systematically studied the diagenesis and geochemistry of the Presqu'ile barrier from east to west (for 400 km) in the Western Canada Sedimentary Basin. The regional geochemical trends offer new interpretations of the diagenesis of the Presqu'ile barrier. These interpretations have immediate applications in terms of the diagenetic study in the other parts of the Western Canada Sedimentary Basin, and probably in sedimentary basins worldwide. The major contributions of this study can be summarized as follows:

- 1. The diagenetic paragenesis of the Presqu'ile barrier is established.
- Four types of dolomites are identified. The origin and timing of these
 dolomites are established on the basis of their distinctive spatial distribution,
 cross cutting relationships, petrographic characteristics, diagenetic paragenesis,
 and geochemical signatures.
- The role of meteoric solution versus hydrothermal dissolution is differentiated in the Pine Point MVT deposits. Meteoric waters caused only minor

dissolution and the majority of dissolution vugs and breccias were produced by hydrothermal fluids during burial. This result has important implications for mineral exploration: MVT deposits are not always related to meteoric karst and mineralization can occur in any available vugs and/or fractures whatever their origin.

- 4. The age of mineralization is constrained by the timing of late-stage saddle dolomites to take place between the Late Cretaceous to early Tertiary.
- 5. This study suggests that diagenetic features in a sedimentary basin, such as hydrothermal dissolution, dolomitization, and mineralization, are related to tectonic evolution of the basin and regional conduit systems. Tectonic thrusting and compression, sedimentary loading, and uplift of a foreland basin can create hydrodynamic systems that initiate large-scale flow of basinal fluids, which played a key role in dolomitization and mineralization along preferential conduit systems in a sedimentary basin, like the Presqu'ile barrier.
- 6. Prior to completion of this thesis, parts of this research have been published, presented as talks, or submitted for publication. The information contained in these papers and abstracts is integrated into the body of the thesis (see following list).

PAPERS:

QING, H. AND MOUNTJOY, E.W., 1990, Petrography and diagenesis of Middle Devonian Presqu'ile barrier -implications on formation of dissolution vugs and breccias at Pine Point and adjacent subsurface, District of Mackenzie: in Current Research, Part D, Geological Survey of Canada, Paper 90-1D, p.37-45.

MOUNTJOY, E.W., QING, H., AND McNUTT, R., in press, Sr isotopes of Devonian dolomites, western Canada: significance regarding sources of dolomitizing fluids: Applied Geochemistry.

ABSTRACTS:

- QING, H. AND MOUNTJOY, E.W., 1989a, Dolomitization of Middle Devonian Presqu'ile barrier at Pinc Point: an indication of open-system diagenesis, in Geol. Assoc. Canada and Mineral. Assoc. Canada Joint Annual Meeting (program with abstr.), p.64.
- QING, H. AND MOUNTJOY, E.W., 1989b, Origin of dissolution vugs and breccias in Presqu'ile barrier (Middle Devonian) at Pine Point: meteoric or hydrothermal karst, in Geological Society of America, abstr. and programs, v.21, No. 6, p.7a.
- QING, H. AND MOUNTJOY, E.W., 1990, Hydrothermal origin of dissolution vugs and breccias in Presqu'ile barrier, host of Pine Point MVT deposits, in 8th International Association of the Genesis of Ore Deposits (IAGOD) Symposium (program with abstracts), p.A250.
- QING, H. AND MOUNTJOY, E.W., 1991a, Dolomitization of Middle Devonian Presqu'ile facies in the Western Canada Sedimentary basin, in Geol. Assoc. Canada and Mineral. Assoc. Canada Joint Annual Meeting (program with abstr.), p.A103.
- QING, H. AND MOUNTJOY, E.W., 1991b, Origin of Middle Devonian Presqu'ile dolomites: evidence from petrography, geochemistry, and fluid inclusions: in Can. Soc. of Petrol. Geol. Annual Meeting (program with abstract), p.115.

ACKNOWLEDGEMENTS

I am greatly indepted to my thesis supervisor, Dr. Eric Mountjoy for his help and encouragement throughout the project. His suggestions, advice, and constructive criticism are greatly appreciated.

Dr. D.F. Sangster (GSC, Ottawa) suggested this project and I appreciate his

valuable advice and encouragement. I thank Dr. K.C. Lohmann (University of Michigan) for O and C isotope analyses, Dr. R. McNutt (McMaster University) for Sr isotope analyses, Dr. S. Jackson (Memorial University of Newfoundland) for REE analyses, and Mr. T. Ahmedali (McGill University) for major and trace element analyses. I thank C. Yang for introducing me to microthemometry techniques.

I extend my thanks to Drs. J. Amthor, T. Barrett, R. Hesse, R. Macqueen, A. Mucci, D. Sangster, and S. Wood for valuable discussions and suggestions, which greatly improved text of the thesis

I am grateful to the geologists of Pine Point Mines of Cominco Ltd, for information, field assistance, and hospitality during my visits in 1986 and 1987. I thank Shell Canada and Westcoast Petroleum Ltd for providing well information, and the Institute of Sedimentary and Petroleum Geology (Calgary) and the B.C. Department of Mines, Core Laboratory (Fort St. John) for assistance during core examination.

For the friendship during my study at McGill, I am indebted to my fellow students, especially H. Chouinard, R. Dechesne, S. Grasby, J. Ko, A. Laflamme, M. Mallamo, X. Marquez, D. McLean, D. Suchy, M. Teare, D. Wang, and S. Zhong.

Financial support for this study came from the Canada-NWT Mineral Developments Agreement 1987-91, Shell Canada, NSERC Grant A2128 to Dr. Mountjoy and McGill scholarships to me.

Finally, I would like to thank my wife, Chao Yang, and my parents in China for their love, encouragement, and support throughout all stages of this study.

ABSTRACT

Four types of dolomites occur in the Middle Devonian Presqu'ile barrier: finecrystalline, medium-crystalline, coarse-crystalline, and saddle. Fine-crystalline dolomite formed penecontemporaneously by Middle Devonian seawater, because it is interbedded with Muskeg anhydrite in the back-barrier facies, and has O and Sr isotopic values of Middle Devonian seawater signatures. Medium-crystalline dolomite is interpreted to have formed: (1) at shallow burial depths by fluids derived from compaction, as indicated by its depleted δ^{18} O values and slightly radiogenic 87Sr/86Sr ratios; or 2) soon after deposition by Middle Devonian seawater derived from the Elk Point basin, as suggested by its spatial distribution. Coarse-crystalline and saddle dolomites formed after sub-Watt Mountain exposure during burial. The homogenization temperatures of saddle dolomite fluid inclusions indicate that dolomitization occurred at temperatures exceeding maximum burial temperatures. The gradual decrease in Sr isotopes and homogenization temperatures with corresponding increase in O isotopes eastward along the Presqu'ile barrier suggests the basin-scale migration of hot and radiogenic dolomitizing fluids updip from west to east along the Presqu'ile barrier. Fluid movement probably was most active during Late Cretaceous and early Tertiary mountain building in conjunction with a gravity-driven flow system caused by uplift of the foreland basin. The Pine Point MVT deposits also occurred at this time since they overlapped with saddle dolomites. Extensive hydrothermal dissolution of carbonates preceded and overlapped with saddle dolomites.

RESUME

On retrouve quatre types de dolomies dans le récif annulaire de Presqu'ile d'âge Dévonien Moyen, soit des dolomies à grains fins, moyens, grossiers, et en selle. Les dolomies à grains fins se sont formées pénécontemporainement par l'action de l'eau de mer dévonienne, parce qu'elles sont interlitées avec les anhydrites de Muskeg dans le faciès arrière-récifal. De plus, elles ont une signature isotopique en O et Sr de l'eau de mer dévonienne. Les dolomies à grains moyens semblent s'être formées à de faibles profondeurs d'enfouissement par des fluides provenant de la compaction, comme le montre les valeurs appauvries de δ^{18} O et le rapport légèrement radiogénique de 87Sr/86Sr; ou peu après le dépôt par des eaux de mer dévoniennes provenant du Bassin d'Elk Point, comme le suggère leur distribution spatiale. Les dolomies grossièrement grenues et en selle se sont formées après l'exposition pré-Watt Mountain pendant l'enfouissement. Les températures d'homogénisation des inclusions fluides des dolomies en selle indiquent que la dolomitisation s'est produite à des températures dépassant les températures maximum d'enfouissement. La diminution graduelle des températures d'homogénisation et des isotopes en Sr, couplée à l'accroissement en isotope d'oxygène vers l'est le long de récif suggère une migration, à l'échelle du bassin, de fluides dolomitisateurs chauds et radiogéniques en amont pendage de l'ouest vers l'est le long du récif Presqu'ile. La circulation des fluides a probablement été plus active au moment de la formation des montagnes, de la fin du Crétacé au début du Tertiaire, ceci en conjonction avec des écoulements gravitaires causés par un soulèvement du bassin d'avant pays. Le gisement de Pine Point de type MVT s'est aussi formé pendant cette période car il chevauche les dolomies en selle. Une dissolution hydrothermale extensive des carbonates a précédé et s'est poursuivie lors de la formation des dolomies en selle.

CHAPTER ONE

INTRODUCTION

1.1 OBJECTIVES

This study is designed to investigate the origin of the various massive dolomites in the Presqu'ile barrier at Pine Point, and in the adjacent subsurface in the Northwest Territories and northeastern British Columbia, using petrography and various geochemical techniques. The main objectives are:

- 1. The study and documentation of the diagenetic features of the barrier, especially diagenetic features across the Watt Mountain unconformity, including: i) the relationships, if any, between subaerial dissolution and the unconformity, and ii) the types and spatial distribution of dolomites above and below the unconformity.
- 2. A systematic study of a series of drill holes across the barrier at Pine Point in order to delineate the spatial distribution of the dolomites and any geochemical trends.
- A study of core samples from the subsurface portion of the Presqu'ile barrier west of Pine Point. The similarities and/or differences in diagenesis between

the Presqu'ile barrier at Pine Point and its subsurface equivalent are compared.

4. An integration of the petrography with geochemical analyses. The following techniques and geochemical analysis are used in this study to constrain the sources and compositions of the dolomitizing fluids for different types of dolomites: i) staining, ii) cathodoluminescence and fluorescence microscopy, iii) oxygen and carbon isotopes, iv) strontium isotopes, v) rare earth elements (REE), vi) fluid inclusions, and vii) trace elements.

Considering both geological and geochemical data, the timing, composition, and source(s) of the dolomitizing fluids are interpreted. The results of this research should improve our understanding of the conditions and timing under which ancient dolomites formed. Since the Presqu'ile dolomites are the host rocks for Mississippi Valley-type (MVT) deposits, they place additional limits on the process of mineralization, especially the origin(s) of solution features and the timing of mineralization.

1.2 METHODS

At Pine Point, a number of open pits and a series of drill holes from three representative cross sections were systematically studied and sampled, and the spatial distribution of the various dolomites mapped. In order to compare the similarities and differences in diagenesis between Pine Point and equivalent strata

in the subsurface, core samples from 32 wells from the downdip, subsurface portion of the Presqu'ile barrier west of Pine Point were studied and sampled (Fig. 1) (20 wells from the NWT in the area between 60° to 61°15' latitude and 116°W to 121°W longitude; and 12 wells from northeastern B.C. between 58° to 60° latitude; 120°W to 122°W longitude). The strata studied and sampled include the Pine Point, Sulphur Point, Slave Point, and Muskeg formations. The location, geologic tops, and cored intervals of the studied wells are listed in Appendix 1. Well history and logs of additional 45 uncored wells from the NWT were also studied.

Approximately 160 thin sections were studied. All were stained with an alizarin-red and potassium ferricyanide mixture, following the procedure outlined by Dickson (1965). Of these, 100 thin sections were observed under the cathodoluminescence microscope, and about 20 thin sections were examined under fluorescence microscopy. Representative dolomite samples were studied under the scanning electron microscope.

Microsamples were analyzed for carbon and oxygen isotopes at the University of Michigan. Powdered carbonate samples ranging from 0.2 to 0.5 mg were drilled from polished slabs using drill bits 100 μm in diameter. These samples were roasted at 380 °C under vacuum for one hour to remove organic matter. Samples were then reacted with anhydrous phosphoric acid at 55 °C for about 10 minutes for calcite and about one hour for dolomite. This was done in an on-line gas extraction system connected to an inlet of a VG 602E ratio mass spectrometer. All the analyses were

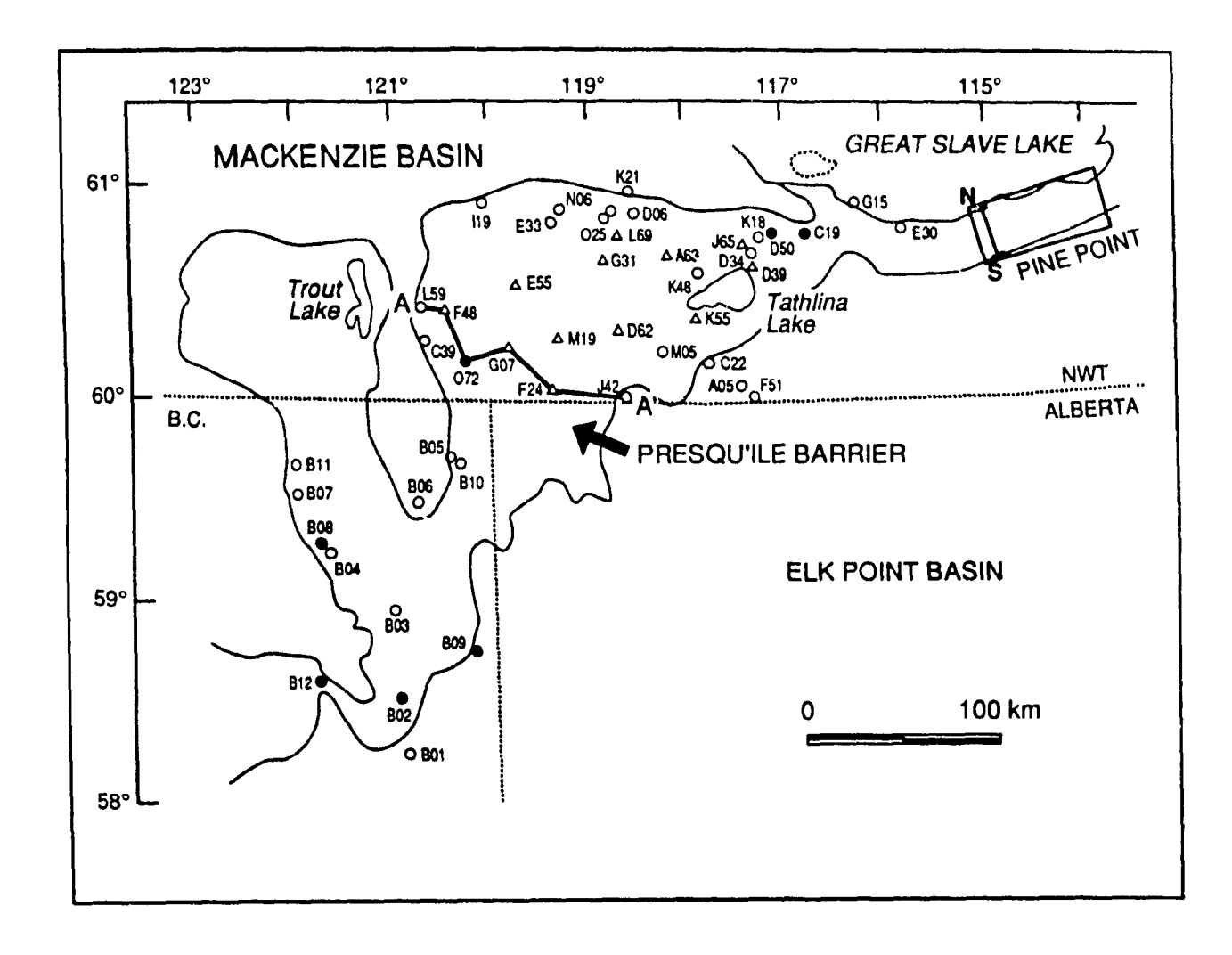


Figure 1 Middle Devonian Presqu'ile barrier and location of the wells studied. Circles and solid dots are wells with core samples. Triangles are wells with no cores. Solid dots indicate wells where dissolution, coarse-crystalline and saddle dolomites occur above the sub-Watt Mountain unconformity. Detailed well information is listed in Appendix 1. N-S cross section is shown in Figure 6. A-A' cross section is shown in Figure 21.

converted to PDB and corrected for ¹⁷O as described by Craig (1957). Analytical results of carbon and oxygen isotopes are given in Appendix 2.

į

Sr isotopes were analyzed at McMaster University. All samples were crushed in stainless steel mortar prior to chemical dissolution. The dolomite and calcite samples were leached in warm and cold 0.5N HCl respectively to extract Sr. For some of the calcites, a similar leaching was done with 0.5N HAc and the measured ⁸⁷Sr/⁸⁶Sr ratios were the same within error. Sr was extracted from the leachate using standard cation exchange techniques with 2.5N HCl. The Sr isotopic analyses were performed on a VG 354 thermal ionization mass spectrometer at McMaster. The sample was loaded as SrCl₂ on a single Ta filament. The error is two sigma from the mean for the internal precision of a single analysis. Typically it is ±0.0025%. The average value of the NBS 987 standard during the course of the study was 0.71022. The sample's isotopic ratios have been normalized against this value. Analytical results of Sr isotopes are given in Appendix 3.

Fluid inclusions from doubly polished thin sections were analyzed at McGill University using a U.S.G.S. design heating-cooling stage. Analytical results of fluid inclusion measurements are given in Appendix 4.

Major (Ca and Mg) and trace elements (Sr, Na, Mn, Fe, K, and Zn) of dolomites and limestones were analyzed at McGill University using an atomic absorption spectrometer. Powdered samples weighing 0.5 g were dissolved in 10 ml 1:1 HCl or 20 ml 1:4 acetic acid for dolomite and calcite respectively and let stand for one hour. Then 30 ml of 30,000 ppm Sr were added to the solutions (for Sr

analysis, 1 ml of 50,000 ppm La or a similar amount of NaCl was used). After digestion, the solutions were filtered with ashless paper and then analyzed. The detection limits are as follows: Al 50 ppm, Ba 40 ppm, Ca 6 ppm, Fe 6 ppm, K 10 ppm, Mg 1 ppm, Mn 2 ppm, Na 5 ppm, and Sr 6 ppm. The stoichiometry of dolomites is calculated from major element concentrations. Analytical results of major and trace elements are given in Appendix 5.

Rare earth elements (REE) were analyzed at Memorial University of Newfoundland, using inductively coupled plasma mass spectrometry (ICP-MS). Samples (0.1 g) were digested in 1N HNO₃ and then analyzed by ICP-MS using the method of standard additions to correct for matrix effects. A sample solution was analyzed in duplicate in each analytical run. A reagent blank and a sample of the CANMET geological reference standard SY-2 were prepared and analyzed with the Reagent contamination is usually insignificant and reagent blank concentrations have not been subtracted from sample concentrations. The detection limits are about 0.01 ppm. Analytical results of RFE are given in Appendix 6. Identification of REE fractionation of the dolomites is done by normalizing the concentration of each REE by its value in average meteoritic chondrite in order to compare this study with previous studies on ancient dolomites that used this standard normalization (e.g. Graf 1984; Dorobek and Filby 1988; Banner et al. 1988a; 1988b). For comparison with literature data, the REE patterns of limestones, FCD, and SD also have been normalized to North America shale composite (NASC).

1.3 PREVIOUS STUDIES

The regional geology, processes of dissolution, dolomitization, and mineralization of Pine Point MVT deposits have been studied by Campbell (1966), Jackson and Beales (1967), Skall (1975), Kyle (1981; 1983), Rhodes et al. (1984), and Krebs and Macqueen (1984). The interpretations of these studies are based mainly on petrography.

A variety of geochemical analyses have been carried out to determine the diagenetic history of the Presqu'ile barrier. Sulphur isotopes were determined for 156 specimens of sulphides, sulphates, elemental sulphur, and pyrobitumen by Sasaki and Krouse (1969). The mean δS³⁴ of 118 sulphide samples is +20.1 ‰, which is similar to the evaporitic anhydrites from the Elk Point Basin (+19 to +20 ‰). Sasaki and Krouse (1969) suggested that the source of sulphur for MVT deposits at Pine Point was Middle Devonian seawater sulphate itself, probably supplied as connate brines or solutions from the contiguous evaporite basin. However, they failed to explain why there was little isotopic fractionation during reduction of sulphate to sulphide.

Lead isotopes of sulphide minerals from different deposits in the Pine Point area are essentially identical, suggesting a uniform and nonradiogenic lead isotopic composition for the Pine Point deposits (Cumming and Robertson 1969; Kyle 1981; Cumming et al. 1990). However, using the same lead-isotope data but different calculation models, the calculated age of mineralization can vary from Pennsylvanian

(Kyle 1981; Cumming et al. 1990), to Permian (Cumming and Robertson 1969), and Cretaceous (Cumming et al. 1990). Thus, the lead-isotope data do not provide an unequivocal resolution of the problem of the age of Pine Point mineralization (Cumming et al. 1990, p.142).

A paleomagnetic study suggested that the age of mineralization at Pine Point is probably Permian (Beales and Jackson 1982). This age determination must be viewed with caution because: 1) these paleomagnetic measurements were performed on unspecified minute amounts of magnetic co-precipitated or entrapped impurities, because neither host carbonates nor sulphide ores are magnetic (Beales and Jackson 1982); 2) the reliability of these measurements cannot be evaluated as they were presented in an abstract.

Sr isotopes were measured from sulphates, carbonates, and fluid inclusions by Medford *et al.* (1984). The ⁸⁷Sr/⁸⁶Sr ratios for fine-crystalline dolomites and pre-ore coarse-crystalline dolomite are close to that of Middle Devonian seawater. Later saddle dolomites associated with mineralization have more variable and radiogenic ratios.

Oxygen and carbon isotopic composition of carbonates (mainly from the overlying Watt Mountain and Slave Point formations) were analyzed by Fritz and Jackson (1972). They suggested that the limestones were dolomitized by evaporitic brines, modified seawater/fresh water, and hydrothermal fluids.

The fluid inclusions, mainly from sphalerite, were studied by Roedder (1968) and Kyle (1981). The homogenization temperatures for sphalerite range from 51 to

99 °C, and salinities from 15 to 23 equivalent weight percent NaCl. Homogenization temperatures measured from one unlocated saddle dolomite range from 90 to 100 °C, and salinities from 15 to 20 equivalent weight percent NaCl. Semiquantitative analysis of individual inclusion decrepitates of Pine Point dolomites by SEM energy dispersive method indicates that fluid composition was dominantly NaCl and CaCl₂, with subordinate KCl and MgCl₂ (Haynes and Kesler 1987).

Organic geochemistry of bitumens were analyzed by Macqueen and Powell (1983), Powell (1984), Powell and Macqueen (1984), Krebs and Macqueen (1984). Two types of bitumen are associated with the Presqu'ile barrier: unaltered and altered. In situ organic matter and unaltered bitumen have a low reflectance ranging from 0.13 to 0.35 %R_n, indicating that it is immature to marginally mature with respect to hydrocarbon generation, and that the host rocks were subjected to generally low-temperature (about 60°C) heating in the Pine Point area. Altered bitumen is intimately associated with saddle dolomite and sulphide minerals. It has a higher values of reflectance from 0.52 to 1.11 %R_o and is interpreted by Macqueen and Powell (1983) and Krebs and Macqueen (1984) to have formed from soluble bitumen by thermochemical sulphate-reducing reactions during dolomitization mineralization at temperatures around 100°C. However, the highest bitumen reflectance of altered bitumen, recently measured by Kirste et al. (1989), suggested paleotemperatures of between 120 and 170°C, after conversion to its vitrinite equivalent.

Conodont colour alteration index (CAI) ranges from 1.0 to 1.5 (D. F. Sangster, pers. comm. 1990). Because there is no indication of local increases in CAI values near the ore deposits or in any specific stratigraphic units, no thermal anomalies can be inferred from the CAI data. The interpreted maximum burial temperatures were in a range of 50 to 100°C.

Using computer modelling, Garven (1985) suggested that the Pine Point ore deposits could have formed during early Tertiary by topography/gravity-driven groundwater flow in the Western Canada Sedimentary Basin.

The apparent apatite fission-track ages of Precambrian basement samples ranges from 30 to 550 Ma (Arne 1991). The presence of apatite grains with fission track ages > 500 Ma indicates that Pine Point district experienced a single phase of heating to maximum paleotemperatures in the range of 80 to 100°C during maximum burial in Cretaceous time (Arne 1991).

1.4 ORGANIZATION OF THE THESIS

The data presented in this thesis will be submitted as six scientific publications. By necessity, there is some overlap of material covered in the separate chapters. The regional geology and stratigraphy are briefly summarized in Chapter 2, which provides relevant background information for the following chapters.

The diagenetic paragenesis of the Presqu'ile barrier is discussed in Chapter 3, which has been published in Qing and Mountjoy (1990, Current Research, Part D, Geological Survey of Canada, Paper 90-D).

The burial and geothermal history of the Presqu'ile barrier is reconstructed in Chapter 4, using the stratigraphic records and geothermal indicators.

The origin of various types of dolomites associated with the Presqu'ile barrier is discussed in Chapter 5, based on evidence from petrography, spatial distribution, diagenetic paragenesis, geochemistry, and fluid inclusions. The data presented in this chapter are to be submitted in three papers. 1) One deals with formation of the Presqu'ile dolomite, which forms the major host rock for the MVT deposits at Pine Point and also forms important hydrocarbon reservoir rocks in the subsurface Presqu'ile barrier. 2) A second paper discusses and compares the petrography, spatial distribution, and geochemistry of different types of dolomite associated with the Presqu'ile barrier. 3) The Sr isotope analyses have been submitted as a third paper, entitled "Sr isotopic composition of Devonian dolomites, Western Canada: significance regarding sources of dolomitizing fluids" (Mountjoy et al. in press).

Rare-earth elements as indicators of water/rock ratios during dolomitization are discussed in Chapter 6 and will be submitted as a fourth paper.

The origin of dissolution vugs and breccias that host MVT deposits has been controversial for a long time. The evidence for hydrothermal dissolution is discussed in Chapter 7, and will be submitted in a fifth paper.

According to the timing of dolomitization, the possible age of Pine Point mineralization is discussed in Chapter 8.

Chapter 9 provides a summary and conclusions of this study.

GEOLOGIC SETTING AND STRATIGRAPHY

2.1 GEOLOGIC SETTING

2.1.1 REGIONAL GEOLOGICAL HISTORY

Á

The Middle Devonian Presqu'ile barrier carbonates are widely distributed in the northern part of the Western Canada Sedimentary Basin, which includes parts of northeastern B.C., northwestern Alberta, and southern NWT (Fig. 2). The Western Canada Sedimentary Basin is a northeasterly thinning we ge of over 6 km of Phanerozoic sedimentary rocks that extends southwest from the Canadian Shield to the Cordilleran thrust belt (Fig. 3). The sedimentary sequence records the evolution of the basin from a continental terrace wedge and cratonic platform to a Mesozoic and Early Tertiary foreland basin that developed during accretion of oceanic terranes onto the western margin of North America (Porter et al. 1982).

The Middle Devonian sedimentation in the Western Canada Basin was preceded by a period of extensive uplift and erosion. In the vicinity of the Pine Point area, the Precambrian basement consists of granites, granite gneiss and quartzite. The oldest Palaeozoic sediments are the basal red beds of the Ordovician Mirage Point

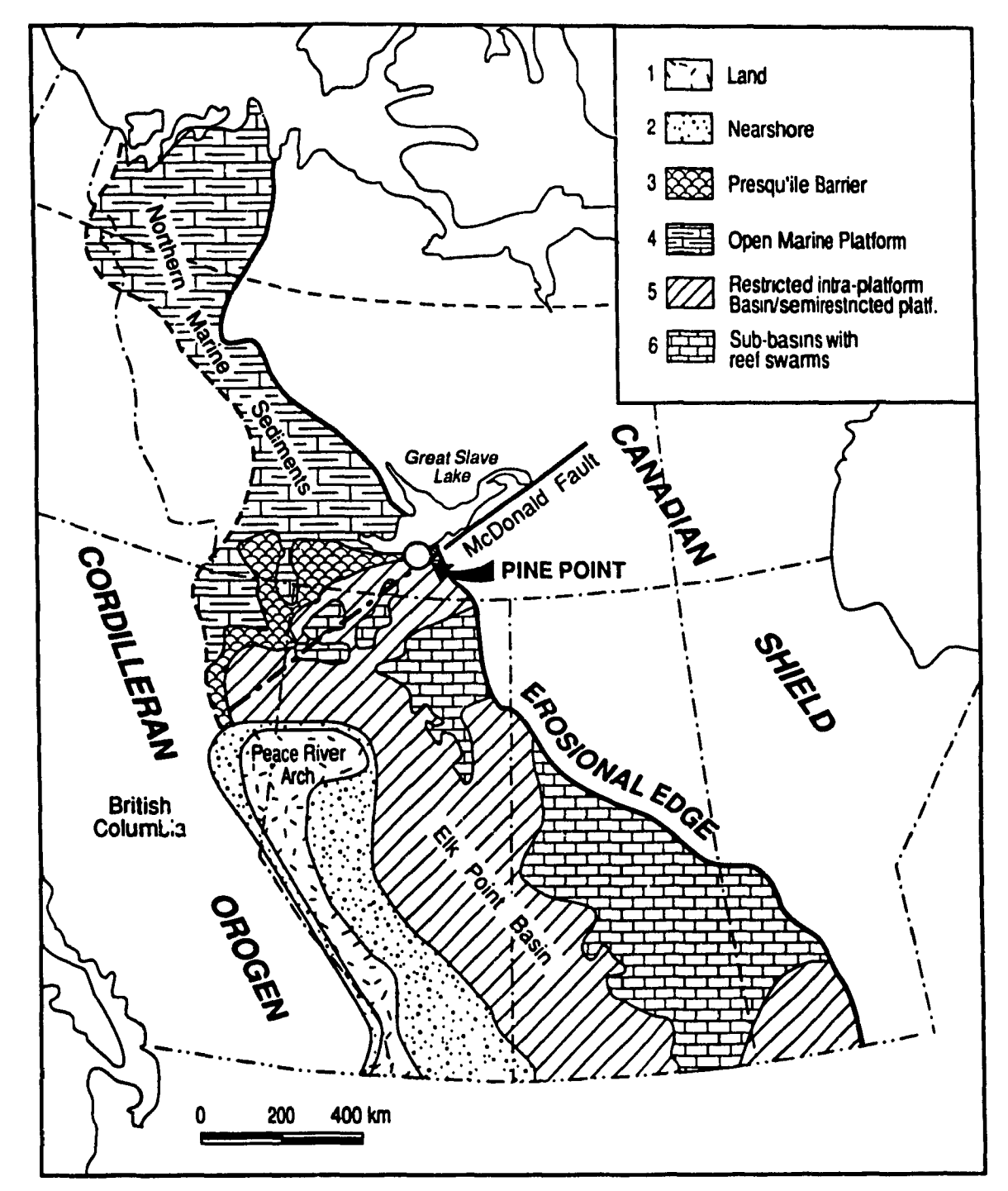


Figure 2 Simplified regional geological map of the Western Canada Sedimentary Basin during Middle Devonian (modified after Moore 1988). The Presqu'ile barrier outcrops in the Pine Point area west of the Canadian Shield. It extends westward into the subsurface of NWT and northeastern B.C. where its present burial depths are 2000 to 2300 m. It separates normal marine sediments to the north from Muskeg evaporites and carbonates to the south. The McDonald Fault is a major basement fault that can be traced from the Canadian Shield into the Pine Point area, northwestern Alberta, and northeastern B.C. The Presqu'ile barrier is shown in detail in Figure 1.

47.79

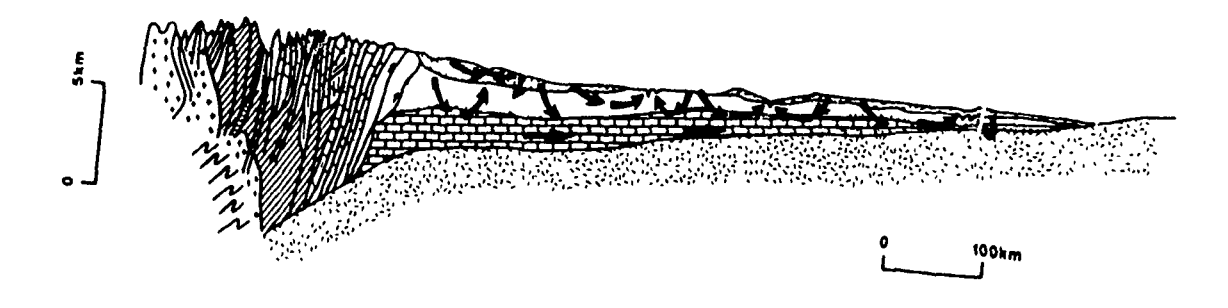


Figure 3 Schematic cross section of the Western Canada Sedimentary basin. The arrows indicate modelled fluid-flow pattern in the basin (from Garven 1989).

Formation (Norris 1965). Neither Silurian nor Lower Devonian strata have been recognized (Norris 1965; Krebs and Macqueen 1984). Deposition of the Middle Devonian Lower Elk Point Group (Eifelian) Chinchaga Formation represents a widespread marine transgression at the end of Eifelian time in the Western Canada Basin (Rhodes et al. 1984). The Chinchaga Formation comprises evaporites, limestones, and dolomites, that unconformably overly older strata (Norris 1965).

The Keg River Formation (Early Givetian) conformably overlies the Chinchaga Formation and represents an open-marine carbonate platform that developed over a wide area (Rhodes et al. 1984). With continued subsidence and marine transgression during Middle Devonian time, the Presqu'ile barrier (also called Keg River, Shekilie...) developed within the northwestern part of the basin. The Presqu'ile barrier is about 400 km kilometres long and extends westward from outcrops in the NWT, into the subsurface of northeastern British Columbia (Fig. 2). It has a variable width from 20 km to about 100 km (Fig. 2). The maximum thickness of the barrier is about 200 m. In the area around Tathlina Lake, the barrier is thinner over the Tathlina Arch. As the Presqu'ile barrier built up to sea level, it restricted the circulation in the southern part of the Western Canada Sedimentary Basin. As a result, normal-marine sediments were deposited on an open-marine platform north of the barrier, and evaporites and carbonates were deposited south of the barrier in the Elk Point basin (Fig. 2). The barrier was subaerially exposed after its development, resulting in an unconformity between the barrier and strata that cover the barrier. Pine Point is located towards the east end of the barrier, on the

south shore of Great Slave Lake (Fig. 2), where various dolomite rocks host more than 80 individual MVT ore bodies.

Generally, Middle Devonian sediments experienced nearly continuous burial during gradual subsidence of the Western Canada Sedimentary Basin from Devonian to Mississippian time. During the Permian and early Mesozoic, the Western Canada Basin was progressively tilted westward (Porter et al. 1982). This tilting caused uplift of the eastern part of basin, resulting in extensive erosion and peneplanation which bevelled the Paleozoic sequence (Krebs and Macqueen 1984).

During Middle Jurassic through Paleocene time, a foreland basin formed in western Canada due to the accretion of oceanic terranes onto the western margin of the North American craton and structural telescoping of the continental terrace wedge (Porter et al. 1982). The foreland basin was filled with over 4 km of a northeasterly thinning clastic wedge (Fig. 3) formed from sediments shed eastward from imbricate thrust slices emplaced during two orogenies, the first during the Late Jurassic to Early Cretaceous, and the second during the Late Cretaceous to early Tertiary (Porter et al. 1982). The Devonian rocks in the Western Canada Sedimentary Basin reached their maximum burial depths during the Late Cretaceous to early Tertiary. During and following the Laramide Orogeny, there was widespread uplift and erosion of Cretaceous and Tertiary rocks in the Western Canada Basin (Hitchon 1984).

2.1.2 STRUCTURAL GEOLOGY

A major basement fault, the McDonald Fault, passes beneath the Pine Point area (Fig. 2). The McDonald Fault forms the boundary between the Slave Province to the northeast and the Churchill Province to the southeast (Ross 1990). Based on aeromagnetic data, the McDonald Fault extends beneath the Palaeozoic cover from Pine Point into northeastern British Columbia (Campbell 1966; Jones 1980; Ross 1990) (Fig. 2). The role of basement faulting with respect to the development of the barrier, and the late stage mineralization and dolomitization remains controversial. Although the trends of dissolution, dolomitization and mineralization do not exactly parallel the McDonald Fault, these trends approximate the projections of the McDonald Fault beneath the Paleozoic cover (Skall 1975; Rhodes et al. 1984). Campbell (1966) suggested that the McDonald fault might have provided a conduit for the ore-forming solutions for the MVT deposits at Pine Point. This is supported by 3 parallel trends of the ore deposits (south, central, and north) along the strike of the Presqu'ile barrier which do not appear to be related to facies changes.

Based on a study of the depositional environments and diagenesis of the Presqu'ile barrier at Pine Point, Skall (1975) suggested that facies development, dolomitization, and mineralization were mutually dependent events, and were influenced by reactivated basement fault systems, which also acted as conduits for subsequent ore solutions. On a regional scale, the renewed activity of basement faults in Devonian time is also supported by the coincidence of linear magnetic

anomalies west of Pine Point with facies front, structure contours, and isopach trends (Belyea 1970). Additionally, these trends remained lines of weakness in post-Devonian time, as indicated by post-Mississippian displacement on the southwest extension of the McDonald Fault (Douglas et al. 1970).

Based on drill hole data and observations in open pits, Rhodes et al. (1984) reported some high-angle faults (with displacements of 2 to 10 m) in the ore zones. These faults appear to be young, displacing all strata (Rhodes et al. 1984). However, the relationship between these faults, the orebodies and dolomites were not described by Rhodes et al. (1984).

2.1.3 PALEOLATITUDE AND PALEOCLIMATE

During the Middle Devonian, the paleolatitude of the study area has been estimated to be within 15° of the paleoequator (Campbell 1987) (Fig. 4). Modelled on today's global wind patterns, the inferred paleolatitude for the Middle Devonian in the Western Canada Basin would indicate a southwesterly prevailing wind direction, which would have set up wave and current circulation patterns that may have influenced facies distribution in Devonian reefal sequences (Campbell 1987). The distribution of modern carbonate shelves and reefs occur predominantly between latitudes 30° N and 30° S, where average water temperature are above 25 °C (Campbell 1987). Evaporites are generally restricted between latitudes 10° and 40°.

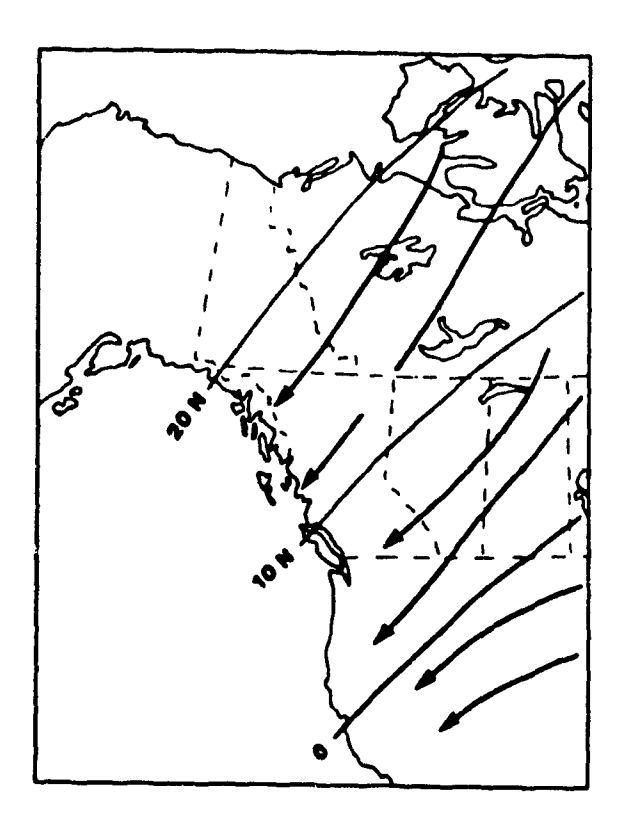


Figure 4 Estimated paleolatitude and surficial wind directions of western North American during the Middle Devonian (from Campbell 1987).

It is reasonable to assume a similar arid tropical climate for Middle Devonian time based on present day climate.

2.1.4 SEA-LEVEL VARIATIONS DURING MIDDLE DEVONIAN

Eustatic fluctuations in sea level through geological time can be caused by either: (1) changes in volume and/or shape of ocean basins, or (2) changes in the volume of seawater, or changes in both (1) and (2) at the same time (Donovan and Jones 1979). In terms of worldwide scale, sea-level changes are a reflection of major tectonic events and/or glaciation, which could profoundly modify the volume (shape) of ocean basins, and the volume of seawater, respectively.

Fluctuations in sea level through geological time were estimated by Vail et al. (1977). The sea-level curve for the Middle Devonian of Western Canada Sedimentary basin is derived from Moore (1988) and Campbell (1987) (Fig. 5). Overall the Devonian is characterized by a steady transgression broken by brief pulses of sea level stillstand and/or lowering (Moore 1988). Throughout most of the Western Canada Sedimentary Basin, a rapid sea-level rise caused a change from evaporitic conditions to normal marine carbonate sediments at the beginning of Keg River time. This is marked by an abrupt change from restricted evaporitic anhydrites and dolostones of the Chinchaga Formation to the basin-wide open-marine carbonate platform of the lower Keg River Formation. With continued subsidence and sea-level rise, the Presqu'ile barrier developed in northeastern British Columbia and the NWT

í

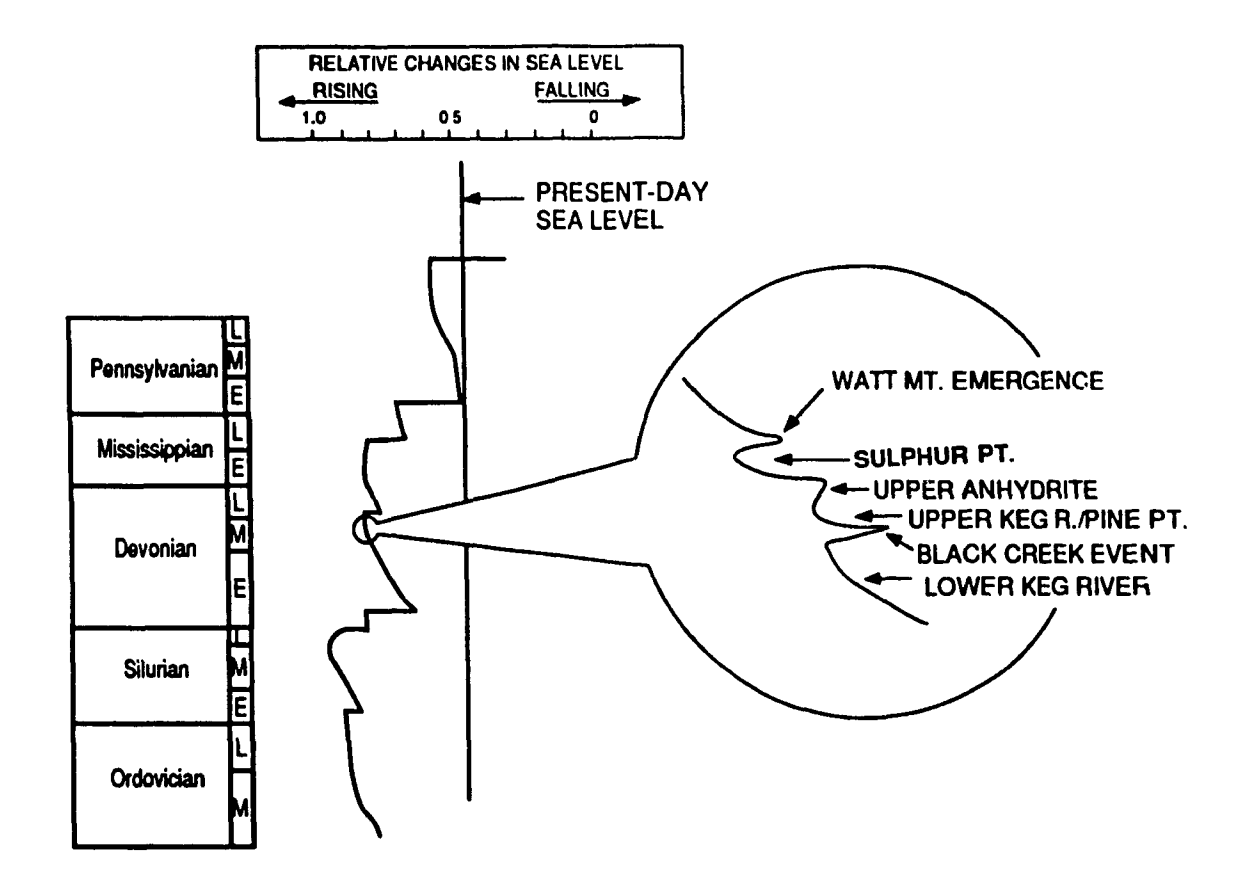


Figure 5 Eustatic sea-level changes during Ordovician to Pennsylvanian (from Vail et al. 1977), and interpreted qualitative curve for the Western Canada Sedimentary Basin during Middle Devonian time (modified after Campbell 1987; Moore 1988).

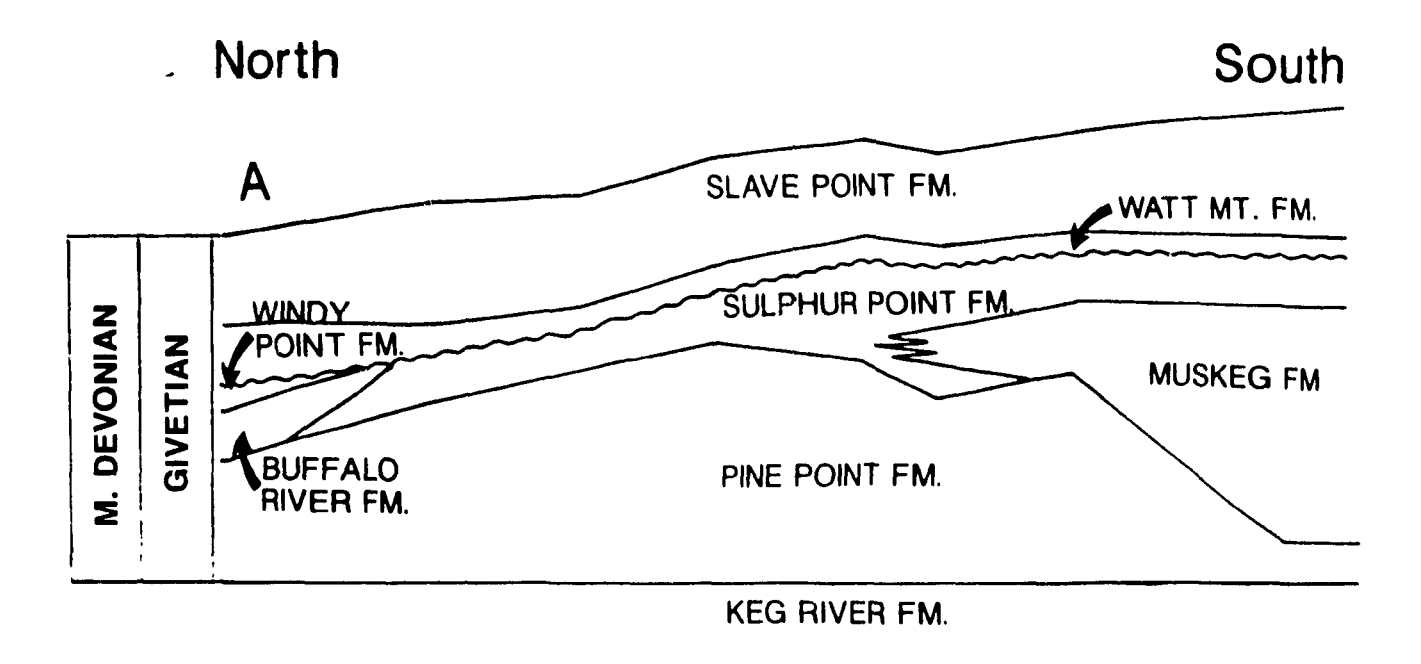
(Fig. 2). South of this barrier, isolated "pinnacle reefs" of the upper Keg River and Winnipegosis Formations developed at the same time on the lower Keg Piver platform (Fig. 2). Two major periods of lowered sea-level are recorded (Moore 1988; Campbell 1987). The first is the Black Creek event, which interrupted reef growth both inside and outside of Presqu'ile barrier and resulted in deposition of halite around the reefs within the Elk Point Basin. When water rose again, some reefs resumed growth; others did not. Evaporitic drawdown eventually terminated Keg River reefs and the Elk Point Basin was filled with evaporitic anhydrite and dolomite of the Muskeg Formation. The Presqu'ile barrier was terminated by a lowering of sea level, resulting in the sub-Watt Mountain unconformity between the Presqu'ile barrier and Watt Mountain and Slave Point strata that cover the barrier.

1

2.2 STRATIGRAPHY ASSOCIATED WITH THE PRESQU'ILE BARRIER

In the Pine Point area, the stratigraphy associated with the Presqu'ile barrier is subdivided as follows (Fig. 6):

- A lowermost carbonate platform: the Keg River Formation, which is composed of grey-brown dolostones with abundant crinoid and brachiopod fragments.
- 2) A carbonate barrier composed of two formations: the lower Pine Point Formation and an upper Sulphur Point Formation. The Pine Point Formation



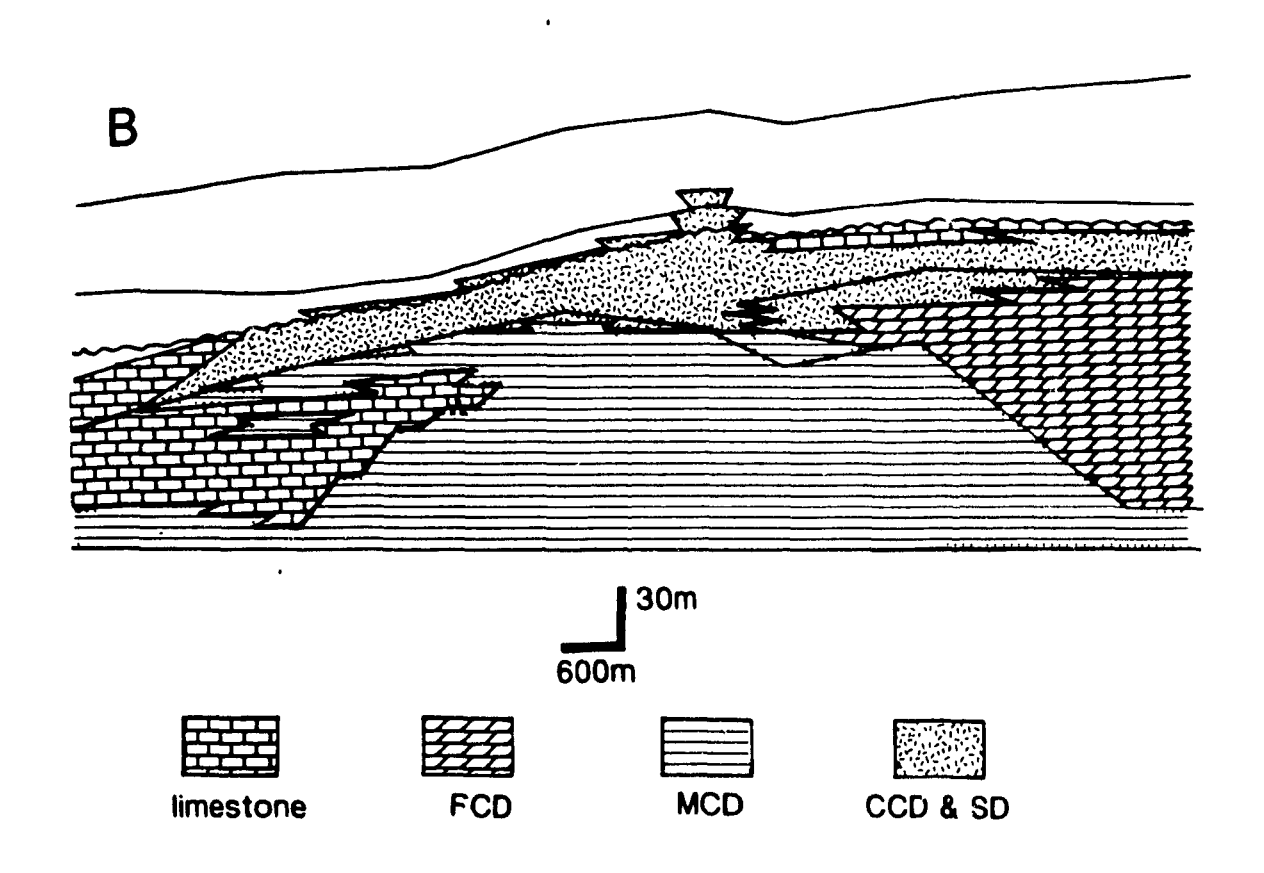


Figure 6 A) Stratigraphy of Presqu'ile barrier in the western part of Pine Point property.

B) Generalized spatial distribution of different types of dolomites associated with Presqu'ile barrier. FCD: fine-crystalline dolomite, MCD: medium-crystalline dolomite, CCD: coarse-crystalline dolomite, SD: saddle dolomite.

is composed of various lithofacies all of which were deposited as limestones, but subsequently dolomitized to medium-crystalline dolomite in the southern and central part of the barrier. The Sulphur Point Formation is composed of light brown/cream limestones, most of which were dolomitized to coarse crystalline (or Presqu'ile) dolomite.

- 3) Back-barrier facies: the Muskeg Formation, which consists of evaporitic anhydrites and dolomites that were deposited in the Elk Point basin on the south side of the barrier.
- 4) fore-barrier facies: Buffalo River and Windy Point formations (Rhodes and others, 1984), which are composed of normal marine shales and carbonates (mainly limestones) that were deposited on a normal marine platform to the north of the Presqu'ile barrier.

Detailed descriptions of the lithofacies of the Presqu'ile barrier can be found in Skall (1975) and Rhodes et al. (1984). The following is a summary from Rhodes et al. (1984).

2.2.1 KEG RIVER FORMATION

The Keg River Formation, a lateral equivalent of the Lower Keg River Member in the subsurface of northern Alberta, is a carbonate platform initiated by a rapid sea-level rise, marking the end of the Lower Elk Point evaporite sedimentation. It consists of grey-brown dolostones with fairly abundant crinoid

and brachiopod fragments, conformably overlying the Eifelian Chinchaga Formation. It maintains a constant thickness of approximately 65 m and represents a widespread open-marine carbonate platform, which forms a laterally continuous and extensive unit.

2.2.2 PINE POINT FORMATION

The Pine Point Formation represents the lower part of the barrier. It consists of dark brown stromatoporoid and coral floatstones, bioclastic grainstones, wackestones, and mudstones (see Rhodes et al. 1984). In the central and southern part of the barrier, the Pine Point Formation is dolomitized (Fig. 6B). The maximum thickness of the Pine Point Formation is about 175 m in the centre of the barrier in the Pine Point area, thinning to both south and north.

2.2.3 SULPHUR POINT FORMATION

The Sulphur Point Formation represents the upper part of the barrier and consists of light brown stromatoporoidal boundstones, bioclastic grainstones, laminated skeletal and pelloidal grainstones. It overlies the Pine Point Formation on the central part of the barrier. Extending south into northern Alberta, it overlies the Muskeg Formation. The maximum thickness of the Sulphur Point Formation is 65 m over the central part of the barrier. It thins to 30 m on the south side of the

barrier, and grades into the Buffalo River Formation north of the barrier. About 60 to 70 % of the Sulphur Point Formation is dolomitized to coarsely crystalline dolomite (Presqu'ile dolomite), which hosts MVT deposits at Pine Point.

2.2.4 MUSKEG FORMATION

In the Elk Point Basin, the Muskeg Formation consists of fine-crystalline dolomites interbedded with laminated anhydrites. In the Pine Point area, the Muskeg Formation is composed of mainly fine-crystalline dolomites with a maximum thickness of about 145 m. The Muskeg Formation overlies the Keg River Formation. It is coeval with the Pine Point Formation and the lower part of the Sulphur Point Formation and represents the evaporitic facies deposited in the restricted back-barrier environment of the Presqu'ile barrier (Fig. 6).

2.2.5 BUFFALO RIVER AND WINDY POINT FORMATIONS

The fore-barrier facies are composed of normal-marine shales and carbonates that were deposited on the north side of the barrier (Fig. 6). These sediments are called Buffalo River and Windy Point formations by Rhodes et al. (1984).

The Buffalo River Formation consists of grey/green shales and lesser carbonates and gradually thickens northward. The formation is 60 m thick on the south shore of the Great Slave Lake (Rhodes et al. 1984).

The Windy Point Formation is composed of argillaceous carbonates, overlying the Buffalo River Formation and flanking the north side of the barrier. The formation reaches a maximum of 50 m on the west shore of the Great Slave Lake at Windy Point (Rhodes et al. 1984).

2.2.6 WATT MOUNTAIN FORMATION

The Watt Mountain Formation consists of green, silty and pyritic shales, locally with nodular and argillaceous limestones or dolostones, limestone breccia, and minor amounts of anhydrite. In the northern Alberta and the adjacent NWT, it has been divided into three members by Meijer Drees (1988): a lower Breccia member; a middle Shale member; and an upper interbedded limestone and shale member. The Breccia member consists of limestone clasts in a shale matrix, indicating the presence of an erosional unconformity. The thickness of the Watt Mountain Formation varies from 10 to 33 m (Rhodes et al. 1984).

2.2.7 SLAVE POINT FORMATION

The Slave Point Formation in the Pine Point area consists of (in a ascending order) a blue-grey calcareous shale (the Amoco shale) sandwiched between two lime mudstones, the mudstones alternating with fine dense dolostones, lime wackestones or packstones, and stromatoporoid and coral floatstones.

2.3 CONCLUSIONS

The Middle Devonian Presqu'ile barrier is a linear carbonate barrier about 400 km long and extends from outcrops in the NWT into the subsurface of northeastern British Columbia. The Presqu'ile barrier restricted seawater circulation in the southern part of Western Canada Sedimentary Basin during Middle Devonian time. As a result, evaporites and carbonates were deposited to the south of the barrier in the Elk Point Basin, whereas normal marine sediments were deposited to the north of the barrier. A major basement fault, the McDonald Fault, occurs in the Pine Point area. Based on magnetic data, it is suggested that the McDonald Fault can be traced from the Canadian Shield into the subsurface of NWT, northwestern Alberta, and northeastern British Columbia. It is not clear whether this basement fault played a role in conducting diagenetic fluids during late stage dolomitization and mineralization.

In the Pine Point area, the stratigraphy associated with the Presqu'ile barrier is subdivided as follows: 1) a lowermost carbonate platform: the Keg River Formation, which is composed of grey-brown dolostones with abundant crinoid and brachiopods fragments; 2) a carbonate barrier composed of two formations: the lower Pine Point Formation and an upper Sulphur Point Formation. The Pine Point Formation consists of various lithofacies all of which were deposited as limestones but subsequently dolomitized to medium-crystalline dolomite in the southern and central part of the barrier. The Sulphur Point Formation is composed of light brown/cream

limestones most of which are dolomitized to coarse-crystalline (or Presqu'ile) dolomite; 3) back-barrier facies: the Muskeg Formation, which consists of evaporitic anhydrites and dolomites that were deposited in the Elk Point basin to the south; and 4) fore-barrier facies: Buffalo River and Windy Point formations, are composed of normal marine shales and carbonates (mostly limestones) that were deposited on a normal marine platform to the north.

DIAGENETIC PARAGENESIS

The Presqu'ile barrier has undergone a complex history of diagenetic alteration in submarine, subaerial, and subsurface environments as the Presqu'ile barrier was invaded by evaporitic brines from the Elk Point Basin, meteoric water during sub-Watt Mountain exposure, and basinal and hydrothermal fluids during burial. The diagenetic features are discussed according to their paragenetic sequence (Fig. 7). Overlapping phases are listed according to their first appearance.

Previous studies (e.g. Jackson and Beales 1967; Fritz 1969; Skall 1975; Kyle 1981; Rhodes et al. 1984; Krebs and Macqueen 1984) of the Presqu'ile barrier examined mainly the relationship between mineralization and dolomitization. The diagenetic features of the limestones are described herein for the first time. This provides additional information and constraints on the origin and timing of dissolution, dolomitization, and mineralization. The petrography and spatial distribution of the dolomites are presented entirely in Chapter 5, and are not repeated here. The dissolution features in the Presqu'ile barrier are discussed in Chapter 7 and only a brief description is provided in this chapter.

3

DIAGENETIC PARAGENESIS OF THE PRESQU'ILE BARRIER

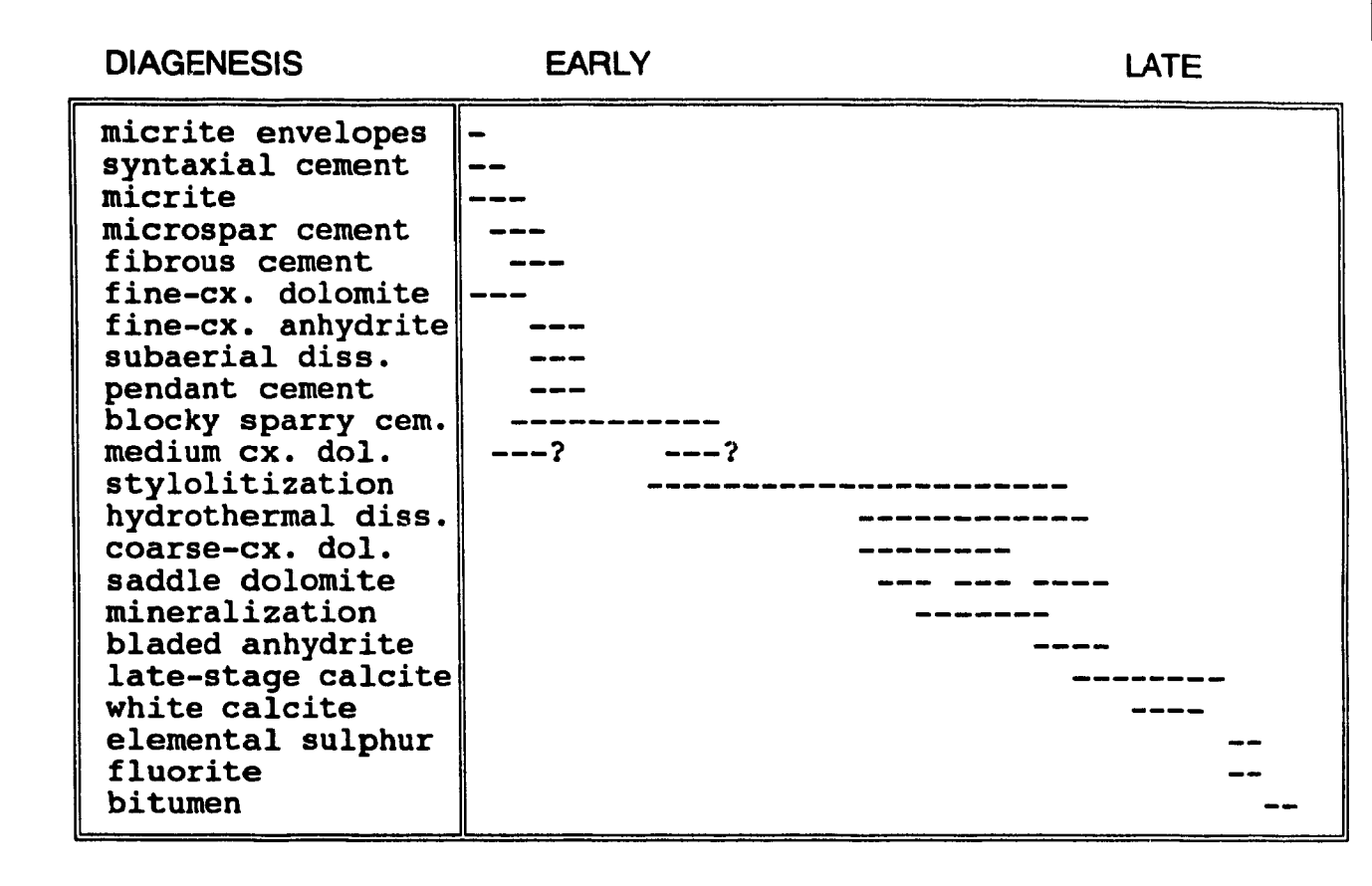


Figure 7 Diagenetic paragenesis of the Presqu'ile barrier derived from petrographic study of open pits and cores.

abbreviations:

cx.=crystalline; dol.=dolomite; diss.=dissolution;

cem.=cement

3.1 SUBMARINE DIAGENESIS

MICRITE ENVELOPE: Micrite envelopes form relatively thin micrite rims (40-100 μm) on fossil fragments (Fig. 8A), especially shell fragments (e.g. gastropod and/or brachiopod). In rare cases, however, an entire fossil fragment may be completely micritized. Micrite envelopes are most abundant in skeletal floatstones of the Sulphur Point Formation.

SYNTAXIAL CEMENT: Syntaxial calcite overgrowths on single crystals of echinoderm fragments occur locally in the upper part of the Sulphur Point Formation (Figs. 8B and 8C). They formed early prior to infilling of micrite.

MICRITE: Micrite (crystals about 5 μm) occurs as a first cement and/or a lime mud filling pore spaces in peloidal wackestones and/or packstones and some skeletal wackestones, mainly in the Pine Point and Sulphur Point formations (Figs. 8A and 8D). It is the most abundant carbonate that fills pore spaces in the Presqu'ile barrier.

MICROSPAR CEMENT: Microspar cement (equant and anhedral crystals 10 up to 30 µm) is common in the limestone portion of the Presqu'ile barrier in the Pine Point and Sulphur Point formations (Fig. 8A). It precipitated after the micrite, but before the submarine fibrous cement. It fills the primary pore spaces in peloidal

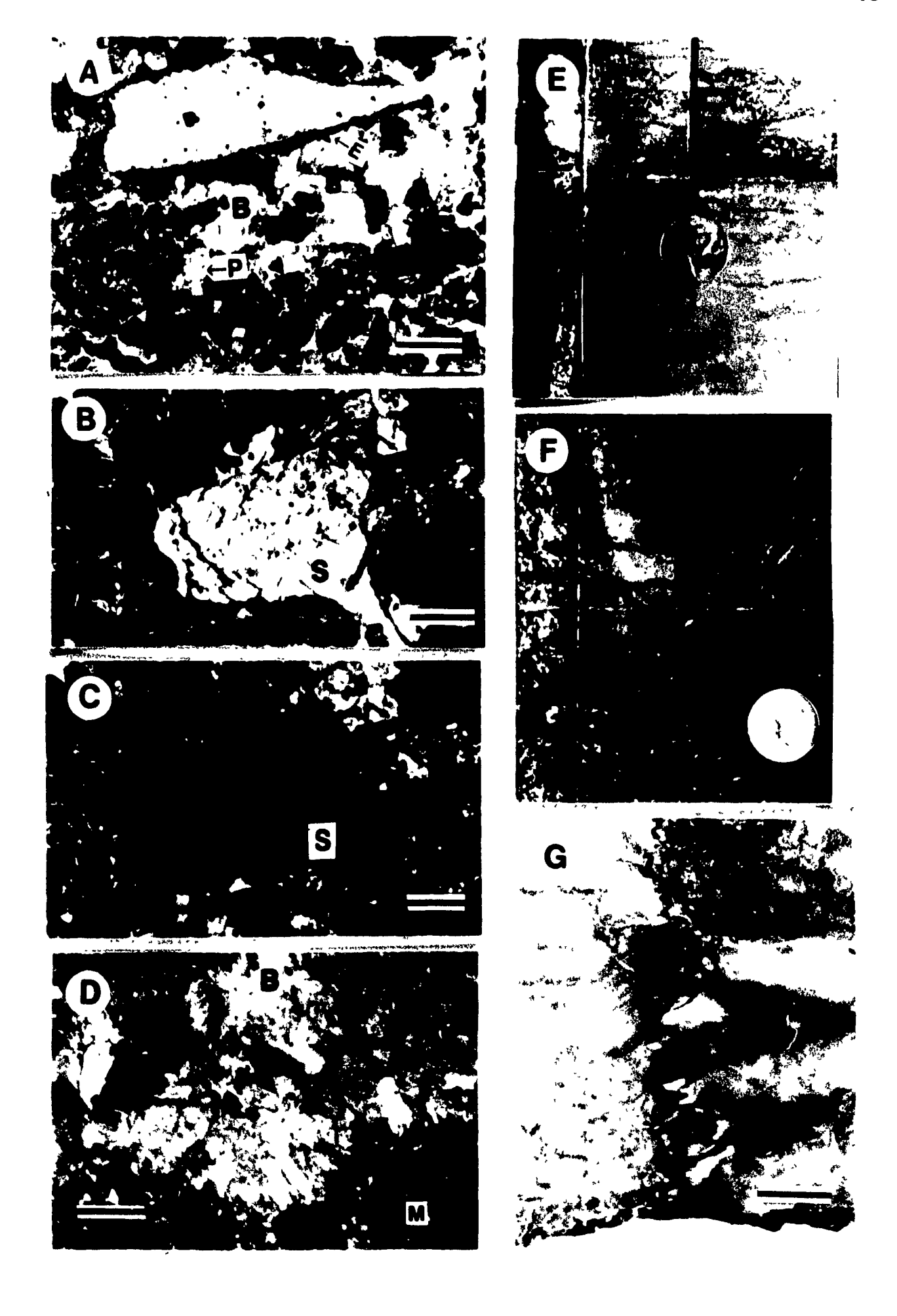
Figure 8A-8D. Calcite cements.

- A) Skeletal and peloidal packstone cemented by: 1) micrite (M), 2) microspar cement (P), and 3) blocky sparry cement (B). Micrite envelope (E) on edge of an echinoderm fragment.
 Location: Sulphur Point Formation, Pit M64, Pine Point. Scale bar 250 μm.
- B) Syntaxial cement (S) on an echinoderm fragment in skeletal and peloidal wackestone. The rest of pore spaces are filled with micrite. Plane light.
 - Location: Sulphur Point Formation, Pit M64, Pine Point. Scale bar 200 µm.
- C) The same view of B) under crossed nicols.
- D) Peloidal wackestone. Peloids are cemented by: micrite (M). The central pore space is filled with fibrous cement (F) and block sparry cement (B). Location: Sulphur Point Formation, Pit M64, Pine Point. Scale bar 400 μm.

Figure 8E-8G. Compaction and stylolitization.

- E) Horizontal stylolites in peloidal packstone. Location: Sulphur Point Formation, well B07, 7211 ft. Coin 1.5 cm.
- F) Horizontal stylolites in peloidal packstone. Location: Sulphur Point Formation, well B07, 7181 ft. Coin 1.5 cm.
- G) A vertical stylolite in stromatoporoid floatstone, which can only develop from horizontal stresses caused by either local structures, or a regional tectonic event.

Location: Sulphur Point Formation, well L-59, 5846. Scale bar 1 cm.



wackestones/packstones and skeletal wackestones and probably represents a submarine cement.

FIBROUS CEMENT: Fibrous cement (elongate calcite crystals 100 to 600 μm long and 25 to 100 μm wide) occurs locally in shelter and interparticle pores in skeletal packstones in the Sulphur Point Formation (Fig. 8D). Most fibrous cements are non-ferroan, but some have ferroan bands about 15 μm along the crystal terminations.

3.2 SUBAERIAL DIAGENESIS

DISSOLUTION VUGS AND BRECCIAS: In the subsurface Presqu'ile barrier west of Pine Point, minor dissolution breccia and vugs occur at the top of the Sulphur Point Formation, just beneath the Watt Mountain unconformity (Fig. 9), suggesting that the exposure of the barrier during Watt Mountain emergence caused dissolution. However the scale of dissolution, which could be directly related to the Watt Mountain unconformity, appears to be small, usually several millimetres (Fig. 9A). These vugs and breccias only occur below the unconformity and usually extend less than a few metres below it. Dissolution vugs and breccias related to the sub-Watt Mountain unconformity are usually filled with green shale matrix (Figs. 9A and 9B).

Figure 9 Subacrial diagenetic features.

A) Subsurface Presqu'ile core across the sub-Watt Mountain unconformity (arrow), showing dissolution vugs related to the unconformity. Note small (1 to 2 cm) size of vugs related to the unconformity, vugs are completely filled with green shale (S).

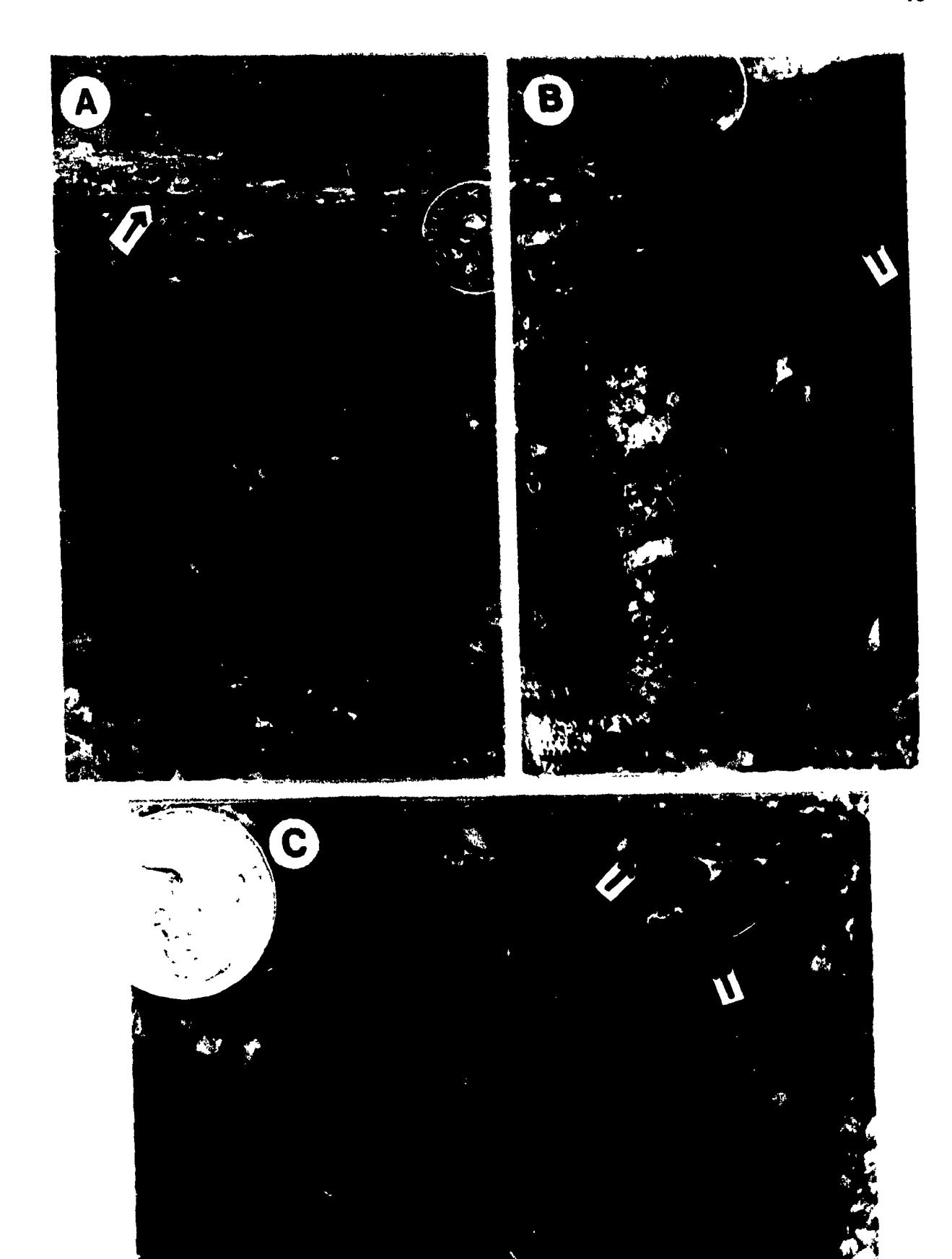
Location: top of the Sulphur Point Formation, well L-59, 1785 m. Coin 1.5 cm.

B) Subsurface core sample, showing solution breccia associated with subaerial exposure during Watt Mountain emergence. The breccia usually occurs immediately beneath unconformity (arrow) and spaces between fragments are filled with green shale (S).

Location: top of the Sulphur Point Formation, well B-11, 2126 m. Coin 1.5 cm.

C) Subsurface Presqu'ile core, showing well preserved dark pendant cements (arrows) diagnostic of vadose diagenesis. Pendant cements were observed only at this locality and extend 12 m below the unconformity.

Location: about 10 m below the unconformity in the Sulphur Point Formation, well L-59, 1776 m. Coin 1.5 cm.



PENDANT CEMENT: Pendant cement was observed in well L-59 (about 300 km west of Pine Point) between 1774.5 to 1778.2 m (Fig. 9C). Abundant pendant cement occurs in dissolution vugs in *Amphipora* rudstone/framestones. These vugs are filled, in paragenetic sequence, with: 1) dark brown pendant cement always occurring on the undersides of fossil fragments; 2) geopetal carbonate silts and muds; 3) milky white calcite cement; and 4) blocky sparry cement in the centre of the pore. Since pendant cements are most likely related to the Watt Mountain unconformity, which occurs at 1768.4 m, the thickness of this Devonian vadose zone is about 10 m in this part of the Presqu'ile barrier.

3.3 SUBSURFACE DIAGENESIS

BLOCKY SPARRY CEMENT: Blocky sparry calcite cement forms limpid to translucent, equant, and usually anhedral crystals of 100 to 1000 µm in size, and post-dates the micrite, microspar, and fibrous cements, filling the remaining pore spaces in the skeletal floatstones and peloidal packstones, and fenestral porosity (Figs 8A and 8D). Most blocky sparry cement is non-ferroan. Minor amounts of ferroan blocky sparry cement occur locally in the Presqu'ile barrier.

COMPACTION AND STYLOLITIZATION: With increasing burial, mechanical compaction is gradually overlapped by chemical compaction and horizontal stylolites form as result of pressure solution (Figs. 8E and 8F). Although

some stylolites may start to develop in limestones at burial depths of about 300 to 500 m, most stylolites probably formed at burial depths greater than 1000 m, because chemical compaction is a continuous process throughout burial history, and probably more commonly developed during deep burial. Thus stylolites indicate transition from early diagenesis to intermediate and deep-burial diagenesis.

Vertical scylolites are observed in the Presqu'ile barrier (Figs. 8G and 19F), and presumably occurred as a result of horizontal stress due to the development of local structure, or regional tectonic events.

HYDROTHERMAL DISSOLUTION: Dissolution features in the Presqu'ile barrier are described and discussed in detail in Chapter 5. The Presqu'ile barrier was invaded by hydrothermal fluids (see Krebs and Macqueen, 1984; Aulstead et al. 1988), resulting in large dissolution vugs and caves in the Pine Point area (from several cm to few m) (Fig. 10A). These vugs and caves are filled with saddle dolomite, and other late diagenetic products (e.g. sulphide minerals, pyrobitumen, and late stage calcite) (Fig. 10). Locally, at Pine Point and also in the subsurface of the NWT and northeastern B.C., large-scale dissolution, brecciation, and associated saddle dolomite occur continuously across the unconformity into the Watt Mountain and Slave Point formations. Therefore, large scale hydrothermal dissolution must have occurred after sub-Watt Mountain exposure.

Figure 10 Hydrothermal dissolution.

A) A hydrothermal dissolution vug in the Presqu'ile barrier is filled with saddle dolomite and late stage calcite.

Location: Sulphur Point Formation, pit X53, Pine Point. Hammer in lower left for scale.

B) Dissolution and brecciation of early stage colloform sphalerite (dark bands, arrows). Post-ore fractures and vugs are filled with saddle dolomite (D), indicating that dissolution, brecciation, and dolomitization postdate mineralization.

Location: Sulphur Point Formation, pit M64, Pine Point. Scale bar 15 cm.

C) Sample from Pine Point, showing hydrothermal dissolution vugs and fractures filled with saddle dolomites (D1, D2, and D3) and sulphide minerals. Some saddle dolomites (D1) precipitated prior to, some (D2) are mixed with, and some (D3) postdate sulphide minerals.

Location: Sulphur Point Formation, Pit X53, Pine Point. Camera lens, 5 cm.









at Pine Point is iron sulphides, sphalerite, and galena (Skall 1975; Kyle 1981; Rhodes et al. 1984; Krebs and Macqueen 1984). These minerals occur as replacements of the host dolomites and/or as open-space fillings in vugs, fractures, and between breccia fragments (Figs. 10B and 10C). The iron sulphides occur as aggregates of fine marcasite (most common) or scattered euhedral pyrite in open spaces. Sphalerite usually occurs as botryoidal bands (Fig. 10B), followed by crystalline sphalerite. Cubic galena crystals precipitated after botryoidal banded sphalerite, partially filling the remaining pore spaces. Sulphide minerals are usually hosted by the coarsely crystalline dolomite in the upper part of the barrier, although some orebodies occur in fine-crystalline dolomite of the back-barrier facies (e.g. in pit X15 and W17, Pine Point). Sulphide minerals precipitated either before saddle dolomite (e.g. marcasite and some botryoidal sphalerite), or overlapped with saddle dolomite (e.g. crystalline sphalerite and galena) (Fig. 10C).

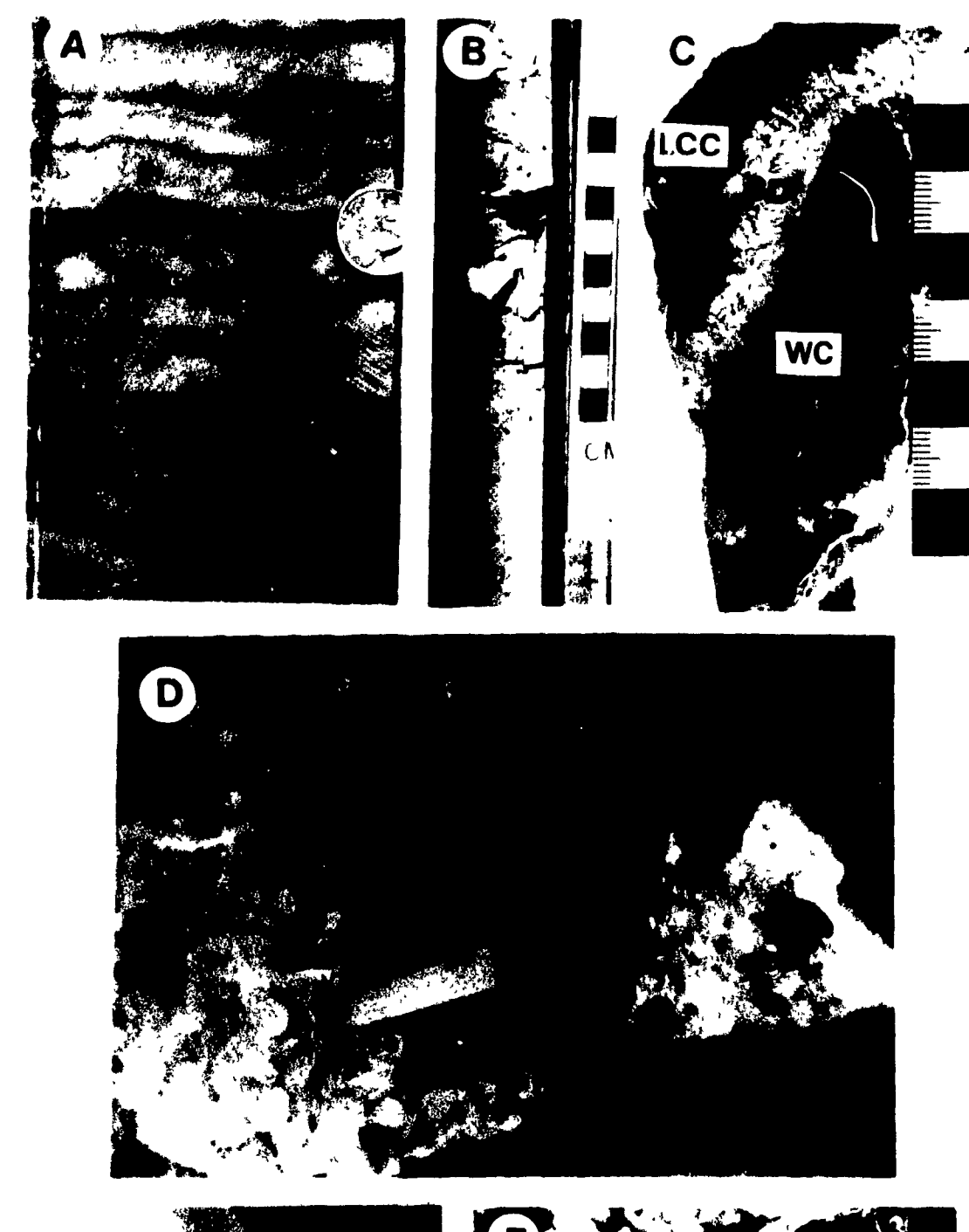
ANHYDRITES: Two types of anhydrite are identified: fine-crystalline and bladed cement. Fine-crystalline anhydrite, usually white and semi-transparent, occurs as nodular masses in vugs and moldic pore spaces, and/or laminae interlayered with laminated fine/medium-crystalline dolomite in the back-barrier facies of the Muskeg Formation (Fig. 11A). In thin section fine-crystalline anhydrite consists of anhedral crystals about 100 µm in length.

Figure 11. Other diagenetic features

- A) Laminated and nodular fine crystalline anhydrite from back-barrier facies. Location: Muskeg Formation, well C-22, 4924 ft. Coin 1.5 cm.
- B) Coarsely crystalline bladed anhydrite in dissolution vugs.

 Location: Muskeg Formation, Pine Point diamond drill hole 2822, 482
 ft. Scale in cm.
- C) Anhedral white calcite that occurs as a thick band (WC) sandwiched between two layers of saddle dolomite (SD). Semi-translucent euhedral LCC postdates SD. Sample has been treated with Alizarin red S.
 Location: Sulphur Point Formation, pit M64, Pine Point. Scale in cm.
- D) Semi-translucent euhedral LCC, varying from 1 to 10 cm. Location: Sulphur Point Formation, pit Y53, Pine Point. Scale in cm.
- E) LCC (C) fills fractures that cross cut saddle dolomite (S) and coarsely crystalline matrix dolomites (M).

 Location: Sulphur Point Formation, well B07, 7242 ft. Coin 1.5 cm.
- F) Dissolution vug filled with banded fluorite (F) and LCC. Location: Sulphur Point Formation, Pit Z65, Pine Point. Pen for scale.







Bladed anhydrite cement consists of white, medium to coarsely bladed anhydrite with euhedral elongate crystals up to 0.5 mm in width and 4.25 mm in length. The contact between the dolomite host rock and the anhydrite cement is sharp. Most of the bladed anhydrite represents a late-diagenetic event that postdates saddle dolomite and fills moldic pores, vugs and some late stage fractures (Fig. 11B).

LATE-STAGE COARSE-CRYSTALLINE CALCITE (LCC): LCC usually forms semi-translucent or white, rhombohedra or hexagonal scalenohedra (Fig. 11D). LCC is commonly observed in large vugs and caves, fractures or breccia, lining the walls and encrusting the earlier saddle dolomite and sulphide minerals (Figs. 11D and 11E). The crystal size varies from a few millimetres to about 20 cm. LCC is found both at Pine Point and in the subsurface NWT and northeastern British Columbia. LCC postdates the sulphide minerals and saddle dolomite.

WHITE CALCITE (WCC): In open pits, WCC is pure white in colour. It is anhedral and occurs as a thick band (1-5 cm) sandwiched between two layers of saddle dolomite (Fig. 11C). WCC is recognized for the first time, as previously it was misidentified as saddle dolomite. WCC is closely associated with the ore bodies and occurs only at Pine Point. Identification of WCC is difficult, because it looks like the white coarsely crystalline saddle dolomite. WCC represents a

dedolomite, because the early stage of saddle dolomite was replaced locally by WCC and WCC retains typical saddle dolomite textures.

ELEMENTAL SULPHUR: Minor amounts of elemental sulphur occur in vugs and fractures at Pine Point. It is either anhedral, as a cement filling dissolution vugs, or occurs as euhedral sulphur crystals (few mm to 5 cm in diameter) partially filling vugs and fractures. In both cases, elemental sulphur postdates SD and LCC.

FLUORITE: Massive fluorite was sampled along the periphery of pit Z65 close to the Watt Mountain unconformity (Fig. 11F). It lines the walls of a large dissolution vug (35 x 60 cm) as a (5 to 10 cm) thick band. In hand specimens, it is usually translucent and has different shades of brown colours. Minor anhedral fluorite is also found in thin sections, replacing LCC.

BITUMEN: Massive black bitumen is common in the Presqu'ile barrier at Pine Point, and has been studied in detail by Macqueen and Powell (1983), Powell and Macqueen (1984), Powell (1984), and Kirste et al. (1989). Massive bitumen is the latest diagenetic product, which postdates LCC, filling some of the remaining vugs and/or fractures.

Two main types of bitumen, unaltered and altered, are associated with the Presqu'ile barrier. Unaltered bitumen is soft and soluble in organic solvents. It represents indigenous organic matter, presumably derived locally from the barrier

sediments. Altered bitumen is brittle and glassy and insoluble in organic solvents. It is intimately associated with saddle dolomite and sulphide minerals and is interpreted to have formed from soluble bitumen by thermochemical sulphate-reducing reactions during dolomitization (CCD and SD) and mineralization at temperatures around 100 °C.

3.4 CONCLUSIONS

The diagenetic features of the Presqu'ile barrier are interpreted to have occurred in submarine, subaerial, and subsurface environments. Submarine diagenesis developed: micrite envelopes, micrite, syntaxial cement, fine crystalline cement, and fibrous cement. Subaerial diagenesis includes the formation of minor small-scale dissolution and brecciation associated with subaerial exposure and minor, very localized pendant cement. Subsurface diagenesis includes: blocky sparry calcite cementation, compaction and stylolitization, hydrothermal dissolution, dolomitization (coarse-crystalline and saddle dolomites), mineralization, and precipitation of various late-stage diagenetic products (e.g. late-stage calcite, bladed anhydrite, elemental sulphur, and bitumen). Subsurface diagenesis has resulted in the most important diagenetic modifications in the Presqu'ile barrier.

BURIAL AND GEOTHERMAL HISTORY

The burial and geothermal history of the Presqu'ile barrier is reconstructed using: (1) the stratigraphic succession, and (2) geothermal indicators. The geothermal indicators include published data on organic geochemistry (Macqueen and Powell 1983; Powell 1984; Powell and Macqueen 1984; Kirste et al. 1989), fission track analysis (Ame 1991), and conodont colour alteration index (CAI) (D.F. Sangster pers. comm. 1989). The burial histories of the Presqu'ile barrier are reconstructed for three selected areas (Fig. 12): 1) northeastern British Columbia (the western section of the barrier which was the most deeply buried); 2) an intermediate section in the NWT (north of the Alberta-B.C. boundary), and 3) Pine Point (eastern section of the barrier, including surface outcrops and the shallowest buried subsurface occurrence).

4.1 BURIAL HISTORY RECONSTRUCTION BASED ON STRATIGRAPHIC RECORDS

END OF MISSISSIPPIAN

From the Devonian until the end of the Mississippian, the Presqu'ile barrier experienced continuous burial as the Western Canada Sedimentary Basin gradually

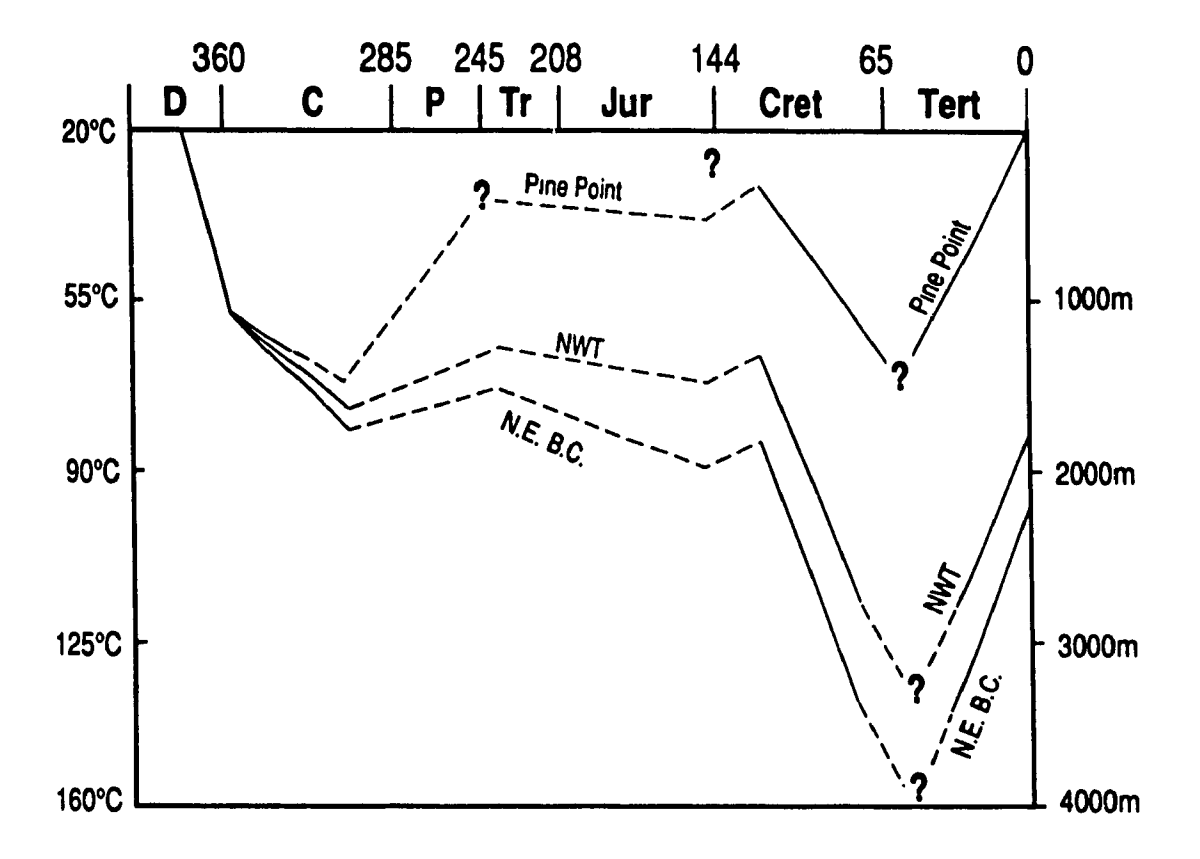


Figure 12. Burial history of the Presqu'ile barrier (top of the Sulphur Point Formation) at Pine Point, NWT north of B.C./Alberta boundary, and N.E. British Columbia.

subsided. Based on drilling data, the estimated original thickness of Middle Devonian to Mississippian strata above the Presqu'ile barrier (strata above the Sulphur Point Formation but below the Cretaceous) is about 1800 m in northeastern British Columbia and about 1600 m in the NWT (north of Alberta-B.C. boundary) (Fig. 12). Since the thickness of all Paleozoic stratigraphic units decreases eastward, it is estimated that the maximum thickness of the Middle Devonian to Mississippian sequence in the Pine Point area is about 1500 m (Fig. 12; see also Krebs and Macqueen 1984). Assuming a geothermal gradient of 35 °C/km and a surface temperature of about 20 °C at the end of Mississippian, the maximum burial temperatures for Presqu'ile barrier at the end of Mississippian would be about 72 °C in the Pine Point area, 76 °C in the NWT north of Alberta-B.C. boundary, and 83 °C in northeastern British Columbia (Fig. 12).

PENNSYLVANIAN TO EARLY CRETACEOUS

1

From Pennsylvanian to Jurassic time, the Western Canada Sedimentary Basin was progressively tilted westward, resulting in uplift, erosion, and peneplanation of the Upper Paleozoic sedimentary rocks in the eastern part of the basin (Porter et al. 1982; Krebs and Macqueen, 1984). The amount of the eroded sequence should increase eastward due to the tilting of the basin, but the exact amount of erosion is difficult to estimate.

1) In northeastern British Columbia, the preserved thickness of the Middle

Devonian to Mississippian strata is about 1700 m. As there are variable amounts of Jurassic sedimentary rocks in northeast British Columbia (Meijer Drees 1986), the estimated maximum burial depths of the Presqu'ile barrier in this region may have been about 1800-2000 m prior to the Early Cretaceous.

- 2) In the NWT north of the Alberta-B.C. boundary, the preserved thickness of the Middle Devonian to Mississippian sequence is about 1300 m, indicating that some of the Mississippian strata were eroded. Although Jurassic sediments were presumably deposited in this area, none are preserved. Thus, the burial depth in the Early Cretaceous was slightly less than that at the end of Mississippian (Fig. 12).
- 3) In the Pine Point area, the exact burial depth of the Presqu'ile barrier in the Early Cretaceous is also unknown, since Cretaceous strata are not preserved in this area. The extent of erosion that occurred from Pennsylvanian through Early Cretaceous time is difficult to estimate, because some Middle Devonian to Mississippian strata may have been eroded after the early Tertiary. In the Tathlina Lake area (e.g. well K55) NWT, about 150 km west of Pine Point, the preserved Devonian Mississippian sequence between the Sulphur Point Formation and Cretaceous strata is about 1000 m (Fig. 13). In the Caribou Mountain area, 100-150 km south of Pine Point, the preserved Devonian Mississippian sequence between the Sulphur Point Formation and Cretaceous deposits is about 400-500 m (Meijer Drees 1986). In the Horn Plateau area, about 150-200 km northwest of the Pine Point area, the preserved Devonian Mississippian sequence between the Sulphur Point Formation and Cretaceous sediments is about 200-400 m (Meijer Drees 1986).

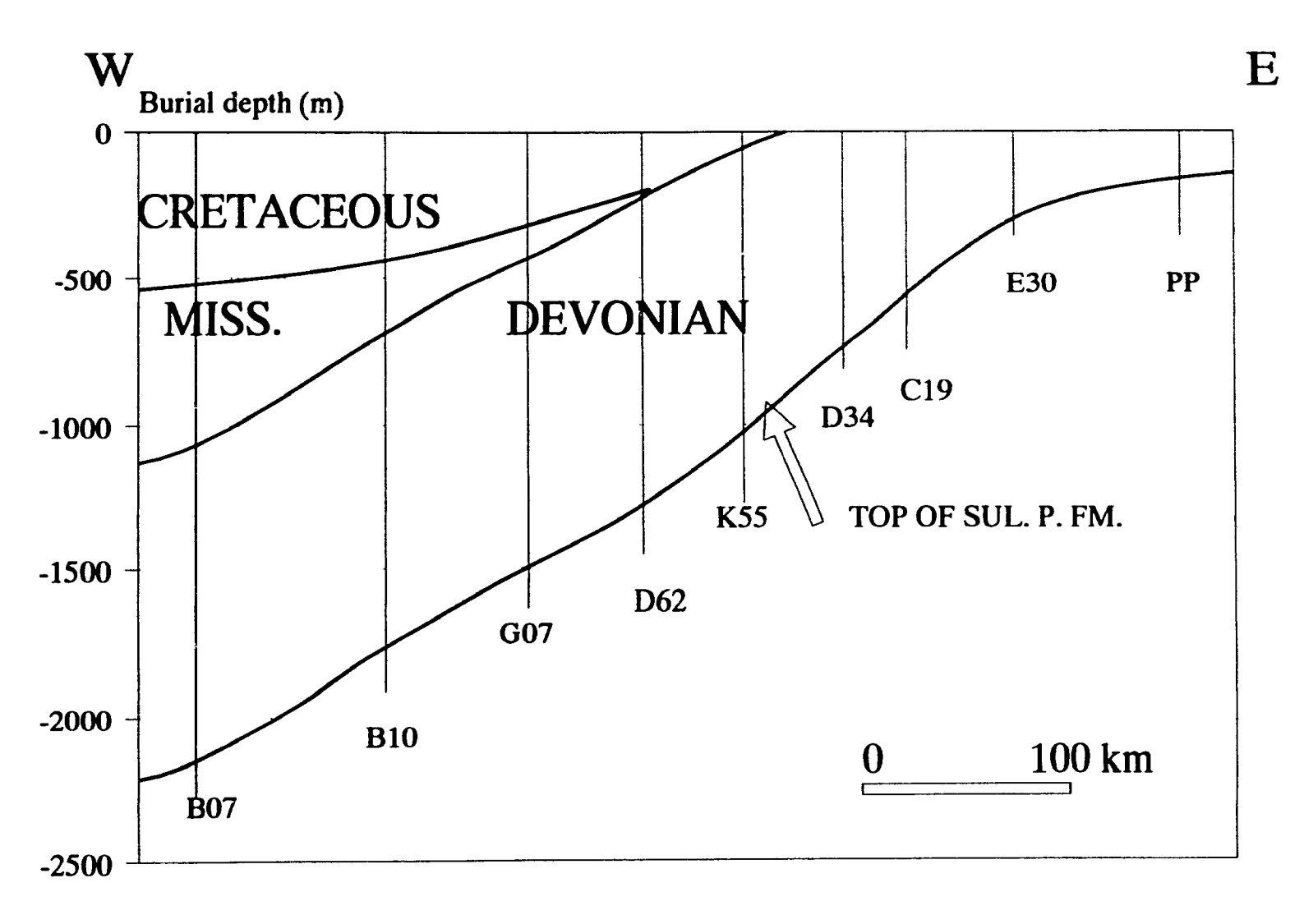


Figure 13. A generalized east-west stratigraphic cross section of the Presqu'ile barrier (see Figure 1 for well locations).

Since the preserved thickness of Paleozoic sediments decreases eastward, it is estimated that much of the Devonian - Mississippian sequence (1200 m to 1300 m) had been eroded before Cretaceous sedimentation in the Pine Point area. The maximum thickness of Devonian - Mississippian strata in the Pine Point area before Cretaceous time, therefore, was probably in the range of 200 m to 300 m (Fig. 12).

END OF EARLY TERTIARY

During the Late Jurassic through early Tertiary, a foreland basin formed in western Canada, due to the collision and accretion of oceanic terranes onto the western margin of North American and structural telescoping of the continental terrace wedge (Porter et al. 1982). Sediments were shed eastward from a series of thrust sheets emplaced in two major deformational phases, the first between Late Jurassic to Early Cretaceous and the second between Late Cretaceous to early Tertiary time (Porter et al. 1982). The foreland basin was filled with a clastic wedge that was over 4 km thick in the west and progressively thinned eastward. In general, Devonian rocks in the Western Canada Sedimentary Basin reached maximum burial in the Paleocene following the deposition of the clastic wedge. As there are about 1800 m of Cretaceous sedimentary rocks preserved in the Trout Lake area (Douglas 1974), the thickness of Cretaceous to early Tertiary sedimentation is estimated to have been about 2000 m in northeastern British Columbia, about 1500-2000 m in the NWT north of Alberta-B.C. boundary, and about 1000 m in the Pine

Point area. Therefore the maximum burial depth for the Middle Devonian Presqu'ile barrier could have reached: 1) about 3500-4000 m in the northeastern British Columbia, 2) about 3000-3500 m in the NWT north of Alberta-B.C. boundary, and 3) about 1200-1300 m in the Pine Point area (Fig. 12). Using a surface temperature of 20 °C and a geothermal gradient of 35 °C/km, the estimated burial temperatures for the Middle Devonian Presqu'ile barrier during early Tertiary time would have been: 1) around 143-160 °C in northeastern British Columbia, 2) about 125-143 °C in the NWT north of Alberta-B.C. boundary, and 3) about 62-66 °C in the Pine Point area (Fig. 12).

PRESENT-DAY

Following the Cordilleran deformation, the Western Canada Sedimentary Basin has been gradually uplifted, resulting in substantial erosion of Cretaceous and Tertiary rocks. The present burial depths of the Middle Devonian Presqu'ile barrier are: 1) about 2000-2500 m in northeastern British Columbia, and 2) about 1500-2000 m in the NWT north of the Alberta-B.C. boundary (Fig. 12). In the Pine Point area, all Upper Devonian, Cretaceous, and Tertiary rocks have been eroded and the Presqu'ile barrier and its hosted orebodies are now at or near the surface (Fig. 12).

4.2 ORGANIC GEOCHEMISTRY

In situ organic matter, bitumens, and heavy oils from the Presqu'ile barrier in the Pine Point area have been systematically studied by Macqueen and Powell (1983), Powell (1984), Powell and Macqueen (1984), Krebs and Macqueen (1984), and Kirste et al. (1989). Both in situ organic matter and unaltered bitumen from the Pine Point area have a low reflectance, ranging from 0.13 to 0.35 %R_o, indicating that they are immature to marginally mature with respect to hydrocarbon generation (Powell and Macqueen, 1984). Based on these reflectance data, the maximum regional geothermal temperatures due to burial were interpreted from 60 °C to 65 °C (Macqueen and Powell 1983; Krebs and Macqueen 1984). This fits the burial history reconstruction for the Pine Point area.

Altered bitumen is intimately associated with saddle dolomite and sulphide minerals. It has higher values of reflectance than the *in situ* organic matter, 0.52 to 1.11 %R_o. Macqueen and Power interpreted the altered bitumen to have formed at temperatures up to 100 °C from soluble bitumen by thermochemical sulphate-reducing reactions during dolomitization and mineralization, suggesting that dolomitization and mineralization events in the Presqu'ile barrier represent thermal anomalies with respect to the maximum regional burial temperatures (60 °C to 65 °C) (Macqueen and Powell 1983; Powell and Macqueen 1984; Powell 1984). A recent study of the optical and compositional characters of these bitumens by Kirste *et al.* (1989) indicates that the highest bitumen reflectance is 1.61% (equivalent to 1.4%

vitrinite reflectance), suggesting paleotemperatures between 120 °C to 170 °C, possibly higher, depending on the duration of heating.

4.3 APATITE FISSION TRACK ANALYSES

Fission track data were obtained from 13 widely spaced samples by Arne (1991): one dolomite (J2 facies, pit X15), and 12 Precambrian basement samples (3 from Pine Point Mine area, 2 from petroleum exploration wells west of Pine Point, and 7 from outcrops from Canadian Shield, north and east of Pine Point). Based on the fission track data, Arne (1991) suggested that the Pine Point district experienced a single phase of heating to maximum paleotemperatures in the range of 80 to 100 °C during maximum burial in Late Cretaceous - Paleocene time. As there is no obvious evidence of "thermal haloes" associated with the ore deposits from his fission track data, Arne (1991) rurther suggested that the maximum temperatures of 80 to 100 °C could have been produced during deep burial to depths of 2 to 3 km, assuming a geothermal gradient of about 30 °C/km. The final cooling from this maximum temperature at Pine Point may have occurred sometime in the Late Cretaceous/early Tertiary (Arne, 1991).

The regional maximum burial paleotemperatures deduced from fission track data (80 °C to 100 °C) are slightly higher than those estimated from reflectance of *in situ* organic matter (60 °C to 65 °C). This discrepancy is probably caused by the fact that all the fission track data (except one) were obtained from Precambrian

basement samples, which could have had a different geothermal history before formation of the Presqu'ile barrier. As fission track data were obtained from widely scattered samples (only four samples from the Pine Point area), more fission track analyses from different facies are needed to verify the existence of the subtle thermal anomalies in the Pine Point area. Therefore the fission track data of Arne (1991) must be used with caution.

4.4 CONODONT COLOUR ALTERATION INDEX

Conodont colour alteration indices (CAI) have been measured from 26 samples in the Pine Point area (D.F. Sangster, pers. comm. 1990). These samples were collected from host dolomites from 3 orebodies (N81, Z64, and X15) and 8 diamond drill holes away from orebodies. The sampled stratigraphic units include:

1) Presqu'ile barrier (i.e. Sulphur Point and Pine Point formations), 2) The Slave Point Formation above the barrier, 3) the Keg River Formation below the barrier, 4) the Buffalo River Formation north of the barrier, and 5) the Muskeg Formation south of the barrier.

CAI of these 26 samples range from 1.0 to 1.5, with no indication of a local increase in values within specific stratigraphic units, or near the ore deposits (D.F. Sangster, pers. comm. 1989). Based on the CAI data, Sangster (pers. comm. 1989) suggested that the Pine Point area could have experienced paleotemperatures of 50 °C to 100 °C over geologic time periods in the range of 10⁷ to 10⁴ years,

respectively.

As CAI can be used to estimate paleotemperatures only approximately, the thermal anomalies of 30-40 °C in Pine Point area could have been too subtle to be detected by CAI methods.

4.5 CONCLUSIONS

The Presqu'ile barrier reached the maximum burial depths during the Late Cretaceous and early Tertiary. Based on the stratigraphic record and geothermal indicators, maximum burial depths for Middle Devonian Presqu'ile barrier may have reached: 1) about 3500-4000 m in northeastern British Columbia, 2) about 3000-3500 m in the NWT north of the Alberta-B.C. boundary, and 3) about 1200-1500 m in the Pine Point area. Assuming a surface temperature of 20 °C and a geothermal gradient of 35°C/km, the estimated maximum burial temperature is about: 1) 143-160 °C in northeastern British Columbia, 2) 125-143 °C in the NWT north of the Alberta-B.C. boundary, and 3) 62-66 °C in the Pine Point area.

The higher reflectances of altered bitumen relative to the *in situ* organic matter suggest that dolomitization and mineralization events in the Pine Point area represented thermal anomalies with respect to the maximum regional burial temperatures (Macqueen and Powell 1983; Powell and Macqueen 1984; Powell 1984).

CHAPTER FIVE

ORIGIN OF MIDDLE DEVONIAN PRESQU'ILE DOLOMITE: EVIDENCE FROM PETROGRAPHY, GEOCHEMISTRY, AND FLUID INCLUSIONS

5.1 INTRODUCTION

The origin of massive replacement dolomites and models of dolomitization have been controversial for a long time, despite intensive research carried out by geologists and geochemists. Dolomite has been interpreted to have formed in many different environments by various fluids (Machel and Mountjoy 1986; Hardie 1987). These include: (1) evaporitic marine brines in sabkha environments (e.g. Adams and Rhodes 1960; Patterson and Kinsman 1982); (2) freshwater/seawater in mixing zones (e.g. Land 1973; Badiozamani 1983; Humphrey 1988; Humphrey and Quinn 1989); (3) normal seawater in subtidal environments (e.g. Saller 1984); (4) various fluids in subsurface environments (e.g. Mattes and Mountjoy 1980; Aulstead and Spencer 1985; Machel and Mountjoy 1986, 1987; Aulstead et al. 1988; Qing and Mountjoy 1989; Machel and Anderson 1989).

The extent of dolomitization is variable in these environments due to variations in the chemical composition of the fluids and the fluid-flow parameters.

Morrow (1982; 1990) and Land (1985) suggested that seawater was the only

abundant source of Mg²⁺ for dolomitization and therefore that subsurface fluids could not result in massive dolomitization due to an insufficient supply of Mg²⁺. Based on close examination of dolomites in modern mixing zones and evaporitic environments, Machel and Mountjoy (1986) and Hardie (1987) concluded that these environments cannot produce massive dolomites and that subsurface dolomitization is probably more abundant than was previously considered.

The unique geologic setting of the Middle Devonian (Givetian) Presqu'ile barrier offers a good opportunity to study the formation of ancient massive dolostones, as well as the relationships of these dolomites to MVT deposits at Pine Point. During the development of the Presqu'ile barrier and its subsequent burial, it was influenced by: 1) evaporated seawater from the Elk Point Basin; 2) meteoric waters during sub-Watt Mountain exposure; and 3) subsurface fluids during burial. Dolomitization could be related to any of these fluids, or any combination of them.

Understanding the origin and distribution of the dolomites in the Presqu'ile barrier is of great economic importance for both the mining and oil industries, as these dolomites host one of the world's largest Mississippi Valley-type (MVT) deposits in the Pine Point area (Rhodes et al. 1984). In the subsurface Northwest Territories (NWT) and northeastern British Columbia, these dolomites are also important hydrocarbon reservoir rocks (e.g. Collins and Lake 1989).

A number of papers have been written on various aspects of the Pine Point ore deposits (e.g. Jackson and Beales 1967; Skall 1975; Kyle 1981 and 1983; Rhodes et al. 1984; Krebs and Macqueen 1984). Little research, especially detailed

geochemistry, has been carried out on the host Presqu'ile dolomite for the Pine Point deposits, except for stable isotope analyses by Fritz and Jackson (1972) and Sr isotope analyses by Medford et al. (1984). As Rhodes et al. (1984, p.1051) state, "the barrier complex provides a major research opportunity to examine the petrography and chemistry of ancient dolomites and their precursor limestones. Until such a project is undertaken, comments on the manner and timing of dolomitization at Pine Point are somewhat speculative."

This chapter is designed to investigate the origin of the various dolomites in the Presqu'ile barrier at Pine Point, and in the subsurface of NWT and northeastern B.C., using petrography and various geochemical techniques, which include: i) oxygen and carbon isotopes, ii) strontium isotopes, iii) fluid inclusion measurements, and iv) trace elements. The petrography, spatial distribution, and geochemistry of these dolomites are discussed and the origins of the different dolomites interpreted by assessing and integrating all available information.

5.2 PETROGRAPHY AND SPATIAL DISTRIBUTION OF DOLOMITES

Four types of dolomites are associated with the Presqu'ile barrier (Fig. 6B). In a paragenetic sequence, they are: fine-crystalline (FCD); medium-crystalline (MCD); coarse-crystalline (CCD); and saddle (SD). The fine-crystalline dolomite of previous studies is divided into two types of dolomites, fine-crystalline and medium-crystalline, because they have distinctively different petrographic textures,

5.2.1 PETROGRAPHY

FINE-CRYSTALLINE DOLOMITE (FCD)

FCD is either brown or grey in hand sample (Fig. 14). Fossils and sedimentary structures are well preserved in FCD. Dolostones composed of FCD are generally tight, with very low porosity. Fractures and vugs in these dolostones are usually filled with fine-crystalline anhydrite.

Microscopically, FCD consists of subhedral to euhedral dolomite crystals, ranging from 5 to 25 μ m (avg. 8 μ m) without undulatory extinction (Fig. 14C). However, the crystal size increases (to 100 μ m) near orebodies, suggesting neomorphism by later mineralizing fluids. Under the scanning electron microscope, FCD consists of euhedral crystals with smooth uncorroded crystal surfaces (Fig. 14D). Micro, intracrystalline pores (1-10 μ m) in FCD crystals are rare. FCD has low intercrystalline porosity because of its interlocking texture.

MEDIUM-CRYSTALLINE DOLOMITE (MCD)

MCD is medium to dark brown, either porous or tight, depending on the presence or absence of intercrystalline porosity (Fig. 15). Fossils and sedimentary

Figure 14. Petrographic features of fine-crystalline dolomite (FCD)

A) Hand sample fine-crystalline dolomite.

Location:

Muskeg Formation, Pine Point diamond drill hole 2162, 614

ft. Scale in cm.

B) Fine-crystalline dolomite with anhydrite nodus and interlayer.

Location:

Muskeg Formation, Pine Point diamond drill hole 2162, 645

ft. Scale in cm.

C) Thin section photomicrography of fine-crystalline dolomite with anhedral dolomite crystals ranging from 15 to 25 μm .

Location:

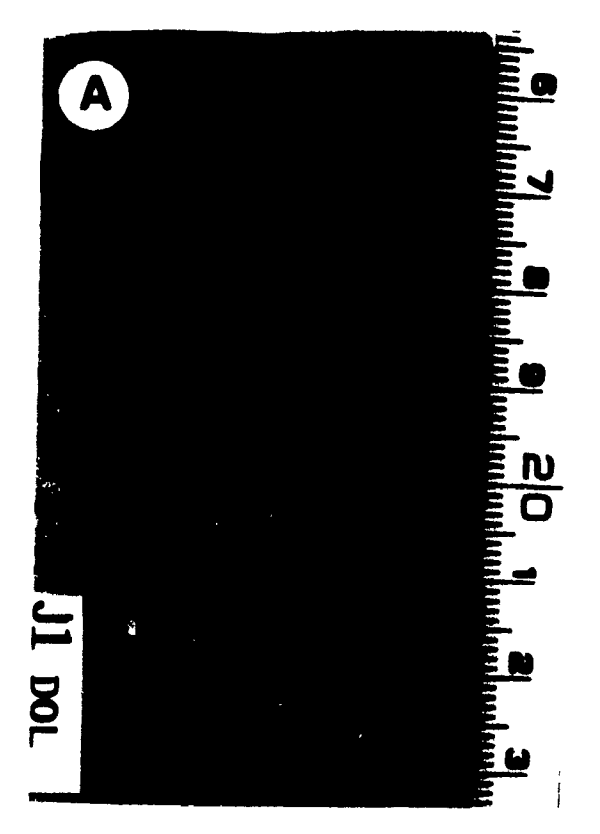
Muskeg Formation, well C-22, 3192 ft. Scale bar 200 µm.

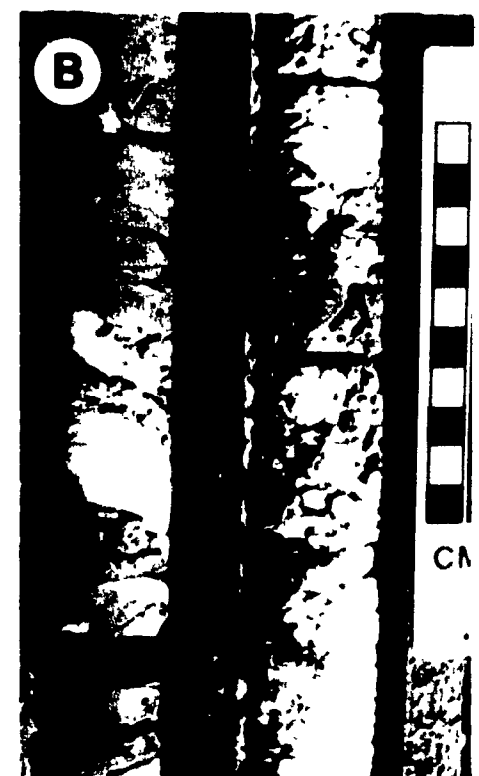
D) SEM photomicrography of FCD. Euhedral dolomite crystals have smooth and uncorroded surface with rare micro intracrystal pores (arrow).

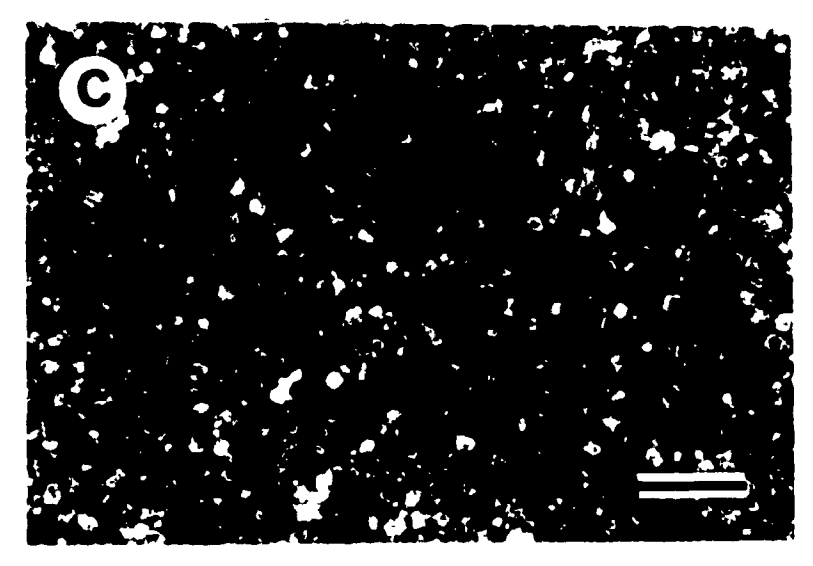
Location:

Muskeg Formation, Pine Point diamond drill hole 2162, 645

ft. Scale bar 10 µm.







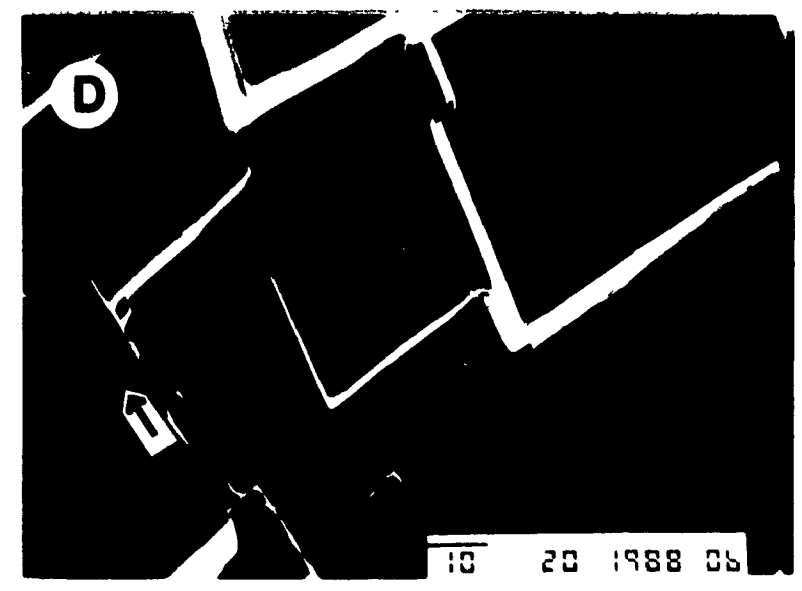


Figure 15. Petrographic features of medium-crystalline dolomite (MCD).

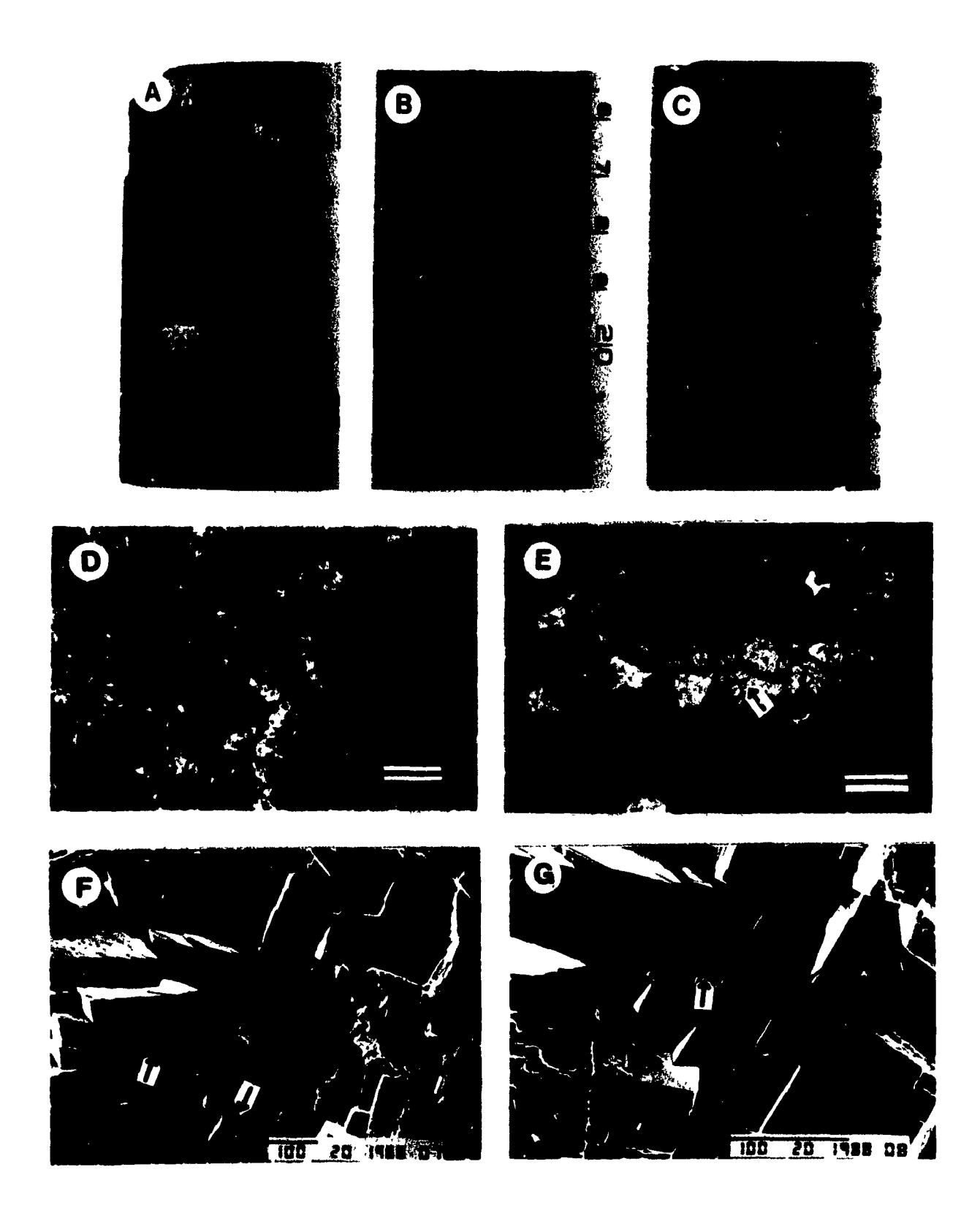
- A) Core sample of MCD with well preserved dolomitized fossil fragments.

 Location: Pine Point Formation, Pine Point diamond drill hole 2813, 530 ft. Scale in cm.
- B) Core sample of MCD with moldic and vuggy porosity.

 Location: Pine Point Formation, Pine Point diamond drill hole 2813, 870 ft. Scale in cm.
- C) Core sample of MCD with well developed intercrystalline porosity.

 Location: Pine Point Formation, Pine Point diamond drill hole 2822,

 452 ft. Scale in cm.
- D) Thin section photomicrograph of MCD. Some crystals have cloudy centres and clear rims, suggesting possible neomorphism or recrystallization.
 Location: Pine Point Formation, Pine Point diamond drill hole 2813, 642 ft. Scale bar 200 μm.
- E) Thin section photomicrograph of MCD. Note in the centre, a previous vug or intercrystalline pore is now filled with clearer dolomite crystals (arrow), suggesting that some dolomite could formed later as cements.
 Location: Pine Point Formation, Pine Point diamond drill hole 3306, 330 ft. Scale bar 200 μm.
- F) SEM photomicrograph of MCD. Subhedral dolomite crystals have variable amounts of intracrystal pores (arrows).
 Location: Pine Pint Formation, Pine Point diamond drill hole 2813, 530 ft. Scale bar 100 μm.
- G) Close up of F. Scale bar 100 µm.



textures are generally recognizable in MCD (Fig. 15A). Secondary dissolution vugs and fractures are locally developed in MCD dolostones (Fig. 15B) and are partially filled with minor amounts of late-stage saddle dolomite or anhydrite.

Microscopically, MCD is composed of anhedral to subhedral dolomite crystals (150- 250 μm, avg. 200 μm), with well defined crystal boundaries (Fig. 15D). No undulatory extinction was observed. Some MCD crystals have clear rims toward the pore centres (Figs. 15D and 15E), suggesting neomorphism of MCD by later diagenetic fluids. MCD appears red/orange under cathodoluminescence. Blotches of bright orange can be observed along crystal boundaries, suggesting neomorphism. Under SEM (Figs. 15F and 15G), MCD consists of anhedral-subhedral crystals with variable amounts of intra- and intercrystalline porosity, suggesting possible dissolution by later diagenetic fluids.

COARSE-CRYSTALLINE DOLOMITE (CCD)

CCD is either light brown or buff. The original sedimentary features, early diagenetic cements, and organic fabrics in CCD are mostly destroyed but locally preserved as relics (Figs. 16A and 16B). At CCD/limestone contacts, CCD clearly replaces the limestones, precluding the possibility that CCD is a neomorphic modification of earlier dolomites (Fig. 16C). CCD contains a large variety of vugs and fractures, ranging in size from a few millimetres to a few meters (Fig. 16B and 16D). These vugs host MVT deposits at Pine Point (Fig. 16E), and also create

- Figure 16. Hand sample and outcrop sample of coarse-crystalline dolomite (CCD) and saddle dolomite (SD).
 - A) Core sample of CCD with vuggy porosity.

 Location: Sulphur Point Formation, Pine Point drill hole 2813, 268 ft.

 Scale in inch (3.05 cm).
 - B) Core sample of CCD from subsurface Presqu'ile barrier, showing that well developed vugs in CCD are partially filled massive saddle dolomite (SD). The curved crystal surfaces, which are typical of saddle dolomite, can be observed on some saddle dolomite crystals.

 Location: Sulphur Point Formation, well B12, 6775 ft. Coin 1.5 cm.
 - C) Irregular contact between limestone (LS) and CCD. CCD clearly replaces limestone and has not reworked an earlier dolomite.

 Location: Sulphur Point Formation, pit M64, Pine Point. Hammer for scale.
 - Vugs and fractures in CCD are filled with saddle dolomite (SD) and late-stage calcite (C) forming a "zebra" texture.
 Location: Sulphur Point Formation, pit X53, Pine Point. Swiss knife for scale.
 - E) Vugs and breccias in ... CCD are filled with saddle dolomite (D) and marcasite (M). The lambda plution vug is about 50 cm across.

 Location: Sulphur Point attion, pit L37, Pine Point. Pen for scale.

excellent reservoir rocks for hydrocarbons in the subsurface of the NWT and northeastern British Columbia.

In thin section, CCD consist of subhedral to anhedral dolomite crystals, ranging from 500 µm to 2 mm (Figs. 17A and 17B). Under cross-polarized light, CCD exhibits undulatory extinction within a single CCD crystal. In partially dolomitized rocks, CCD replaces blocky sparry calcite cement and other earlier diagenetic products (Fig. 17C). Locally CCD precipitated along stylolites in limestones, indicating that CCD formed during or after stylolitization (Fig. 17D). Under the cathodoluminescence microscope, CCD exhibits a generally uniform, dull red luminescence. Under the scanning electron microscope, CCD appears as interlocking, anhedral crystal mosaics (Fig. 17E and 17F), and displays excellent intracrystalline microporosity, suggesting that dissolution probably occurred after this phase of dolomitization.

SADDLE DOLOMITE (SD)

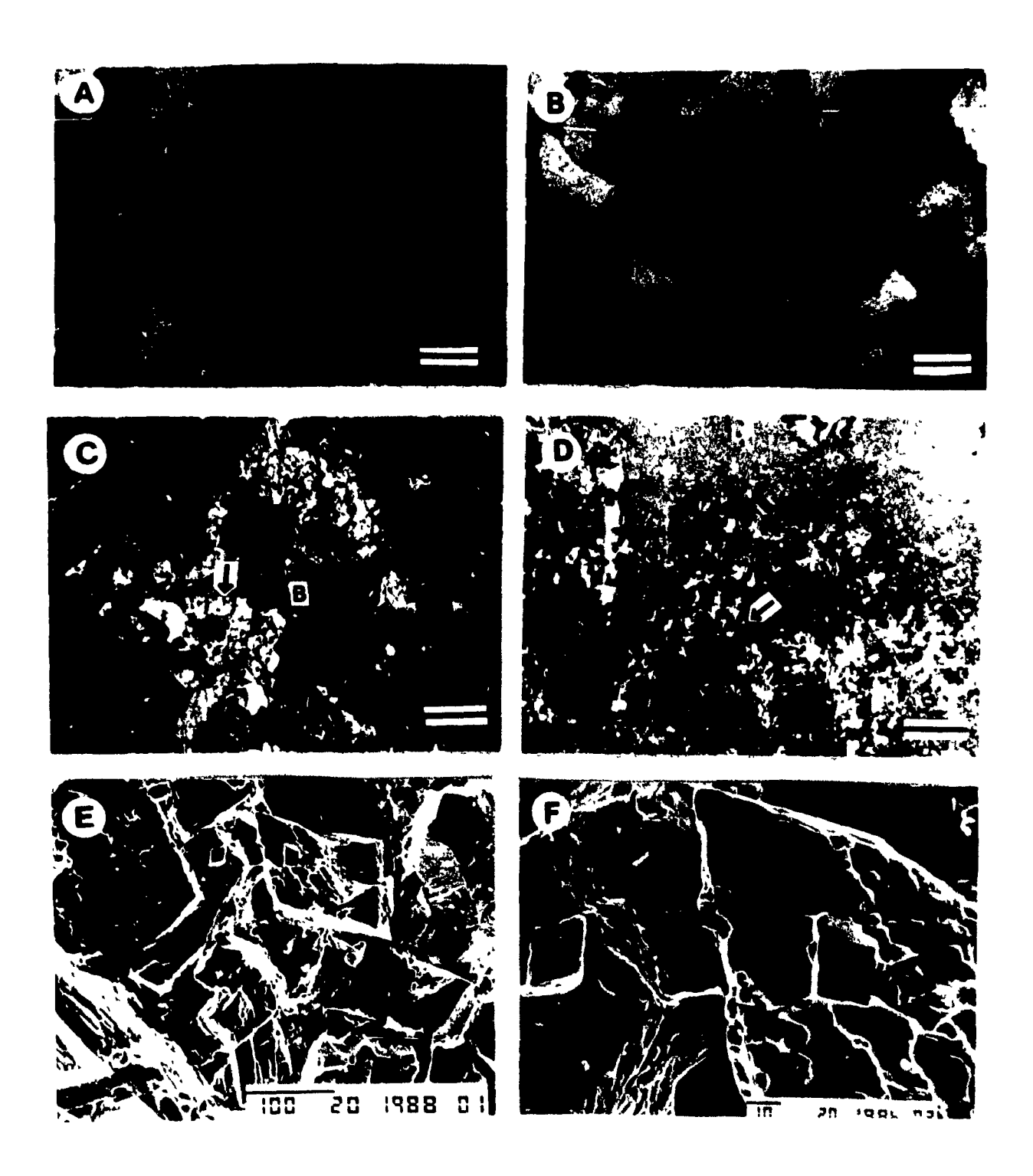
In hand specimens, SD has a distinctive white colour (Figs. 16B, 16D, and 16E), although pink and grey colours also occur locally. SD usually consist of coarse (millimetre-sized) dolomite crystals. The crystal shape ranges from rhombohedral, with slightly curved faces through increasing face curvature, to symmetrical saddle forms (Fig. 16B). SD occurs mainly as cement in vugs and fractures in CCD (Figs. 16B, 16D and 16E). Minor SD was also observed associated

Figure 17. Thin section and SEM photomicrography of CCD

- A) Thin section photograph of CCD. Anhedral dolomite crystals range from 500 μm to 2 mm.
 Location: Sulphur Point Formation, pit M64, Pine Point. Scale bar 500 μm
- B) View of A) under crossed nicols. CCD crystals exhibit undulatory extinction.
- C) Thin section photomicrograph showing blocky sparry calcite cement (B) was partially replaced by CCD crystals (arrow).

 Location: Sulphur Point Formation, pit M64, Pine Point. Scale bar 500 µm
- D) Thin section made from the cut in upper right corner of core sample in Figure 8E. Coarse crystalline-dolomite crystals precipitated along stylolites. Location: Sulphur Point Formation, well B07, 7211 ft. Scale bar 1 mm.
- E) SEM photograph of CCD. Anhedral/subhedral dolomite crystals have abundant intracrystalline micropores.

 Location: Sulphur Point Formation, pit N81, Pine Point. Scale 100 μm.
- F) A closer view of E). Scale 100 μm.



with FCD and MCD, as a thin rim lining vugs and fractures, postdating these dolomites. SD is usually associated with sulphide minerals at Pine Point (Figs. 10B and 10C). Some SD is pre-mineralization. Some SD is syn-mineralization because it alternates with sulphide minerals. Some SD postdates mineralization, filling vugs and fractures that cross cut the sulphide minerals (Figs. 10B and 10C). Therefore the timing of SD overlaps with mineralization at Pine Point.

Under cross-polarized light, SD crystals have a diagnostic sweeping extinction pattern (Figs. 18A and 18B). Under cathodoluminescence microscope, SD generally shows a uniform, dull red luminescence (Figs. 18C and 18D). Some SD has slightly deeper red cores and lighter red rims. One SD sample from BO6 from subsurface B.C. shows bright luminescence at the crystal terminations.

5.2.2 SPATIAL DISTRIBUTION OF DOLOMITES

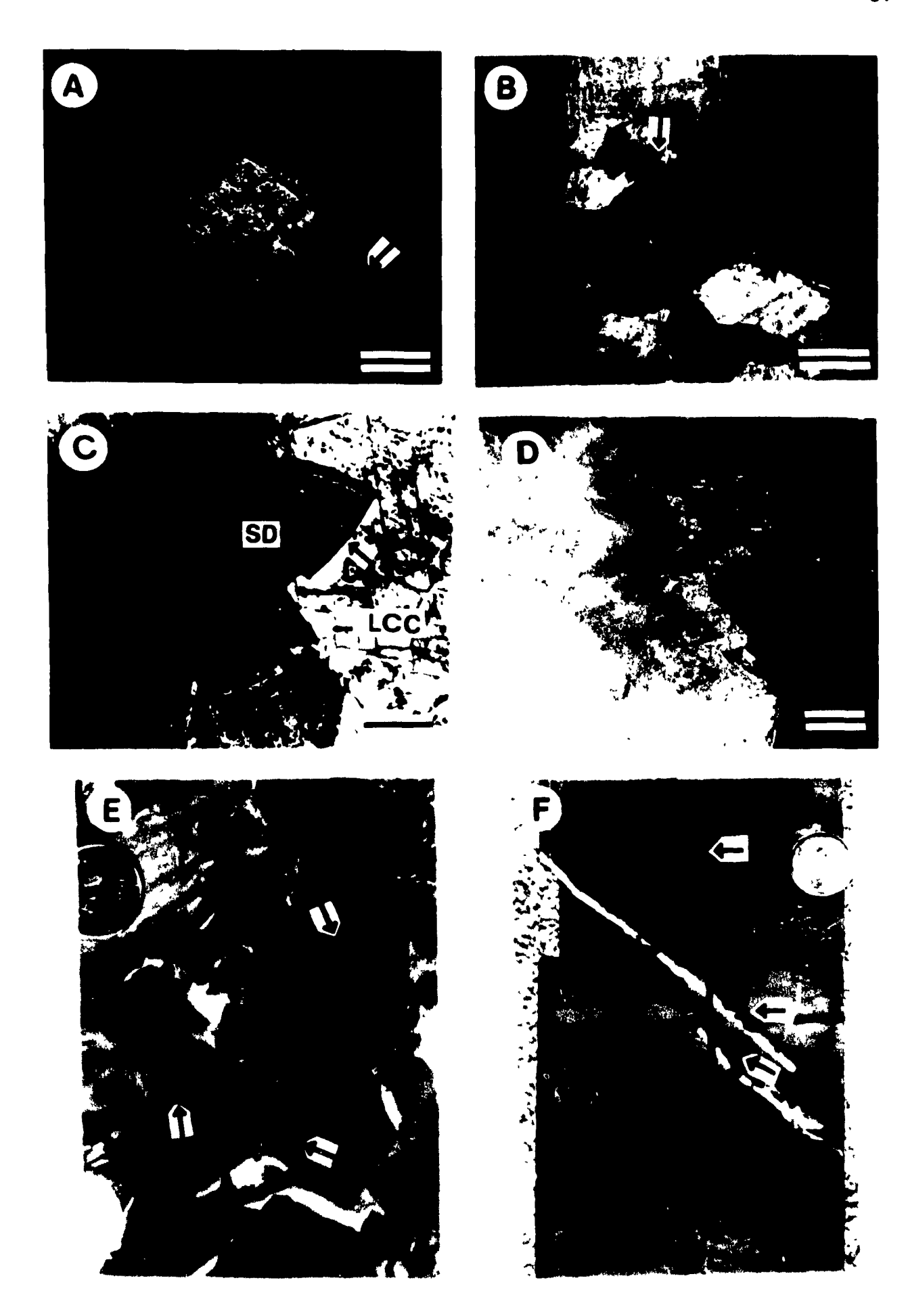
FCD is found only in the back-barrier facies on the south side of the Presqu'ile barrier in the Muskeg Formation (Fig. 6B). The Muskeg Formation consists of FCD interbedded with evaporitic anhydrite and extends from the Presqu'ile barrier into the Elk Point Basin to the south.

MCD is the most abundant dolomite type in the Pine Point Formation, which forms the lower part of the Presqu'ile barrier (Fig. 6B). However, at Pine Point MCD occurs only in the southern part of the Presqu'ile barrier, which is in direct contact with evaporitic anhydrite and FCD of the Muskeg Formation in the Elk Point

Figure 18. Petrographic features of saddle dolomite (SD).

- Thin section photomicrograph of saddle dolomite crystals with curved crystal boundary (arrow). Plane light. Location: Sulphur Point Formation, pit M64, Pine Point. Scale bar 500 µm.
- View of A) under crossed nicols, showing sweeping extinction (arrow). B)
- Thin section photomicrograph of saddle dolomite crystals (SD) with curved crystal boundary (arrow). Late-stage calcite (LCC) precipitated after saddle dolomite. Plane light.
 - Location: Sulphur Point Formation, pit X51, Pine Point. Scale bar 500 µm.
- D) View of C) under cathodoluminescence light. Saddle dolomite is uniform bright orange with occasional weak zonations. LCC (dark) is not luminescent.
- Breccia filled with white saddle dolomites. Some low amplitude stylolites (arrows) in different fragments have different orientations, indicating that brecciation occurred after the onset of stylolitization. Location: Sulphur Point Formation, NWT well K-48, 3076 ft. Coin 1.5 cm.
- Low amplitude horizontal stylolites cross cut by a vertical stylolite. Both horizontal and vertical stylolites were cross cut by oblique fractures that are filled with saddle dolomite, suggesting that saddle dolomite postdates both types of stylolites.

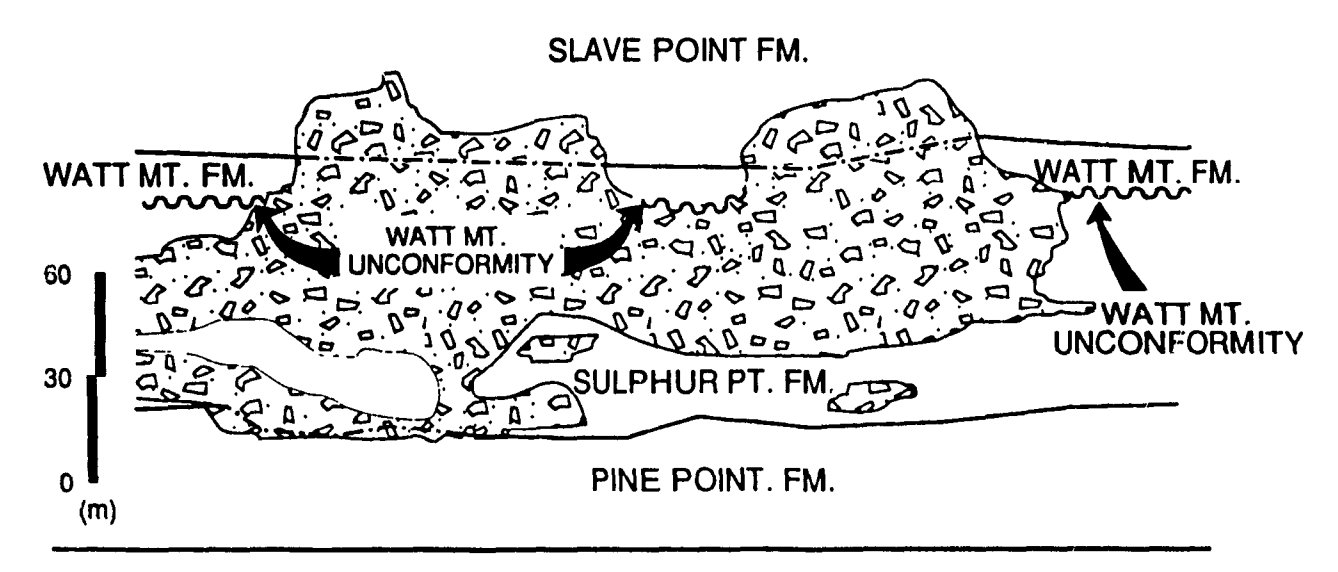
Location: Sulphur Point Formation, NWT well O-72, 5860 ft. Coin 1.5 cm.



Basin. The northern part of the barrier is preserved as limestones (Fig. 6B). In the Pine Point area, there are two layers of very porous sucrosic MCD. One is at the base of the Pine Point Formation, called the B Spongy Member by Rhodes et al. (1984), and the other occurs just below the coarse-crystalline dolomite. These porous sucrosic dolomites, however, have not been observed in cores from the subsurface west of the Pine Point property, perhaps due to poor well control and the few cored intervals in the region.

4

CCD, along with vug and fracture filling SD, is called Presqu'ile dolomite by some geologists. In the early mining days, Presqu'ile dolomite was thought to be a reefal development and was given formation status. It is now known to be a secondary dolomitization that cuts across formation boundaries (e.g. Rhodes et al. 1984). At Pine Point, Presqu'ile dolomite commonly occurs in the lower and middle parts of the Sulphur Point Formation, while variable amounts of the upper part of the Slave Point Formation are preserved as limestones (Fig. 6B). However, in the western part of the Pine Point property where the strata above the unconformity were preserved (e.g. N18, W85, and G03), Presqu'ile dolomite extends higher stratigraphically across the unconformity into the Watt Mountain and the lower part of the Slave Point formations (Figs. 19 and 20). Presqu'ile dolomite is also observed cross-cutting the unconformity in the subsurface of the NWT and NE B.C. (Fig. 21). In well O-72, Presqu'ile dolomite extends for about 45 m above the unconformity into the Slave Point Formation (Fig. 21). However in adjacent well F-48, the Sulphur Point Formation and the upper 90 m of Pine Point Formation are



Dissolution, dolomitization, and mineralization

Figure 19. Cross section of pit N81 (Pine Point), showing that dissolution, dolomitization, and mineralization occur continuously from the Sulphur Point Formation, across the sub-Watt Mountain unconformity, into the Watt Mountain and Slave Point Formations (Modified after Rhodes et al. 1984).

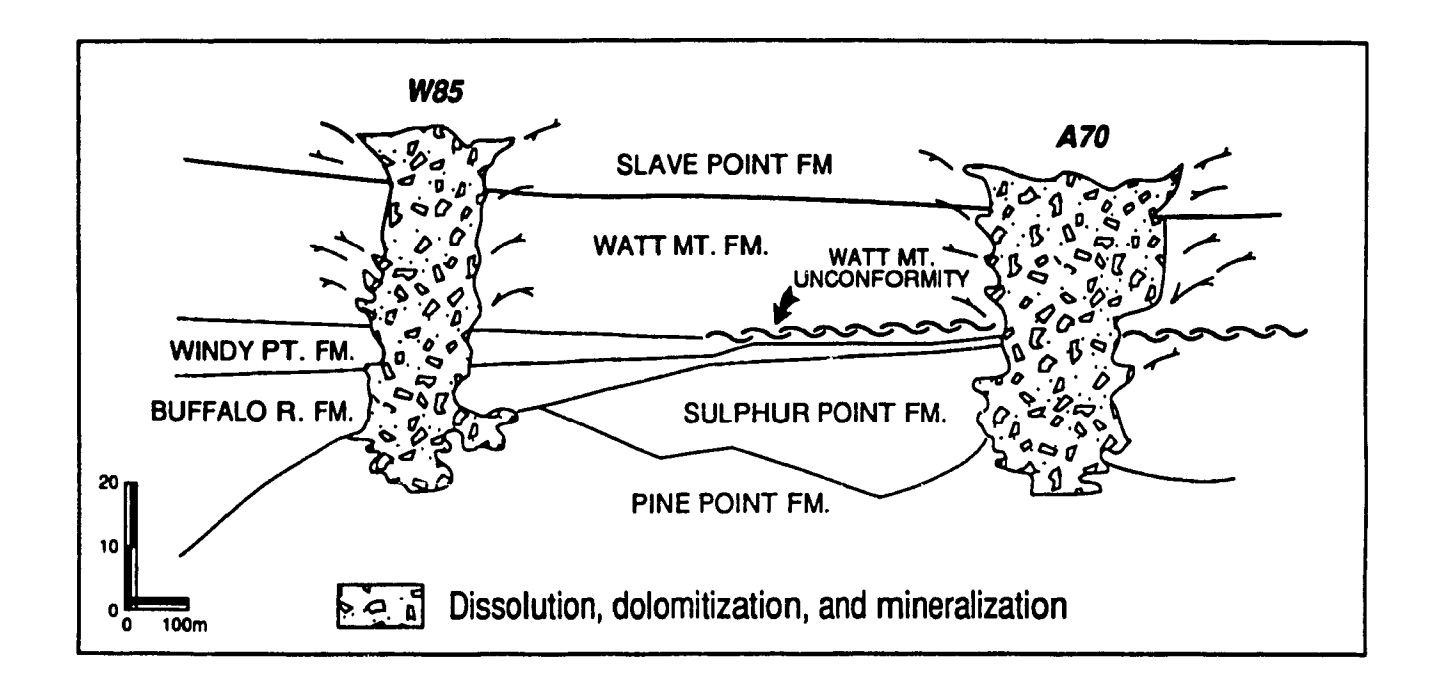


Figure 20. Cross section of pits W85 and A70 (Pine Point), showing that dolomitization and large-scale dissolution occur continuously across the sub-Watt Mountain unconformity (Modified after Rhodes et al. 1984).

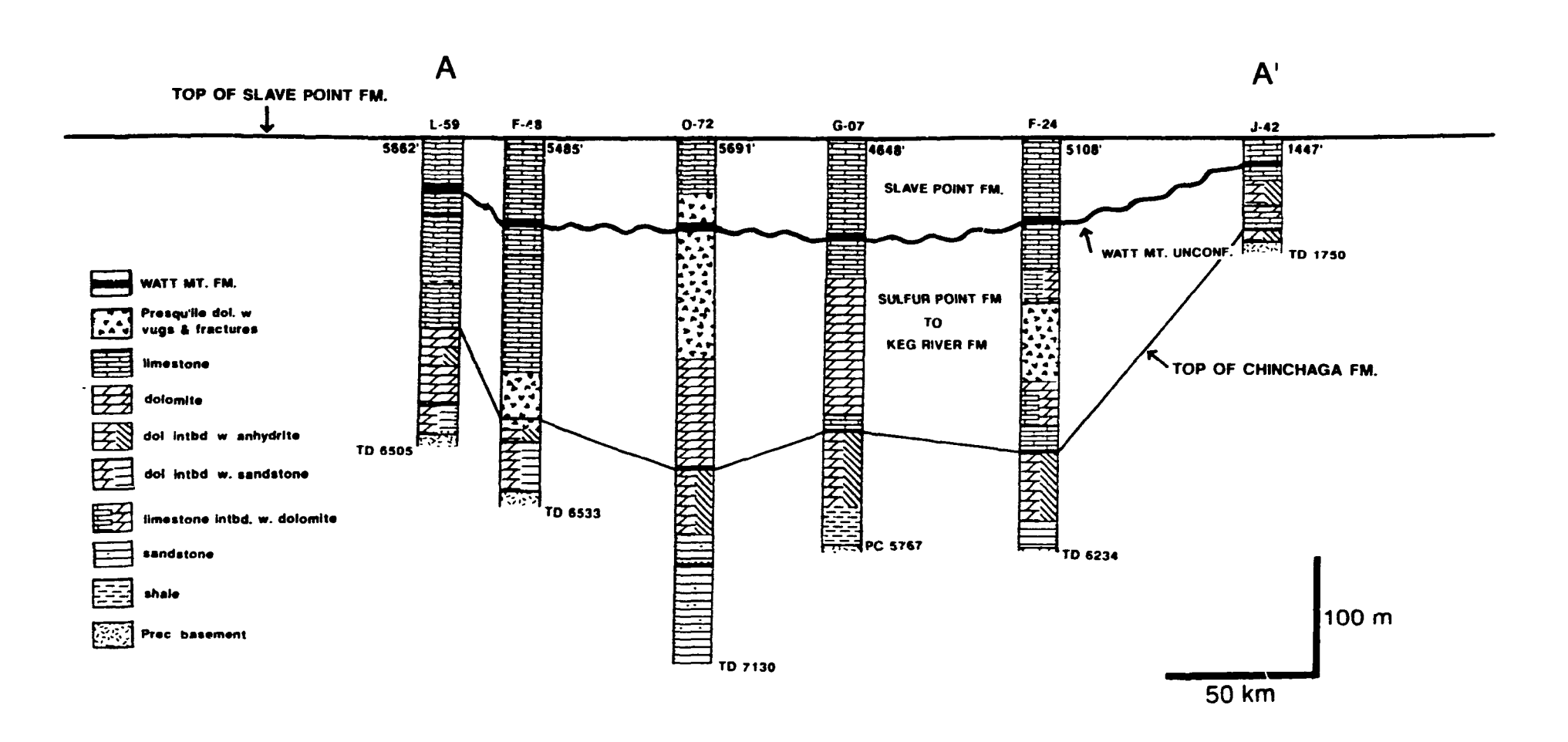


Figure 21. Cross section A-A' from subsurface Presqu'ile barrier from NWT (see Fig. 1 for location). The dolomitization is not directly related to the sub-Watt Mountain unconformity, and Presqu'ile dolomitization extends across the unconformity in well O-72.

limestones, and Presqu'ile dolomite occurs 120 m (between 1865 and 1887 m) below the unconformity (Fig. 21). Similarly in well F-24, tight limestones occur below the sub-Watt Mountain unconformity and Presqu'ile dolomite occurs 61 m below the unconformity (Fig. 21). Presqu'ile dolomite was also observed to occur above the unconformity in 6 other subsurface wells (in the NWT C-19, F-24, O-72, and D-50; in NE British Columbia, B-8 and B-12. Solid dots in Fig. 1).

5.3 OXYGEN AND CARBON ISOTOPES

Assuming bulk solution equilibrium, the δ^{18} O values of dolomites could be controlled by: the δ^{18} O values of dolomitizing fluids, the δ^{18} O values of limestone precursor, the water/rock ratio, and the temperature (Land 1980; 1983). Although the dolomite/water fractionation factor is poorly constrained, it is generally accepted that dolomite that precipitates in isotopic equilibrium with water should be about 2-4 ‰ heavier than coexisting calcites (Land 1980). During later diagenesis, the original δ^{18} O values may be modified and/or re-set.

In this study, different dolomites and calcite components from Pine Point and the adjacent subsurface of the NWT and northeastern British Columbia were systematically sampled and analyzed for oxygen and carbon isotopes (Appendix II).

5.3.1 RESULTS

CALCITE FOSSIL FRAGMENTS

Oxygen and carbon isotopes were measured on brachiopod, crinoid, and *Amphipora* fragments from the Presqu'ile barrier (Fig. 22). Two calcite brachiopod fragments from the Sulphur Point Formation have δ^{18} O values of -3.8 and -4.2 ‰ PDB. Their δ^{13} C values are similar, at 1.8 and 1.9 ‰ PDB, respectively. Three crinoid fragments were analyzed, with average δ^{18} O of -8.01 ‰ PDB and δ^{13} C of -0.17 ‰ PDB. Two *Amphipora* fragments were analyzed. One has a δ^{18} O value of -8.5 ‰ PDB and δ^{13} C value of -0.5 ‰ PDB. The other yields δ^{18} O of -10.7 ‰ PDB, and δ^{13} C of -2.3 ‰ PDB. The δ^{18} O values of brachiopod fragments are much heavier than crinoids and *Amphipora* fragments, suggesting that brachiopods tend to preserve the original oxygen and carbon isotope values better than crinoids and *Amphipora*.

DOLOMITES

FCD, MCD, CCD and SD contain progressively lighter δ^{18} O values (Fig. 23). Three FCD sampled from the Elk Point Basin yield δ^{18} O value of -1.6 to -3.8 % PDB. FCD sampled from the open pits around the orebodies, which is coarser (up to 100 μ m, A-FCD in Fig. 23), are more depleted in δ^{18} O, varying from -6.7 to -7.9

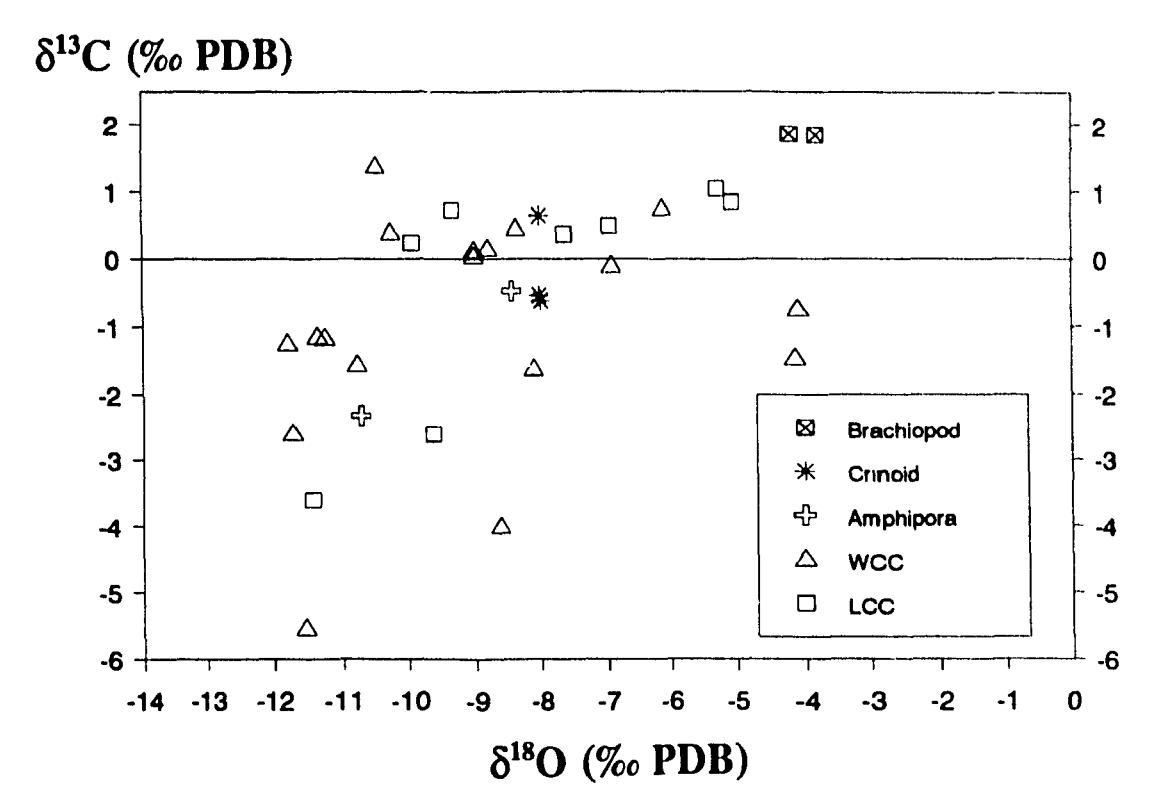


Figure 22. Cross plot of $\delta^{18}O$ and $\delta^{13}C$ for calcite fossil fragments, late-stage coarse-crystalline calcites (LCC), and white calcites (WCC).

Figure 23. Cross plot of $\delta^{18}O$ and $\delta^{13}C$ values for various types of dolomites and brachiopod fragments.

abbreviations:

FCD:

fine-crystalline dolomite

A-FCD:

fine-crystalline dolomite associated with mineralization;

MCD:

medium-crystalline dolomite;

CCD-PP:

coarse-crystalline dolomite from Pine Point;

CCD · SUB:

coarse-crystalline dolomite from the subsurface of the

NWT and northeastern B.C.;

SD-PP:

saddle dolomite from Pine Point;

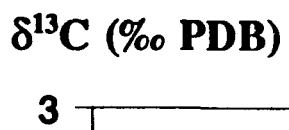
SD-SUB:

saddle dolomite from the subsurface of the NWT and

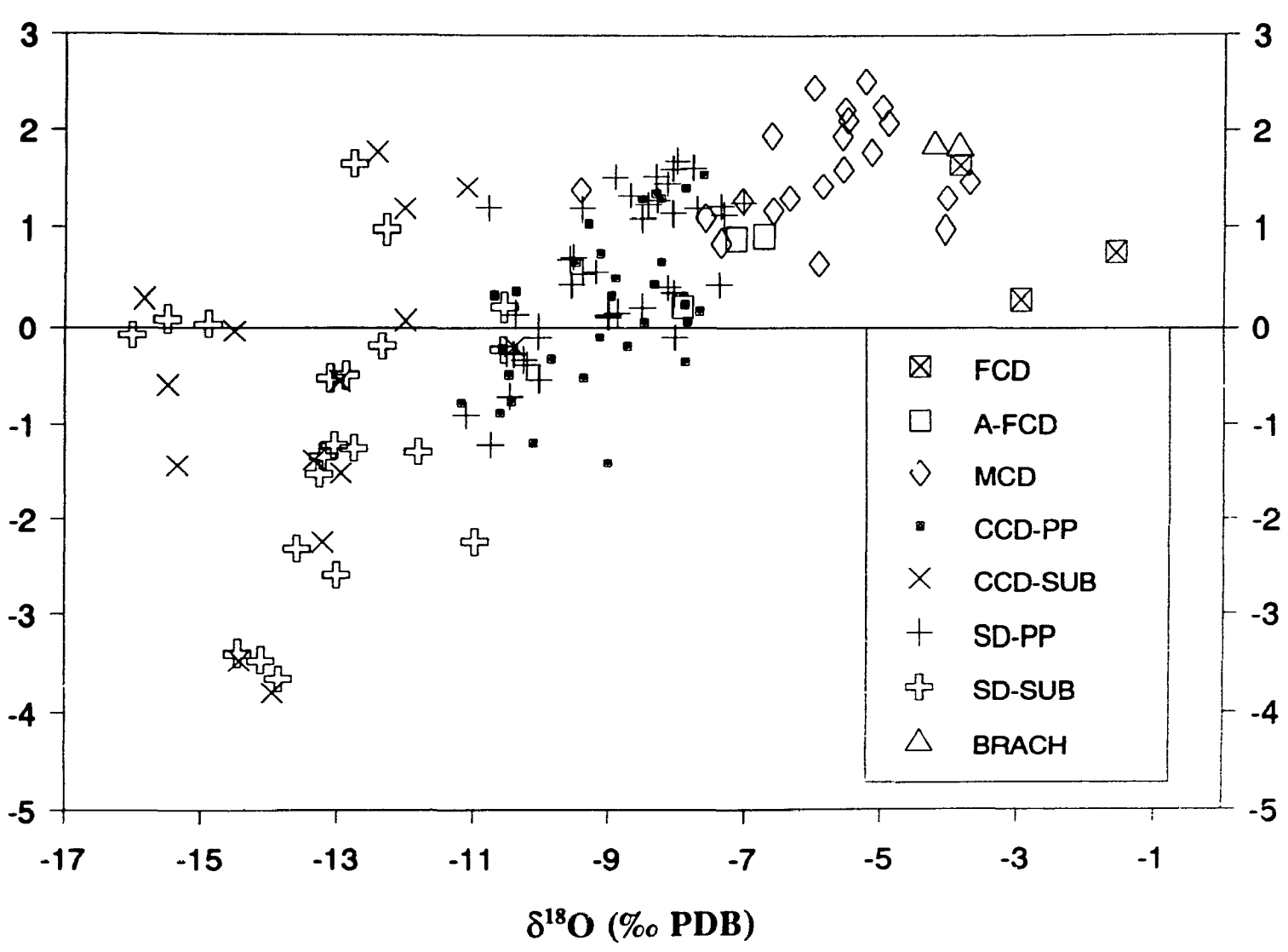
northeastern B.C.;

BRACH:

brachiopod.



j



% PDB.

Twenty-one MCD samples were analyzed for oxygen and carbon isotopes, with δ^{18} O values from -3.7 to -9.4 % PDB (avg. -5.9 % PDB) and δ^{13} C from 0.6 to 2.5 % PDB (avg. +1.6 % PDB).

Forty-five CCD and sixty-one SD samples were analyzed for oxygen and carbon isotopes. The δ^{18} O and δ^{13} C values of CCD and SD are similar, with δ^{18} O varying from -7.0 to -16.0 ‰ PDB, and δ^{13} C values from +1.7 to -3.8 ‰ PDB. The average δ^{18} O of CCD and SD from the Pine Point area are -9.1 and -9.0 ‰ PDB, respectively, which is distinctly heavier than CCD and SD from the subsurface Presqu'ile barrier, which are -13.3 and -13.1 ‰ PDB respectively.

WHITE CALCITE

Eighteen white calcite samples were analyzed for $\delta^{18}O$ and $\delta^{13}C$. White calcite has the most variable $\delta^{18}O$ and $\delta^{13}C$ values, with $\delta^{18}O$ ranging from -11.79 to -4.1 % PDB and $\delta^{13}C$ from -5.54 to 1.37 % PDB (Fig. 22).

LATE-STAGE COARSE-CRYSTALLINE CALCITE

Nine late-stage coarse-crystalline calcite crystal were analyzed. Similar to white calcite, late-stage calcite crystals have quite variable $\delta^{18}O$ and $\delta^{13}C$ values, with most of $\delta^{18}O$ falling between -11.4 and -5.3 ‰ PDB and $\delta^{13}C$ between -5.5 and

5.3.2 DISCUSSION

O ISOTOPE SIGNATURE OF MIDDLE DEVONIAN SEAWATER

It is important to estimate the initial marine calcite isotopic composition in order to determine the extent of liagenetic alteration. At present, two compatible yet different components, abiotic marine cements and brachiopods, are used to establish a marine calcite baseline for δ^{18} O and δ^{13} C (Meyers and Lohmann 1985; Given and Lohmann 1985; Popp *et al.* 1986; Veizer *et al.* 1986). The overall agreement of records of secular trends suggests that both may be employed to define patterns of δ^{18} O variation.

Because inorganically precipitated aragonite and high-Mg calcite marine cements are almost isotopically in equilibrium with ambient seawater, therefore physical and chemical information on ancient seawaters can be obtained from analysis of these marine cements (Gonzalez and Lohmann 1985). Unfortunately submarine cements sufficiently large for isotopic sampling have not been found in the cores and samples from the Presqu'ile barrier, therefore only brachiopods were used to establish a Middle Devonian marine calcite value in this study.

Brachiopod shells are composed of low-Mg calcite and the initial isotopic compositions are commonly well preserved, provided they are checked for

neomorphic changes under cathodoluminescence (Popp et al. 1986; Veizer et al. 1986). However, even then one must be careful as both δ^{18} O and δ^{13} C values of non-luminescent brachiopods could also be modified during diagenesis (Rush and Chafetz 1990). In the Presqu'ile barrier, brachiopods with shells sufficiently large for isotopic sampling are rare. Two brachiopod shell fragments from the Sulphur Point Formation have $\delta^{18}O$ -3.8 and -4.2 % PDB and $\delta^{13}C$ 1.8 and 1.9 % PDB. respectively (Fig. 22). These values are similar to the average δ^{18} O values (-3.7+0.2) % PDB) of nonluminescent portions of well preserved brachiopods in the Middle Devonian limestones from various places in North America (Popp et al. 1986). The δ^{18} O values of these brachiopod are also in general agreement with the δ^{18} O values of calcite submarine cements (-5.1 % PDB) from the Rainbow buildups in the Middle Devonian Keg River Formation in the Black Creek sub-basin south of the Presqu'ile barrier (Qing and Mountjoy 1989). Therefore, the δ^{18} O values of these brachiopods are probably close to the δ^{18} O values of primary marine calcites and have not been altered significantly from their original values during later diagenesis. They are used to estimate the δ^{18} O value of Middle Devonian seawater in the study area.

Taking an average δ^{18} O value of -4 ‰ PDB for Middle Devonian marine calcite, the δ^{18} O value of Middle Devonian seawater was calculated to be -2.0 ‰ SMOW, using a temperature of 25 °C and equations proposed by Friedman and O'Neil (1977):

$$10^3 \ln \alpha_{\text{calcite-fluid}} = 2.78 \times 10^6 \text{ T}^{-2}(^{\circ}\text{K}) - 2.89 \tag{1}$$

where:
$$\alpha_{\text{calcite-fluid}} = \frac{\delta^{18}O_{\text{calcite}} + 1000}{\delta^{18}O_{\text{fluid}} + 1000}$$

$$\delta_{\text{SMOW}} = 1.03086 \ \delta_{\text{PDB}} + 30.86$$
 (2)

The calculated δ^{18} O value of Middle Devonian seawater in the Pine Point area supports the earlier conclusions that Middle Devonian seawater was depleted in δ^{18} O by about 2-3 ‰ SMOW relative to modern seawater (Popp *et al.* 1986; Qing and Mountjoy 1989).

FINE-CRYSTALLINE DOLOMITE

Using -2 to -3 ‰ SMOW as the δ^{18} O values of Middle Devonian seawater, dolomite precipitated in bulk solution equilibrium with it at a temperature of 25 °C should have δ^{18} O values of between -1.2 and -2.2 ‰ PDB, using equations (2) and (3):

$$10^3 \ln \alpha_{\text{delernite-fluid}} = 3.2 \times 10^6 \text{ T}^2 (^{\circ}\text{K}) - 3.3$$
 (3) (Fritz & Smith 1970)

where:
$$\alpha_{dolomste-fluid} = \frac{\delta^{18}O_{dol} + 1000}{\delta^{18}O_{fluid} + 1000}$$

$$\delta_{\text{SMOW}} = 1.03086 \ \delta_{\text{PDB}} + 30.86$$
 (2)

The heaviest δ^{18} O of the unaltered FCD is -1.58 ‰ PDB, which falls within the range of Middle Devonian seawater dolomite, suggesting that the dolomitizing fluids for FCD were probably seawater. However. FCD sampled around orebodies at Pine Point are more depleted in δ^{18} O values (-6.7 to -7.9 ‰ PDB) and clearly have been modified by higher temperature diagenetic fluids during later stage mineralization and dolomitization. This is also reflected in the increase in crystal size (from 25 μ m to 100 μ m) of FCD that are close to the ore deposits.

MEDIUM-CRYSTALLINE DOLOMITE

The heaviest δ^{18} O value for MCD is -3.7 ‰ PDB, although δ^{18} O values for most MCD fall between -5 to -7.6 ‰ PDB. Taking the neaviest δ^{18} O value of -3.7 ‰ PDB as a possible original δ^{18} O signature of MCD and assuming that the temperature during dolomitization was 25 °C, the calculated δ^{18} O values of the dolomitizing fluids should be -5.5 ‰ SMOW, which is 2 to 3 ‰ SMOW lighter than the best estimated values for Middle Devonian seawater. Among others, this discrepancy can be explained in the following three ways:

1. The δ^{18} O values of MCD could have originated from compaction fluids of Middle Devonian seawater parentage during shallow to intermediate burial at slightly elevated temperatures. Such fluids would have δ^{18} O values similar to seawater, or slightly heavier, as a result of recrystallization of the rock matrix in the pore fluids of seawater parentage (Machel and Anderson, 1989).

Taking the most positive δ^{18} O value of -3.7 ‰ PDB as the possible original δ^{18} O signature of MCD and -2 ‰ SMOW as representative of Middle Devonian seawater, the temperature during formation of MCD would be about 39 °C, calculated using equations (2) and (3). This assumes that the measured δ^{18} O values for MCD are the original δ^{18} O signature and were not altered during later diagenesis.

2. If the dolomitizing fluids for MCD were Middle Devonian seawater, the initial δ^{18} O values for MCD must have been around -2.2 to -1.2 % PDB, or even heavier if dolomitizing fluids were evaporated Middle Devonian seawater (e.g. evaporatic brines in the Elk Point Basin). However, the depleted δ^{18} O values could have resulted from neomorphism of MCD at elevated temperatures during later diagenesis.

It has been suggested that dolomites can form as a Ca-rich, poorly ordered metastable phase, which would experience crystal enlargement and chemical modification during progressive stabilization (Lana 1985). Dolomites usually achieve their final chemical compositions and petrographic textures at elevated temperatures in the subsurface, which would obscure the initial chemical and petrographic properties to various degrees (Land 1985). As MCD is generally porous and permeable, it was probably neomorphosed in the later hydrothermal fluids which were responsible for CCD, SD, and mineralization (Qing and Mountjoy, 1990). Neomorphism of MCD is also suggested by the gradual depletion of δ^{18} O values for those samples that

occur closer to CCD and SD in vertical δ¹⁸O profiles. In Pine Point drill hole 2813 (Fig. 24), MCD has δ¹⁸O values of about -4 ‰ PDB for samples from about 100 m (300 ft) below the CCD/MCD boundary. The δ¹⁸O values of MCD decrease upward and reach -7 ‰ PDB close to CCD/MCD boundary, suggesting that MCD may have been modified by later diagenetic fluids that were responsible for CCD. A similar trend is also found in drill hole 2822 in the Pine Point area (Fig. 24)

- 3. The observed δ¹⁸O values could have resulted from influence of meteoric waters, which were about 4-6 ‰ SMOW lighter than Middle Devonian seawater, during sub-Watt Mountain exposure. This is unlikely because (see also Chapter 7 for details):
 - i) Meteoric-seawater mixing zones would have occurred on both the scuth and north flanks of the Presqu'ile barrier during the sub-Watt Mountain exposure. However, MCD is restricted to the lower southern part of the barrier (Fig 6B). The absence of MCD in the northern part of the barrier, suggests that MCD did not form in a meteoric-seawater mixing zone environment.
 - ii) The lack of vadose textures and meteoric cements in the Pine Point limestones suggests that the influence of meteoric waters during sub-Watt Mountain exposure was limited.
 - iii) In vertical profiles of δ^{13} C (Fig. 24), MCD has a consistent and narrow range of positive δ^{13} C values throughout the whole sequence of the

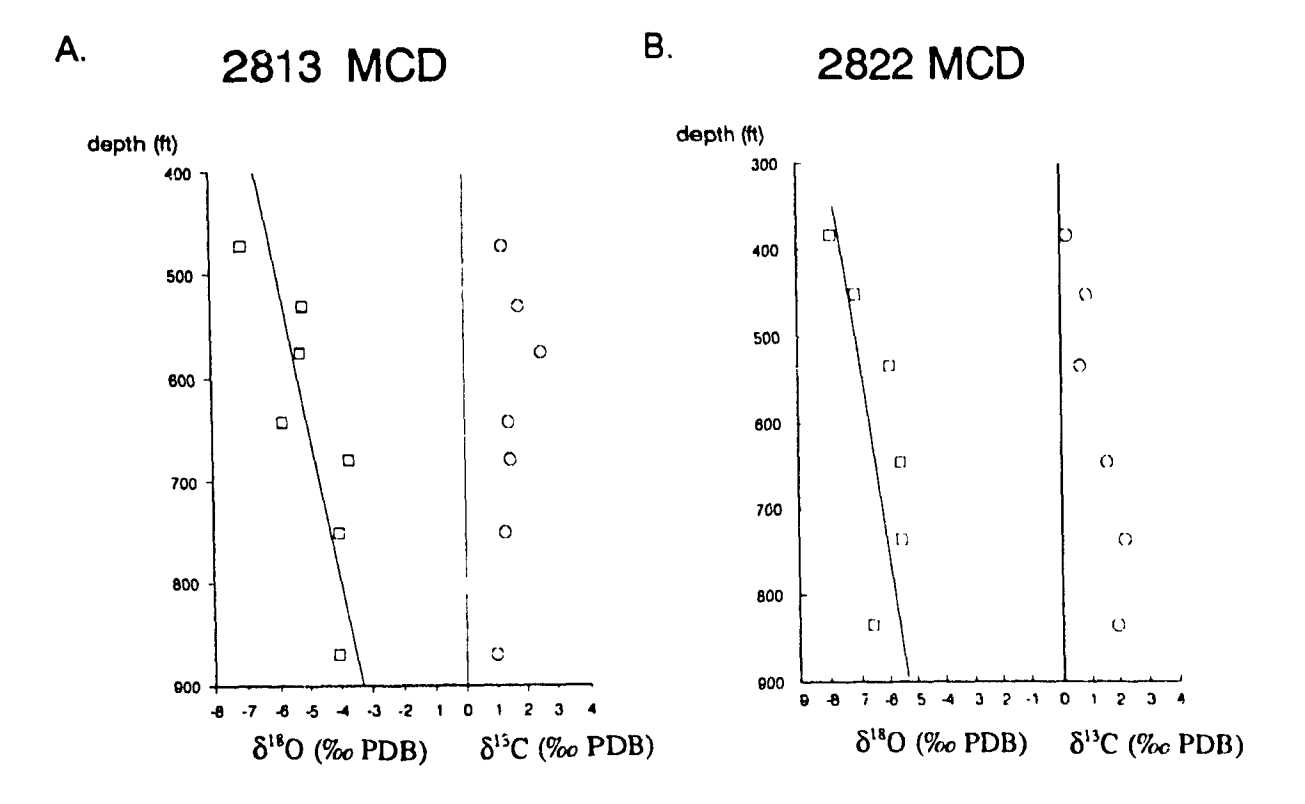


Figure 24. δ^{18} O and δ^{13} C profiles of MCD from drill holes 2813 and 2822 from Pine Point area.

MCD sampled closer to the CCD (top of the profile) have lighter $\delta^{18}O$ values, suggesting that MCD probably have been modified by later diagenetic fluids that precipitated CCD. The consistent positive $\delta^{13}C$ value suggests little influence of meteoric diagenesis associated with subaerial exposure.

buildups, suggesting that the influence of meteoric water during the formation of MCD was negligible. If carbonate sediments have undergone mineralogical stabilization in meteoric water associated with subaerial exposure, they generally have a wide range of δ^{13} C values due to incorporation of lighter carbon from the decomposition of organic matter or from the atmosphere, and progressive addition of heavier carbon from interaction with the carbonate host rock (Allan and Matthews 1982; Given and Lohmann 1986).

vi) The regional climate was arid during Middle Devonian (Schmidt et al. 1985; Walls and Burrowes 1985), and the barrier was probably in contact with hypersaline brines during exposure. Therefore, if there was any influence of fresh water on the barrier, it was probably minor.

Based on the spatial distribution of MCD, lack of meteoric diagenetic features, uniform positive δ^{13} C values, and paleoclimate during the Middle Devonian time, it seems unlikely that the formation of MCD in the Presqu'ile barrier was associated with meteoric waters during the sub-Watt Mountain exposure. MCD in the Presqu'ile barrier was, therefore, probably formed: 1) during shallow to intermediate burial at slightly elevated temperatures by fluids derived from compaction, and/or 2) soon after deposition of the Pine Point Formation by Middle Devonian seawater from the Elk Point Basin.

COARSE-CRYSTALLINE AND SADDLE DOLOMITES

As CCD and SD are closely associated with each other and have similar δ^{18} O and δ^{13} C values, they are discussed jointly in this section. Concerning their oxygen and carbon isotopes, several important features are:

- 1) CCD and SD are much more depleted in δ^{18} O than FCD and brachiopods that presumably have preserved Middle Devonian seawater signatures (Fig. 23). The δ^{18} O values of CCD and SD are also significantly more depleted than MCD (Fig. 23).
- 2) The δ¹⁸O values of Pine Point CCD and SD are heaviest, and gradually decrease from east to west along the Presqu'ile barrier (Figs. 25; 26; and Table 1).

Table 1. Variations of maximum burial depths and $\delta^{18}O$ values of coarse-crystalline and saddle dolomites in different parts of the Presqu'ile barrier.

	Pine Point	Tathlina L. (SUB1)	W. Tathlina L. NE B.C. (SUB2)
	East		West
max. burial depth based on strat. record	1.3-1.5 km	2-2.5 km	3-4 km
avg. δ ¹⁸ O of CCD	-9.1 ‰ PDB	-11.9 ‰ PDB	-13.9 ‰ PDB
avg. δ ¹⁸ O of SD	-9.0 ‰ PDB	-11.8 ‰ PDB	-13.5 ‰ PDB

SD and CCD from the Pine Point open pit and outcrops have δ^{18} O values from -7 to -11 ‰ PDB, averaging -9.0 and -9.1 ‰ PDB, respectively. In the

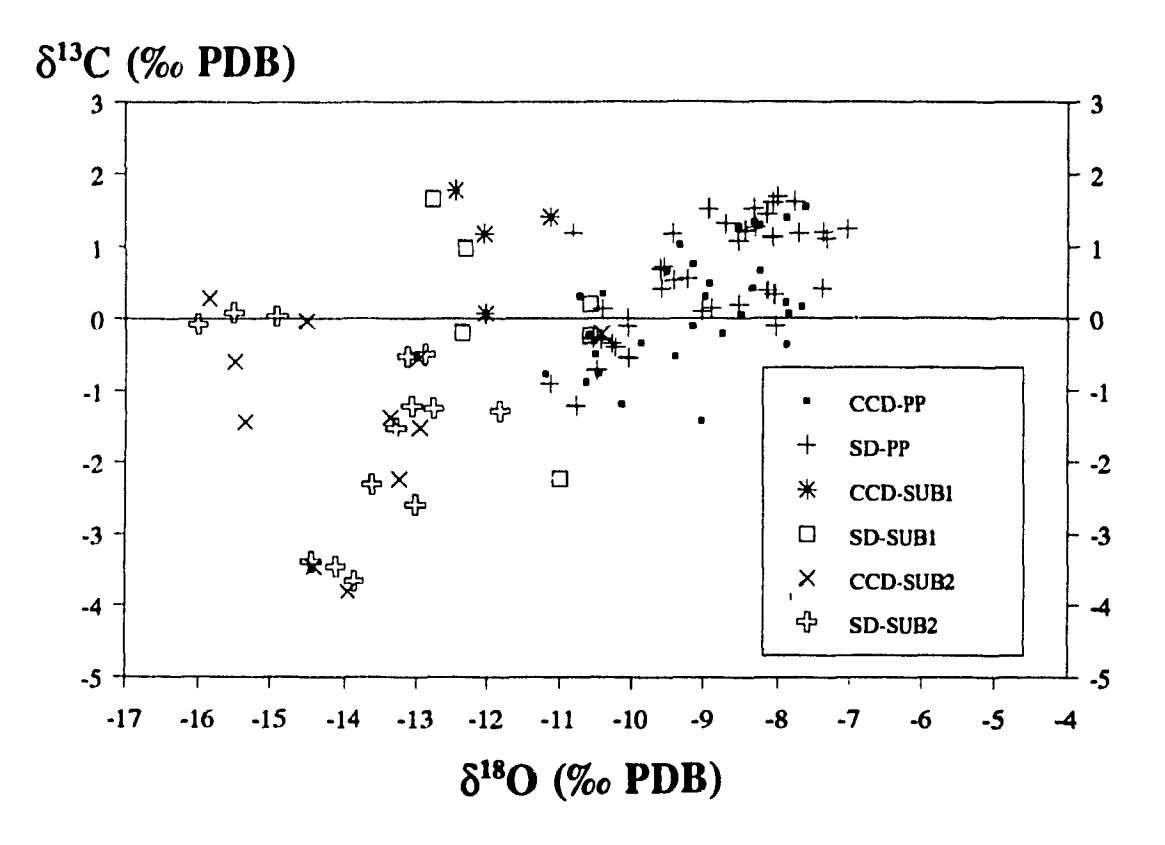


Figure 25. Cross plot of $\delta^{18}O$ and $\delta^{13}C$ values of CCD and SD from different localities. The $\delta^{18}O$ value of CCD and SD gradually decrease from the east (Pine Point area) to the west (northeastern British Columbia) with increasing present burial depths.

- 1) CCD-PP and SD-PP refer to CCD and SD samples from Pine Point area;
- 2) CCD-SUB-1 and SD-SUB-1 refer to CCD and SD samples from west of Pine Point to the Tathlina Lake area with present burial depths less than 1000 m;
- 3) CCD-SUB2 and SD-SUB2 refer to CCD and SD samples from west of Tathlina Lake and northeastern British Columbia with present burial depths from 1000 to 2500 m.

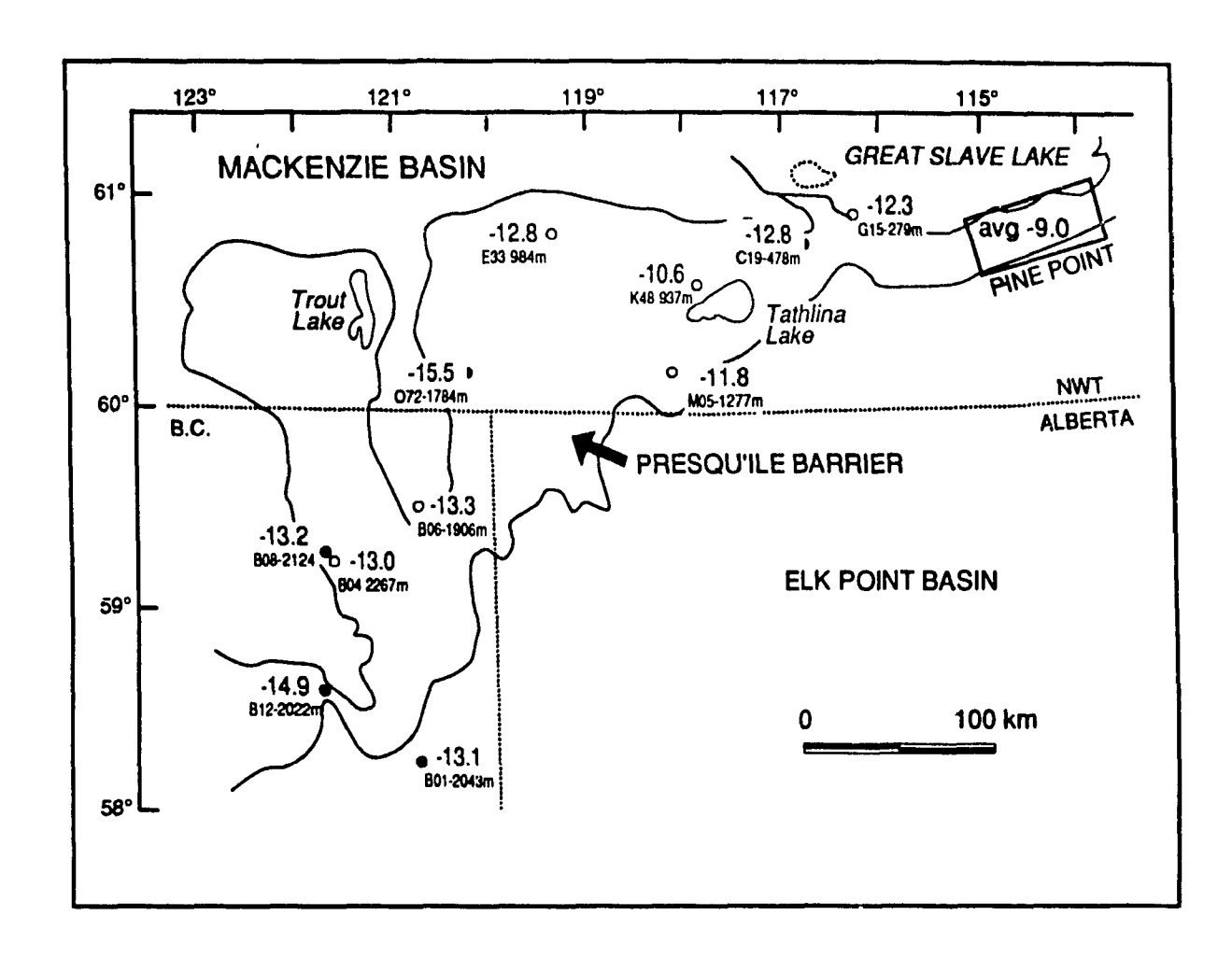


Figure 26. Variation of δ^{18} O values of saddle dolomites along the Presqu'ile barrier.

area west of Pine Point to the Tathlina Lake (SUB-1 in Fig. 25), δ^{18} O of SD and CCD varies from -11 to -13 ‰ PDB, averaging -12.2 and -11.9 ‰ PDB, respectively. Further west in the subsurface of the NWT and northeastern British Columbia (SUB-2 in Fig. 25), SD and CCD are most depleted in δ^{18} O, ranging from -13 to -16 ‰ PDB, averaging -13.5 and -13.9 ‰ PDB, respectively. The gradual depletion of δ^{18} O values of CCD and SD westward along the Presqu'ile barrier is mainly attributed to the higher temperatures at which they formed as indicated by fluid inclusion data (discussed later).

- CCD and SD have similar δ¹⁸O and δ¹³C values at the same locality (Fig. 25; Table 1), suggesting that both CCD and SD formed from dolomitizing fluids with similar δ¹⁸O values.
- 4) CCD and SD occur continuously above the sub-Watt Mountain unconformity in some places. These is no appreciable difference in the oxygen and carbon isotopes between dolomites above the unconformity and dolomites below it (Fig. 27), suggesting that CCD and SD, both above and below the unconformity, were of the same origin and formed at about the same time. Therefore CCD and SD must post-date the sub-Watt Mountain exposure and could not have formed in a meteoric-seawater mixing zone during sub-Watt Mountain exposure.
- 5) The δ¹³C values for CCD and SD are generally more negative than FCD and MCD. At Pine Point, the δ¹³C values for CCD and SD range from -1.6 to +1.6 ‰ PDB, which partially overlap with, but are slightly more depleted

δ¹³C (‰ PDB)

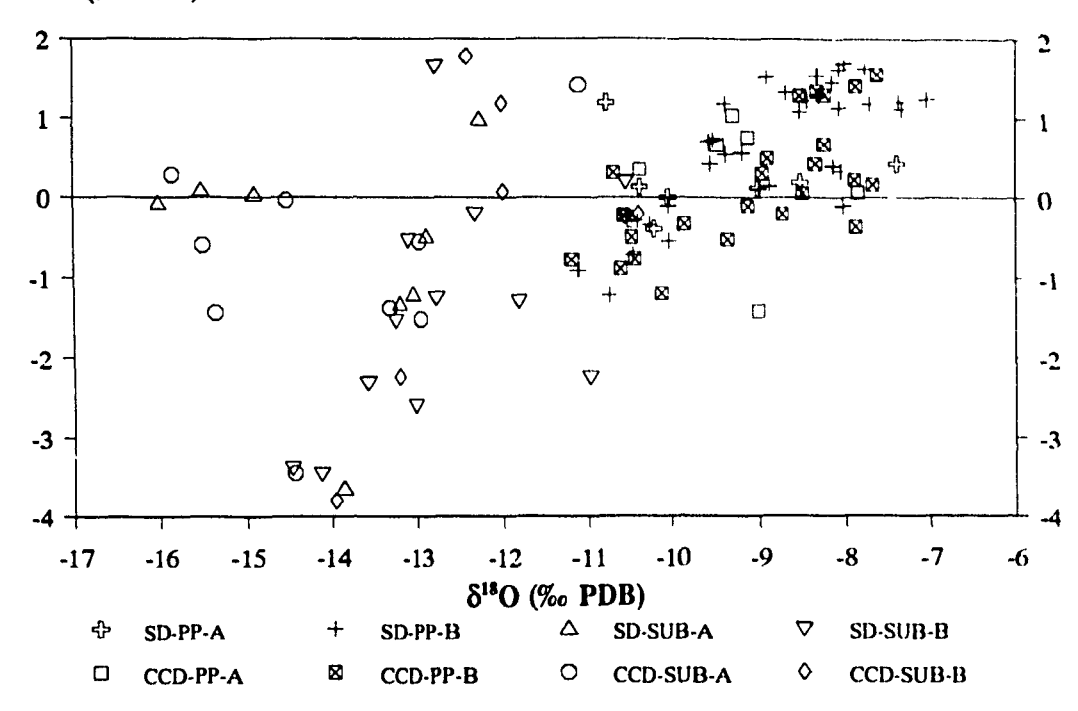


Figure 27. Comparison of δ^{18} O and δ^{13} C of CCD and SD above sub-Watt Mountain unconformity with those below it.

- 1) SD-PP-A: saddle dolomite above the unconformity, Pine Point area;
- 2) SD-PP-B: saddle dolomite below the unconformity, Pine Point area;
- 3) SD-SUB-A: saddle dolomite above the unconformity, subsurface of NWT and N.E. British Columbia;
- 4) SD-SUB-B: saddle dolomite above the unconformity, subsurface of NWT and N.E. British Columbia;
- 5) CCD-PP-A: coarse-crystalline dolomite above the unconformity, Pine Point area;
- 6) CCD-PP-B: coarse-crystalline dolomite below the unconformity, Pine Point area;
- 7) CCD-SUB-A: coarse-crystalline dolomite above the unconformity, subsurface of NWT and N.E. British Columbia;
- 8) CCD-SUB-B: coarse-crystalline dolomite below the unconformity, subsurface of NWT and N.E. British Columbia.

than, δ^{13} C of Middle Devonian seawater (+1 to +2 ‰ PDB). In the subsurface of the NWT and northeastern British Columbia, δ^{13} C values for SD and CCD vary from -3.7 to +0.3 ‰ PDB, which are from 1 to 5 ‰ PDB lighter than Middle Devonian seawater. One possibility for this slightly depleted δ^{13} C is that it reflects 12 C-enriched CO₂ generated by the oxidation of organic matter during hydrocarbon generation and/or thermochemical sulphate reduction (TSR).

The average δ^{13} C values of organic matter extracted from the adjacent Rainbow subbasin are -28 ‰ PDB (Clark and Philp 1989). Taking +2 ‰ PDB as representative of the inorganic carbon (e.g. the original limestone) and -28 % PDB as representative of organic carbon, for a dolomite with δ^{13} C value of -3.7 ‰ PDB (the most depleted ones from northeastern B.C.), approximately 19 % of the carbon would be derived from organic matter. The increasing δ^{13} C values of dolomites indicate less input from organic carbon. For example, for dolomites with δ^{13} C values ranging from -1.5 to +0.5 % PDB (as some CCD and SD from Pine Point area, Fig. 25), the required proportion of organic carbon in the dolomites would vary from 12 % to 5 % respectively. According to this calculation, the possible amounts of organic carbon added during formation of CCD and SD in the Presqu'ile barrier are relatively small, varying from a few percent to about 20 %. Thus, the dominant carbon input (more than 80 %) would be inorganic carbon generated through dissolution of Middle Devonian marine carbonates.

Late-stage coarse-crystalline and white calcites have similar ranges of oxygen and carbon isotopes (Fig. 22). The depleted δ^{18} O values of LCC and WCC relative to brachiopod fragments suggest that LCC nad WCC were precipitated from warm diagenetic fluids, as indicated by homogenization temperatures of fluid inclusions in LCC (discussed later). The δ^{13} C values of LCC and WCC are similar to those of CCD and SD. The slightly depleted δ^{13} C values indicate input of the light carbon possibly from alteration of organic matters during hydrocarbon generation and/or thermochemical sulphate reduction as discussed above.

5.4 Sr ISOTOPES

Analysis of marine carbonates indicates that the ⁸⁷Sr/⁸⁶Sr ratio of oceans has varied systematically throughout Phanerozoic time, but has apparently been constant in the open ocean at any given time (Fig. 28) (Burke *et al.* 1982). The time-dependent variation of ⁸⁷Sr/⁸⁶Sr ratio in the oceans results from changing proportions of Sr contributed to the oceans from different sources (Faure 1986). According to Faure (1986), the ⁸⁷Sr/⁸⁶Sr ratio of seawater is controlled by the mixing of Sr from three sources: (1) volcanic rocks, (2) sialic rocks of the continental crust, and (3) marine carbonate rocks. A: isotopic fractionation of Sr during carbonate precipitation is negligible, the Sr isotopic composition of marine carbonate minerals are assumed

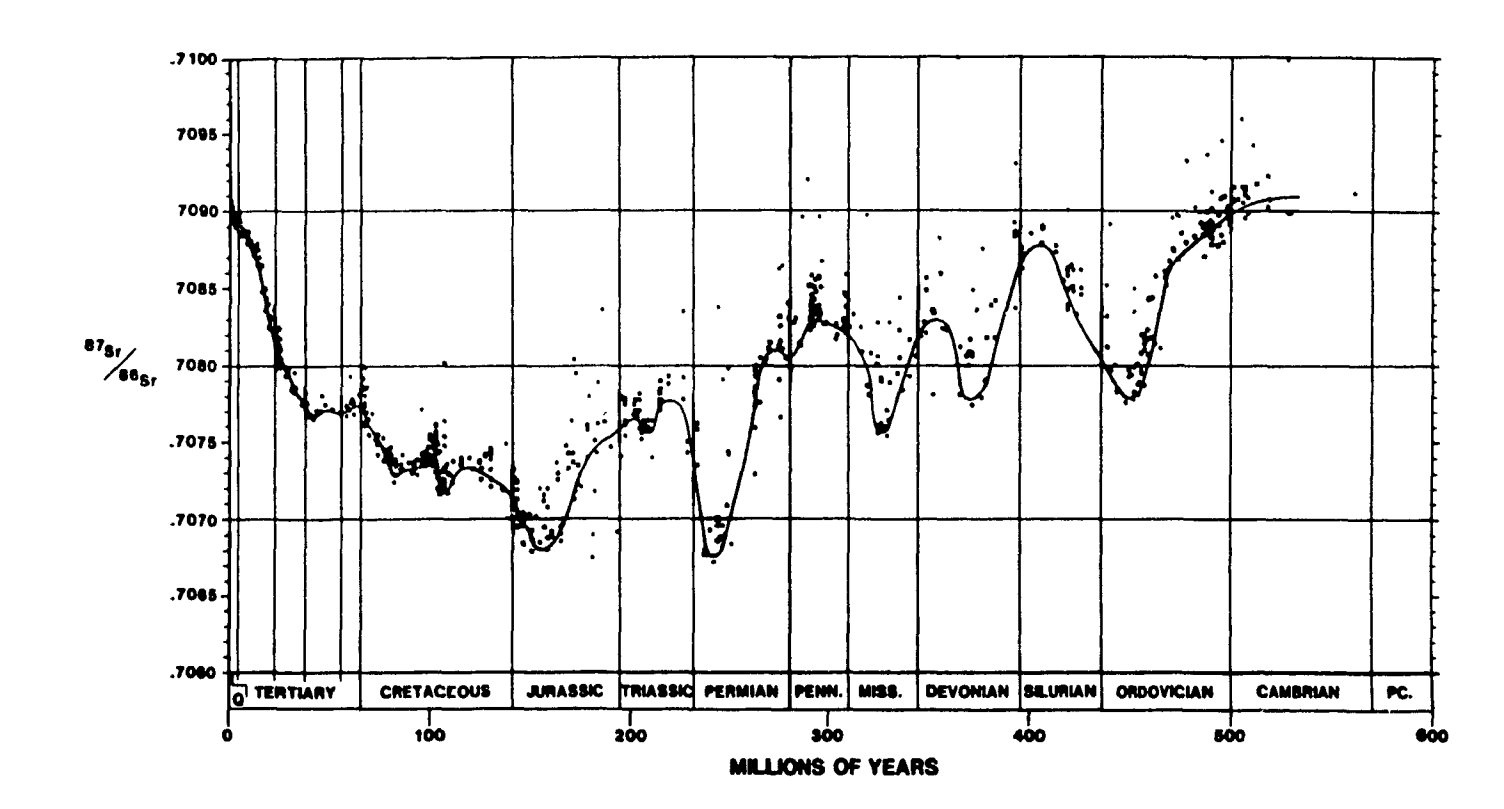


Figure 28. Variation of ⁸⁷Sr/⁸⁶Sr ratios through geological time (from Burk *et al.* 1982)

to be identical to those of seawater at the time of deposition (Veizer 1983). Therefore, unaltered Middle Devonian marine carbonate rocks should have a ⁸⁷Sr/⁸⁶Sr ratio similar to Middle Devonian seawater, which is estimated to be between 0.7078 and 0.7081 (Burke *et al.* 1982). This estimate is used below to determine post-depositional diagenetic changes.

50 samples were analyzed for Sr isotopes in this study (Fig. 29 and Appendix 2). The data presented in this section have been submitted in a manuscript entitled "Sr isotopic composition of Devonian dolomites, Western Canada: significance regarding source of dolomitizing fluids" (Mountjoy et al. in press).

5.4.1 RESULTS

Three FCD yield ⁸⁷Sr/⁸⁶Sr ratios of 0.7079 to 0.7081 (Fig. 29A). These FCD were sampled from subsurface petroleum exploration wells in the Elk Point Basin 5 km south of the Presqu'ile barrier. One sample of primary anhydrite associated with these FCD has a ⁸⁷Sr/⁸⁶Sr ratio of 0.7078. Two FCD sampled in the open pits of the Pine Point Mine have slightly higher ⁸⁷Sr/⁸⁶Sr ratios (0.7082 and 0.7083).

Three MCD analyzed for Sr isotope have ⁸⁷Sr/⁸⁶Sr ratios from 0.7081 to 0.7087 (Fig. 29B). The average ⁸⁷Sr/⁸⁶Sr ratio of MCD (0.7084) is close to, but slightly higher than Middle Devonian seawater.

Five Pine Point CCD samples yield ⁸⁷Sr/⁸⁶Sr ratios from 0.7082 to 0.7088 (avg. 0.7085), slightly more radiogenic than Middle Devonian seawater (Fig. 29C).

Figure 29. ⁸⁷Sr/⁸⁶Sr ratios of dolomites associated with the Presqu'ile barrier. The best estimated ⁸⁷Sr/⁸⁶Sr ratio of Middle Devonian seawaters, according to Burke *et al.* (1982), ranges from 0.7079 to 0.7081.

A) FCD: fine-crystalline dolomite;

A-FCD: fine-crystalline dolomite associated with mineralization;

B) MCD: medium-crystalline dolomite;

C) CCD-PP: coarse-crystalline dolomite, Pine Point area;

CCD-SUB2: coarse-crystalline dolomite, west of Tathlina Lake and

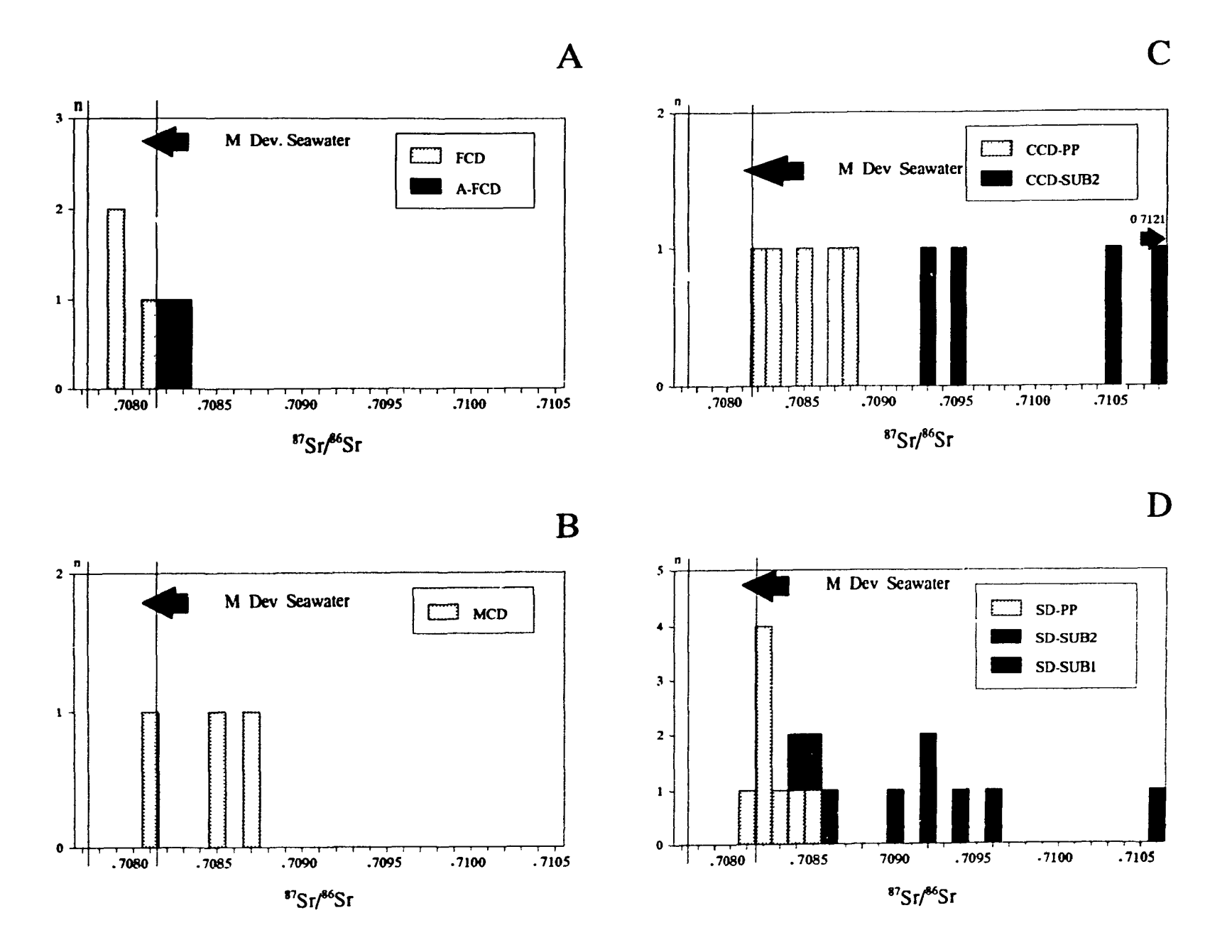
N.E. British Columbia;

D) SD-PP: saddle dolomite, Pine Point area;

SD-SUB1: saddle dolomite, west of Pine Point to Tathlina Lake.

SD-SUB2: saddle dolomite, west of Tathlina Lake and N.E.

British Columbia;



; \$

Four CCD samples from the deeper subsurface have ⁸⁷Sr/⁸⁶Sr ratios from 0.7093 to 0.7121 (avg. 0.7104), much more radiogenic than Middle Devonian seawater (SUB-2 in Fig. 29C).

-

1

The ⁸⁷Sr/⁸⁶Sr ratios of SD are similar to those of CCD (Fig. 29D). Eight Pine Point SD samples yield ⁸⁷Sr/⁸⁶Sr ratios from 0.7081 to 0.7085 (avg. 0.7083), slightly more radiogenic than Middle Devonian seawater (Fig. 29D). In the area west of Pine Point to the Tathlina Lake, the ⁸⁷Sr/⁸⁶Sr ratios of 3 SD samples vary from 0.7084 to 0.7086 (avg. 0.7085) (SD-SUB1 in Fig. 29D). West of the Tathlina Lake to northeastern B.C., six SD samples have ⁸⁷Sr/⁸⁶Sr ratios from 0.7090 to 0.7106 (avg. 0.7095), and are much more radiogenic than Middle Devonian seawater (SUB-2 in Fig. 29D).

Four late-stage coarse-crystalline calcite (LCC) samples yield ⁸⁷Sr/⁸⁶Sr ratios from 0.7105 to 0.7161 (avg. 0.7135) (Fig. 30), similar to the LCC analyzed by Medford *et al.* (1984). The ⁸⁷Sr/⁸⁶Sr ratios for seven white calcite samples are also very radiogenic, ranging from 0.7128 to 0.7147 (avg. 0.7131) (Fig. 30), except for one sample 0.7085.

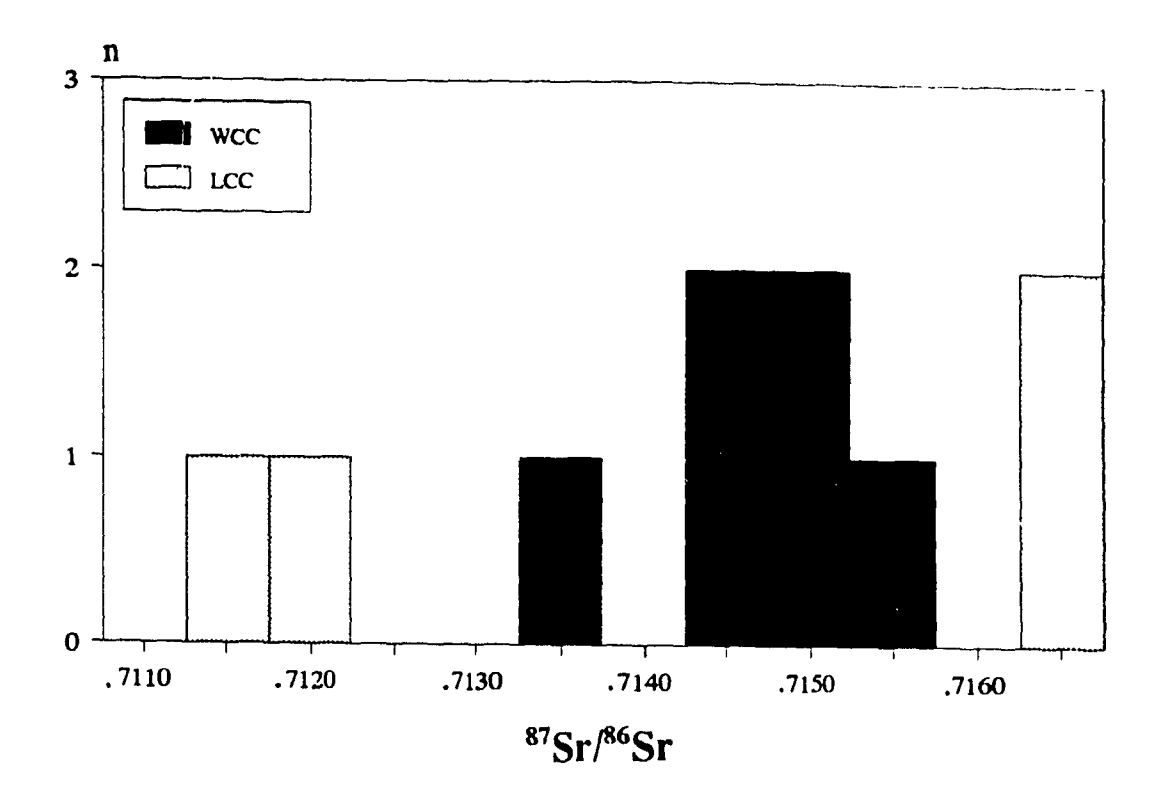


Figure 30. 87Sr/66Sr ratios of late-stage coarse-crystalline calcite (LCC) and white calcite (WCC).

5.4.2 DISCUSSION

FINE-CRYSTALLINE DOLOMITE

The Sr isotopes values of FCD (0.7079-0.7080) are within the range of the best estimated ⁸⁷Sr/⁸⁶Sr ratio of Middle Devonian seawater (0.7078 to 0.7081, see Burke *et al.* 1982). This strongly supports the interpretation that the dolomitizing fluids for FCD were Middle Devonian seawater, and that the original Sr isotope signature, similar to their oxygen isotopes, was not significantly affected by later diagenesis. These values are comparable with the ⁸⁷Sr/⁸⁶Sr ratio (0.7080) of coeval dolomites of the Middle Devonian Winnipegosis reef complexes of Dawson Bay, Manitoba, which were interpreted to be dolomitized by fluids of Middle Devonian seawater parentage (Teare 1990; Mountjoy *et al.* in press). The slightly higher ⁸⁷Sr/⁸⁶Sr ratios of FCD from the Pine Point open pits suggest that their original ⁸⁷Sr/⁸⁶Sr signature was probably partially modified by later diagenetic fluids.

MEDIUM-CRYSTALLINE DOLOMITE

The ⁸⁷Sr/⁸⁶Sr ratios of MCD are close to, but slightly higher than, Middle Devonian seawater. Two possible interpretations are:

1) The ⁸⁷Sr/⁸⁶Sr ratios of dolomitizing fluids for MCD were slightly higher than that of Middle Devonian seawater. The initial ⁸⁷Sr/⁸⁶Sr signature of MCD was

- not altered during later diagenesis.
- 2) The dolomitizing fluids had a ⁸⁷Sr/⁸⁶Sr ratio similar to that of Middle Devonian seawater, but their original Sr isotope signature was increased slightly during later diagenesis.

The second interpretation is preferred, because one of three samples has a ⁸⁷Sr/⁸⁶Sr ratio (0.7081) similar to the estimated Middle Devonian seawater. The other two more radiogenic samples were probably modified by later diagenetic fluids with slightly radiogenic ⁸⁷Sr/⁸⁶Sr ratios as indicated by clear rims at the crystal edges.

COARSE-CRYSTALLINE AND SADDLE DOLOMITE

The ⁸⁷Sr/⁶⁶Sr ratios of SD and CCD are similar, increasing gradually and consistently from east to west along the Presqu'ile barrier (Table 2; Fig. 31).

Table 2. Variation of maximum burial depth and average ⁸⁷Sr/⁸⁶Sr ratio of coarse-crystalline and saddle dolomites in different parts of the Presqu'ile barrier.

	Pine Point	Tathlina L. (SUB1)	W. Tathlina L. NE B.C. (SUB2)
	East		West
max. burial depth based on strat. record	1.3-1.5 km	2-2.5 km	3.5-4 km
avg. 87Sr/86Sr ratio of CCD	0.7085		0.7104
avg. 87Sr/86Sr ratio of SD	0.7083	0.7085	0.7097

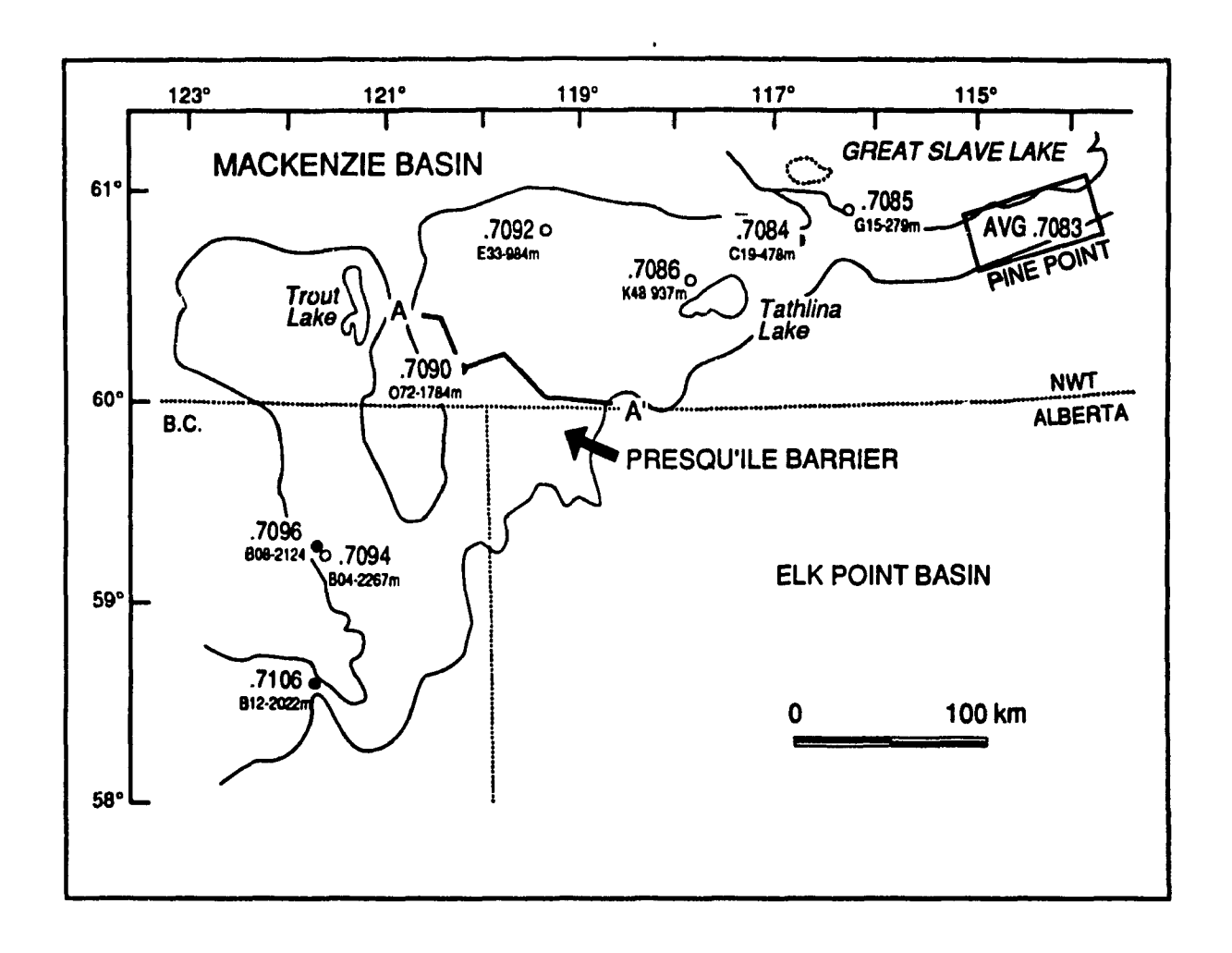


Figure 31. Variation of ⁸⁷Sr/⁸⁶Sr ratios of saddlo dolomite along the Presqu'ile barrier.

CCD from Pine Point open pit and outcrops have the lowest ⁸⁷Sr/⁸⁶Sr ratios, averaging 0.7085. However CCD samples from NWT west of the Tathlina Lake and northeastern B.C. are very radiogenic, averaging 0.7104.

The ⁸⁷Sr/⁸⁶Sr ratios of saddle dolomites from Pine Point are only slightly more radiogenic than Middle Devonian seawater, averaging 0.7083 (Fig. 31). In the area west of Pine Point to the Tathlina Lake, the ⁸⁷Sr/⁸⁶Sr of SD are slightly more radiogenic, averaging 0.7085 (Fig. 31). In the NWT west of the Tathlina Lake, the ⁸⁷Sr/⁸⁶Sr ratios of SD vary from 0.7090 to 0.7092, which are much more radiogenic than Middle Devonian seawater (Fig. 31). Further west in the northeastern British Columbia, the ⁸⁷Sr/⁸⁶Sr ratios are the most radiogenic, ranging from 0.7094 to 0.7106. One SD from the Rainbow F buildup southeast of Presqu'ile barrier yields a ⁸⁷Sr/⁸⁶Sr ratio of 0.7099, similar to the deeper subsurface saddle dolomites from the Presqu'ile barrier.

The gradual increase in ⁸⁷Sr/⁸⁶Sr ratios of CCD and SD (Figs. 29C; 29D; 31) from east to west along the Presqu'ile barrier suggest that the sources of the radiogenic Sr probably came from the deeper subsurface to the west. Presumably these fluids became less and less radiogenic as they moved from west to east updip along the Presqu'ile barrier.

Alternatively, the less radiogenic CCD and SD in the Pine Point area may indicate that the dolomitizing fluids in the Pine Point area have reworked the surrounding Middle Devonian limestones and dolomites. Therefore, more Sr isotope analyses of carbonates in the area adjacent to Pine Point would help to provide an

The Presqu'ile dolomite was interpreted by Morrow et al. (1986; 1990) and Aulstead et al. (1988) to connect 100 km to the north with the Manetoe dolomite (or facies), a diagenetic dolomite that developed in the Lower and Middle Devonian carbonates of the Mackenzie shelf in the southern Yukon and NWT. The ⁸⁷Sr/⁸⁶Sr ratios of seven saddle dolomites range from 0.7094 to 0.7128, and for three replacement dolomites, from 0.7091 to 0.7092 (Morrow et al. 1990), which are much more radiogenic than CCD and SD from the Pine Point area but are similar to CCD and SD from the subsurface NWT and northeastern British Columbia. The radiogenic Sr isotopes were attributed to the circulation of dolomitizing fluids through the underlying basement and clastic rocks (Aulstead et al. 1988; Morrow et al. 1990).

The Sr isotopes of replacement dolomite from the Nisku Formation (0.7089-0.7107 avg. 0.7092) and the Middle-Upper Devonian Swan Hills Formation (0.7082-0.7104) were more radiogenic than Devonian seawater (Machel and Anderson 1990; Kaufman et al. 1990). The Nisku dolomite was interpreted to have been dolomitized by fluids that had acquired radiogenic Sr through interaction with clastics before or during dolomitization (Machel and Anderson 1989). Replacement dolomites from the Swan Hills Formation, however, were suggested to have formed during shallow burial with a Sr isotopic signature similar to Devonian scawater, but were later neomorphosed in ⁸⁷Sr enriched fluids during deep burial (Kaufman et al. 1990).

LATE-STAGE COARSE-CRYSTALLINE CALCITE AND WHITE CALCITE

The ⁸⁷Sr/⁸⁶Sr ratios of LCC and WCC are similar, representing the most radiogenic carbonate phase precipitated in the Presqu'ile barrier (Fig. 30). The similar ⁸⁷Sr/⁸⁶Sr ratios of LCC and WCC, together with petrographic evidence, suggest that LCC and WCC were probably precipitated from similar fluids. LCC represents calcite directly precipitated from diagenetic fluids, whereas WCC represents calcitized saddle dolomite. The Sr isotopic signatures of WCC are similar to radiogenic SD (avg. 0.7110) analyzed by Medford *et al.* (1984). As WCC looks similar to SD in hand samples, possibly some of the radiogenic saddle dolomites analyzed by Medford *et al.* were contaminated with WCC, or possibly were dedolomitized.

5.4.3 SOURCES OF RADIOGENIC Sr

A cross plot of 87 Sr/ 86 Sr ratios and 518 O values of various types of dolomites associated with the Presqu'ile barrier (Fig. 32) reveals a trend of gradual increase in 87 Sr/ 86 Sr ratios coupled with a decrease in 518 O values in these dolomites. Unaltered FCD has the lowest 87 Sr/ 86 Sr (0.7079) and the heaviest 518 O (-1.6 to -3.8 % PDB). Both strontium and oxygen isotopes of FCD are close to the estimated Middle Devonian seawater values, suggesting that the dolomitizing fluids were Middle Devonian seawaters. MCD has slightly higher 87 Sr/ 86 Sr ratios (0.7081 to 0.7087) and

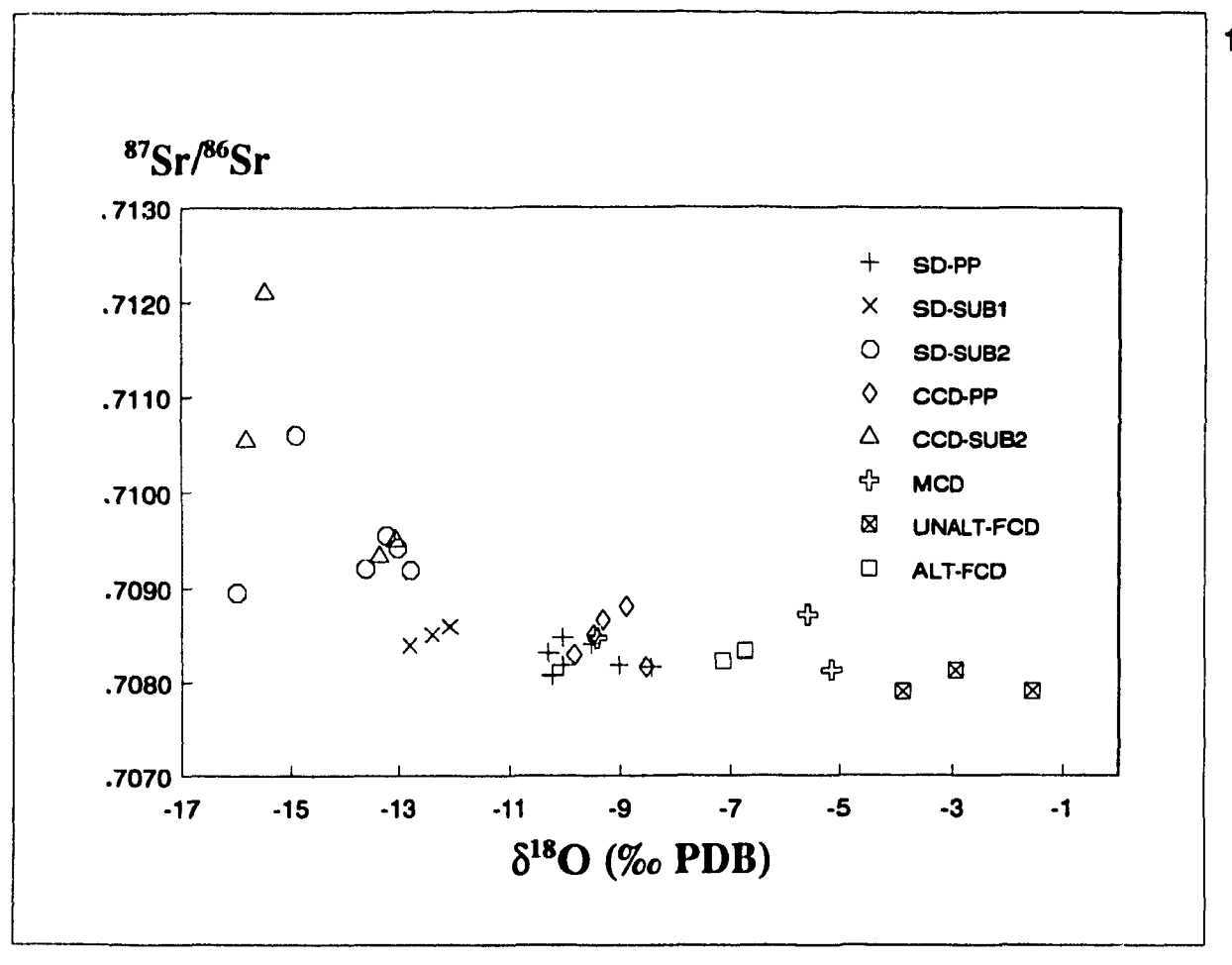


Figure 32. Cross plot of ${}^{87}\text{Sr}/{}^{86}\text{Sr}$ ratios and $\delta^{18}\text{O}$ values of various dolomites associated with Presqu'ile barrier.

is depleted in δ^{18} O (-3.7 to -9.4 ‰ PDB). SD and CCD from Pine Point have 87 Sr/ 86 Sr ratios similar to MCD, whereas their δ^{18} O values are much more depleted (-8.5 to -10.5 ‰ PDB) than estimated seawater dolomites. SD and CCD from the subsurface Presqu'ile are most radiogenic in 87 Sr/ 86 Sr (0.7090 to 0.7122) and most depleted in δ^{18} O (-13 to -16 ‰ PDB). It is unlikely that these radiogenic 87 Sr/ 86 Sr ratios and light δ^{18} O values were caused by meteoric waters, because fluid inclusion data (see discussion later) indicate that these saddle dolomites were precipitated from warmer (120-171°C) fluids than the Pine Point saddle dolomites (93-106°C).

In the Edmonton area of the Western Canada Sedimentary Basin, the present-day basin fluids display three distinct zones in terms of ⁸⁷Sr/⁸⁶Sr ratios (Connolly *et al.* 1990a; 1990b). Fluids in the Upper Cretaceous zone have distinctly low ⁸⁷Sr/⁸⁶Sr ratios (as low as 0.7058) and fluids in the lower Cretaceous to Jurassic have intermediate ⁸⁷Sr/⁸⁶Sr ratios. The fluids in the deepest Paleozoic reservoirs are the most radiogenic, ranging from 0.7076 to 0.7129 with most fluids being more radiogenic than 0.7095 (Connolly *et al.* 1990b). Two formation water samples from the Upper Devonian Nisku Buildup are also radiogenic with ⁸⁷Sr/⁸⁶Sr ratios from 0.7122 to 0.7128 (H. G. Machel pers. comm. 1991). This indicates that the fluids presently in the Paleozoic reservoirs, given the right chemical conditions, would precipitate coarse-crystalline dolomites, saddle dolomites, and late-stage calcites with radiogenic ⁸⁷Sr/⁸⁶Sr ratios similar to those observed in the subsurface Presqu'ile barrier and other areas in the Western Canada Basin.

Because of low to intermediate 87 Sr/66 Sr ratios in the formation waters of the

Cenozoic and Mesozoic strata (Connolly et al. 1990b), it appears that topographically driven fluids, which passed through the Mesozoic and early Tertiary clastic wedge during the Cretaceous and early Tertiary, have contributed little radiogenic Sr to the fluids in the Paleozoic level of the basin. Two likely sources of radiogenic Sr could be: 1) the underlying Precambrian crystalline and metamorphic basement; or 2) from clastic sequences downdip in the Lower Cambrian Gog Group and the feldspathic grits of the Late Proterozoic Windermere Supergroup (Mountjoy et al. in press). The ⁸⁷Sr/⁸⁶Sr ratios for Precambrian basement rocks range from 1.0932 to 1.3097 and for Cambrian shales from 0.7431 to 0.7757 (Connolly et al. 1990b). Brines analyzed from wells in the exposed parts of the Precambrian Shield vary from 0.7070 to 0.7550, with most values ranging from 0.7150 to 0.7300 (McNutt et al. 1990). Similar values should be expected for brines in the basement beneath the Western Canada Sedimentary Basin.

1

1

5.5 FLUID INCLUSIONS

Two-phase (aqueous liquid-vapour) fluid inclusions were analyzed from 14 saddle dolomite samples from 11 localities, 4 calcite samples from 4 localities, and 4 quartz samples from one locality (Appendix 4). There are two types of inclusions: primary and secondary. Primary inclusions form at the time of crystal growth, and are commonly concentrated in planes parallel to growth zones. Secondary inclusions are entrapped at any time after crystal growth has been completed. They generally

occur along healed fractures that cut crystal boundaries. The fluid inclusions measured in this study are thought to be primary in origin.

Homogenization temperatures (Th) are measured during heating runs. This is the temperature at which two phases (aqueous liquid-vapour in our study) initially contained in an inclusion are homogenized into a single phase. Homogenization temperatures provide an estimate of the **minimum** temperature at which the fluid was trapped.

The initial (or eutectic) melting temperatures (Te) and final melting temperatures (Tm) are measured during freezing runs. Initial melting temperatures provide information about the compositions of the fluids contained in the inclusions (Table 3).

Table 3. Eutectic temperatures for some chloride salt systems (data from Crawford 1981)

KCl	-10.6°C	KCl-NaCl	-22.9°C
NaCl	-20.8°C	MgCl ₂ -NaCl	-35.0°C
MgCl ₂	-33.6°C	CaCl ₂ -NaCl	-52.0°C
CaCl ₂	-49.8°C	MgCl ₂ -CaCl ₂ -NaCl	-57.0°C

The final melting temperature is the temperature at which the last ice or salthydrate melts. Total salinity can be calculated from the final melting temperature using the equation of Potter et al. (1978):

 $ws = 1.76958 (D) - 4.2384x10^{-2}(D)^2 + 5.2778x10^{-4}(D)^3$

where:

ws is the equivalent weight percent NaCl; and

D is the freezing point depression in °C.

5.5.1 RESULTS

SADDLE DOLOMITE

Saddle dolomites contain two-phase aqueous liquid-vapour (LV) fluid inclusions (Fig. 33). Inclusions are found in growth bands close to crystal edges. Therefore the data derived from these inclusions represent fluids present during the last stages of dolomitization. Fluid inclusions in saddle dolomite are very small, about 5 μ m, and have irregular to elongated shapes (Fig. 33). Some samples contain abundant inclusions, while others contain only a few.

The homogenization temperatures of fluid inclusions in saddle dolomites range from 85 to 210 °C and depend on the location and present burial depth of the sample (Figs. 34). The homogenization temperatures gradually increase from Pine Point westward along the Presqu'ile barrier, as present burial depths increase from Pine Point, to the subsurface of the NWT and northeastern British Columbia (Figs. 35 and 36).

1) The average homogenization temperatures of saddle dolomite from the Pine

Figure 33. Photomicrograph showing two-phase aqueous fluid inclusions.

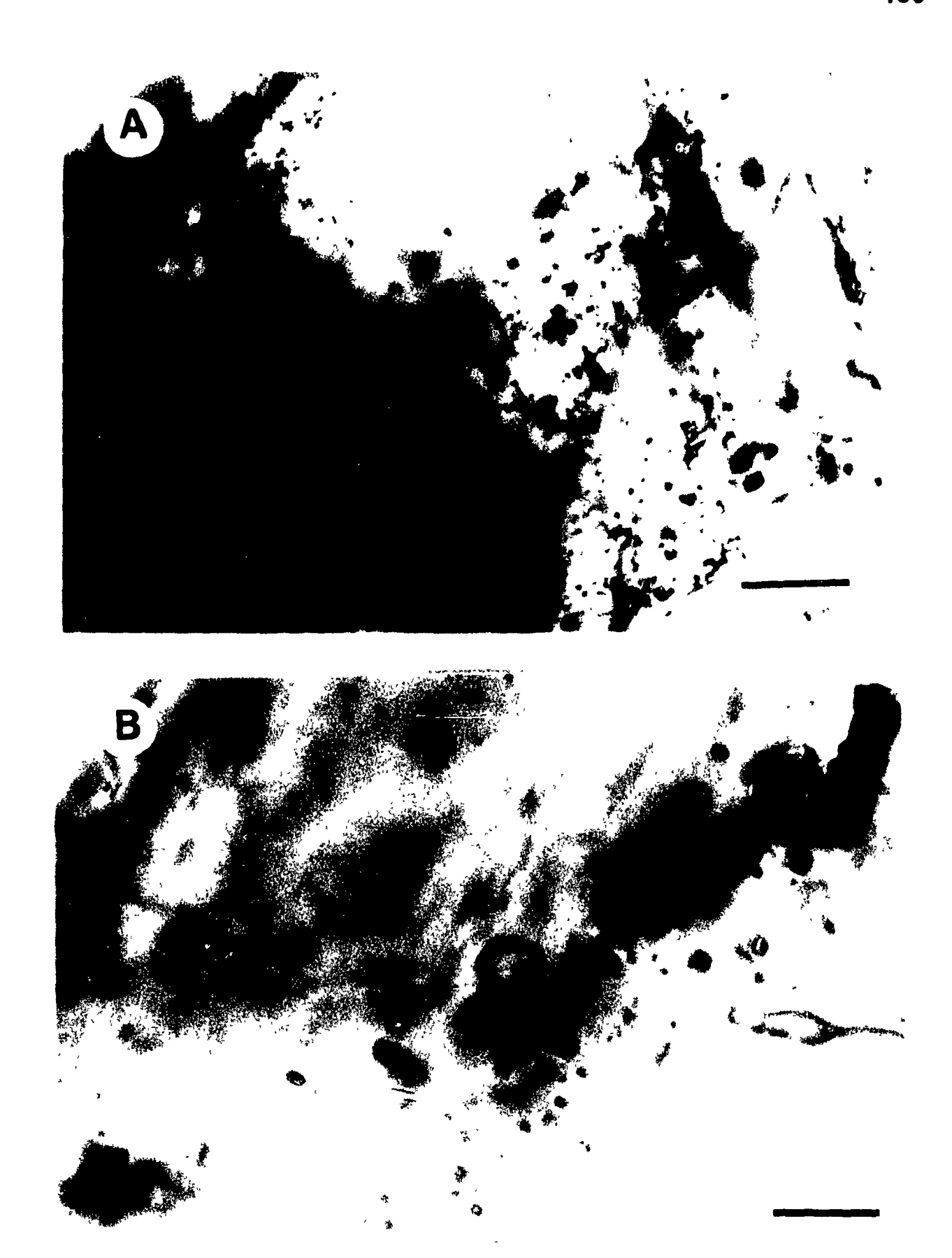
- A) Two-phase aqueous fluid inclusion in saddle dolomite crystal.

 Location: Sulphur Point Formation, pit N81, Pine Point.

 Scale bar 50 μm.
- B) Two-phase aqueous fluid inclusion in late-stage calcite.

 Location: Sulphur Point Formation, well B07, 7242 ft.

 Scale bar 100 μm.



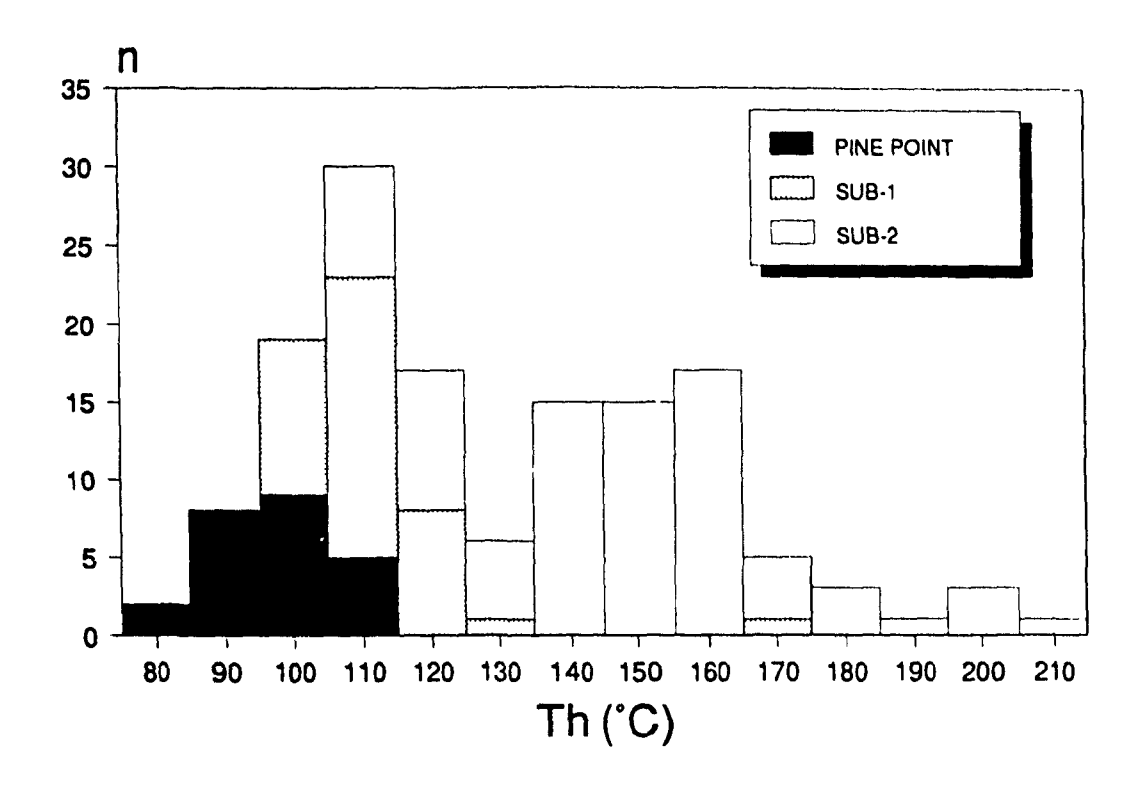


Figure 34. Homogenization temperatures of saddle dolomites from the Presqu'ile barrier.

SUB-1: samples from west of Pine Point to the Tathlina Lake area;

SUB-2: samples from NWT west of the Tathlina Lake and northeastern B.C.

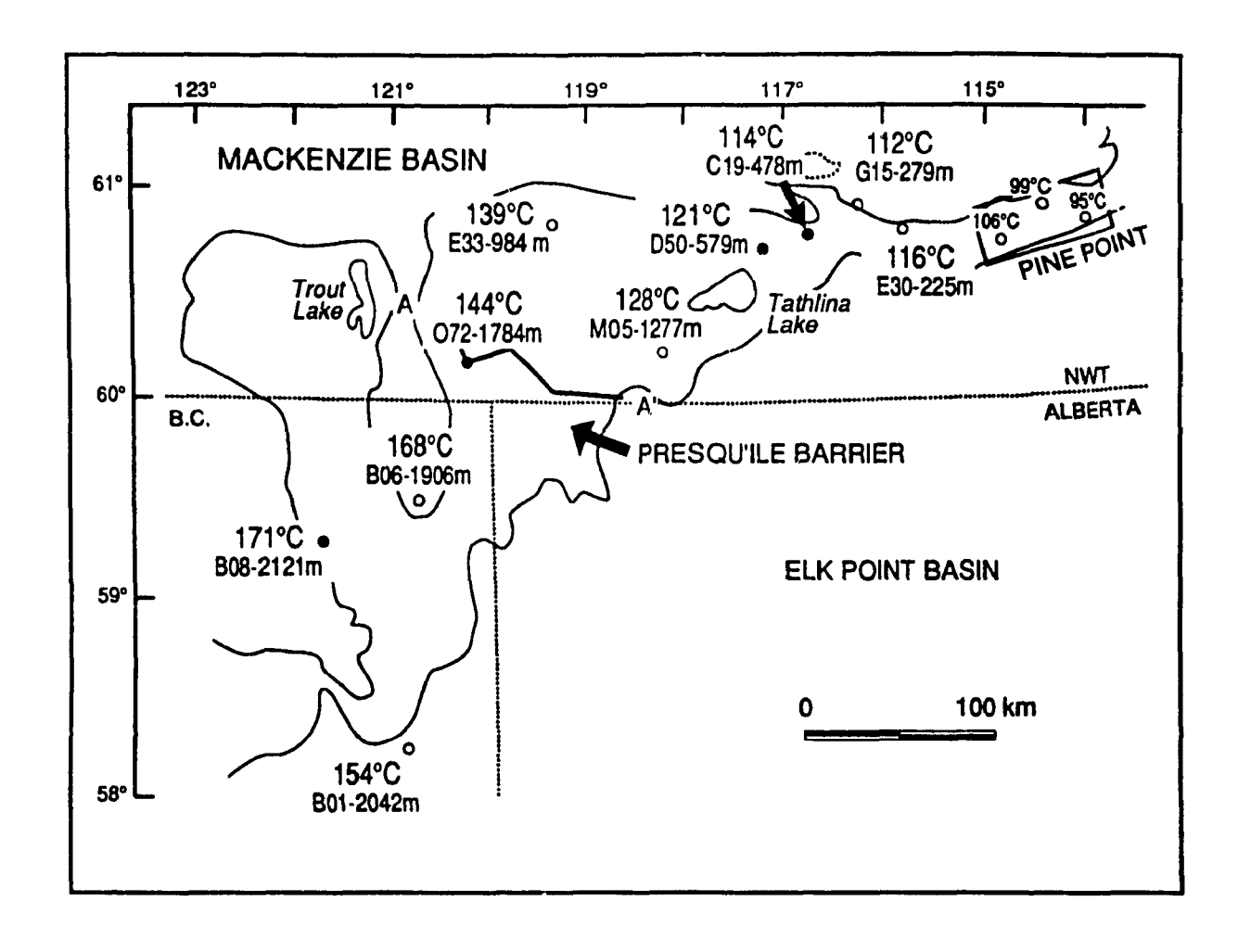


Figure 35. Variation of average homogenization temperatures of fluid inclusions in saddle dolomites along the Presqu'ile barrier.

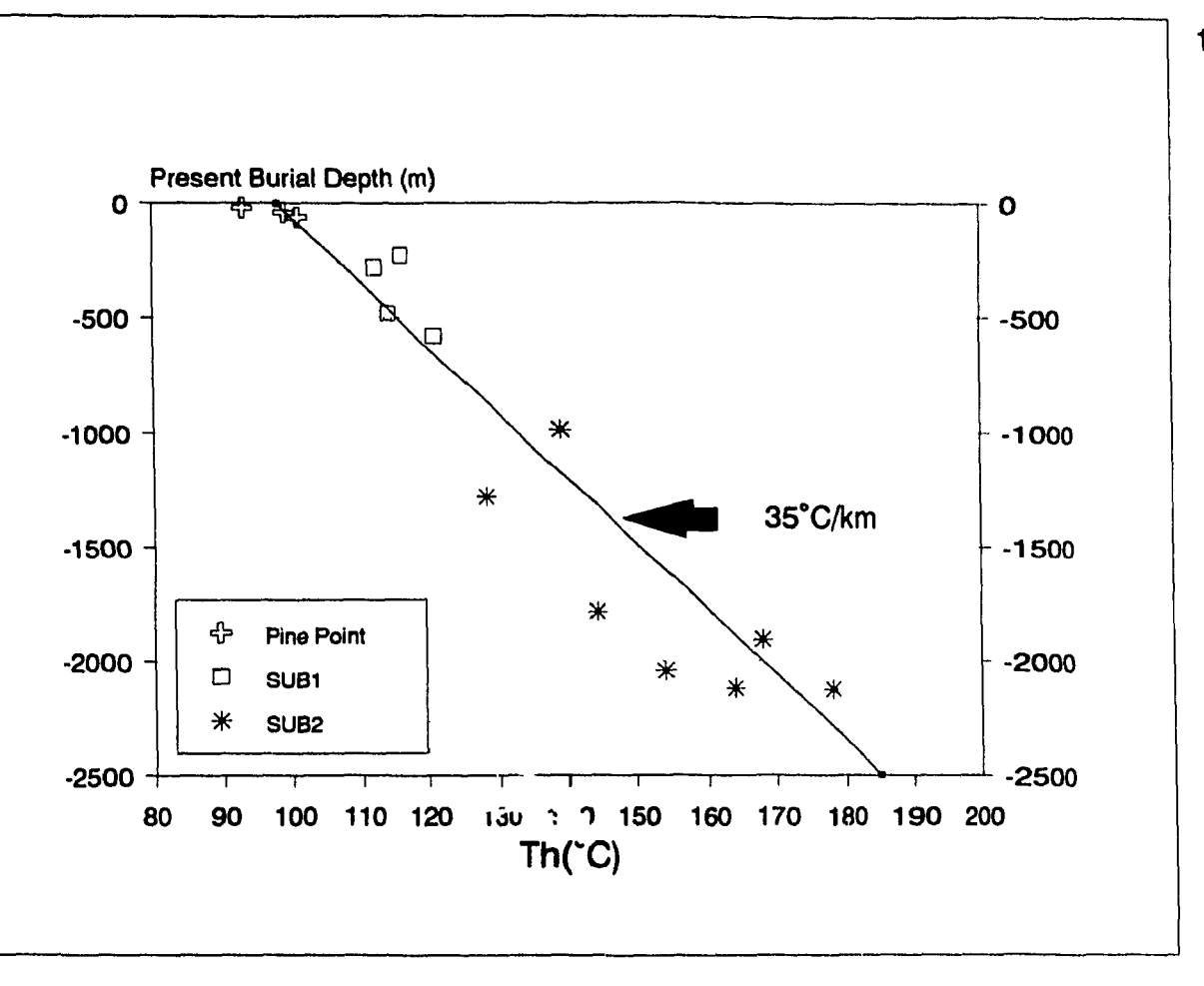


Figure 36. Average homogenization temperature (Th) of saddle dolomites vs their present burial depths. Homogenization temperatures increase westward with increasing present burial depths, and fit on a line of 35 °C/km.

SUB-1: samples from west of Pine Point to the Tathlina Lake area;

SUB-2: samples from NWT west of the Tathlina Lake and northeastern B.C.

Point open pits is 92 °C for pit X51, 99 °C for pit P24, and 106 °C for pit N81. These temperatures are similar to Roedder's measurements (90-100 °C) from one Pine Point SD sample from an unspecified location (Roedder 1968).

- 2) In the area west of Pine Point to Tathlina Lake, the average homogenization temperatures of saddle dolomite from 4 wells (E30, G15, C19 and D50) increase from 112 °C to 121 °C, whereas the present burial depth increases from 225 m to 580 m.
- 3) Further west in the NWT west of Tathlina lake (well M05, E33, and O72, present burial depths of the Presqu'ile barrier range from 1000 m to 1800 m) the average homogenization temperature of saddle dolomite reaches 128 °C to 144 °C.
- 4) In the subsurface of northwestern British Columbia, Th ranges from 154 °C to 171°C (present burial depths 1900 m to 2200 m).

Initial and final melting temperatures in some saddle dolomites are difficult to accurately determine due to the small size of the inclusions. Final melting temperatures range between -7 and -34 °C (Fig. 37), correspond to salinities ranging from 10 to 31 wt % equivalent NaCl, which are 3 to 9 times the salinity of seawater. The measured initial temperatures range from -22 to -65 °C, with most occurring in the range of -40 to -60 °C (Fig. 38), indicating that the fluid inclusions contain a multicomponent salt system with dissolved NaCl, CaCl₂, KCl, and MgCl₂ (see Table 3). Semiquantitative analysis of individual inclusion decrepitates of Pine Point

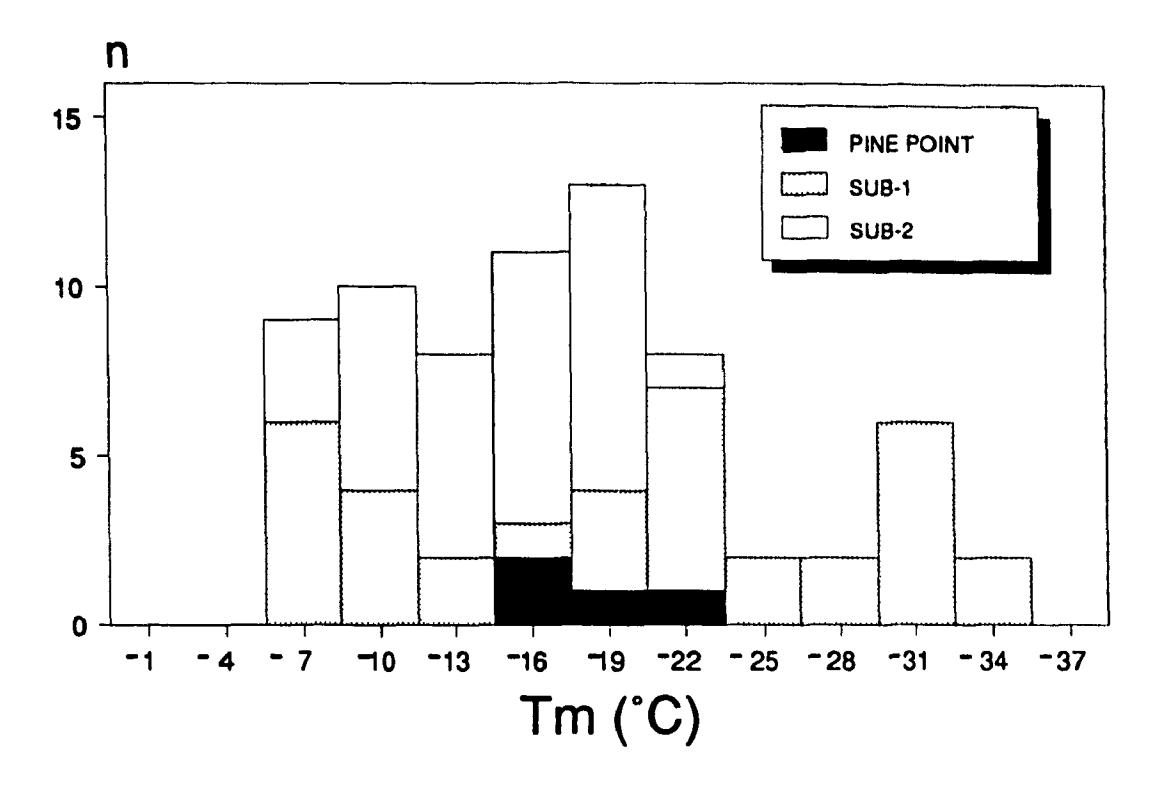


Figure 37. Final melting temperatures (Tm) of saddle dolomite fluid inclusion.

SUB-1: samples from west of Pine Point to the Tathlina Lake area;

SUB-2: samples from NWT west of the Tathlina Lake and northeastern B.C.

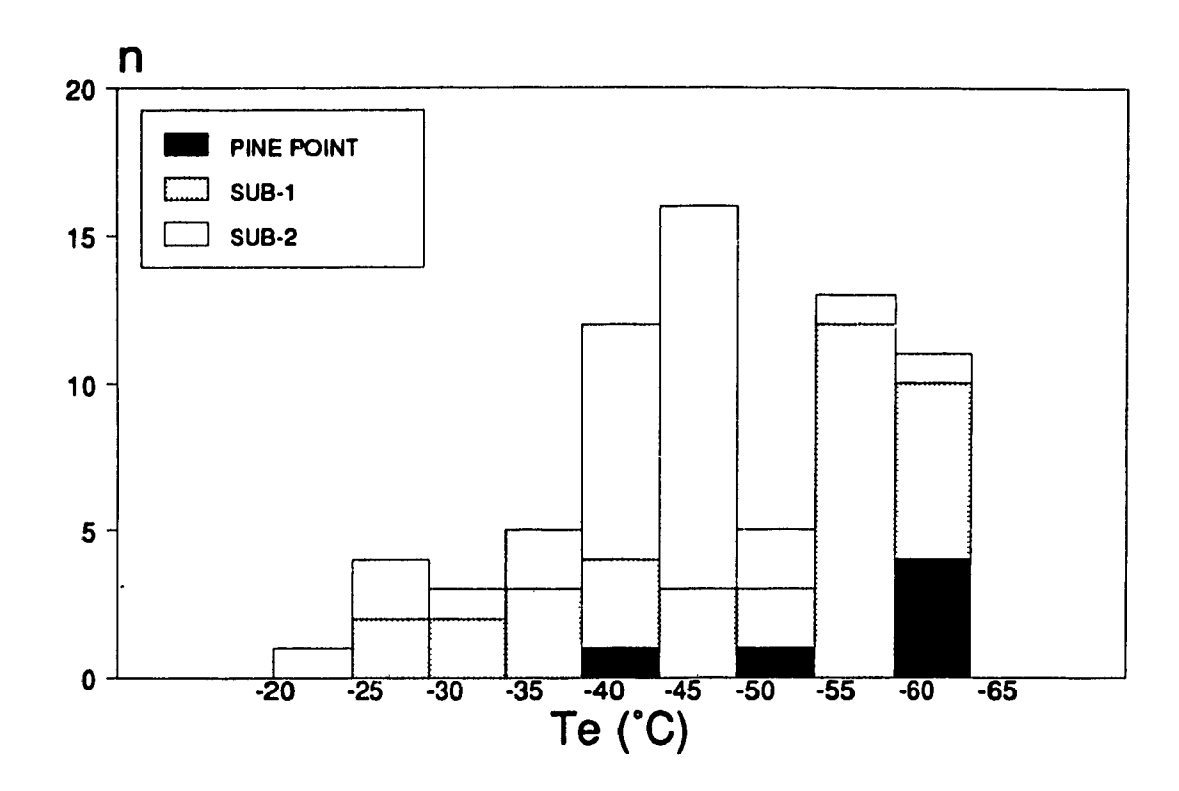


Figure 38. Initial melting temperatures (Te) of saddle dolomite fluid inclusions.

SUB-1: samples from west of Pine Point to the Tathlina Lake area;

SUB-2: samples from NWT west of the Tathlina Lake and northeastern B.C.

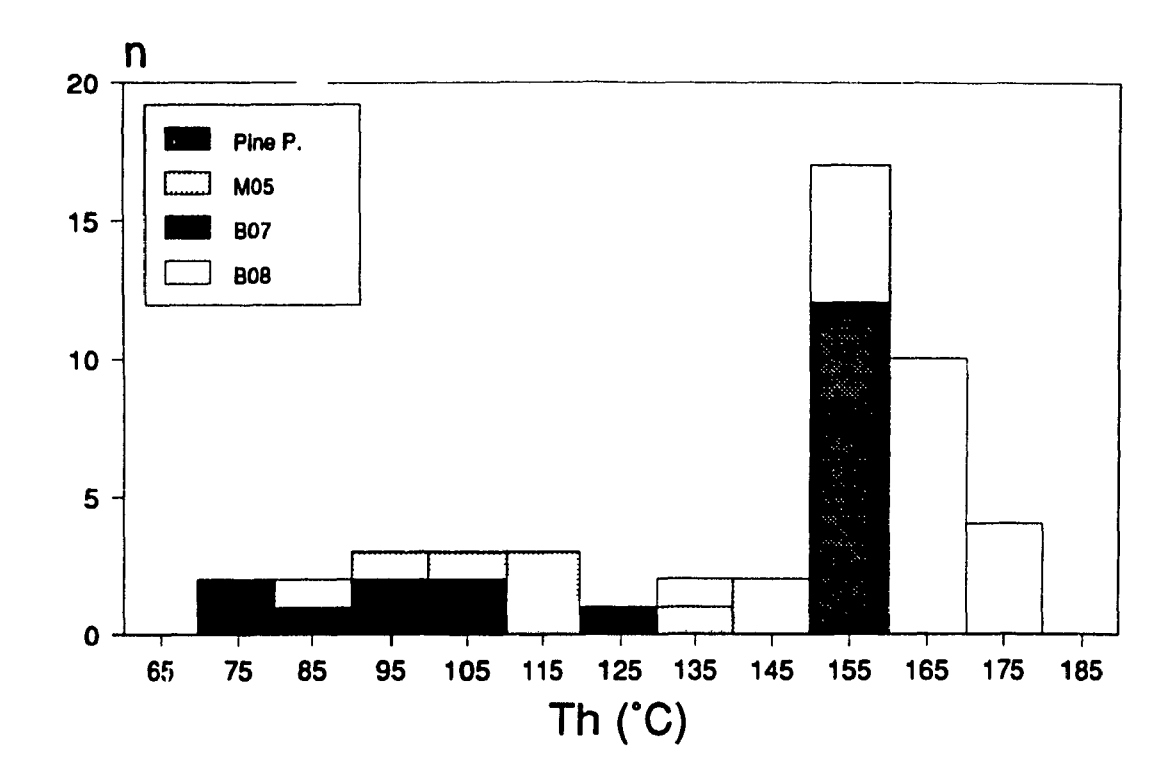
dolomites, using a SEM energy dispersive method, indicates that the fluid composition is dominantly NaCl and CaCl₂ with subordinate KCl and MgCl₂ (Haynes and Kesler 1987).

LATE-STAGE COARSE-CRYSTALLINE CALCITE

Fluid inclusion data of late-stage calcite were obtained from four localities: one from Pine Point (N81), one from subsurface NWT (M05), and two from the subsurface of northeastern British Columbia (wells B07 and B08).

Late stage coarse-crystalline calcites contain two-phase (LV) aqueous inclusions (Fig. 33). Homogenization temperatures of calcite fluid inclusions range from 70 to 176 °C (Fig. 39). Similar to the homogenization temperature of saddle dolomites, the homogenization temperatures of late-stage calcites also increase westward along the Presqu'ile barrier with increasing present burial depth (Fig. 40). However, the average Th of late-stage calcite is usually about 10 °C lower than the Th of saddle dolomites from the same location (Fig. 40).

The final melting temperatures of fluid inclusions in these calcites range from -3.6 to -15.1°C (Fig. 41), which are 5 to 18 °C higher than the final melting temperatures of the saddle dolomites from the same locations. The corresponding salinities for calcites range from about 6 to 19 equivalent wt % NaCl, 2 to 5.5 times the salinity of seawater, suggesting that calcites precipitated from slightly less saline fluids than saddle dolomites from the same location.



1

Figure 39. Homogenization temperatures of fluid inclusions in late-stage coarsecrystalline calcites (LCC). Numbers refer to well locations, see Figure 1.

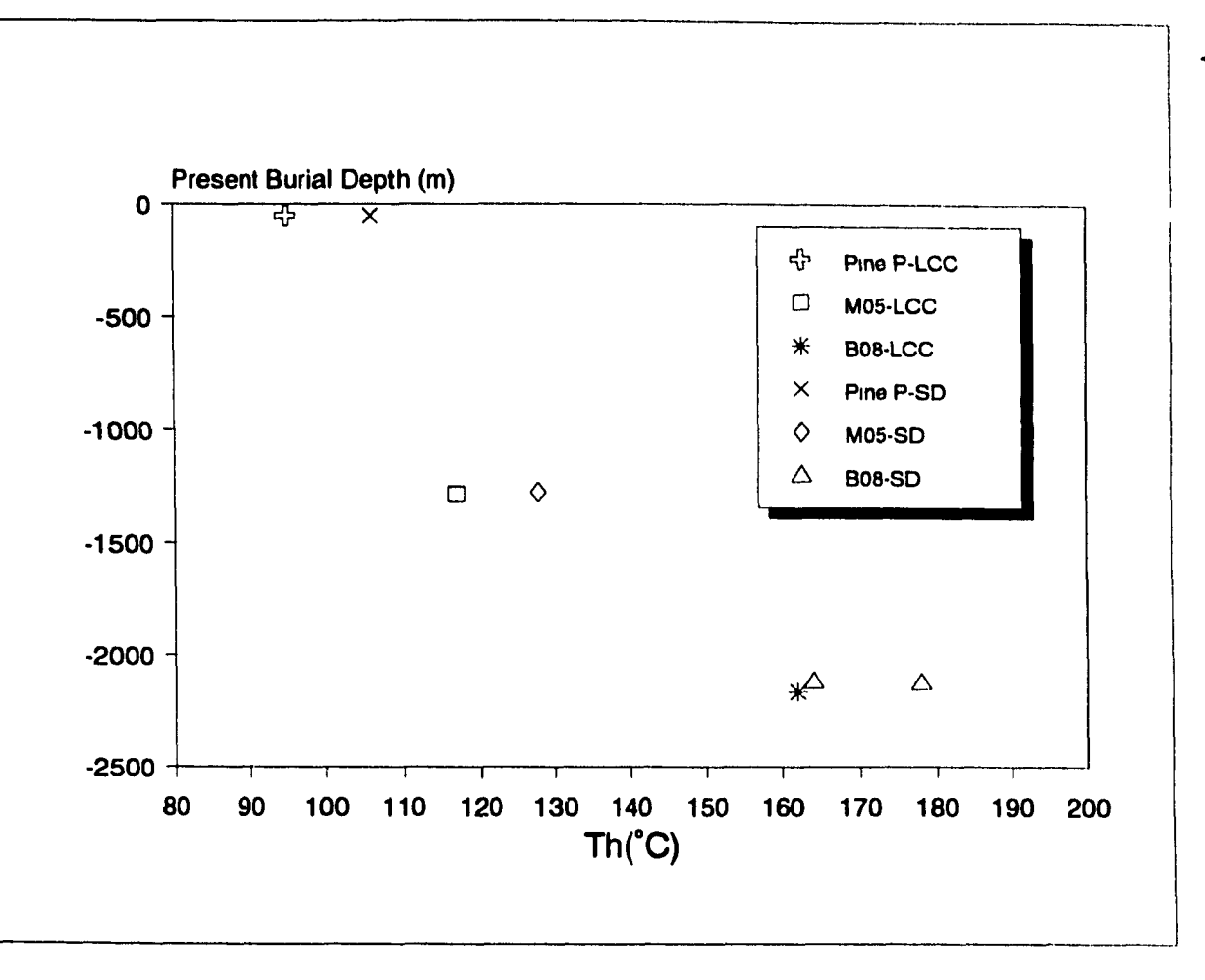


Figure 40. Cross plot of average homogenization temperature of fluid inclusions in late-stage coarse-crystalline calcites (LCC) and burial depths. Homogenization temperatures of saddle dolomite fluid inclusions from the same locations are also plotted for comparison. Numbers refer to well locations, see Figure 1.

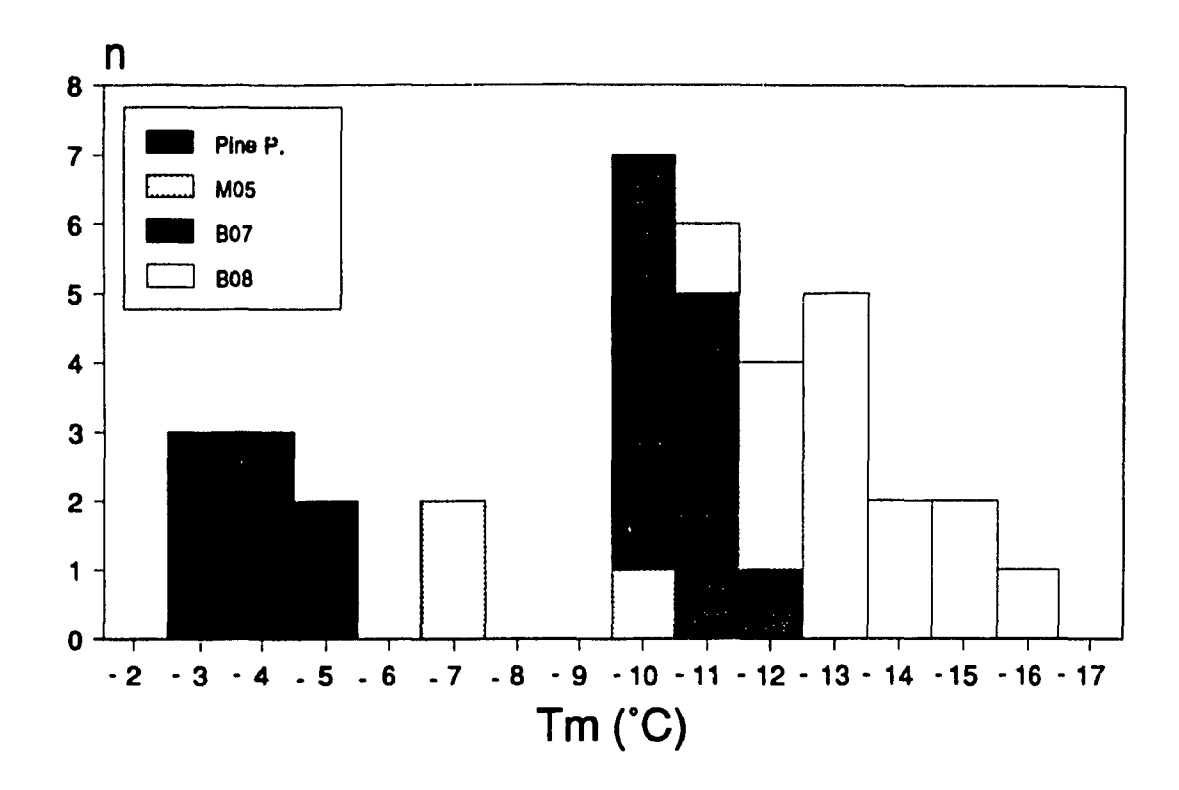
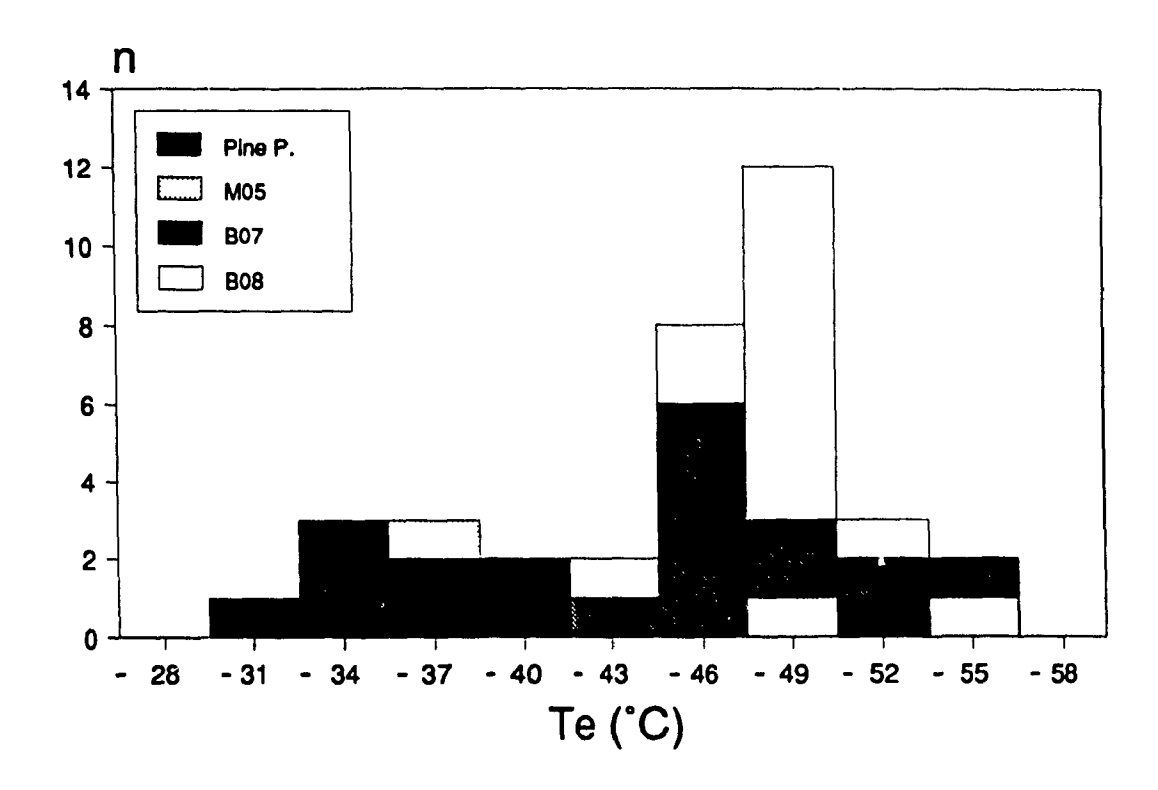


Figure 40. Cross plot of average homogenization temperature of fluid inclusions in late-stage coarse-crystalline calcites (LCC) and burial depths. Homogenization temperatures of saddle dolomite fluid inclusions from the same locations are also plotted for comparison. Numbers refer to well locations, see Figure 1.



f . 1

Figure 41. Final melting temperatures (Tm) of fluid inclusions in late-stage coarse-crystalline calcites. Numbers refer to well locations, see Figure 1.

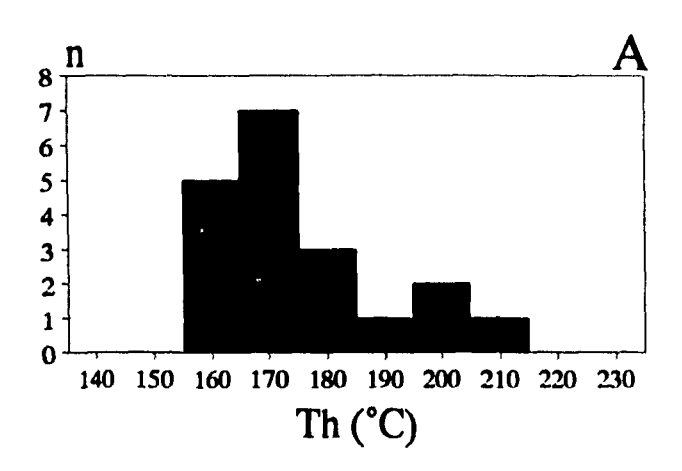
The measured initial melting temperatures range from -30 to -55 °C (Fig. 42), indicating that the fluid inclusions in calcites contain a multicomponent salt system of NaCl-CaCl₂, possibly with minor amounts of MgCl₂ (Table 3).

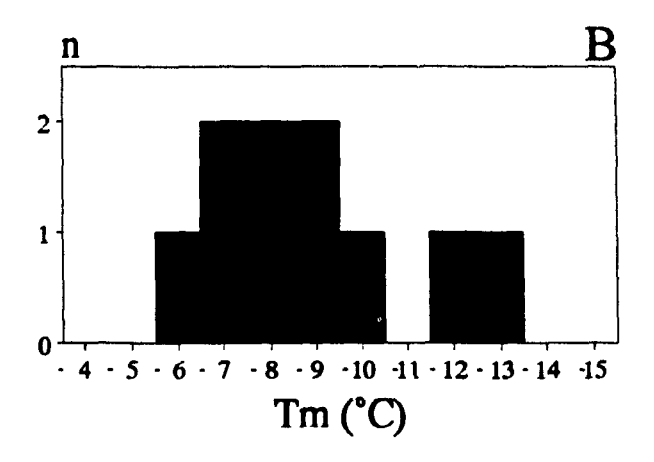
QUARTZ

Quartz was found only in well B08 at 2119 m (6952'), occurring as euhedral crystals precipitated on saddle dolomite. Fluid inclusions in the quartz are two-phase, aqueous liquid-vapour inclusions. Homogenization temperatures of the fluid inclusions range from 165 to 211 °C (avg. 180 °C, Fig. 43), which is about 15 °C higher than the coexistent saddle dolomite.

The final melting temperatures of the fluid inclusions in quartz range from -6.8 to -13.6 °C (avg. -9.4 °C, Fig. 43), which are much lower than the coexistent saddle dolomite (avg. -18 °C) and slightly lower than late-stage calcite (avg. -11 to -13 °C), suggesting that quartz was precipitated from less saline fluids (10 to 17 wt% NaCl equivalent).

The initial melting temperatures of the fluid inclusions in quartz range from -27 to -43 °C (Fig. 43), averaging -33.7 °C. These temperatures are slightly higher than the average initial temperatures of -48 °C for both saddle dolomite and calcite from the same location. This suggests that the quartz fluid inclusions still contain a multicomponent salt system of NaCl and MgCl₂, but possibly with much less CaCl₂ content, compared with fluids from which saddle dolomite and calcite





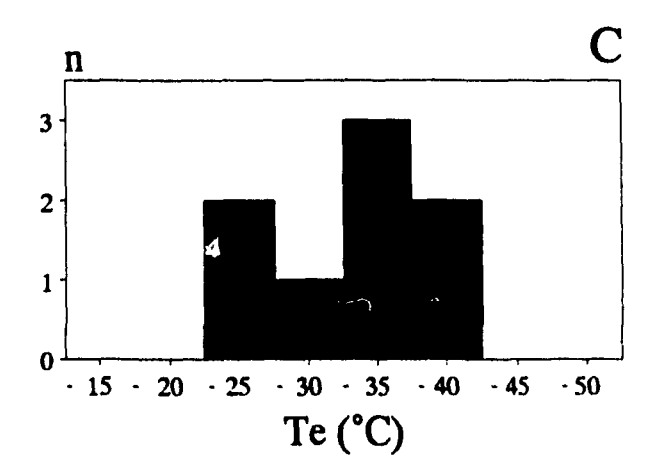


Figure 43. Fluid inclusion temperatures of quartz.

Location: Sulphur Point Formation, well B08, 6952 ft.

A) homogenization temperature, B) initial melting temperature, and C) final melting temperature.

5.5.2 DISCUSSION

The homogenization temperatures of fluid inclusions and the present burial depths of saddle dolomites are plotted in Figures 34. The gradual increase of homogenization temperatures of fluid inclusions in saddle dolomites appears to be related to the westward increase of burial depths of the Presqu'ile barrier and fits a line with a geothermal gradient of 35 °C/km (Fig. 34). The average homogenization temperature is about 99 °C for Pine Point samples and about 168 °C for saddle dolomites from northeastern British Columbia. If these homogenization temperatures represent normal burial temperatures, the calculated depths of saddle dolomite formation would be about 2300 m at Pine Point, and about 4300 m in the northeastern British Columbia (Fig. 44), assuming a surface temperature of 20 °C and a geothermal gradient of 35 °C/km. However, as homogenization temperatures represent only minimum trapping temperatures, pressure corrections have to be applied to determine the actual (trapping) temperatures at which the saddle dolomites precipitated (Table 4). The maximum burial depths based on the stratigraphic reconstruction (see Chapter 4) are used in pressure-correction calculation for different parts of the Presqu'ile barrier.

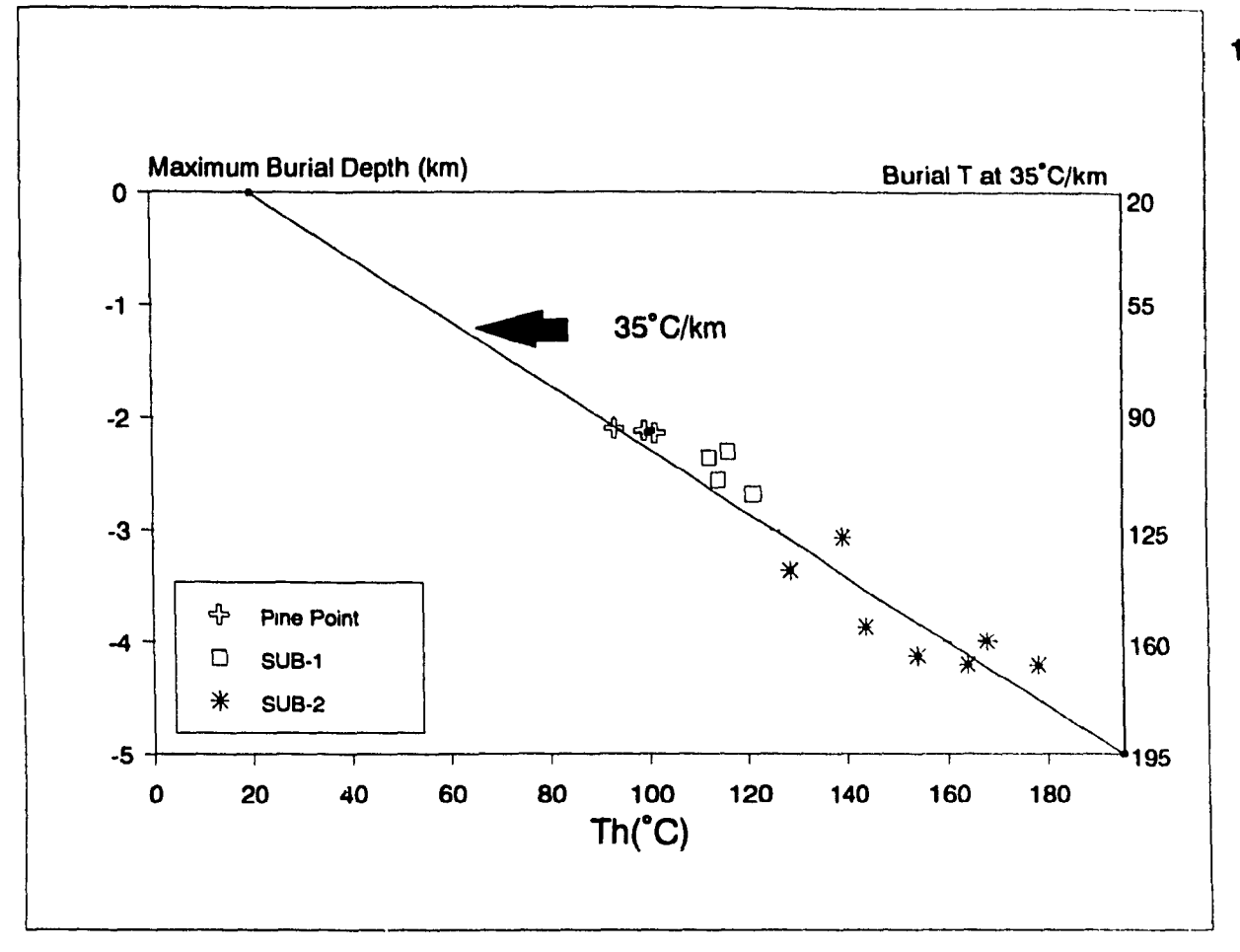


Figure 44. Homogenization temperatures of Presqu'ile saddle dolomites vs calculated burial depths, assuming a surface temperature of 20 °C and a geothermal gradient of 35 °C/km.

Table 4. Comparison of pressure-corrected homogenization temperatures and estimated maximum burial temperatures*.

	Pine Point	Tathlina L.	N of B.C-A.B	NE B.C.
max. burial depth based on stratigraphic reconstruction	1500 m	2000 to 2500 m	3000 to 3500 m	3500 to 4000 m
max. burial T based on a geothermal gradient 35 km/°C	66 °C	90-107 °C	125-143 ℃	143-160 ℃
corrected Th under hydrostatic condition	106 °C	125-127 ℃	160-163 ℃	187-190 °C

^{*} the maximum burial temperatures are calculated, using a geothermal gradient of 35°C/km and a surface temperature of 20 °C.

Assuming a hydrostatic condition and using isochores for 20 eq. wt.% NaCl (which is calculated from the average final melting temperature), the pressure-corrected homogenization temperatures for saddle dolomites would be around 106 °C for the Pine Point area, 130 °C for the Tathlina Lake area, 160 °C for the NWT north of B.C./Alberta boundary, and 190 °C for northeastern B.C. (Table 4). Based on the stratigraphic reconstruction of these area and assuming a geothermal gradient of 35°C/km and a surface temperature of 20 °C, the maximum burial temperatures are estimated to be about 66 °C in the Pine Point area, about 125-143 °C in the NWT north of B.C./Alberta border, and about 143-160 °C in the northeastern B.C. (Table 4). Unless there were abnormally high geothermal gradients, the pressure-corrected homogenization temperatures would exceed the maximum burial temperatures. Therefore it is reasonable to interpret the corrected homogenization temperatures as

resulting from a regional hydrothermal event. The gradual decrease in homogenization temperatures eastward along the Presqu'ile barrier suggests that dolomitizing fluids moved updip from west to east along the Presqu'ile barrier.

Similar to the Presqu'ile saddle dolomites, the systematic change of homogenization temperatures with geographic location is also observed in the calcite and quartz that are associated with the Manetoe dolomite north of the Presqu'tle barrier. The homogenization temperatures of late-stage calcite increase systematically from 110 °C to 190 °C from the north (e.g. 62.5°N and 122.9°W, as in well Berry F-71) to the south (e.g. 60.0°N and 124.3°W, as in well Beaver River YT G-01), which were interpreted to be due to differences in burial depths (about 700 m in the north and 4000 m in the south) during Cretaceous time (Aulstead et al. 1988). The homogenization temperatures of Manetoe dolomite, however, are distinctly different. There is no relationship between homogenization temperatures and geographic locations in the Manetoe dolomite (Aulstead et al. 1988; Morrow et al. 1990), suggesting that Manetoe dolomite may have formed in a different way from Presqu'ile dolomite.

Using equation 3 and the measured homogenization temperatures and δ^{18} O values of the Presqu'ile saddle dolomites, the δ^{18} O values of dolomitizing fluids are calculated to be -1 to +5 ‰ SMOW (Fig. 45). These values are 1 to 8 ‰ SMOW heavier than the best estimated δ^{18} O values of Middle Devonian seawater (Fig. 45), suggesting that dolomitizing fluids vere burial brines, rather than diluted seawater from a mixing zone environment as suggested by Kyle (1981, 1983). This is also

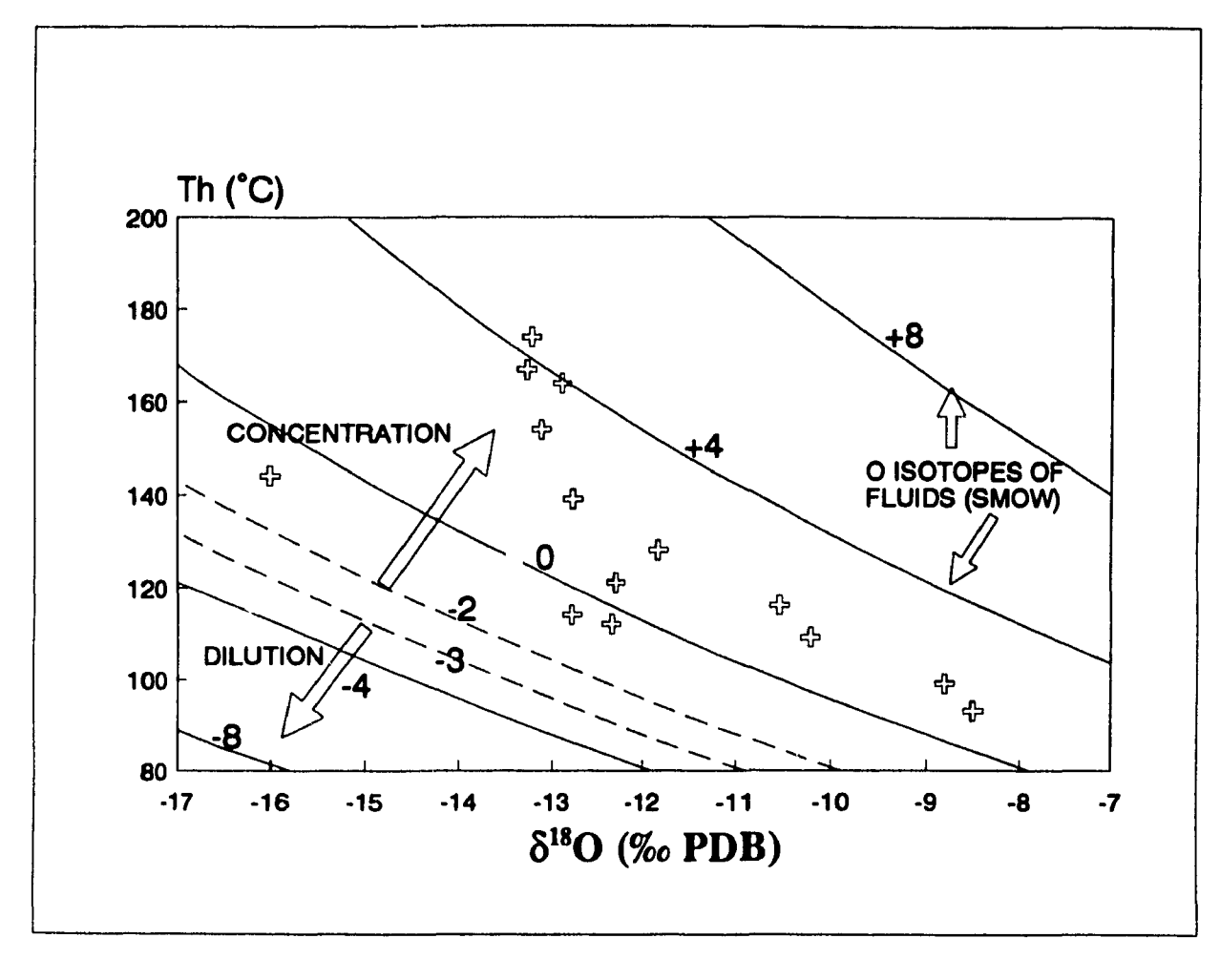


Figure 45. Cross plot of homogenization temperature and δ^{18} O values of saddle delomite. δ^{18} O value of dolomite is controlled by the temperature and δ^{18} O value of fluid, and can be expressed by the equation of Fritz and Smith (1970): $10^3 \ln \alpha_{\text{dolomate-fluid}} = 3.2 \times 10^6 \text{T}^2(^{\circ}\text{T}) - 3.3$. The graph is constructed using this equation. The average homogenization temperature is plotted against δ^{18} O value of dolomite to yield the δ^{18} O values of dolomites were precipitated varies from -1 to +5 % SMOW, which are heavier than the best estimated δ^{18} O values of Middle Devonian seawater are -2 to -3 % SMOW (dash lines), according to the calculation of this study (section 5.3.2) and study by Popp et al. (1986). Using the pressure-corrected homogenization temperatures, the δ^{18} O values of the dolomitizing fluids would be even heavier.

indicated by the final melting temperatures, which suggest that the salinities of the dolomitizing fluids range from 10 to 31 wt% equivalent NaCl, or about 3 to 9 times the salinity of seawater.

Fluid inclusions in sphalerite were studied by Roedder (1968) and Kyle (1981). The homogenization temperatures for sphalerite range from 51 to 99 °C, slightly lower than those of saddle dolomite. Measurements of Tm suggested that sulphide minerals were precipitated from fluids with salinities from 15 to 23 equivalent weight percent NaCl, similar to the salinities of the saddle dolomite inclusions.

Fluid inclusions from saddle dolomite and late-stage calcite from the same localities are compared in order to determine the evolution of basin-fluid chemistry. Figure 46 is a cross plot of homogenization and final melting temperatures of SD and late-stage calcite from 1) pit N81, Pine Point, 2) well M05, NWT, and 3) well B08 northeastern B.C. In all three localities, late-stage coarse-crystalline calcite precipitated after saddle dolomites from fluids of slightly lower temperatures but much lower salinities (Fig. 46). Similar to saddle dolomites, the homogenization temperatures of fluid inclusions in late-stage calcites also increase westward with increasing present burial depth (Fig. 40), suggesting that late-stage calcites probably precipitated in a similar hydrodynamic regime.

In well B08, fluid inclusions in saddle dolomite above the sub-Watt Mountain unconformity has similar homogenization and final melting temperatures to those in saddle dolomite below the unconformity (Fig. 46), suggesting that the dolomites

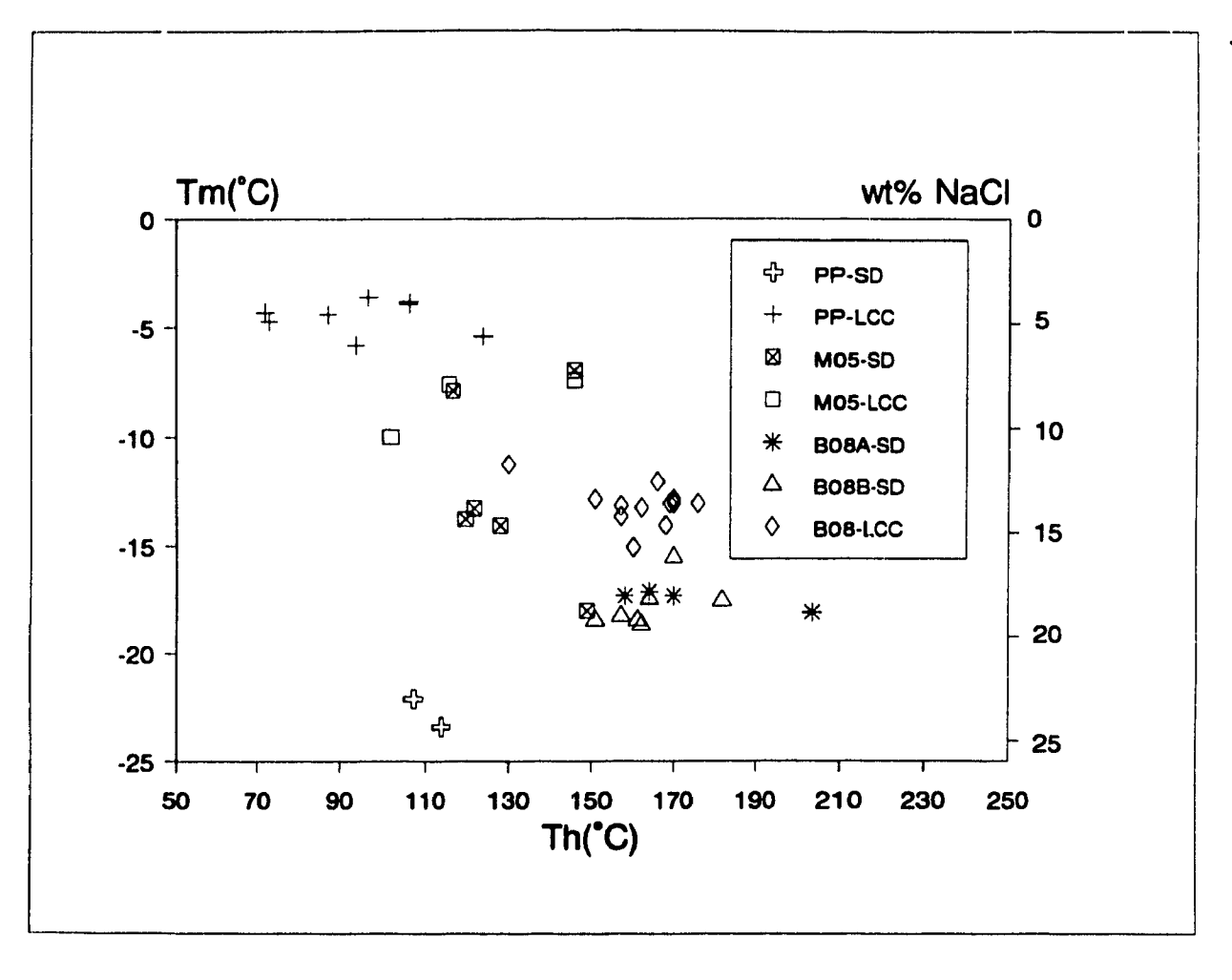


Figure 46. Cross plot of homogenization temperature (Th) and final melting temperature (Tm) for saddle dolomites (SD) and late-stage coarse-crystalline calcites (LCC) from: 1) Pine Point (pit N81), 2) NWT (well M05), and 3) northeastern B.C. (well B08). B08A is sample above the sub-Watt Mountain unconformity; B08B is sample below the sub-Watt Mountain unconformity.

formed during the same hydrothermal event from similar fluids.

5.6 TRACE ELEMENTS

Trace elements that substitute in the carbonate lattice are governed by the distribution coefficient (D). The distribution coefficient for trace elements in CaCO₃ in an open system at equilibrium is given by (McIntire 1963; Kinsman 1969):

$$D = \frac{(m_{Me}/m_{Ca})_{calcute}}{(m_{Me}/m_{Ca})_{fluid}}$$

where m indicates molar concentration, and Me represents the trace element.

When D > 1, the precipitated solid phase will contain, relative to Ca, higher Me concentrations than the fluid from which this solid phase precipitated. The opposite will apply for trace elements with D < 1. Depletion (or enrichment) will be proportional to the deviation of D from unity (Veizer 1983).

Results of element analysis, however, have to be treated with caution, because of the following factors:

1) Trace elements can also be incorporated into carbonate minerals in many other ways, in addition to substituting for Ca²⁺ or Mg²⁺ in the carbonate lattice (see Veizer 1983), e.g, a) as non-carbonate phases, e.g. in clay minerals, in fluid inclusions, etc.; b) occupying lattice positions which are free due to structural defects; c) adsorbed due to remnant ionic charges; and d) occurring in interstices between lattice planes. Non-carbonate contamination may frequently be a problem for Na, Fe,

and Mn.

- 2) Distribution coefficients vary during precipitation of a single solid phase depending on the physical-chemical conditions, such as temperature and kinetic factors (Veizer 1983). In particular, the rate of precipitation appears to be a dominant controlling factor of D, e.g. a D < 1 is enhanced (or D > 1 is diminished) with an increasing rate of precipitation (Lorens 1981; Mucci 1988).
- 3) Studies by Reeder and Prosky (1986) and Reeder and Grams (1987) indicate that trace element concentration varies within a single carbonate crystal, resulting in sector zoning in these crystals. Trace element concentrations may vary within single concentric zones because face-specific factors influence trace element uptake during crystal growth (Paquette and Reeder 1990). This could result in serious problems when trace element concentrations are measured by microanalytical methods. Paquette and Reeder (1990) suggest that the effects of these sector-related types of zoning on trace element contents are comparable to or larger than rate effects and must be considered in trace-element modelling of diagenetic processes.
- 4) Recrystallization and in some cases precipitation of carbonates in aqueous fluids may occur in thermodynamic **disequilibrium** with the bulk solution, therefore the composition of bulk solution cannot be back-calculated accurately (Machel 1990).
- 5) Most carbonate precipitation is due to direct (shells) or indirect biogenic factors (changing of environmental conditions, such as pH). The process of biogenic fractionation (or vital effect) may lead to reduction, or enrichment of trace element contents in the calcite (Veizer 1983).

6) Our understanding of trace elements in dolomites is severely limited by the fact that dolomite has not been synthesised in the laboratory at room temperatures. D_{dolomite} was commonly estimated from D_{calcite} based on the assumption that cations with ionic radii larger than Ca⁺² will substitute proportionally more in Ca site of dolomite, whereas those smaller than Ca⁺², would substitute in the Mg site (Kretz 1982). Although equilibrium concentrations of trace elements in dolomite calculated using the reasoning of Kretz (1982) have been widely used in the literature (e.g. Table 3-3 in Veizer, 1983), some of these D_{dol} have been modified recently. Vahrenkamp and Swart (1990) suggested that D^{Sr}_{dol} is dependent on the concentration of Ca in dolomite (D for other trace elements might also be a function of Ca content, but we do not know). For stoichiometric dolomite, D^{Sr}_{dol} is 0.0118, but it increases by about 0.0039 for every additional mol% of CaCO₃ in nonstoichiometric dolomite. This D^{Sr}_{dol} is substantially lower than previously suggested (e.g. 0.025-0.06 Veizer 1983; 0.06 Baker and Burns 1985).

For these reasons, previously suggested $D_{dolomite}$ is not well constrained and mu * be used with caution.

5.6.1 RESULTS

Trace elements were analyzed for 123 bulk samples and are summarized in Appendix 5. Only Sr and Mn display recognizable trends in some dolomites from the Presqu'ile barrier. For other measured elements, the changes in concentrations are very irregular and no clear trends were identified.

Sr content decreases from FCD, to MCD, CCD and SD (Fig. 47), whereas Mn increases from FCD, to MCD, CCD and SD (Figs. 48 and 49). FCD has the highest Sr concentrations, ranging from 55 to 225 ppm (avg. 105 ppm) (Figs. 47A and 49). The Sr concentrations in MCD are much lower than FCD, but slightly higher than CCD and SD, ranging from 30 to about 79 ppm (avg. 50 ppm) (Figs. 47B and 49). The Sr concentrations in CCD and SD are similar, varying from 30 to about 70 ppm (avg. 47 ppm) (Figs. 47C; 47D, and 49).

The Mn contents in the four types of dolomite change antipathetically to Sr (Figs. 48 and 49). The Mn content in FCD is the lowest among the four types of dolomite, ranging from 25 to 160 ppm (avg. 86 ppm). The average Mn content in MCD is 161 ppm, which is higher than FCD but lower than CCD and SD. The Mn contents in CCD and SD are highest among four types of dolomites, averaging 227 and 253 ppm respectively.

5.6.2 DISCUSSION

From a recent study of the Sr contents of Miocene marine dolomites from Little Bahama Bank, Vahrenkamp and Swart (1990) suggested that the amount of Sr in dolomite is not only related to the Sr content of the fluids from which dolomites precipitated but is also related to the stoichiometry of the dolomite crystals (Fig. 50). Assuming that Sr generally replaces Ca in the carbonate crystal lattice due to their similar ionic radius, $D_{sr}^{dolomste}$ can be defined as a function of Sr and Ca, by

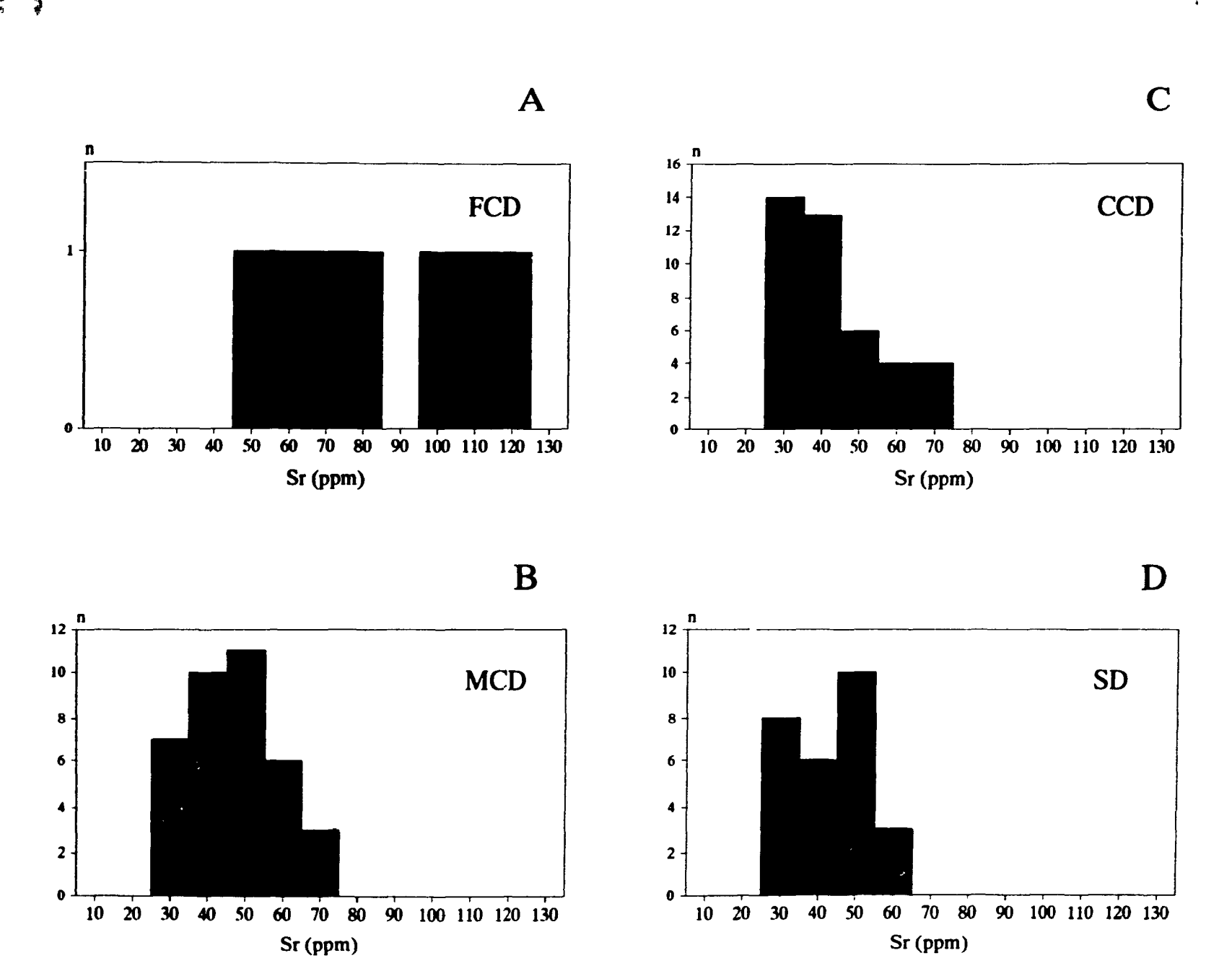


Figure 47. Sr concentration (ppm) of different dolomites. n = number of samples.

One FCD with 225 ppm Sr is not shown.

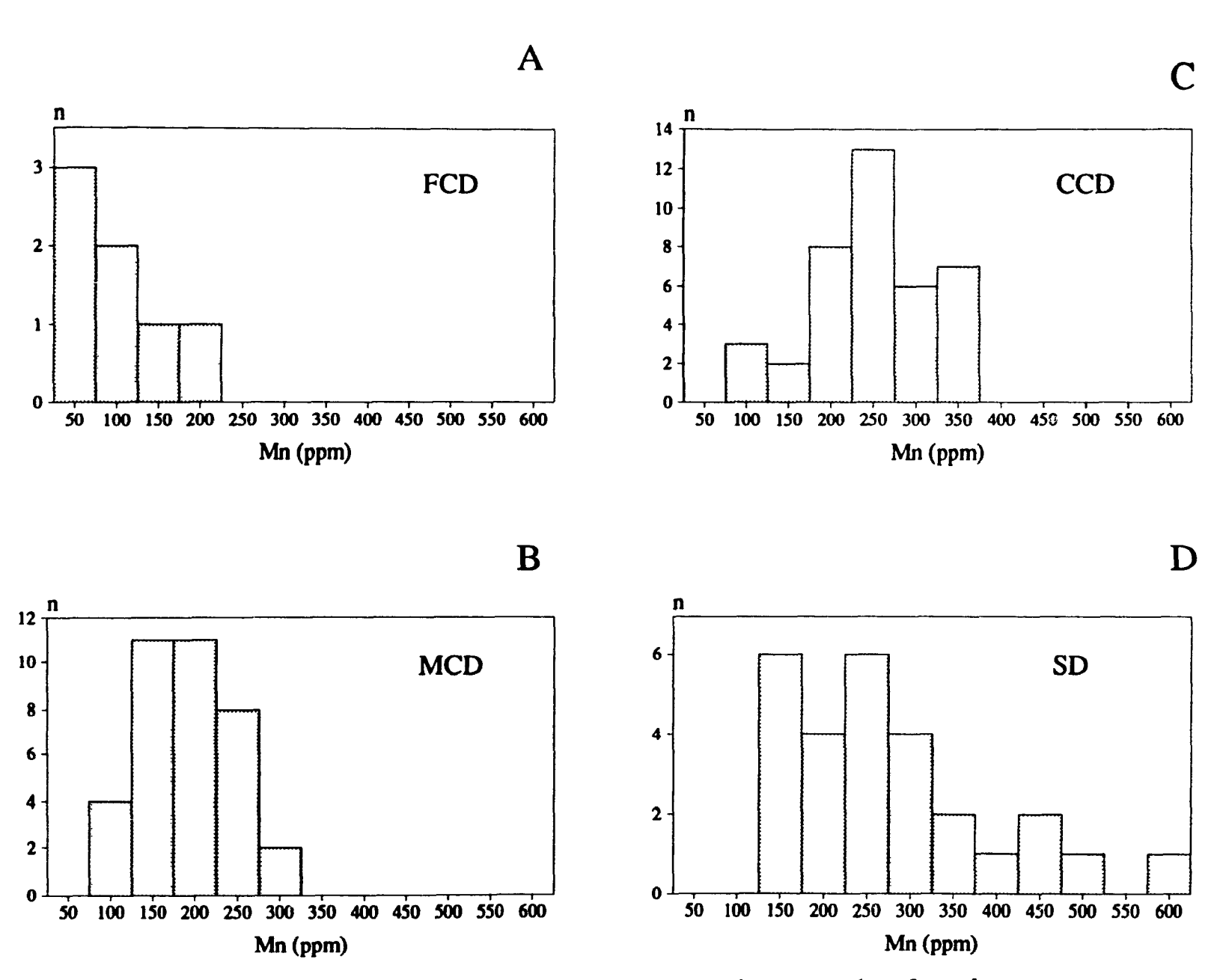


Figure 48. Mn concentration (ppm) of different dolomites. n= number of samples.

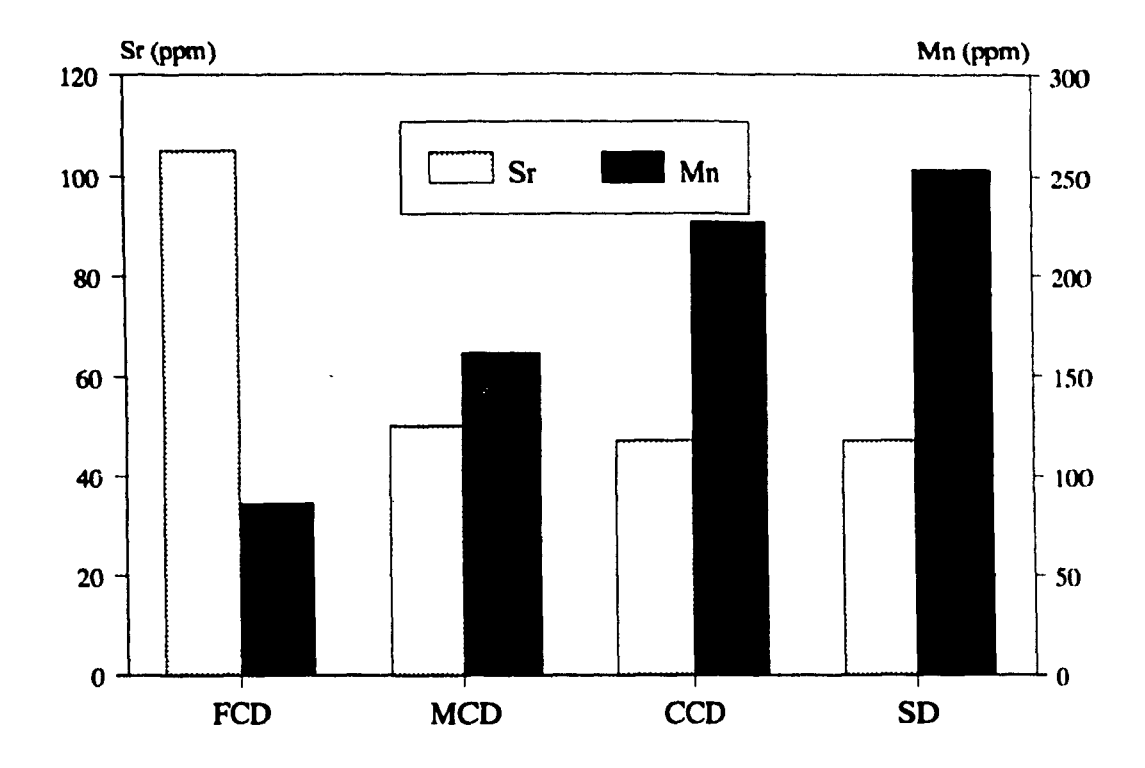


Figure 49. Average Sr and Mn contents (ppm) of different dolomites.

*نى*د

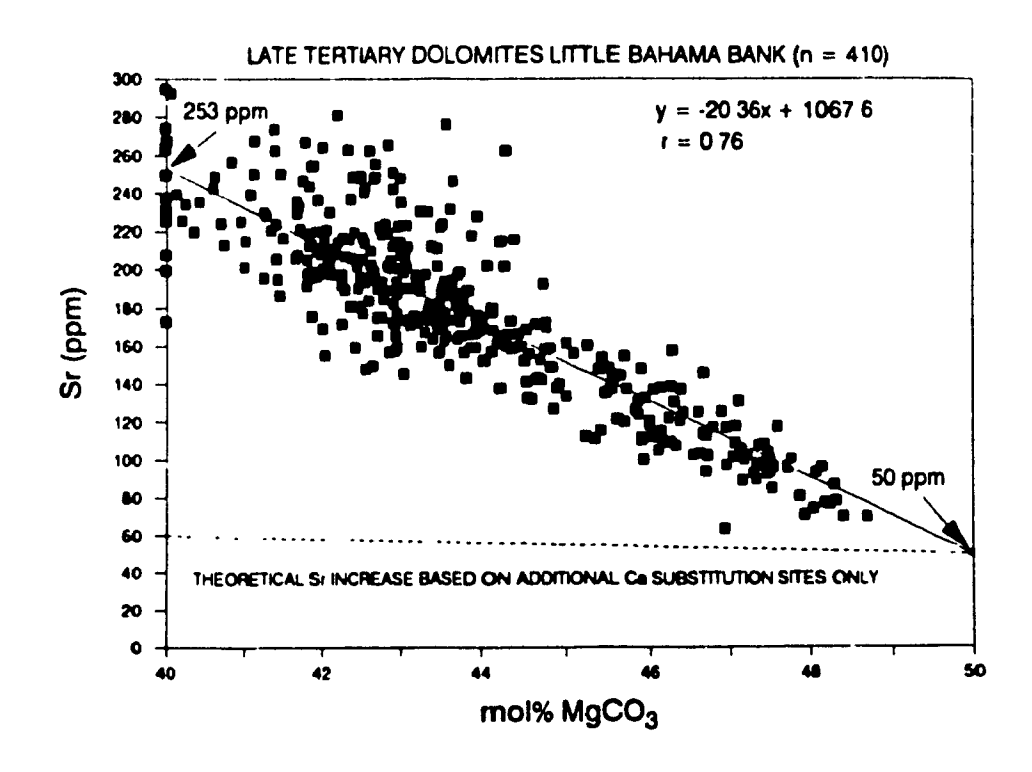


Figure 50. Cross plot of Sr (ppm) and mol % MgCO₃ for seawater dolomite from Little Bahama Bank (from Vahrenkamp and Swart 1990).

using the equation proposed by Vahrenkamp and Swart (1990):

$$D_{Sr}^{\text{dolomite}} = \frac{[50 + 20X]/Ca_{\text{dolomite}}}{[Sr^{2+}/Ca^{2+}]_{\text{fluid}}}$$

in which X = excess mol% of $CaCO_3$ in dolomite.

A $D_{sr}^{dolomate}$ of 0.0118 was suggested for stoichiometric dolomite, and this coefficient increases by about 0.0039 for every additional mol % CaCO₃ in nonstoichiometric dolomite (Vahrenkamp and Swart 1990).

Therefore a stoichiometric dolomite precipitated in equilibrium with seawater should have a Sr content of about 50 ppm, and 20 ppm Sr would be added for every excess mol % CaCO₃ in nonstoichiometric dolomite (Vahrenkamp and Swart 1990).

The reason for this increase is not known, but it may be due to rapid precipitation of nonstoichiometric dolomite which may favour the uptake of Sr, as well as the incorporation of Ca in Mg sites (Vahrenkamp and Swart 1990). Based on this, dolomite with 50-51 mol % CaCO₃ precipitating in equilibrium with seawater should have a Sr content of about 50-70 ppm, much lower than 128-155 ppm suggested by Machel and Anderson (1989), or 470-550 ppm suggested by Veizer (1983). However nonstoichiometric marine dolomites with 60 mol % CaCO₃ could have a Sr content as high as 250 ppm.

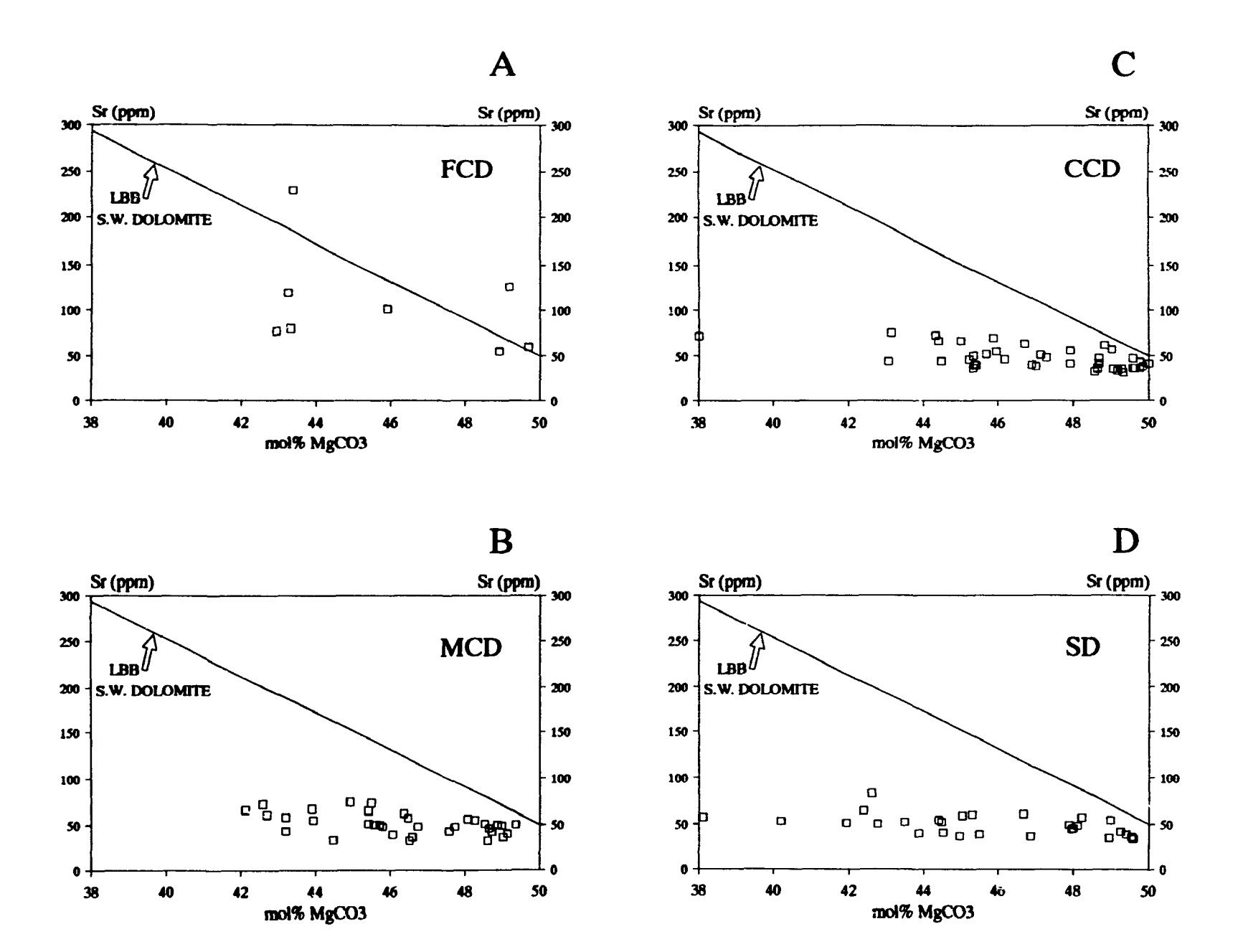
The Sr concentrations of FCD range from 55 to 225 ppm, and the relationship

between Sr concentration and mol % CaCO₃ is similar to Little Bahama seawater dolomites (Fig. 51A), suggesting that FCD may have formed from fluids with Sr²⁺/Ca²⁺ ratios similar to those of modern seawater. MCD, CCD, and SD are nonstoichiometric with 50 to 60 mol % CaCO₃ (Figs. 51B, 51C, and 51D). The relationship between Sr contents and mol % CaCO₃ deviates from the Little Bahama seawater dolomites (Figs. 51B, 51C, and 51D), suggesting that 1) the Sr²⁺/Ca²⁺ ratios of the dolomitizing fluids were modified from seawater; or 2) these dolomites were recrystallized and modified after dolomitization by diagenetic fluids with Sr²⁺/Ca²⁺ ratios different from seawater.

Mn concentration in carbonate is highly dependent upon precipitation rate and the [Mn2+]/[Ca2+] ratio of the folution (Pingitore et al. 1988; Mucci, 1988). The equilibrium concentration of Mn in calcite precipitated from seawater is 1 ppm (Veizer 1983). Seawater dolomite contains a similar amount of Mn (Veizer 1983). In the Presqu'ile barrier, the average Mn concentrations of various dolomite types are much higher than this. Because the distribution coefficients of Mn in carbonates are greater than one, Mn is preferentially incorporated into carbonates during diagenesis (Veizer 1983; Land 1985). In the Presqu'ile barrier, the average Mn increases from 86 ppm in FCD, to 161 ppm in MCD, 227 ppm in CCD, and 253 ppm in SD. FCD probably formed in seawater with low concentrations of divalent Mn, and hence contains the lowest amounts of Mn. The gradually increasing Mn contents in MCD, CCD and SD may be caused by: 1) decreasing precipitation rate (Pingitore et al. 1988; Mucci, 1988); 2) a change in the diagenetic environment (more reducing

Figure 51. Cross plots of Sr (ppm) and mol % MgCO₃ for dolomites from Presqu'ile barrier.

A) FCD; B) MCD; C) CCD; and D) SD.



with increasing burial), and/or 3) a change in the composition of the dolomitizing fluids (e.g. [Mn2+]/[Ca2+] ratio of the solution). As a result, more Mn was incorporated into dolomite crystal lattices during later dolomitization and possibly neomorphism.

5.6.3 FLUID-FLOW DIRECTION DURING DOLOMITIZATION

Machel (1988) recently proposed a qualitative mathematical model to identify fluid-flow direction during dolomitization using the bulk trace-element compositions of massive dolostones. The direction of flow of the dolomitizing fluids could be used as a criteria for helping to choose among various dolomitization models. If the Presqu'ile barrier was dolomitized by compactional fluids during shallow burial (Qing and Mountjoy 1989), or by rising fluids along faults and fractures (Aulstead *et al.* 1988), the direction of fluid flow should be upward. If Presqu'ile barrier was dolomitized by topography-driven flow (Garven 1985), the fluid flow should be lateral.

According to Veizer (1983) and Machel (1988), elements with distribution coefficients smaller than one (e.g. Sr) should increase downflow, if dolomites precipitate as cements (e.g. saddle dolomite in the Presqu'ile barrier), and/or if the dolomitizing fluid has a molar Sr/Ca ratio that is equal to or lower than that of the limestone precursor (in the situations where dolomites replace limestones). If dolomitizing fluids have a molar Sr/Ca greater than that of the limestone precursor,

Sr should decrease downflow. Elements with distribution coefficients larger than one (e.g. Mn) should decrease downflow if dolomite is precipitated as cements. In the case of the replacement of a limestone precursor, Mn trends could be sympathetic or antipathetic to those of Sr depending on the molar ratio of Mn/Ca of the dolomitizing fluid. Variations of Sr and Mn have been used to interpret the fluid-flow directions during dolomitization in the Cambrian Bonneterre Formation of southeast Missouri (Greggs and Shelton 1986) and the Devonian Nisku Formation in the Western Canada Sedimentary Basin (Machel 1988).

In an attempt to identify the direction of fluid flow during dolomitization, trace elements were systematically analyzed from seven wells in this study, with five wells from the Pine Point area (2813, 2822, 2729, 3306, and 2162), and two from the subsurface of northeastern British Columbia (B8 and B12). The samples analyzed in these wells usually cover vertical distances between 50 m and 250 m. Among 7 wells analyzed, four of them (2162, 3306, 2822, and 2813) were systematically sampled for MCD six (2729, 3306, 2822, 2813, B8, B12) for CCD, and two (B8 and B12) for SD.

Changes in the Sr and Mn concentrations were found in a few vertical profiles (Figs. 52 and 53). The antipathetic changes of Sr and Mn were observed only in well 2813 (Fig. 52A). In well 2813, Mn in MCD increases whereas Sr decreases upward, suggesting that the direction of fluid flow during dolomitization was probably vertical. An upward increase in Mn in MCD was also observed in well 2822 (Fig. 52B).

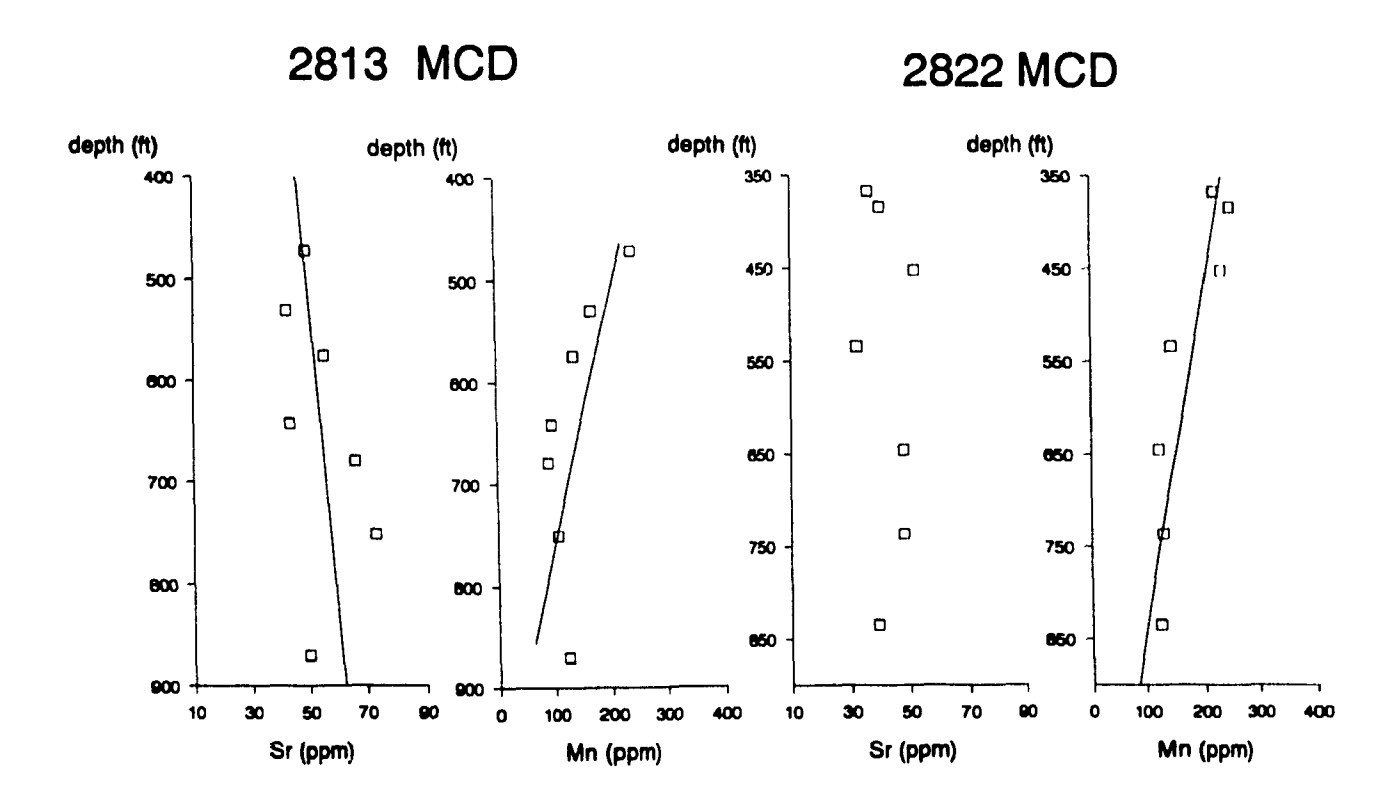


Figure 52. Vertical profiles of Sr and Mn of MCD for Pine Point diamond drill holes 2813 and 2822.

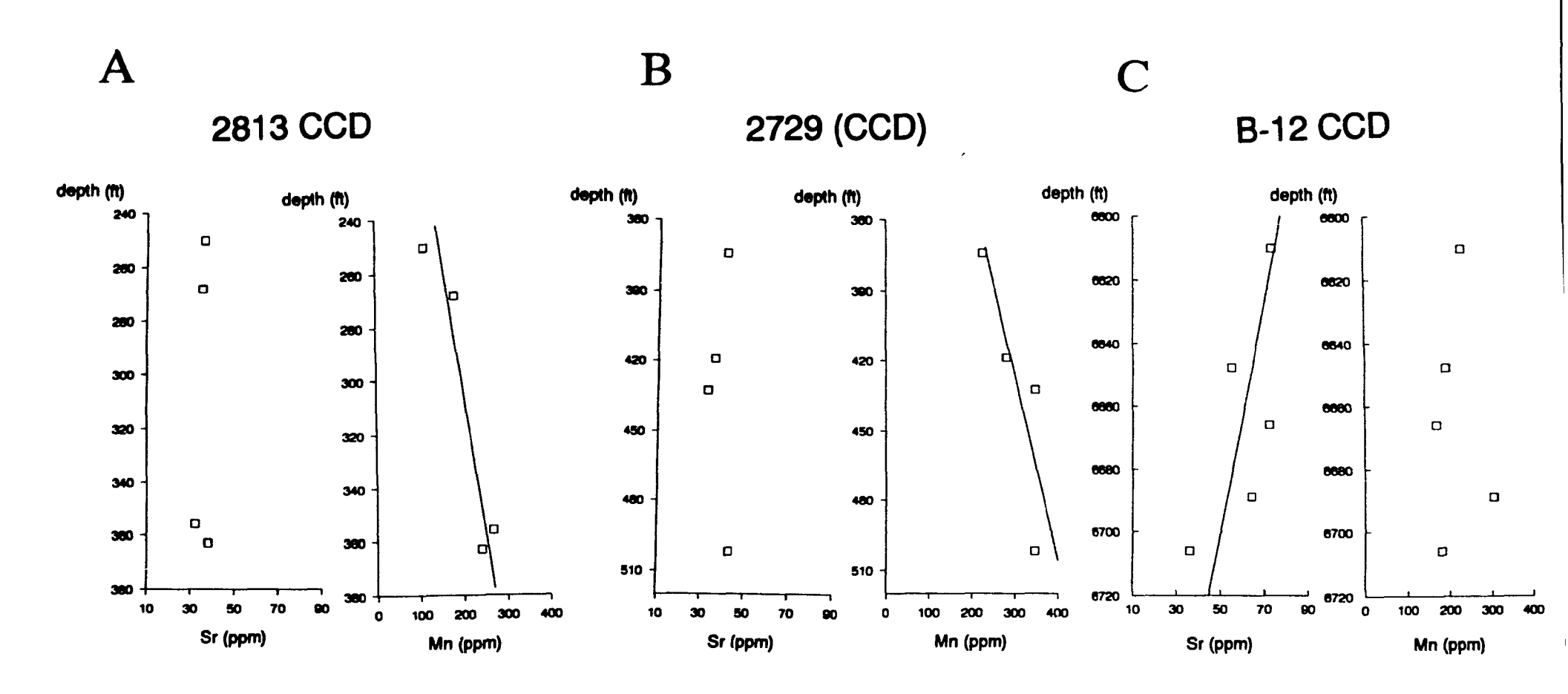


Figure 53. Vertical profiles of Sr and Mn of CCD.

A) well 2813, Pine Point. B) well 2729, Pine Point. C) B12, B.C.

In CCD of well 2813, Mn concentrations decrease upward opposite to the upward increase in Mn in MCD of the same well (Figs. 52A and 53A). Possibly the direction of fluid flow during the formation of CCD may have been opposite to that for MCD. An upward decrease of Mn in CCD also occurs in well 2729 (Fig. 53B). An upward increase of Sr in CCD was observed in well B12 (Fig. 53C). No systematically vertical changes of trace elements were found in saddle dolomites from the Presqu'ile barrier.

There are no appreciable systematic changes of Sr or Mn contents in other wells, therefore the fluid flow direction during dolomitization can not be derived from these data.

Sr and Mn concentrations of the saddle dolomites were also plotted according to the geographic locations (Figs. 54 and 55). Unlike the systematic changes in homogenization temperatures, O and Sr isotopes along the Presqu'ile barrier, there are no trends in Sr or Mn concentrations along the Presqu'ile barrier. Therefore the regional fluid-flow direction during dolomitization can not be derived from trace elements in this case.

Failing to find evidence for the direction of a regional fluid flow based on trace element analyses suggests that several factors may hamper a proper interpretation, as was discussed in the section on trace elements. Furthermore, the model proposed by Machel was based on a number of assumptions (Machel 1988). Among others, fluid composition, temperature, and pressure are assumed to remain constant; the flow rate is constant and flow direction is linear; the limestone

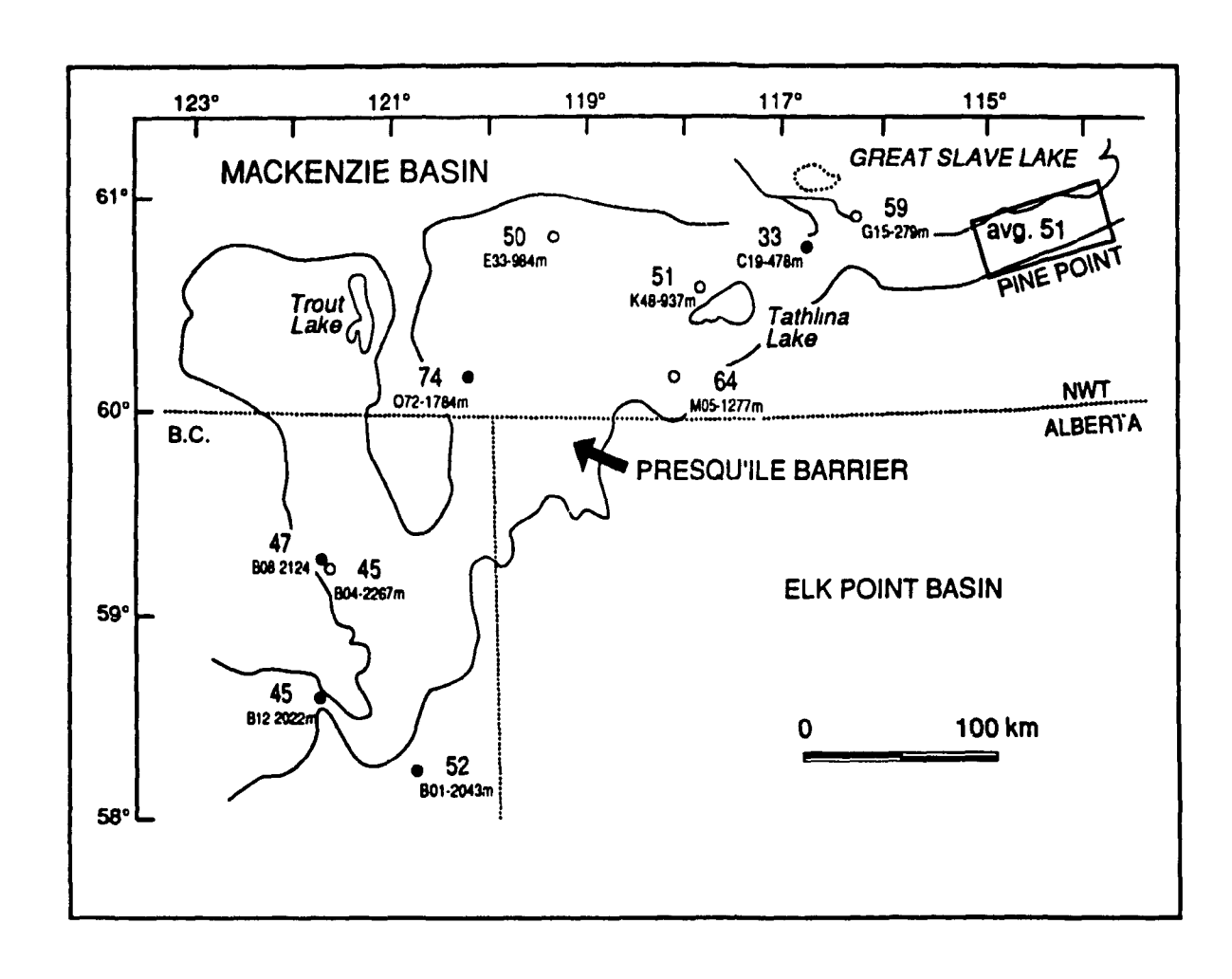


Figure 54. Variation of Sr concentration (ppm) of saddle dolomite in the Presqu'ile barrier.

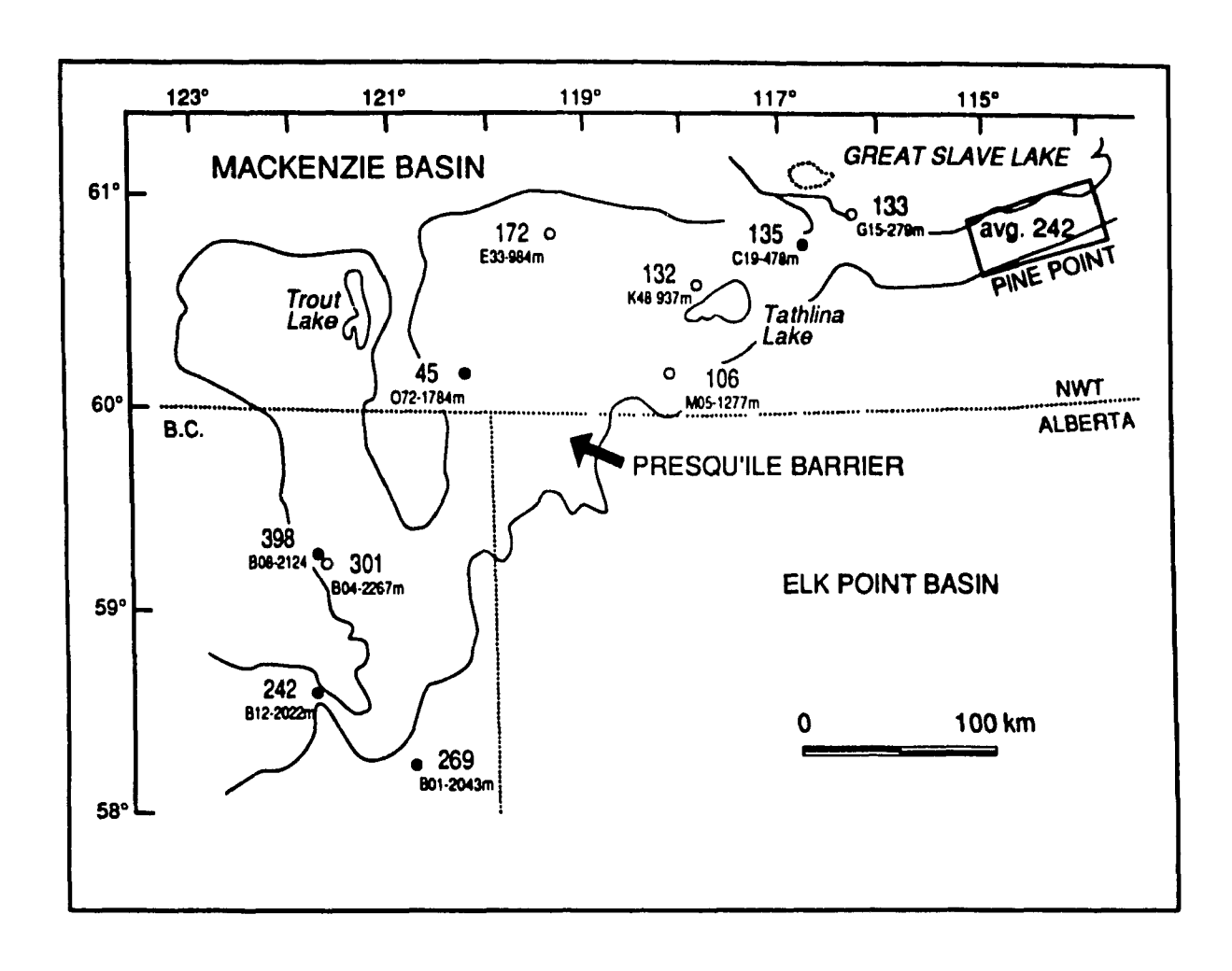


Figure 55. Variation of Mn concentration (ppm) of saddle dolomite in the Presqu'ile barrier.

precursor is compositionally and texturally homogeneous and contains few or no impurities (e.g. clay minerals, organic matter); the dolomite crystals must not be recrystallized later, or recrystallization must have taken place in a closed system with respect to the trace elements under consideration.

Some of these assumptions are difficult to meet in the case of dolomitization in the Presqu'ile barrier. For example, fluid compositions, temperatures, and pressures changed systematically along the Presqu'ile barrier, as indicated by the different Sr isotopes, homogenization temperatures, and in different parts of the Presqu'ile. The neomorphism of early MCD is also evident from cloudy centres and clear rims of dolomite crystals and their depleted oxygen isotopes. "Even if only some of these unfavourable conditions are realized", there may be no recognizable trends in trace elements (Machel 1988; p.122). This is probably why there are no appreciable systematic changes of trace elements in the majority of the wells analyzed along the Presqu'ile barrier.

5.7 DISCUSSION AND CONCLUSIONS

The Presqu'ile barrier has undergone diagenetic alteration in a variety of diagenetic environments. It probably was invaded by evaporitic brines from the Elk Point Basin, meteoric water during sub-Watt Mountain exposure, and basinal hydrothermal fluids during burial.

đ

A number of models (or hypotheses) have been proposed for the

dolomitization associated with the Presqu'ile barrier (Table 5).

Table 5. Previously proposed models of the dolomitization of the Presqu'ile barrier.

	FCD and MCD	CCD and SD	
Fritz and Jackson 1972	FCD: evaporated brines. MCD: modified seawater.	CCD: hydrothermal fluids	
Skall 1975	MCD: seepage reflux of evaporative brines.	pre-mineralization hydrothermal brines during post-Givetian times, or possibly post-Middle Devonian.	
Kyle 1981; 1983	evaporative pumping of seawater through the barrier.	mixing zone environment during sub-Watt Mountain exposure	
Krebs and Macqueen 1984	MCD: seepage reflux during early diagenesis.	CCD mixing zone environment superimposed by hydrothermal fluids SD: hydrothermal fluids	
Rhodes et al. 1984	J facies formed early in an arid evaporitic environment.	mixing zone environment during sub-Watt Mountain exposure	

These interpretations are based primarily on petrographic studies. Skall (1975) and Kyle (1981; 1983) suggested that the evaporitic brines of Elk Point Basin were responsible for the formation of the fine crystalline dolomite. The coarse crystalline dolomites were interpreted to have formed in a mixing zone during the Watt Mountain erosion (Kyle, 1981 and 1983; Rhodes et al., 1984). The white sparry saddle dolomite was interpreted as having precipitated from ascending hydrothermal brines (Krebs and Macqueen 1984).

The following interpretations are based on petrography, spatial distribution,

cross cutting relationships, diagenetic paragenesis, geochemistry, and fluid inclusion studies.

5.7.1 FINE-CRYSTALLINE DOLOMITE

- 1) FCD is restricted to the back-barrier facies and is interbedded with Muskeg evaporitic anhydrites in the Elk Point Basin.
- 2) The heaviest δ^{18} O value of FCD (-1.58 ‰ PDB) is within the range of calculated δ^{18} O values of dolomite precipitated from Middle Devonian seawater.
- 3) The \$7Sr/\$6Sr ratios of unalterer FCD range from 0.7079-0.7080, which corresponds to the estimated \$7Sr/\$6Sr ratio of Middle Devonian seawater (Burke et al. 1982). This suggests that the dolomitizing fluids for FCD were most probably Middle Devonian seawater and their original Sr isotope signature, similar to their oxygen isotopes, was not significantly affected by later diagenesis.
- 4) The relationship between Sr concentration and mol % CaCO₃ for FCD is similar to the Miocene marine dolomite from Little Bahama Bank, suggesting that FCD was formed in normal seawater or slightly modified seawater with "normal" [Sr²⁺]/[Ca²⁺].

Because FCD is interbedded with anhydrite in the Elk Point Basin, and because its δ^{18} O values and 87 Sr/ 86 Sr ratios are similar to those estimated and

calculated for Middle Devonian seawater dolomite, FCD probably formed penecontemporaneously at or just below the sea floor from Middle Devonian seawater. However, FCD sampled near the Pine Point orebodies has been altered during mineralization by later diagenetic fluids, as indicated by an increase in crystal size (up to $100 \mu m$), depleted $\delta^{18}O$ values (-6.7 to -7.1 % PDB), and slightly increased $^{87}Sr/^{86}Sr$ ratios (0.7082-0.7083).

5.7.2 MEDIUM-CRYSTALLINE DOLOMITE

- 1) MCD occurs in the lower part of the Presqu'ile barrier in the Pine Point Formation and is restricted to the southern and central (lower) part of the barrier. The northern part of the barrier remains undolomitized.
- 2) The heaviest δ¹⁸O values for MCD is -3.7 ‰ PDB, slightly depleted compared with the estimated δ¹⁸O signature of Middle Devonian seawater dolomites. However, the δ¹⁸O values of most MCD fall between -5 to -7 ‰ PDB, and are much more depleted than the estimated δ¹⁸O signature of Middle Devonian seawater dolomites.
- Three MCD were analyzed for ⁸⁷Sr/⁸⁶Sr ratios. One MCD has a ⁸⁷Sr/⁸⁶Sr ratio of 0.7081, comparable to the estimated ⁸⁷Sr/⁸⁶Sr ratio of Middle Devonian seawater. The ⁸⁷Sr/⁸⁶Sr ratios of the other two are 0.7085 and 0.7087, slightly more radiogenic than Middle Devonian seawater.
- 4) Sr concentration in MCD ranges from 30 to 79 ppm, averaging 50 ppm. The

relationship between Sr concentration and mol% CaCO₃ deviates from that of the Little Bahama seawater dolomites.

The data from the present study place constraints on but do not provide an unequivocal conclusion, concerning the origin of MCD. Among several possibilities, MCD could have occurred:

- during shallow burial at slightly elevated temperatures from fluids derived by means of compaction of strata: a) from downdip in the western part of the basin, and/or b) from the Elk Point or Mackenzie basins adjacent to the Presqu'ile barrier;
- soon after sedimentation of the Pine Point Formation by Middle Devonian seawater derived from the Elk Point Basin.

The geochemistry of MCD, especially the depleted δ^{18} O values and slightly radiogenic 87 Sr/ 86 Sr ratios, strongly support the first interpretation.

The second interpretation is based on the spatial distribution of MCD. The absence of MCD in the upper part of the barrier suggests that MCD probably formed soon after sedimentation. The restriction of MCD to the lower southern and central part of the barrier suggests dolomitizing fluids may have been derived from the Elk Point Basin, preferentially dolomitizing limestones adjacent to the Elk Point Basin. However the original O and Sr isotope signatures of MCD could have been modified during later neomorphism. In the Pine Point area, the δ^{18} O values of MCD have been systematically analyzed in wells 2813 and 2822. In well 2813, δ^{18} O values of

4

MCD vary from -7 ‰ PDB for samples close to CCD/MCD boundary, to -4 ‰ PDB for samples 100 m below the CCD/MCD boundary, suggesting that δ^{18} O values of MCD may have been modified by later diagenetic fluids that were responsible for CCD (Fig. 24). A similar trend in δ^{18} O is also found in well 2822.

5.7.3 COARSE-CRYSTALLINE AND SADDLE DOLOMITE

- 1) CCD and SD are closely associated with each other, occurring mainly in the upper part of the Presqu'ile barrier. Because of the intimate association of CCD and SD and their similar δ¹⁸O and δ¹³C values, ⁸⁷Sr/⁸⁶Sr ratios, and trace element concentrations, CCD and SD are interpreted to be dolomitized by diagenetic fluids of similar chemical compositions. CCD represents dolomitized limestones whereas SD occurred after CCD as dolomite cements that fill vugs and fractures 11 CCD.
- 2) Locally CCD and SD extend continuously across the sub-Watt unconformity.
 The geochemical signatures (e.g δ¹8O, δ¹3C, 87Sr/66Sr) and fluid inclusions
 (only in SD) of dolomites above the unconformity are similar to those below
 it. Therefore, these dolomites occurred after the sub-Watt Mountain exposure.
- 3) Both CCD and SD postdate stylolites, suggesting these dolomites occurred during burial. Although the onset of stylolitization can start in limestones at burial depths of 300 to 500 m, most stylolites probably formed at burial depths greater than 1000 m as chemical compaction and stylolitization are

continuous processes throughout burial.

- The timing of mineralization has been broadly constrained during two periods:

 1) Pennsylvanian to Permian by lead isotopes dating (Kyle 1981; Cumming et al. 1990), and paleomagnetic dating (Beales and Jackson 1982); or 2)

 Late Cretaceous to early Tertiary by fission track dating (Arne 1991) and computer modelling of basin hydrodynamics (Garven 1985). Therefore, the earliest possible timing of dolomitization is Pennsylvanian.
- is about 106 °C for Pine Point area and about 190°C for northeastern B.C. and the oxygen isotopes of CCD and SD (-7.0 to -16.0 ‰ PDB) suggest that CCD and SD formed at temperatures that exceed the maximum burial temperatures (65 °C at Pine Point and 160 °C in northeastern B.C.). CCD and SD are probably related to the regional influx of hydrothermal fluids, or to abnormally high othermal gradients in the Presqu'ile barrier. The low reflectance of ... '... ganic matter compared with relatively high reflectance of altered bitumen suggests that both late dolomites and mineralization are related to a hydrothermal event or events (Macqueen and Powell 1984; Krebs and Macqueen 1984).
- 6) The homogenization temperatures of SD fluid inclusions (Fig. 35), and the ⁸⁷Sr/⁸⁶Sr ratios of both SD and CCC (Fig. 31) gradually decrease from northeastern B.C. eastward updip along the Presqu'ile barrier, whereas the

δ¹⁸O values of CCD and SD (Fig. 26) become heavier eastward along the Presqu'ile barrier. The variation of homogenization temperatures, Sr and O isotopes along the Presqu'ile barrier are summarized in Table 6.

Table 6. Variation of maximum burial depth, ⁸⁷Sr/⁸⁶Sr, δ¹⁸O, and pressurecorrected fluid inclusion homogenization temperatures for saddle dolomite in different parts of the Presqu'ile barrier.

		Pine Point	Tathlina L. (SUB1)	NWT, W. of Tathlina L. & NE. B.C. (SUB2)
		East		West
max. burial depth		1.3-1.5 km	2-2.5 km	3-4 km
avg. 87Sr/86Sr ratio	SD	0.7083	0.7085	0.7097
	CCD	0.7085		0.7104
avg. δ¹8O (‰ PDB)	SD	-9.0	-11.8	-13.5
	CCD	-9.1	-11.9	-13.9
avg. pressure corrected Th	SD	106 °C	125-127 °C	160-190 °C

PROPOSED DOLOMITIZATION MODEL FOR CCD AND SD

The systematic and consistent increase in oxygen isotopes, decrease in homogenization temperatures and Sr isotopes, from northeastern B.C. eastward to the Pine Point area (Table 6) suggest a large-scale migration of hot and radiogenic dolomitizing fluids from west to east in the Presqu'ile barrier. As dolomitizing fluids moved eastward updip along the Presqu'ile barrier, the temperature of the fluids

gradually decreased and the radiogenic Sr was diluted by less radiogenic formation waters. Eastward updip flow of basin brines was probably established when hot fluids with radiogenic Sr were expelled tectonically from deeply buried sediments and crystalline basement due to tectonic thrusting and compression, sedimentary loading, and uplift of the foreland basin (Fig. 56).

真

According to Oliver (1986), when sedimentary rocks are buried beneath thrust sheets in zones of convergence, hot fluids would be expelled from sedimentary rocks by tectonic loading and these fluids would move updip into adjacent parts of the continent (Fig. 56). In the Western Canada Sedimentary Basin, tectonic deformation occurred in two main episodes, the first during the Late Jurassic to Early Cretaceous, and the second during the Late Cretaceous to Paleocene. Some dolomites could have occurred during the first episode. However, the main stage of dolomitization probably occurred during the second episode because: 1) fluid migration was probably more active during the Late Cretaceous to early Tertiary because a more extensive gravity-driven flow system was formed by uplift of the Cordilleran and foreland basin (Fig. 57) (Garven 1985; 1989); 2) the Western Canada Sedimentary Basin reached maximum burial during the Late Cretaceous and early Tertiary, which would make it easier to attain the temperatures of the dolomitizing fluids.

The Presqu'ile barrier is a linear carbonate buildup about 400 km long, extending eastward from the Cordilleran Orogenic belt to the Canadian Shield (Fig. 2). It probably has acted as a deeply buried regional porous and permeable conduit

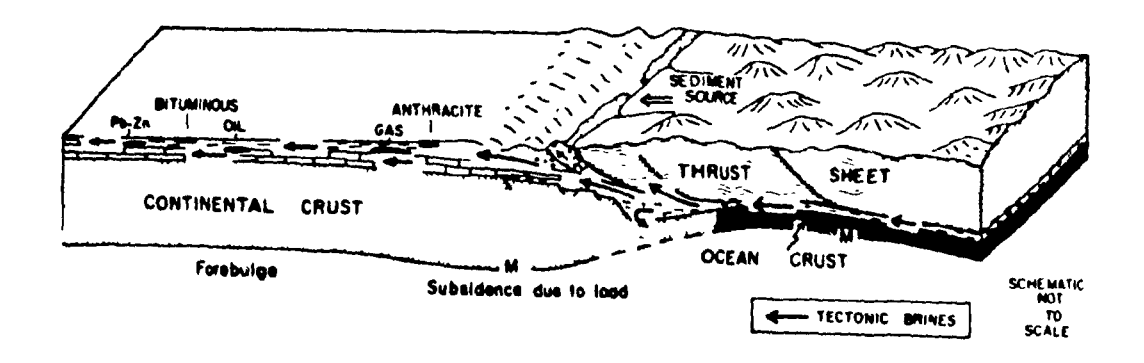


Figure 56. When sedimentary rocks are buried beneath thrust sheets, the fluids from the pores and hydrated minerals are expelled and injected into adjacent continent via conduit systems. These tectonically expelled fluids may play an important role in the diagenesis of sedimentary basin in terms of dolomitization, mineralization, as well as hydrocarbon migration (from Oliver 1986).

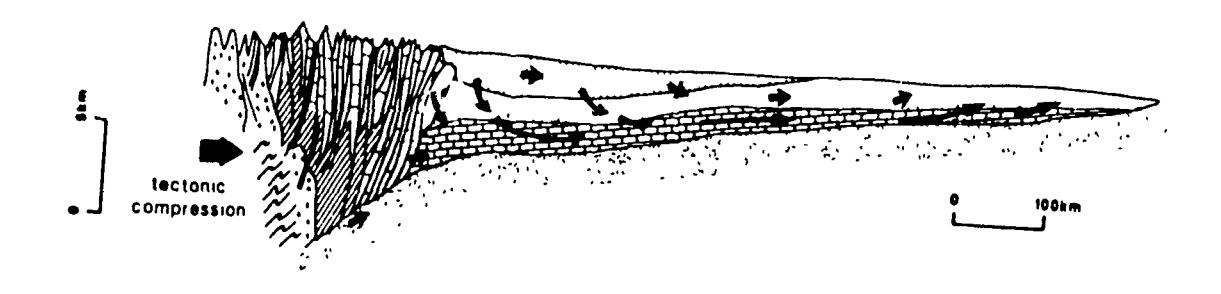


Figure 57. Schematic cross section of the Western Canada Sedimentary Basin during the Tertiary, soon after tectonic compression and foreland uplift. The arrows indicate modelled fluid-flow patterns (from Garven 1989).

system throughout most of its history. When hot fluids with radiogenic Sr were expelled tectonically from deeply buried sediments and the crystalline basement into the Presqu'ile barrier, the temperatures in the conduit increased, thus explaining why the homogenization temperatures of saddle dolomite fluid inclusions exceed the maximum burial temperatures of the Western Canada Sedimentary Basin. As the fluids moved updip eastward along the Presqu'ile barrier, they would gradually cool, resulting in the gradual eastward decrease in homogenization temperatures of SD, and corresponding increases in δ^{18} O values of SD and CCD.

The eastward decrease of the ⁸⁷Sr/⁸⁶Sr ratio suggests that ⁸⁷Sr enriched fluids derived from the deeper subsurface to the west were progressively diluted as they moved updip. The radiogenic fluids could have come from deeper buried sediments and/or from the crystalline basement downdip from the Presqu'ile barrier during tectonic thrusting and compression. This would result in the CCD and SD precipitated in the western part of the Presqu'ile barrier being the most radiogenic. As dolomitizing fluids moved eastward along the Presqu'ile barrier, the radiogenic Sr was gradually mixed with less radiogenic formation waters. As a result the ⁸⁷Sr/⁸⁶Sr ratio of CCD and SD decreased eastward along the Presqu'ile barrier.

Based on a study of the horizontal asymmetry of sulphide minerals in flatfloored vugs at Pine Point, Kesler et al. (1972) concluded that the net flow direction was up-dip along the barrier. This predicted flow direction is consistent with and supports the model of dolomitization proposed in this study.

The movement of meteoric waters into the Western Canada Sedimentary

Basin from uplifted mountains is supported by final melting temperatures of fluid inclusions in late-stage calcites, and the chemical and isotopic composition of the present day formation waters. In the Presqu'ile barrier, late-stage coarse-crystalline calcites precipitated from fluids of lower salinities (6 to 9 eq. wt.% NaCl) than saddle dolomites from the same locality (15 to 23 eq. wt% NaCl), based on measurements of the final melting temperatures (Fig. 46), indicating dilution of brines by meteoric waters. In the Edmonton area of the Western Canada Sedimentary Basin, the present day basin fluids display three distinct zones in terms of 87 Sr/ 86 Sr ratios, δ^{18} O values, and chemical compositions (Connolly et al. 1990a; 1990b). The δ^{18} O values of seven present day formation waters from Devonian carbonate reservoirs (Nisku and Leduc formations) range from -4.5 to -7.2 % SMOW (Connolly et al. 1990b). These values are depleted relative to oxygen isotopic equilibrium values of -1 to +5 % SMOW calculated from homogenization temperatures and δ^{18} O of SD (Fig. 45). The depleted δ^{18} O values in the present formation waters may be due to the regional influx of fresh water into the basin subsequent to the Laramide Orogeny (Connolly et al. 1990b). Inorganic chemical analyses suggested that the chemical composition of these formation waters was a mixture of a residual evaporated brine that has been diluted by post-Laramide but pre-present day meteoric water (Connolly et al. 1990a).

The formation of the coarsely crystalline dolomites and saddle dolomites in the Presqu'ile barrier have been interpreted to have resulted from the circulation of heated residual brines of the Elk Point basin that rose from depths of several kilometres along faults during an inferred Late Devonian thermal event (Aulstead et al. 1986; Morrow et al. 1990). The earliest possible timing of such a thermal event would be Pennsylvanian according to the age of mineralization.

The decrease of 87 Sr/ 86 Sr ratios and trapping temperatures with the corresponding increase of δ^{18} O values eastward along the Presqu'ile barrier support an interpretation of a large-scale migration of hot and radiogenic dolomitizing fluids from west to east. Eastward updip flow of basin brines was probably established by tectonic and sedimentary loading and by a gravity-driven flow system as a result of Cordilleran uplift during the Late Cretaceous and Paleocene. The homogenization temperatures, δ^{18} O, and δ^{87} Sr/ δ^{86} Sr together best fit and support this model.

RARE-EARTH ELEMENT GEOCHEMISTRY OF DOLOMITES IN THE PRESQU'ILE BARRIER: IMPLICATIONS FOR WATER/ROCK RATIOS DURING DOLOMITIZATION

6.1 INTRODUCTION

Trace elements and stable isotopes are commonly analyzed in carbonates to gain insights into the processes of diagenesis and dolomitization. Rare-earth element (REE) studies on dolomites, although only at a preliminary stage, can provide important information on the origin and diagenetic history (e.g Graf 1984; Dorobek and Filby 1988). Recent studies by Banner et al. (1988a; 1988b) suggest that REE patterns of the original limestones, unlike the trace elements and oxygen and carbon isotopes, are generally not affected during dolomitization, and that very large water/rock ratios (>10⁴) are required to alter REE patterns during diagenesis. Therefore, REE analysis may provide useful information on the process of dolomitization, especially with respect to water/rock ratios during dolomitization and subsequent neomorphism or recrystallization. Water/rock ratios are very important parameters for dolomitization in the subsurface environment, as there is a dispute whether enough Mg-bearing fluids are available for subsurface dolomitization (e.g. Morrow 1982; Land 1985; Machel and Mountjoy 1986; Hardie 1987). If insufficient

fluids were available, the so-called burial dolomites might only represent neomorphosed (or recrystallized) earlier dolomites (Morrow 1982; Land 1985).

In the Pine Point area (Northwest Territories, Canada), dolomites of the Presqu'ile barrier host one of the largest Mississippi Valley-type (MVT) deposits in the world. In the subsurface of the Northwest Territories and northeastern British Columbia, these dolomites also form important reservoir rocks for hydrocarbon exploration. Understanding the origin of these dolomites is important for both mineral and petroleum exploration and exploitation. REE concentrations were determined from 29 samples from Presqu'ile barrier as part of a regional study of dolomitization in the Presqu'ile barrier (Appendix 6). Identification of REE fractionation of the dolomites is done by normalizing the concentration of each REE by its value in average meteoritic chondrite in order to compare our study with previous studies on ancient dolomites that used this standard normalization (e.g. Graf 1984; Derobek and Filby 1988; Banner et al. 1988a; 1988b). For comparison with the literature data, the REE patterns of limestones, FCD, and SD also have been normalized to the North America shale composite (NASC).

6.2 RESULTS

Two samples of pelloidal grainstone from the Sulphur Point Formation in the Pine Point area have REE patterns similar to those of the North America shale composite (NASC), showing overall sub-horizontal trends when normalized to

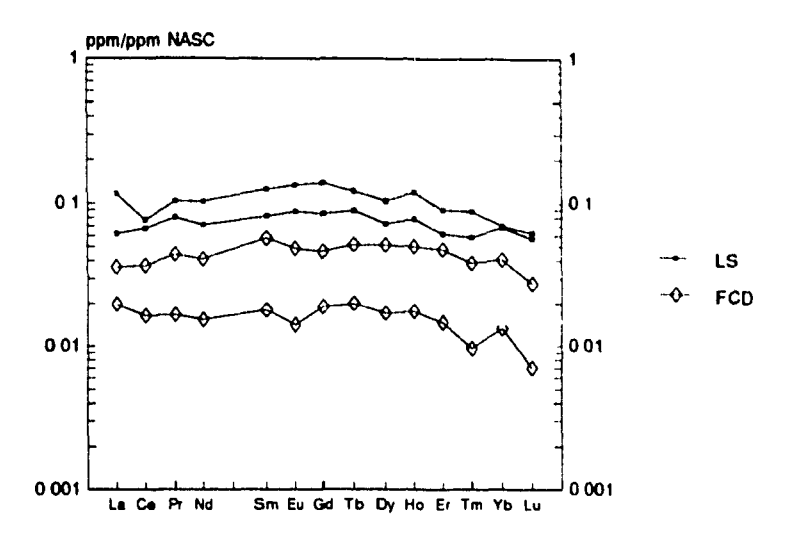
NASC (Fig. 58A). When normalized to chondrite, the pelloidal limestones display strong light REE enrichments and distinct negative Eu anomalies (Fig. 58B).

The REE patterns for two unaltered FCD samples from the Muskeg Formation about 5 km south of the barrier are similar to marine limestones and NASC, showing sub-horizontal trends when normalized to NASC (Fig. 58A). Relative to chondrite, FCD is strongly enriched in light RFE but depleted in Eu (Fig. 58B).

The REE patterns of five MCD samples of the Pine Point Formation from drill holes in the Pine Point area are different from those of limestone and FCD. Relative to chondrite, the REE patterns are inclined from La to Sm, nearly horizontal from Gd to Tm, and inclined again for Yb and Lu. MCD patterns also have distinct negative Ce and Eu anomalies (Fig. 59).

Five CCD samples (with three from the Pine Point area, one from the subsurface of the NWT, and one from northeastern B.C.) were analyzed for REE. The REE patterns of CCD from the Pine Point area are generally different from those of marine limestones. Relative to chondrite, the Pine Point samples are enriched in light REE with variable REE contents and slightly negative Ce anomalies. One sample also has a distinct negative Eu anomaly (Fig. 60). The REE pattern for CCD from the subsurface of the NWT does not have a negative Ce anomaly (Fig. 60). CCD from northeastern B.C. has distinct negative La and Ce anomalies (Fig. 60).

Six SD from the Pine Point area and 2 from the subsurface of northeastern B.C. were analyzed for REE (Fig. 61). The REE patterns of Pine Point samples are similar to those from the subsurface of B.C. SD has REE patterns quite different



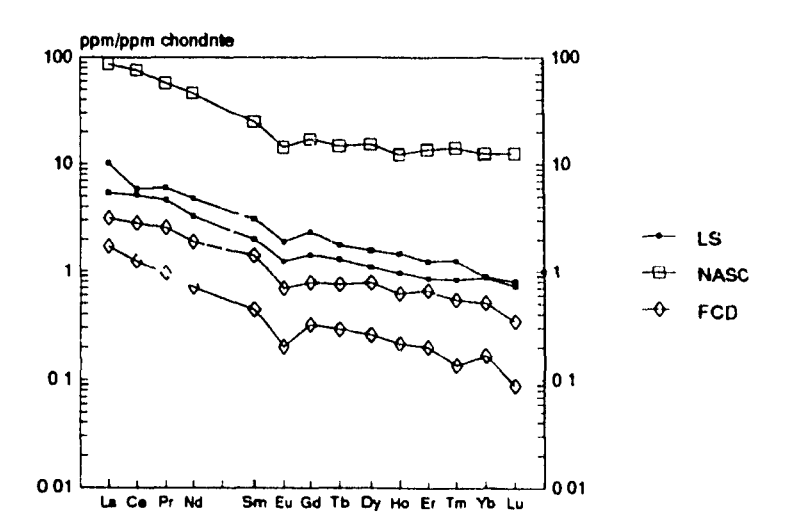


Figure 58. A) REE patterns of limestones (solid squares) and fine-crystalline dolomite (diamonds), normalized to North American shale composite (NASC).

B) REE patterns of limestones (solid squares), FCD (diamonds), and NASC (open squares), normalized to chondrite.

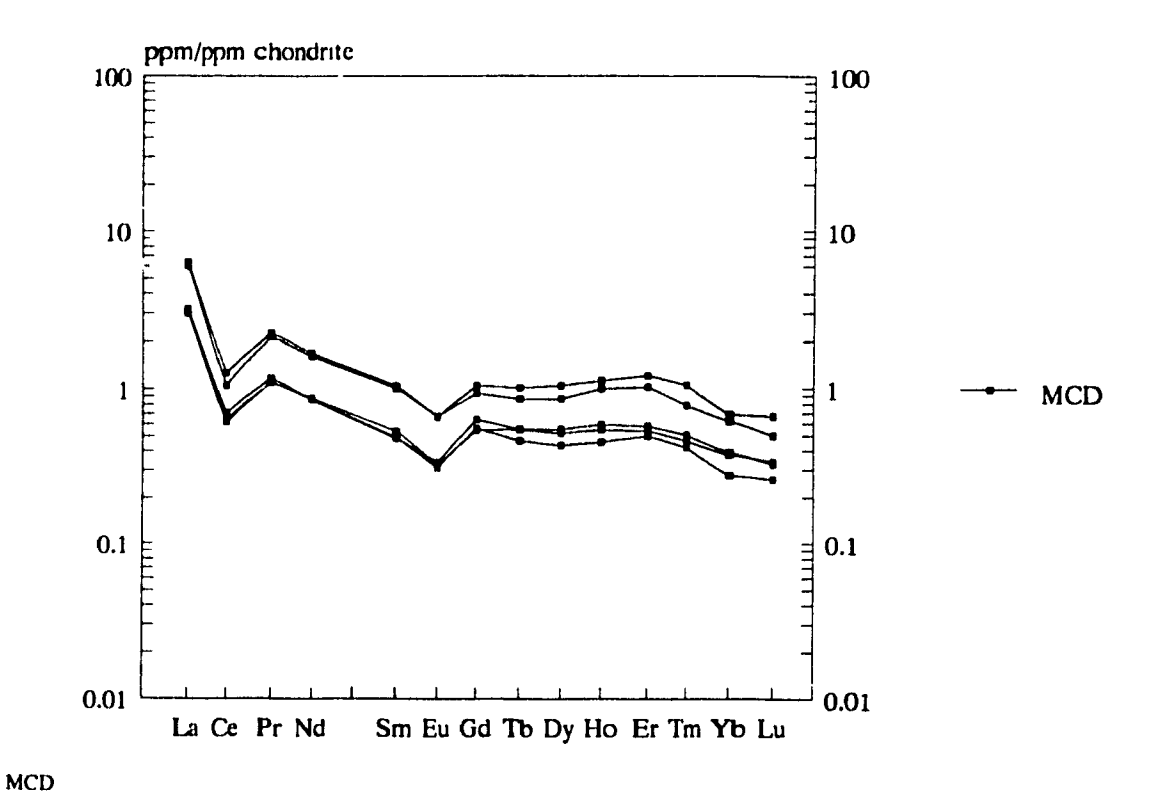


Figure 59. REE patterns of medium-crystalline dolomites (chondrite normalized). All the samples are from Pine Point.

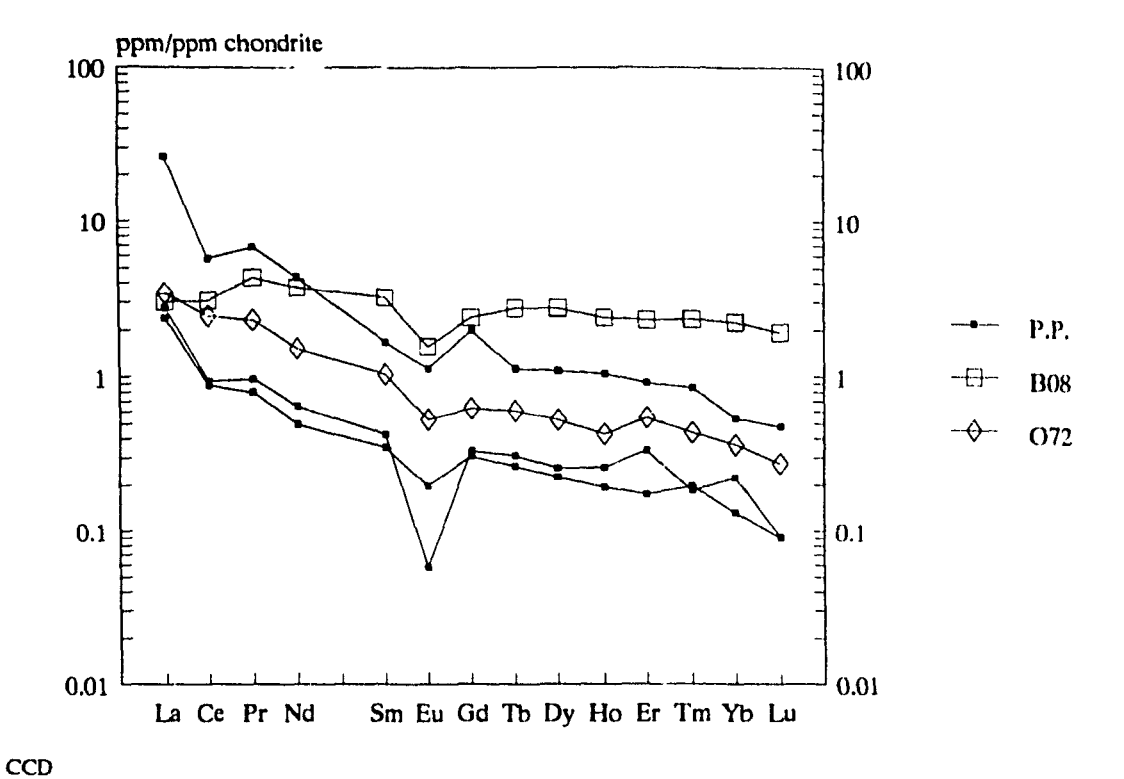
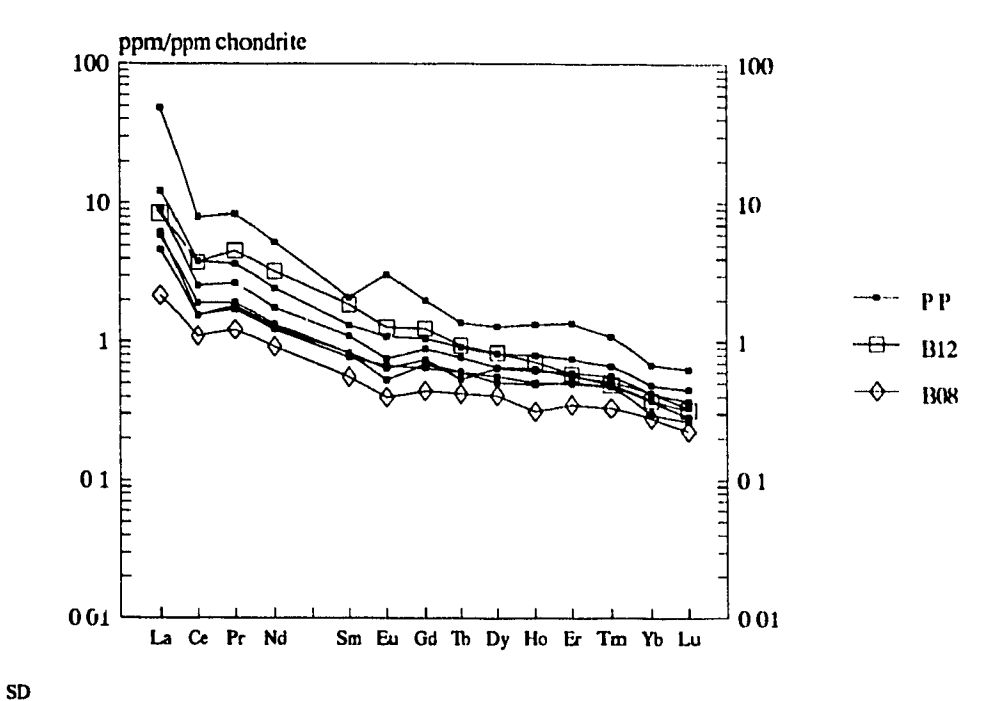


Figure 60. REE patterns of coarse-crystalline dolomites (chondrite normalized). Pine Point samples in solid squares, sample from well 072 (NWT) in diamonds, and sample from well B08 (northeastern B.C.) in open squares.



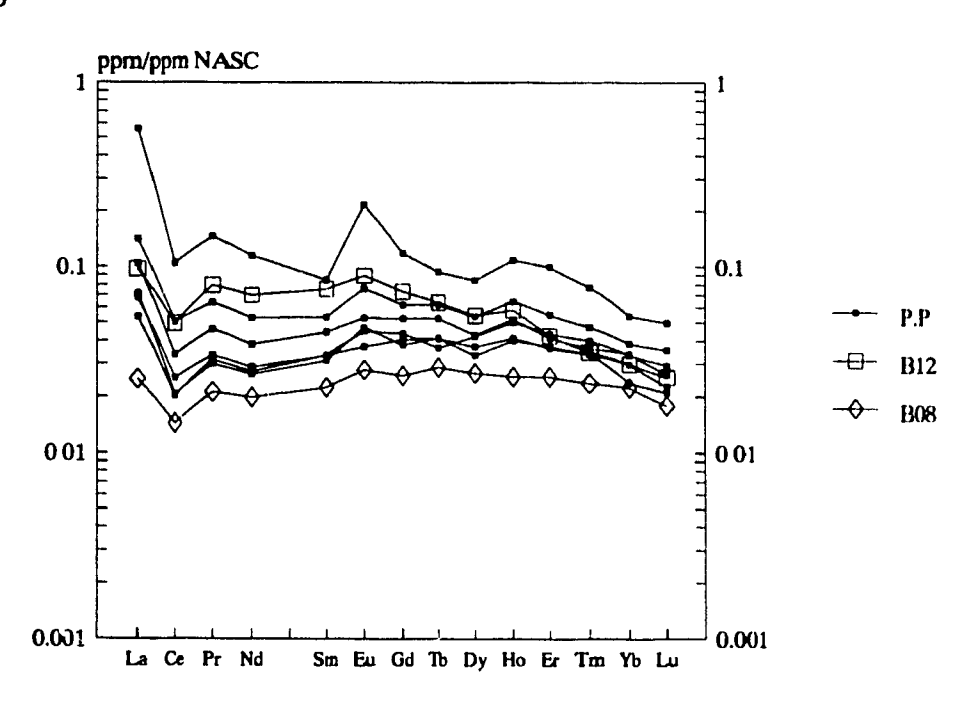


Figure 61. REE patterns of saddle dolomites. Pine Point samples in solid squares, sample from well B08 (northeastern B.C.) in diamonds, and sample from well B12 (northeastern B.C.) in open squares.

A) chondrite normalized, and B) NASC normalized.

from those of marine limestones. Relative to chondrite, SD samples are enriched in light REE, with moderately negative Ce anomalies (Fig. 61A). One Pine Point SD sample has a positive Eu anomaly. When normalized against NASC (Fig. 61B), most SD samples are enriched in La but slightly depleted in the heavy REE (Er-Lu). Most of the samples show a slight positive and one Pine Point sample shows a distinct Eu anomalies relative to NASC (Fig. 61B).

The REE patterns of 5 Pine Point WCC samples have a inclined base line, with enrichments of light REE. It shows a distinctive enrichment in La. All samples have a slight negative Ce anomaly (Fig. 62).

The REE patterns of three Pine Point LCC samples have slight positive La anomalies and negative Ce anomalies (Fig. 62). One sample is depleted in the heavy REE (Tm-Lu) (Fig. 62).

6.3 DISCUSSION

The concentration of REE in dolomite is probably influenced by the following factors (Humphris 1984; Dorobek and Filby 1988): 1) the concentration of the REE in the original unaltered rocks; 2) the concentration of REE in the dolomitizing fluids; 3) the partitioning of the REE between the dolomitizing fluids and precipitating dolomite; and 4) water/rock ratios during diagenesis. High water/rock ratios indicate open systems while low water/rock ratios indicate closed systems. Massive dolomitization is usually thought to take place in an open system because

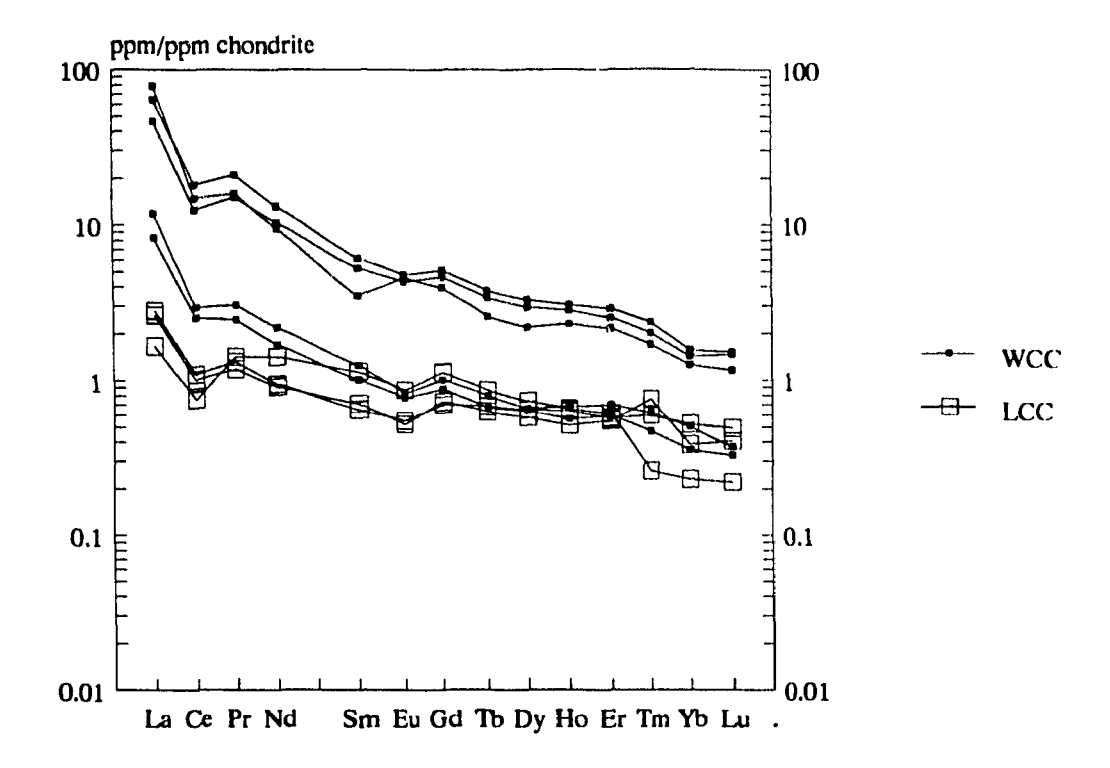


Figure 62. REE patterns of late-stage coarse crystalline calcite (LCC) and white calcite (WCC), chondrite normalized. All samples from Pine Point.

of the large amounts of Mg needed for dolomitization (e.g. Morrow 1982; Land 1985; Machel and Mountjoy 1986).

The REE presumably could be incorporated into carbonate minerals in the following ways similar to other trace elements (see Veizer 1983): 1) substituting for Ca²⁺ or Mg²⁺ in the carbonate lattice; 2) occurring as separate REE carbonate phases; 3) occurring in interstices between lattice planes; 4) occupying lattice positions which are free due to structural defects; 5) adsorbed due to remnant ionic charges; 6) occurring in fluid inclusions; and 7) as non-carbonate phases, such as clay minerals, authigenic feldspar, quartz.

Little is known concerning the importance of these factors, except for substitution in the carbonate lattice, which is governed by the *distribution coefficient* (K_D). The distribution coefficient for a individual REE in CaCO₃ in an open system at equilibrium is given by (Palmer 1985):

$$K_{D} = \frac{(m_{REE}/m_{Ca})_{calcite}}{(m_{REE}/m_{Ca})_{fluid}}$$

7

where m indicates molar concentration.

REE abundances in most natural waters, e.g. seawater, river water, ground water, and in some hydrothermal waters, are extremely low, varying from 10⁻⁶ to 10⁻³ ppm (McLengan 1989). High-temperature acidic hydrothermal solutions can have REE concentrations exceeding 10⁻³ ppm (McLennan 1989). Carbonates precipitated from seawater are enriched in REE by several orders of magnitude relative to the seawater. The estimated partition coefficients for REE, therefore, are very large, on

partition coefficients are on the order of 10² for Quaternary biogenic calcite (Scherer and Seitz 1980; Palmer 1985). The measured effective REE partition coefficients vary from 1400 for La to about 460 for Lu for Jurassic marine limestones from southern Germany, indicating relative enrichment of the light REE (Parekh et al. 1977).

As REE concentrations in carbonate rocks are usually 10² to 10³ times higher the diagenetic carbonates formed from the than REE in the natural waters, neomorphism and/or replacement of the previous carbonates should have REE patterns similar to those of the original unaltered carbonates. According to Dorobek and Filby (1988) and Banner et al. (1988a; 1988b), if water/rock ratios are low, REE patterns of the diagenetic minerals will resemble those of the original rock, because the REE will be derived largely from the dissolution of the rock. Quantitative modelling by Banner et al. (1988a; 1988b) indicates that very large water/rock ratios (>10⁴) are required to alter REE patterns in diagenetic carbonates (Fig. 63). Because concentrations of O, Sr, and C in the diagenetic fluids and carbonates are significantly higher than those of REE, the water/rock ratios required to alter the original O, C, and Sr isotopes of carbonates are several order-of-magnitude lower, depending on the fluid and rock concentrations (Banner et al. 1988a; 1988b) (Fig. 63).

The REE patterns for FCD are similar to those of the marine limestones, suggesting that the formation of FCD did not significantly alter the REE patterns of

豫..

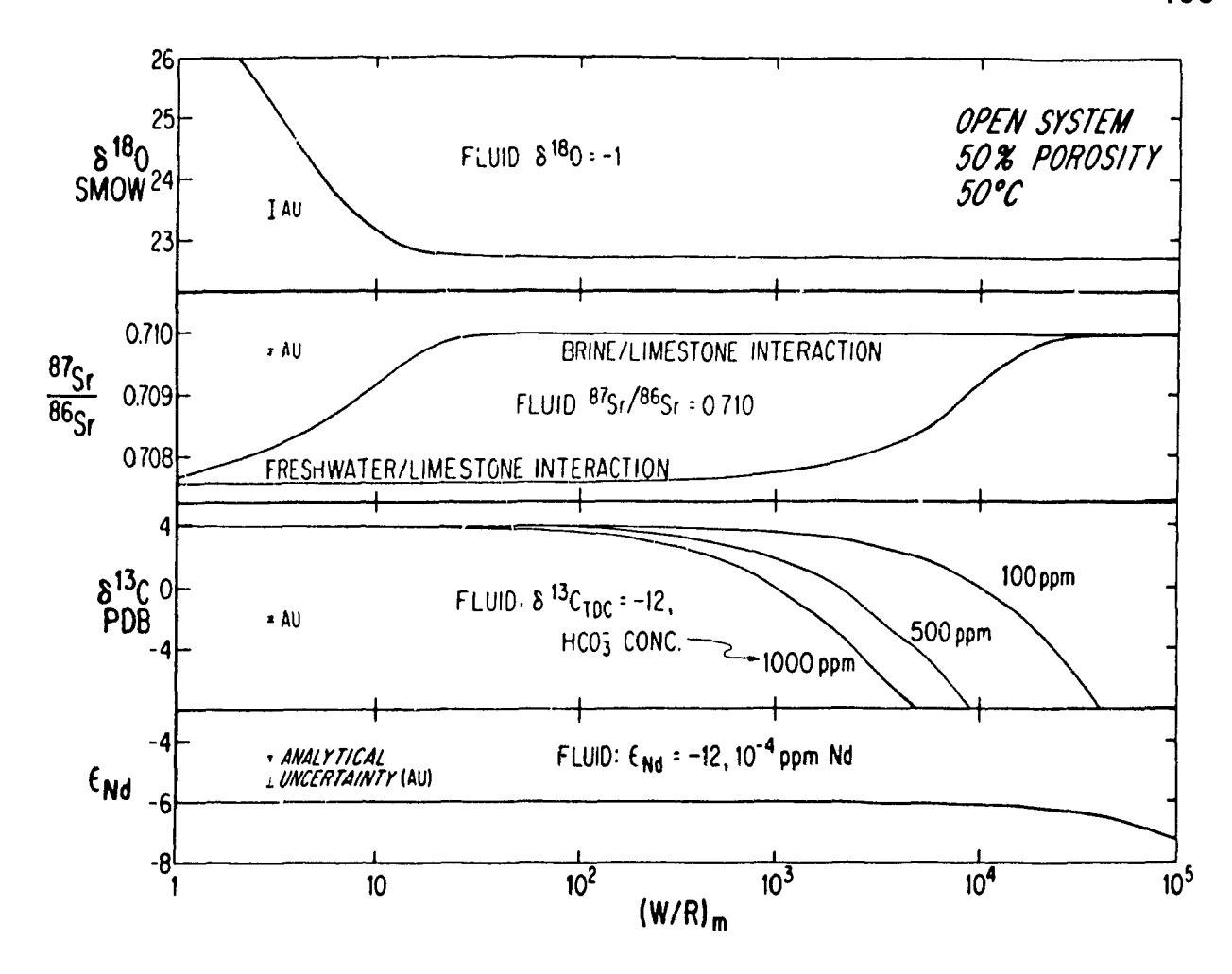


Figure 63. Variations in the isotopic composition of O, Sr, C, and Nd during open-system recrystallization of limestone as function of increasing molar water/rock ratio, (W/R)m. Owing to the differences in the concentrations of these elements in diagenetic fluids and carbonates, there are significant differences in the water:rock ratios required to alter the original rock composition. O isotopes significantly deviate from the original rock composition at water:rock of 10. C and Sr isotopic composition respond at variable rates, depending on the fluids compositions. For Nd isotopes, no significant changes from the original rock composition are obtained at water:rock ratios of up to $5x10^4$ (from Banner et al. 1986).

the parent carbonates. Based on petrographic studies and geochemical analysis, FCD is interpreted to be limestones that were dolomitized penecontemporaneously at or just below the sea floor by Middle Devonian seawater in the Elk Point Basin. As FCD generally has low permeability, the diagenetic fluids responsible for later mineralization and dolomitization had little access to FCD, and did not significantly affect the REE patterns and other geochemical characteristics of FCD. This interpretation is also supported by restriction of FCD to the back-barrier facies in the evaporitic Elk Point Basin, where it is interbedded with evaporitic anhydrites (Fig. 6B). In addition, Sr isotope values for FCD fall on the curve for Middle Devonian seawater (Burke *et al.* 1982). Three FCD samples have δ^{18} O values range from -1.6 to -3.8 % PDB, close to the equilibrium values with Middle Devonian seawater.

MCD has REE patterns different from limestones and FCD. The origin of MCD is not certain. MCD could have formed in at least two different diagenetic settings: (1) during shallow burial at slightly elevated temperatures by fluids derived from compaction of sedimentary rocks a) from downdip in the western part of basin, and/or b) from Elk Point Basin; (2) soon after sedimentation by Middle Devonian seawater from the adjacent the Elk Point Basin. The first interpretation is supported by the geochemical data (especially depleted δ^{18} O values) as discussed earlier.

The second interpretation is mainly based on the spatial distribution of MCD.

The absence of MCD in the upper part of the barrier (Fig. 6B) suggests that MCD probably formed soon after sedimentation. The restriction of MCD to the southern and central part of the Presqu'ile barrier (Fig. 6B) suggests that dolomitizing fluids

may have been derived from the Elk Point Basin (south of the Presqu'ile barrier). Therefore, limestones adjacent to the Elk Point Basin would have been preferentially dolomitized, whereas the northern part barrier remains undolomitized (Fig. 6B). If Middle Devonian seawater from the Elk Point Basın was the dolomitizing fluid for MCD, MCD should have geochemical signatures of Middle Devonian seawater, with δ^{18} O from -1.2 to -2.2 ‰ PDB, 87 Sr/ 86 Sr from 0.7078 to 0.7081, and REE patterns similar to those of marine limestones and FCD. However, the average δ^{18} O value of 21 MCD samples from the Pine Point area is 5.9 % PDB, the average value of 87Sr/86Sr of 3 MCD samples is 0.7084, and REE patterns of 5 MCD samples are distinctly different from those of FCD. These geochemical analyses suggests that MCD was probably neomorphosed during later diagenesis. As MCD is generally porous and permeable, it may have been modified by later diagenetic fluids, which formed CCD and SD. The different REE patterns of MCD, compared with those of marine limestones and FCD, suggest that MCD may have been neomorphosed in a diagenetic system with a large water/rock ratio.

Because of the close association between CCD and SD, and the similarity of their oxygen, carbon, and Sr isotopes (Chapter 5), CCD and SD are interpreted to have formed from similar dolomitizing fluids. High La/Ce ratios distinguish CCD and SD from limestone and FCD. Unlike FCD, the REE patterns of CCD and SD are quite different from undolomitized marine limestones of the Presqu'ile barrier, indicating that water/rock ratios during dolomitization were very high. At Pine Point, CCD and SD host one of the largest MVT deposits in the world. The formation of

MVT deposits demands a regional fluid flow to transport sufficient Pb and Zn for mineralization (Anderson 1983; Garven 1985; Anderson and Macqueen 1976). If the ore-forming period was 0.5 to 5.0 million years, with a flow rate of 1 to 5 m/yr, as suggested by Garven (1985), the water/rock ratios for mineralization at Pine Point would vary from 0.5 x 10^6 to 25×10^6 . These rates are much larger than the minimum ratios (5 x 10^4) required to alter the REE patterns of carbonates (Banner et al. 1988), assuming their calculations and assumptions are correct.

In the Pine Point district and the adjacent subsurface of the Northwest Territories and northeastern British Columbia, both CCD and SD extend continuously from the Sulphur Point Formation, across the Watt Mountain unconformity, and into the lower part of the Slave Point Formation (Qing and Mountjoy 1990; Rhodes et al. 1984). Thus, the formation of CCD and SD clearly postdates the deposition of the Slave Point Formation, and they could not have formed in a mixing zone associated with the Watt Mountain Formation as previously suggested by Kyle (1981; 1983). Locally, CCD precipitated along stylolites in limestones, suggesting that it probably formed at burial depths of more than 500-1,000 m.

In the Presqu'ile barrier, 87 Sr/ 86 Sr ratios and homogenization temperatures decrease with a corresponding increase in δ^{18} O values from northeastern British Columbia eastward to Pine Point. These geochemical trends suggest that hot, radiogenic fluids probably moved updip from west to east along the Presqu'ile barrier. Such a large-scale fluid migration most probably occurred during the

tectonic and sedimentary loading in the Western Canada Sedimentary Basin, when hot fluids were expelled from the deeper part of the basin west of the Presqu'ile barrier by tectonic thrusting and compression and by a gravity-driven flow system as a result of foreland basin uplift.

The REE patterns for WCC and LCC are different from those discussed above. As LCC precipitated after sulphide minerals and saddle dolomites in the vugs and fractures, its FEE patterns may represent the REE compositions of diagenetic fluids after mineralization.

In another MVT district, the Viburnum Trend, southeast Missouri, the REE geochemistry of the carbonate rocks from the Bonneterre Formation is similar to that of the Presqu'ile dolomites. The REE patterns of unmineralized dolostones in the Viburnum Trend are similar to patterns of adjacent limestones (Graf 1984), suggesting that the late-diagenetic fluids responsible for Pb-Zn mineralization had little influence on the unmineralized dolostones. By contrast, the mineralized dolostones and saddle dolomites have very different REE patterns (Graf 1984), suggesting that these dolomites resulted from different fluids with very high water/rock ratios.

Dolomitization and subsequent recrystallization do not always significantly modify the original limestone REE signatures. Such a case is demonstrated by Banner et al. (1988a; 1988b) for dolomites in the Burlington-Keokuk Formation of Iowa, Illinois, and Missouri. Two major episodes of regionally extensive dolomitization (dolomite I and its recrystallized product, dolomite II) were recognized

1

and correlated in the Burlington-Keokuk Formation. These dolomites were interpreted to have formed in distinctly different diagenetic environments based on differences in petrography, trace element abundances, and stable and strontium isotopic compositions. Dolomite I was interpreted to have formed in a seawater-freshwater mixing environment associated with a regional meteoric-groundwater system established beneath late Mississippian/early Pennsylvanian unconformities. Dolomite II was interpreted to represent recrystallization of dolomite I in warm subsurface fluids. Although dolomitization and subsequent recrystallization produced profound textural and compositional changes with respect to cathodoluminescence, Sr, O and C isotopes, they did not significantly alter REE patterns of the original carbonates. This indicates that there are differences in the mobility of Sr, O, and REE during diagenesis and dolomitization (Banner et al. 1988a; 1988b).

The REE study of the regionally extensive Burlington-Keokuk dolomites suggests that dolomitization and subsequent recrystallization do not necessarily modify REE signatures of the original carbonates, although dolomitization generally requires large amounts of fluid to transport Mg²⁺ to the reaction site (Morrow 1982; Land 1985; Machel and Mountjoy 1986; Hardie 1987). Very large water/rock ratios are required to alter REE patterns, as appears to be the case for dolomitization in the Presqu'ile barrier at Pine Point, and in the Bonneterre Formation of the Viburnum Trend.

6.4 CONCLUSIONS

Fine-crystalline dolomite (FCD) is interpreted to have formed penecontemporaneously by seawater and/or evaporated seawater in the Elk Point Basin. REE patterns of FCD are similar to those of marine limestones, suggesting that late diagenetic fluids did not significantly modify REE patterns of FCD.

Medium crystalline dolomite (MCD) probably formed at shallow burial depths by compactional fluids, or soon after sedimentation by Middle Devonian seawater derived from the Elk Point basin. Compared with marine limestones and FCD, MCD has different REE patterns. This, together with the depleted O isotopes and slightly radiogenic Sr isotopes of MCD, suggesting that MCD was probably neomorphosed in an open diagenetic system with high water/rock ratios. Because MCD is very porous and permeable, its REE patterns may have been modified by later diagenetic fluids that were responsible for formation of CCD, SD, and sulphate minerals.

The REE patterns for coarse-crystalline dolomite (CCD) and saddle dolomite (SD) are different from those of limestones and FCD. CCD is interpreted as a replacement of limestones, whereas SD precipitated as dolomite cement soon after CCD. Water/rock ratios during dolomitization were probably high, resulting in distinctive REE patterns for CCD and SD. CCD and SD are interpreted to have been dolomitized by hot fluids expelled from deeply buried sediments by tectonic

thrusting and compression and by a gravity-driven flow system as a result of foreland basin uplift in the Cordilleran orogenic belt.

The different REE patterns of the four types of dolomites in the Presqu'ile barrier suggest that enormous volumes of fluids were available for subsurface dolomitization. The specific sources of the fluids and their driving mechanism need to be carefully identified in each case.

À

HYDROTHERMAL ORIGIN OF DISSOLUTION VUGS AND BRECCIAS IN PRESQU'ILE BARRIER, HOST OF PINE POINT MVT DEPOSITS

7.1 INTRODUCTION

Mississippi Valley-type (MVT) deposits hosted in carbonate rocks are closely associated with dissolution vugs and breccias, and the origin of these solution features is still controversial (e.g. Ohle 1985; Sangster 1988). Some workers related these vugs and breccias to meteoric karst systems (or unconformities) (e.g. Harris 1971; Kyle 1981; Rhodes et al. 1984). Mineralization was considered to be a later, separate diagenetic event. For most MVT deposits, "support for meteoric dissolution is largely circumstantial and little or no clear cut evidence has yet been recognized" (Sangster 1988; p.114). Others suggested that the most important part of dissolution, insofar as the orebodies were concerned, was accomplished by warm hydrothermal fluids (e.g. Bogacz et al. 1970; Dzulynski 1976; Sass-Gustkiewicz et al. 1982; Anderson 1983; Ohle 1985; Anderson and Garven 1987; Sangster 1988).

Carbonate rocks of the Middle Devonian Presqu'ile barrier host one of the world's largest MVT deposits at Pine Point and these carbonates were subjected to considerable dissolution and brecciation. The dissolution features at Pine Point were interpreted by some authors as a classic example of meteoric karst that formed during the sub-Watt Mountain exposure (e.g. Kyle 1981; 1983; Ford and Williams 1990).

However, others suggest that hydrothermal fluids also played a role in the formation of these dissolution features (e.g. Skall 1975; Rhodes *et al.* 1984; Krebs and Macqueen 1984) (Table 7). The objective of this chapter is to discuss which fluids and processes caused major dissolution in the Presqu'ile barrier at Pine Point.

Table 7. Some previous interpretations on formation of dissolution vugs.

AUTHORS	PROPOSED TIME	EVIDENCE
Kyle 1981; 1983	during sub-Watt Mountain exposure	vugs, fractures, and CCD occur below the unconformity.
Krebs & Macqueen 1984	PennPermian emergence	vadose silt and "eyebrow texture" indicating influence of meteoric water.
Rhodes <i>et al</i> . 1984	initiated during sub-Watt Mountain exposure and reactivated later	Slave Point Fm. was foundered and collapsed into the dissolution features.

Understanding the timing and origin of dissolution and the distribution of the porous host rocks is important for both mineral and hydrocarbon exploration strategies. Also the results from this study have implications for other MVT districts, where hydrothermal dissolution may have been overlooked and incorrectly attributed to subaerial solution.

7.2 DISSOLUTION FEATURES AT PINE POINT AND ADJACENT SUBSURFACE

ą,

The origin and timing of the dissolution features at Pine Point is controversial (Table 7). Based on observations from open pits from the eastern and central part of the Pine Point mine, Kyle (1981) deduced that dissolution was restricted to below sub-Watt Mountain unconformity, and, therefore, suggested that the solution events occurred during the sub-Watt Mountain exposure. Rhodes et al. (1984) proposed that the dissolution was initiated during the sub-Watt Mountain exposure and reactivated later based on the fact that dissolution features extend into the overlying Slave Point Formation. Krebs and Macqueen (1984), however, suggested that solution occurred later during Pennsylvanian-Permian emergence. It is difficult to determine how much dissolution resulted from the action of meteoric waters during sub-Watt Mountain exposure in the Presqu'ile barrier at Pine Point, because late diagenesis, especially dolomitization and mineralization, greatly obscures the earlier diagenetic features. To address this problem, core samples from 32 wells (Appendix 1 and Fig. 1) from the adjacent subsurface Presqu'ile barrier were studied. As these wells are not related to any ore deposits, the influence of the later stage hydrothermal fluids is more easily identified. If the dissolution at Pine Point was caused mainly by meteoric waters during the sub-Watt Mountain exposure, then similar features should also be observed in the Presqu'ile barrier in the adjacent subsurface, because the sub-Watt Mountain unconformity represents a widespread regional subaerial exposure

SCALE OF DISSOLUTION

In seven wells from the subsurface NWT and northeastern British Columbia, cores were sampled across the Watt Mountain/Sulphur Point contact in the Presqu'ile barrier. In these wells, dissolution, which can be directly related to the sub-Watt Mountain unconformity, is small in scale. Some dissolution breccia and vugs occur at the top of the Sulphur Point Formation, just beneath the sub-Watt Mountain unconformity (Fig. 9). These vugs are small, 1 to 2 centimetres, and are commonly filled with a green shale matrix (Fig. 9A). Solution breccias occur only locally and are restricted to several metres immediately beneath the unconformity at the top of the Sulphur Point Formation (Fig. 9B).

The solution and brecciation associated with the MVT deposits at Pine Point, in contrast, are extensive and occur on a much larger scale. Solution features were observed in all of the MVT orebodies and the size of vugs ranges from a few centimetres to a few metres (Fig. 10). The solution features at Pine Point are well described by Kyle (1981), Rhodes and others (1984), Krebs and Macqueen (1984), and Qing and Mountjoy (1990).

In the subsurface, the material that fills dissolution vugs and breccias related to the sub-Watt Mountain unconformity differ from those that fill vugs and breccias associated with the MVT deposits at Pine Point. Pendant calcite cement, which is diagnostic of the vadose zone, was observed in one well (Fig. 9C). These pendant cements extend up to 12 metres below the unconformity. Green shale matrix is the most common material that fills dissolution vugs and breccias beneath the unconformity (Figs. 9A and 9B). The origin of the green shale is not certain. It probably represents materials deposited during the subsequent marine transgression and/or formed during subaerial exposure.

Dissolution vugs and breccias associated with the Pine Point ore deposits, in contrast, are not filled with green shale, but are partially filled with saddle dolomite, sulphide minerals, pyrobitumen, and late-stage coarse-crystalline calcite cement (Figs. 10). These products are generally absent in dissolution vugs that are associated with the sub-Watt Mountain unconformity. Pendant cements are not found in the larger vugs and caves at Pine Point.

SPATIAL DISTRIBUTION OF DISSOLUTION FEATURES

If dissolution vugs and breccias at Pine Point were caused mainly by meteoric waters during sub-Watt Mountain exposure, these dissolution features should be

restricted below the unconformity. In the subsurface, the solution vugs and breccias related to the sub-Watt Mountain exposure are restricted to several metres immediately beneath the unconformity. However, at Pine Point large-scale dissolution and brecciation occurs continuously across the unconformity as indicated by the cross sections of open pits N81, W85, and A70 (Figs. 19 and 20). Massive dissolution, dolomitization, and mineralization occur above the unconformity in pit N81 (Figs. 19 and 64). Clearly, dissolution occurred some time after the sub-Watt Mountain exposure.

Our observations at Pine Point suggest that large-scale solution is closely associated with the occurrence of saddle dolomite (Fig. 64), a feature also noted by Rhodes et al. (1984). The dissolution vugs and breccias are "closely associated with Presqu'ile dolomite, such that the two major dissolution trends parallel the zone of maximum Presqu'ile development" (Rhodes et al. 1984, p.1052). Much of the dissolution and mineralization occurs in the Sulphur Point Formation below the unconformity at Pine Point. However, where saddle dolomites and/or mineralization extend from the Sulphur Point Formation, across the unconformity, into the overlying Watt Mountain and Slave Point Formations (e.g. pits N81, W85, and A70), large-scale dissolution and mineralization also cross the unconformity (Figs. 19, 20, and 64).

Extensive dissolution was also observed locally in the subsurface Presqu'ile barrier (e.g. in the NWT: in wells C-19, D-50, O-72, F-48, F-24; in northeastern British Columbia: wells B08 and B12, Fig. 1). The dissolution vugs are not

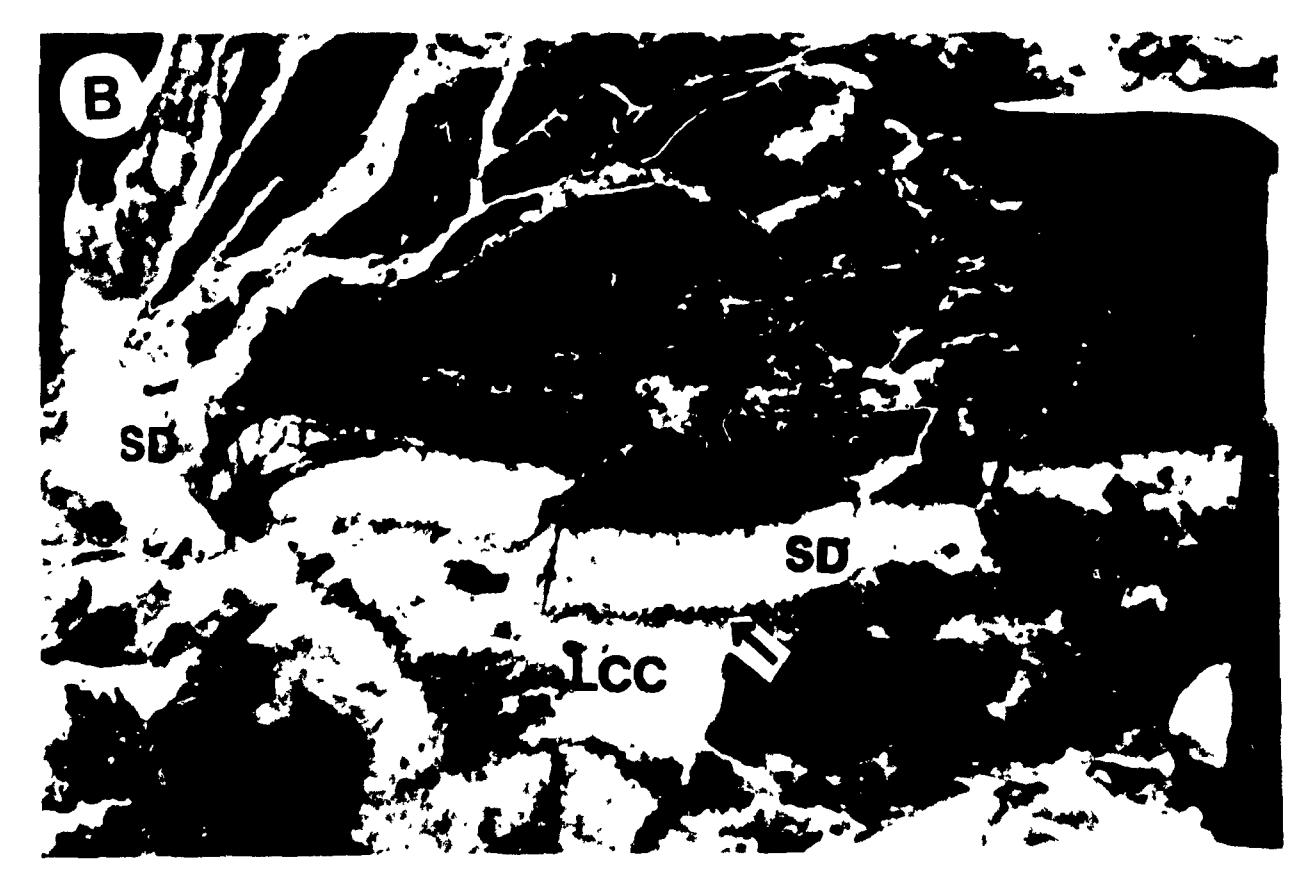
Figure 64.

A) A section about 5 m above the sub-Watt Mountain unconformity Pine Point, showing well developed fractures and dissolution vugs along bedding, which are filled with saddle dolomite, bitumen, and late stage coarse crystalline calcite.

Location: Watt Mountain Formation, pit N81, Pine Point. Scale bar 0.5 m.

B) Closer view of A. Argillaceous coarse-crystalline dolomite of the Watt Mountain Formation is fractured. The fracture and vugs are filled with a thick band of saddle dolomite (SD), which in turn was coated with a thin layer of pyrobitumen (arrow). The late stage calcite crystals (LCC) are the latest diagenetic product in the vugs. Hammer for scale.





restricted to strata below the sub-Watt Mountain unconformity, but rather they are closely related to the presence of saddle dolomites, irrespective of their stratigraphic position. In well O-72, saddle dolomites, as well as large-scale dissolution, extends from the Sulphur Point Formation across the unconformity into the overlying Slave Point Formation (Fig. 21). However, in adjacent well F-48, large-scale dissolution was not observed immediately beneath the sub-Watt Mountain unconformity (Fig. 21). The Sulphur Point Formation and the upper 90 m of Pine Point Formation are limestones in this well. Large-scale dissolution occurred between 1865 and 1887 m (6120 and 6190 ft), where massive saddle dolomites are present (Fig. 21). In well F-24, tight limestones occur below the sub-Watt Mountain unconformity and there is no obvious dissolution associated with the unconformity. However, where saddle dolomite is present 61 m below the unconformity, large-size vugs are present (Fig. 21). The well history reads "drill bit dropped 0.3 m at 1693 m" and at 1898 m "drill rough and fast". These examples suggest that large-scale dissolution is not associated with the unconformity, but rather is closely associated with the occurrence of saddle dolomites.

The fluid-inclusion data from Pine Point and the subsurface Presqu'ile barrier suggest that saddle dolomites were precipitated from very saline (10 to 31 eq. wt.% NaCl), hydrothermal brines (85 to 210 °C) (discussed in Chapter 5), rather than in a mixing zone environment during the sub-Watt Mountain exposure. Fluid inclusions were also measured from saddle dolomites both below and above the sub-Watt Mountain unconformity. Their homogenization, initial and final melting temperatures

are similar (Fig. 46), suggesting that these saddle dolomites precipitated from the same or similar fluids.

In summary, dissolution related to the sub-Watt Mountain exposure in the subsurface differs from the solution features that host the MVT deposits at Pine Point in three aspects: 1) scale of dissolution, 2) materials that fill solution features, and 3) spatial distribution of solution features. Dissolution vugs related to meteoric dissolution during the sub-Watt Mountain exposure are small (usually 1 to 2 cm) and are restricted only to local zones immediately beneath the unconformity, whereas vugs that host MVI deposits at Pine Point are much larger, ranging from centimetres to metres in size, and are more extensive. Dissolution features related to the sub-Watt Mountain unconformity are commonly filled with green shale matrix, locally with pendant calcite cements, while dissolution vugs at Pine Point are commonly filled with saddle dolomite, sulphide minerals, and coarse-crystalline calcite cement. The spatial distribution of these large-scale solution features is not controlled by the sub-Watt Mountain unconformity, but rather is closely associated with the occurrence of saddle dolomites, which is present both above and below the sub-Watt Mountain unconformity. Solution occurred in several phases prior to and associated with saddle dolomites, and the major phase of dissolution clearly postdates the sub-Watt Mountain exposure. The fluid inclusion study indicates that saddle dolomites precipitated from very saline hydrothermal fluids.

7.3 DISCUSSION

The interpretation of a meteoric origin of dissolution vugs and breccias of the Presqu'ile barrier was based on information available in the 70's. At that time, mineral exploration was mainly in the eastern part of the Pine Point property, where strata above the unconformity have been eroded and it was conceivable to assume that dissolution features and mineralization were restricted to the interval below the unconformity. However, in the late 70's and 1980's, mining activities in the western part of the property exposed the strata above the unconformity, and showed that dissolution and mineralization extend continuously across the unconformity.

Therefore, it is unreasonable to attribute the large-scale dissolution that host Pb and Zn deposits at Pine Point to sub-Watt Mountain exposure only. Carbonate dissolution in this region was caused by two different processes: meteoric and hydrothermal.

Undoubtedly some dissolution and brecciation was associated with meteoric water during the sub-Watt Mountain exposure as indicated by subsurface core samples. In their summary, Rhodes et al. (1984; p.1052) stated that "the timing of this karst is not readily proven; however it seems most likely that it was *initiated* in periods of subaerial exposure" before the deposition of the Watt Mountain Formation and "it has been reactivated" later. Earlier meteoric dissolution during the sub-Watt Mountain exposure, combined with possible tectonic fracturing (Skall 1975) and local dissolution of anhydrite (Beales and Hardy 1980), probably enhanced the porosity and

permeability in the barrier and produced some of the conduits for passage of later hydrothermal fluids. Krebs and Macqueen (1984) suggested that the dissolution vugs and fractures may have been enhanced by meteoric waters during the Pennsylvanian-Permian emergence, when the Presqu'ile barrier at Pine Point was uplifted and much of the Devonian-Mississippian sequence was eroded as a result of a progressively westward tilting of the Western Canada Sedimentary Basın. However it is difficult to estimate how much dissolution occurred during this period. Krebs and Macqueen (1984) also suggested that dissolution developed during the Pennsylvanian-Permian emergence may have continued during the main mineralization stage.

However, meteoric water during the sub-Watt Mountain exposure caused only minor dissolution. The large scale dissolution vugs and breccias were produced by hydrothermal fluids in the subsurface after formation of stylolites.

PROCESSES OF DISSOLUTION

The dissolution associated with ore deposition may be closely related to acidity generated by H₂S, sulphate reduction, and/or diagenesis of organic matter before and during mineralization.

Acidity Generated by H₂S: H₂S generates acid either by precipitating sulphide or through oxidation by porewaters. This, in turn, will cause dissolution and brecciation of the carbonate rocks. If sulphate reduction started before the arrival of

metal-bearing brines, oxidation of H₂S generated during sulphate reduction in the pore fluids may have caused pre-mineralization dissolution and brecciation (Anderson 1983; Anderson and Garven 1987):

$$H_2S + 2O_2 = SO_4^{-2} + 2H^+$$

According to Anderson (1983) and Anderson and Garven (1987), sulphide precipitation is an acid-generating process, which inevitably causes solution vugs and breccias in the host carbonate rocks:

$$Zn^{2+} + H_2S = ZnS + 2H^+$$

Therefore, it is not surprising that dissolution and brecciation postdates mineralization in the Pine Point deposits (Figs. 10B and 10C). The brecciated ores and dolomite-filled veins that cut sulphide were also described by Krebs and Macqueen (1984) as evidence of dissolution and brecciation associated with mineralization.

Sulphate Reduction: Some saddle dolomites could also result from sulphate reduction (Anderson 1983; Anderson and Garven 1987; Machel 1987a, 1987b; Krouse et al. 1988):

$$2CaSO_4 + Mg^{+2} + 2CH_4 = CaMg(CO_3)_2 + Ca^{-2} + 2H_2S + 2H_2O.$$

The lateral extent of the dissolution and brecciation events caused by the hydrothermal fluids is indicated by saddle dolomite, since it is usually the first stage of cement to fill these vugs and breccias. In this case, the dissolution vugs and breccias associated with saddle dolomite are not necessarily linked to the sulphide mineralization (Anderson and Garven 1987). Instead they are probably related to thermochemical sulphate reduction by light hydrocarbon gases in deep carbonate reservoirs. This helps to explain dissolution associated with saddle dolomites in the subsurface Presqu'ile barrier and elsewhere in the Western Canada Sedimentary Basin where sulphide minerals are rare or absent.

Organic Matter Alteration: The dissolution of the host carbonate rocks and precipitation of saddle dolomites in MVT deposits may also be related to the thermal alteration of organic matter, which is abundant in the Pine Point area (Macqueen and Powell 1983). Thermal alteration of organic matter by hydrothermal solutions could cause a diagenetic sequence of carbonate dissolution, precipitation, and renewed dissolution (Spirakis and Heyl 1988; 1990). The initial dissolution is related to the production of organic acids that were produced by the heating of organic matter. As heating continues, organic acids begin to break down to carbon dioxide and methane. Addition of carbon dioxide to a solution with an organic-acid pH buffer decreases the solubility of carbonates, thus carbonates precipitate. At still higher temperatures, organic acids quickly degrade, so that the pH buffer is lost. Without a buffer, the continual addition of carbon dioxide then lower; the pH and causes carbonate

Cooling of CO₂-rich Warm Brines: At a given P_{CO2}, the saturation concentration of dissolved carbonate increases in solution as temperature decreases. Therefore, cooling of CO₂-rich thermal brines may result in extensive solution of carbonates, forming hydrothermal cave systems. The dissolution caves in the Mississippian limestone and dolomite of the Black Hills (South Dakota) were suggested to have been formed by cooling CO₂-rich waters (Bakalowicz *et al.* 1987). However, as CO₂-rich basinal fluids migrate updip along regional aquifers to shallower depths, decreasing hydrostatic pressure in rising water may allow partial degassing of CO₂, resulting in precipitation of hydrothermal dolomites and calcites. This would account for regionally extensive saddle dolomite cement that is genetically and spatially associated with localized MVT deposits throughout the Ozark region (Leach *et al.* 1991).

Organic matter, dissolved organic species, and dissolution of carbonate minerals have been suggested as sources of CO₂ (e.g. Machel 1987a, 1987b; Spirakis and Heyl 1988, 1990). CO₂ could also be derived from silicate hydrolysis of clay minerals during diagenesis in the adjacent and down-dip shale basin (Hutcheon and Abercombie 1990).

The above mentioned processes probably enhanced and modified earlier dissolution features, resulting in the extensive dissolution features that host MVT

deposits at Pine Point. Therefore, the role of the sub-Watt Mountain exposure forming extensive karst and solution features has been over-emphasized. In terms of the majority of dissolution vugs and breccias that host sulphide minerals, the main dissolution events are not controlled by the sub-Watt Mountain exposure, but rather formed much later during burial when hydrothermal fluids invaded the Presqu'ile barrier. This accounts for the presence of saddle dolomite and sulphide minerals both above and below the sub-Watt Mountain unconformity.

The Watt Mountain shale formed a relatively impermeable unit that restricted the later hydrothermal fluid flow within the barrier. Because of this, most dissolution generally occurs within the Sulphur Point Formation below the Watt Mountain shale. Locally, however, hydrothermal fluids breached the shale cover, resulting in locally extensive hydrothermal dissolution in the Watt Mountain and Slave Point formations above the unconformity. This late-stage hydrothermal dolomitization and dissolution overprinted and obliterated most of the earlier unconformity-related meteoric solution system.

It is unlikely that the saddle dolomite above the unconformity formed later than the saddle dolomite below the unconformity by either chemical reworking (Rhodes et al. 1984) or rejuvenation (Ford and Williams 1990). Their similar geochemical signatures (e.g. δ^{18} O, δ^{13} C, δ^{87} Sr/ δ^{86} Sr, and fluid inclusion temperatures, Chapter 5) suggest that these saddle dolomites formed during the same event from similar fluids. Similarly, the associated dissolution features that occur both below and above the unconformity may have been produced by similar solutions during a

major dissolution event(s).

TIMING OF DISSOLUTION

Petrographic evidence suggests that dissolution and brecciation postdate stylolitization (Figs. 18E and 18F). Figure 18F shows that horizontal stylolites are truncated by a vertical stylolite. Both horizontal and vertical stylolites are cross cut by a fracture that is filled with saddle dolomite, suggesting that fracturing occurred after stylolitization. Some low amplitude stylolites can be observed in the clasts in a breccia (Fig. 18E). The different angles of these stylolites with respect to the orientation of the core (arrows in Fig. 18E) indicate that brecciation occurred after the formation of these stylolites. Although some stylolites may have developed in carbonates at burial depths of about 500 m, most stylolites probably formed at burial depths greater than 1000 m, because stylolitization is a continuous process during burial and can be used to separate early diagenesis from intermediate to deep burial diagenesis. Thus, dissolution and brecciation must have occurred at minimum burial depths of about 500 m and most probably more than 1000 m.

In the Pine Point area, some of the vugs and breccias postdate coliform sphalerite, which formed during the early stages of mineralization (Figs. 10B). Some fractures postdate crystalline sphalerite and galena that formed during the main stage of mineralization (Fig. 10C). This indicates that the main dissolution events preceded and overlapped saddle dolomites and were caused by subsurface hydrothermal fluids.

The ages of mineralization are constrained to occur from Pennsylvanian to early Tertiary, by different dating methods (Kyle 1981; Beales and Jackson 1982; Garven 1985; Arne 1989; and Cumming et al. 1990). Thus, the dissolution associated with mineralization is much later than the sub-Watt Mountain exposure, and is certainly post Devonian. Fluid-inclusion data indicate that the saddle dolomites were precipitated from very saline, hydrothermal brines. On the basis of the burial history and the gradual increase of homogenization temperatures of saddle dolomite fluid inclusions from Pine Point westward towards the Cordilleran orogenic belt, it is suggested that the hydrothermal fluids, which were responsible for dolomitization and mineralization, were expelled from deeply buried sediments and the crystalline basement to the west by tectonic compression and gravity-driven flow, most probably during maximum burial in the Late Cretaceous to early Tertiary.

COMPARISONS

Hydrothermal dissolution associated with saddle dolomite also occurs elsewhere in the Western Canada Sedimentary Basin. Carbonates of the Middle Devonian Keg River Formation south of the Presqu'ile barrier also contain vugs with saddle dolomite cement, which are interpreted to have been caused by hydrothermal fluids (e.g. Aulstead and Spencer 1985; Qing and Mountjoy 1989). Similarly, studies by Packard et al. (1990) and Mountjoy and Halim-Dihardja (1991) suggest that dissolution vugs and breccia in the Wabamun Formation on the east side of the Peace

River Arch, Alberta, south of the Presqu'ile barrier, were caused by hydrothermal solutions that precipitated saddle dolomites. Hydrothermal solutions were also suggested to be responsible for some of the dissolution of the host carbonates and the precipitation of saddle dolomites in Lower and Middle Devonian Manetoe facies that occur in the Mackenzie basin north of the Presqu'ile barrier (Morrow et al. 1986; Aulstead et al. 1988) and Upper Devonian Nisku buildups in the Western Canada Sedimentary Basin southwest of Edmonton (Machel 1987; Machel and Anderson 1989). Thus, hydrothermal dissolution associated with saddle dolomites is a common phenomenon in the Devonian carbonates of the Western Canada Sedimentary Basin. Hydrothermal solution and subaerial exposure can produce somewhat similar appearing solution vugs and breccias. For solution events associated with secondary dolomitization, it is crucial to establish the timing of dissolution events and not simply relate solution to the nearest unconformity.

Ĭ

7.4 CONCLUSIONS

The role of the sub-Watt Mountain exposure in forming extensive karst and solution features in the Middle Devonian Presqu'ile barrier has been over-emphasized. Only minor dissolution and brecciation occurred during the sub-Watt Mountain exposure. Occurrences of large scale solution are closely associated with hydrothermal fluids that also precipitated saddle dolomites and sulphide minerals.

Dissolution related to the sub-Watt Mountain exposure differs from subsurface dissolution associated with the MVT deposits at Pine Point in at least three aspects: 1) the size of yugs related to the sub-Watt Mountain exposure is small, usually 1 to 2 cm, while dissolution vugs that host MVT deposits at Pine Point are much larger, varying from a few centimetres to several metres; 2) dissolution vugs and breccias related to the sub-Watt Mountain unconformity are commonly filled with green shale, and locally with pendant calcite cements. Dissolution vugs at Pine Point are commonly filled with late-stage saddle dolomite, sulphide minerals, and calcite; 3) dissolution features that resulted from sub-Watt Mountain exposure only occur below the sub-Watt Mountain unconformity, while large-scale vugs and breccias, observed at Pine Point and in the subsurface NWT and northeastern British Columbia, extend continuously from below the unconformity to strata above it. The main dissolution events clearly postdate sub-Watt Mountain exposure. Petrographic evidence indicates that dissolution and brecciation postdate stylolites, and therefore, must have occurred during burial. At Pine Point, the main dissolution events preceded and/or overlapped saddle dolomite. In addition later dissolution postdates the early stages of mineralization, indicating that solution overlaps mineralization.

Fluid inclusion measurements indicate that the saddle dolomites from both below and above the sub-Watt Mountain unconformity are similar and precipitated from very saline, warm hydrothermal fluids. Therefore dissolution that precedes and overlaps saddle dolomites was caused by subsurface hydrothermal fluids. Hydrothermal dissolution and dolomitization almost completely overprints and

obliterates the earlier unconformity-related meteoric dissolution features at Pine Point.

Meteoric karst has been inferred to have been responsible for extensive solution and brecciation in many MVT districts. In many cases, there is no direct evidence to support a meteoric origin for the solution and the timing of solution is not sufficiently well constrained. The results of this study have important implications for other MVT districts and evidence for meteoric-karst should be critically re-examined. In cases like Pine Point, the influence of subaerial exposure has been over-emphasized and later hydrothermal dissolution overlooked up to now.

CHAPTER EIGHT

TIMING OF MINERALIZATION AT PINE POINT INFERRED FROM DIAGENESIS OF HOST DOLOMITES

8.1 PREVIOUS DATING FOR PINE POINT DEPOSITS

One of the unsolved problems in defining mineralization models for MVT deposits at Pine Point is that the age of mineralization has been constrained only within broad limits between the Pennsylvanian and Early Tertiary (Table 8).

Table 8. Inferred timing for Pine Point MVT deposits

AUTHOR(S)	PROPOSED TIME	METHOD
Kyle (1981)	Pennsylvanian	lead isotopes
Cumming et al. (1990)	Pennsylvanian to Early Tertiary	lead isotopes
Cumming and Robertson (1969)	Permian	lead isotopes
Beales and Jackson (1982)	Permian (?)	paleomagnetic measurements
Garven (1985)	Late Cretaceous to Early Tertiary	computer modelling
Arne (1991)	Cretaceous	fission track

A uniform and nonradiogenic lead isotopic composition for the Pine Point deposits has been demonstrated by several isotopic studies (Cumming and Robertson 1969; Kyle 1981; Cumming et al. 1990). However, using the same lead isotope data but different models for calculation, the interpreted age of mineralization has ranged from Pennsylvanian (Kyle 1981; Cumming et al. 1990), to Permian (Cumming and Robertson 1969), and Cretaceous (Cumming et al. 1990). Although Cumming et al. (1990) favour the interpretation that mineralization occurred during Pennsylvanian time, the lead isotope data do not provide an unequivocal resolution concerning the age of Pine Point mineralization (Cumming et al. 1990, p.142).

ž

Paleomagnetic studies suggested that age of mineralization at Pine Point may be Permian (Beales and Jackson 1982). This age determination has to be used with caution because: 1) these paleomagnetic measurements were performed on unspecified minute amounts of magnetic co-precipitated or entrapped impurities, since neither host carbonates nor sulphide ores are magnetic (Beales and Jackson 1982); and 2) the reliability of these measurements cannot be evaluated as they were presented in an abstract.

The apparent apatite fission track ages of Precambrian basement samples range from 30 to 550 Ma (Arne 1991). The presence of apatite grains with fission track age > 500 Ma indicates that the Pine Point district has experienced a single phase of heating to maximum paleotemperatures in the range of 80 to 100°C during maximum burial in Late Cretaceous time (Arne 1991). Based on these fission track data, Arne (1991) suggested that mineralization at Pine Point occurred during

maximum burial in Cretaceous time. As 12 out of 13 of Arne's measurements were made on the apatite from Precambrian samples which could have represented paleotemperatures before Devonian time, these calculated ages have to be used with caution.

Using computer-generated models of fluid movements and paleotemperatures in the Western Canada Sedimentary Basin, Garven (1985) suggested that the Pine Point ore deposits could have formed during Early Tertiary by topography/gravity-driven groundwater flow in the Western Canada Sedimentary Basin. However this modelling needs supporting geological evidence.

8.2 DISCUSSION

None of the methods discussed above can provide an unequivocal resolution of the problem of the age of mineralization for the Pine Point MVT deposits. Since mineralization is closely associated with saddle dolomites at Pine Point, as discussed under diagenetic paragenesis in Chapter 4, the timing of the formation of saddle dolomites provide additional constraints on the age of mineralization.

Petrographic study indicates that saddle and coarsely crystalline dolomites: 1) locally occur continuously ecross the Watt Mountain unconformity into the overlying Slave Point Formation, and 2) postdate stylolites. The dolomitization, therefore, must have occurred after sub-Watt Mountain exposure during burial.

The pressure corrected homogenization temperature of SD is about 190 °C in northeastern B.C. and 105 °C at Pine Point, decreasing updip along the Presqu'ile barrier. These temperatures exceed the maximum burial temperatures of the region, calculated using a normal geothermal gradient (35 °C/km) and a surface temperature of 20 °C, and therefore suggest a hydrothermal event. The systematic decrease of ⁸⁷Sr/⁸⁶Sr ratios and trapping temperatures (with corresponding increase in δ^{18} O values) of saddle dolomites from west to the east suggest a large-scale migration of hot, radiogenic dolomitizing fluids from west to east. These fluids were possibly expelled from deeply buried sediments and the crystalline basement during two episodes of tectonic thrusting and compression, the first during Late Jurassic to Early Cretaceous, and the second during Late Cretaceous to early Tertiary. Mineralization at Pine Point could have started as early as Late Jurassic. However, the main stage of mineralization probably occurred during the second episode of tectonic thrusting and compression, because the gravity-driven flow system appears to have been more active during Late Cretaceous to early Tertiary as a result of foreland basin deformation and uplift (Garven 1985; 1989) and also because the Western Canada Sedimentary Basin reached maximum burial during this period of time, which could provide an adequate supply of hotter brines in the deeper part of the basin.

Similarly, the MVT deposits of the Ozark Mountains have been genetically linked to the Ouachita foldbelt tectonism by Leach and Rowan (1986). Leach and Rowan (1986) suggested that MVT deposits in the Ozarks probably formed by hot subsurface brines that migrated updip onto the southern flank of the North American

Craton, in response to deformation of the Arkoma foreland basin and uplift of the Ouachita Mountains, during the late Paleozoic collision of the Llanortian and North American plates. This interpretation is supported by a regional trend of decreasing fluid inclusion homogenization temperatures northward away from Ouachita foldbelt (Leach and Rowan 1986), similar to that of the Presqu'ile barrier in the Western Canada Sedimentary Basin. From a recent study of petroleum migration in the Illinois basin, Bethke et al. (1991) suggested that the long-range migration of basinal fluids occurred late in the basin's history during a Mesozoic period of regional groundwater flow that was set up by tectonic uplift in the southern basin. Therefore, it is clear from these examples that uplift of a foreland basin may create a hydraulic system for large-scale migration of basinal fluids, which could play key roles in mineralization and dolomitization along preferential conduit systems in sedimentary basins.

8.3 CONCLUSIONS

The age of mineralization of MVT deposits at Pine Point has been constrained within broad limits between the Pennsylvanian and early Tertiary by various dating methods, although none of these methods provided an unequivocal answer. Since mineralization is closely associated with saddle dolomites at Pine Point, the timing of saddle dolomites provides additional constraints on the age of mineralization.

Petrographic study indicates that saddle and coarsely crystalline dolomites: 1) locally occur continuously across the sub-Watt Mountain unconformity, and 2) postdate stylolitization. The dolomitization, therefore, must have occurred after the sub-Watt Mountain exposure during burial.

The systematic decrease of 87 Sr/ 86 Sr ratios and trapping temperatures (with corresponding increase in δ^{18} O values) of saddle dolomites eastward along the Presqu'ile barrier suggests that a hot, radiogenic fluid from the west, was possibly expelled from deeply buried sediments and the crystalline basement by tectonic thrusting and compression and by a gravity-driven flow system as a result of the uplift of the foreland basin. These data support an interpretation that the timing of mineralization probably occurred during Late Cretaceous and early Tertiary time when the Western Canada Sedimentary Basin reached maximum burial depths.

CHAPTER NINE

SUMMARY AND CONCLUSIONS

9.1 DIAGENETIC PARAGENESIS

The Presqu'ile barrier has undergone diagenetic alteration in submarine, subaerial, and subsurface environments. The diagenetic features that occurred in a submarine environment include: micrite envelope, micrite, syntaxial cement, fine crystalline cement, fibrous cement. Only minor, localized pendant cement and minor small-scale dissolution and brecciation are interpreted to be associated with the sub-Watt Mountain exposure in a subaerial environment. Subsurface diagenesis resulted in the most important modifications in the Presqu'ile barrier, and includes: blocky sparry calcite cement, compaction and stylolitization, hydrothermal dissolution, dolomitization, anhydrite, late-stage coarse-crystalline calcite, white calcite, elemental sulphur, fluorite, and bitumen.

9.2 DOLOMITIZATION

Four types of dolomites are associated with the Presqu'ile barrier. In a paragenetic sequence, they are: fine-crystalline (FCD); medium-crystalline (MCD);

coarse-crystalline (CCD); and saddle (SD). The origin and timing of these dolomites are established on the basis of their distinctive spatial distributions, cross cutting relationships, petrographic characteristics, diagenetic paragenesis, and geochemical signatures.

FINE-CRYSTALLINE DOLOMITE

1

Ý

- 1) FCD is restricted to the back-barrier facies and is interbedded with Muskeg evaporitic anhydrites in the Elk Point Basin.
- 2) The heaviest δ^{18} O value of FCD is -1.58 ‰ PDB, which is within the range of calculated δ^{18} O values (-1.2 to -2.2 ‰ PDB) for dolomites that would precipitate from Middle Devonian seawater.
- 3) The ⁸⁷Sr/⁸⁶Sr ratios of unaltered FCD range from 0.7079 to 0.7080, corresponding to the estimated ⁸⁷Sr/⁸⁶Sr ratio of Middle Devonian seawater (Burke *et al.* 1982).
- 4) The REE patterns of FCD are similar to those of marine limestones from the Presqu'ile barrier.
- 5) The relationship between Sr concentration and mol% CaCO₃ for FCD is similar to the Miocene marine dolomite from Little Bahama Bank.

FCD probably formed penecontemporaneously at or just below the sea floor by Middle Devonian seawater, because it was interbedded with anhydrite in the Elk Point Basin, and because its δ¹⁸O values, ⁸⁷Sr/⁶⁶Sr ratios, REE patterns, and Sr concentrations are similar to those estimated and calculated for Middle Devonian seawater dolomites.

However, FCD sampled near Pine Point orebodies has been altered during mineralization by later diagenetic fluids, as indicated by an increase in crystal size, depleted δ^{18} O values (-6.7 to -7.9 % PDB), and slightly increased 87 Sr/ 86 Sr ratios (0.7082-0.7084).

MEDIUM-CRYSTALLINE DOLOMITE

- 1) MCD occurs in the lower part of the Presqu'ile barrier in the Pine Point Formation and is restricted to the southern and central (lower) part of the barrier. The northern part of the barrier remains undolomitized.
- 2) The heaviest δ¹⁸O values for MCD is -3.7 ‰ PDB, slightly depleted compared with the estimated δ¹⁸O signature of Middle Devonian seawater dolomites. However, the δ¹⁸O values of most MCD fall between -5 to -7 ‰ PDB, and are much more depleted than the estimated δ¹⁸O signature of Middle Devonian seawater dolomites.
- 3) Three MCD were analyzed for ⁸⁷Sr/⁸⁶Sr ratios. One MCD has a ⁸⁷Sr/⁸⁶Sr ratio of 0.7081, comparable to the best estimated ⁸⁷Sr/⁸⁶Sr ratio of Middle Devonian seawater. The ⁸⁷Sr/⁸⁶Sr ratios of the other two are 0.7085 and 0.7087, slightly more radiogenic than Middle Devonian seawater.

- 4) REE patterns of MCD are different from those of marine limestones and FCD.
- 5) Sr concentration in MCD ranges from 30 to 79 ppm, averaging 50 ppm. The relationship between Sr concentration and mol% CaCO₃ deviates from that of the Little Bahama seawater dolomites.

The data from the present study place constraints, but do not provide an unequivocal conclusion, concerning the origin of MCD. Among several possibilities, MCD could have formed:

- during shallow burial at slightly elevated temperatures from fluids derived by
 means of compaction of strata: a) from downdip in the western part of the
 basin, and/or b) from the Elk Point and Mackenzie basins adjacent to the
 Presqu'ile barrier;
- soon after sedimentation of the Pine Point Formation by seawater and/or evaporated seawater derived from the Elk Point basin;

The geochemistry of MCD, especially the depleted δ^{18} O values, strongly support the first interpretation.

The second interpretation is based mainly on the spatial distribution of MCD.

The absence of MCD in the upper part of the barrier suggests that MCD probably formed soon after sedimentation. The restriction of MCD to the lower southern and central part of the barrier suggests dolomitizing fluids may have been derived from

the Elk Point Basin, preferentially dolomitizing limestones adjacent to the Elk Point Basin. However the original O and Sr isotope signatures of MCD could have been modified during later neomorphism. In both well 2813 and 2812, the vertical profiles of MCD δ^{18} O values are clearly more depleted close to CCD/MCD boundary, suggesting that δ^{18} O values of MCD may have been modified by later diagenetic fluids that were responsible for CCD. REE patterns of MCD are different from those of marine limestones and FCD, suggesting that water/rock ratios during neomorphism were probably high.

COARSE-CRYSTALLINE AND SADDLE DOLOMITES (CCD and SD)

- 1) CCD and SD are closely associated with each other. Because of the intimate association of CCD and SD, their similar δ¹⁸O values, ⁸⁷Sr/⁸⁶Sr ratios, and trace element concentrations, CCD and SD are interpreted to be dolomitized by diagenetic fluids of similar chemical compositions. CCD represents dolomitized limestones, whereas SD occurred after CCD as dolomite cement filling vugs and fractures in CCD.
- Locally CCD and SD extend above the sub-Watt Mountain unconformity, suggesting that CCD and SD formed after sub-Watt Mountain exposure.
- In the Presqu'ile barrier, CCD and SD postdate stylolites, suggesting that dolomitization formed during burial.
- 4) SD overlaps mineralization in the Pine Point area. The timing of

- mineralization has been broadly constrained between Pennsylvanian to early Tertiary by various dating methods.
- 5) Forty-five CCD and 61 SD samples were analyzed for δ¹8O values. Both types of dolomites have similar ranges of δ¹8O values, varying from -7 to -16 ‰ PDB and gradually increasing eastward along the Presqu'ile barrier from northeastern B.C. to Pine Point.
- The ⁸⁷Sr/⁸⁶Sr ratios of CCD and SD are lowest at Pine Point, and gradually increase westward along the Presqu'ile barrier. Eight Pine Point SD samples yield ⁸⁷Sr/⁸⁶Sr ratios from 0.7081 to 0.7085 (avg. 0.7083, slightly more radiogenic than Middle Devonian seawater). In the area west of Pine Point to the Tathlina Lake, the ⁸⁷Sr/⁸⁶Sr ratios of three SD samples vary from 0.7084 to 0.7086 (avg. 0.7085). West of the Tathlina Lake to northeastern B.C., six SD samples have ⁸⁷Sr/⁸⁶Sr ratios from 0.7090 to 0.7106 (avg. 0.7095, much more radiogenic than Middle Devonian seawater).

The ⁸⁷Sr/⁸⁶Sr of CCD are similar to those of SD. Five Pine Point CCD samples yield ⁸⁷Sr/⁸⁶Sr ratios from 0.7082 to 0.7088 (avg. 0.7085). Four CCD samples from the deeper subsurface are much more radiogenic, with ⁸⁷Sr/⁸⁶Sr ratios from 0.7093 to 0.7121 (avg. 0.7104).

7) The homogenization temperatures of saddle dolomite fluid inclusions from 14 locations vary from 85 to 210 °C, and gradually decrease from northeastern B.C. (155 to 171 °C) to Pine Point (95 to 106 °C). The pressure-corrected homogenization temperatures exceed the maximum burial temperatures of the

- region. Therefore, the formation of CCD and SD probably represent regional hydrothermal event(s).
- 8) REE patterns of CCD and SD differ from those of marine limestones and FCD, suggesting that the water/rock ratios during dolomitization were probably high, resulting in REE patterns distinctly different from the parent limestones.

The gradual decrease in 87 Sr/86 Sr ratios and homogenization temperatures (with corresponding increase in δ^{18} O values) from northeastern B.C. to Pine Point suggests a large-scale migration of hot and radiogenic dolomitizing fluids updip from west to east along the Presqu'ile barrier. The eastward updip flow of basin brines was probably established by the tectonic thrusting and compression, sedimentary loading, and uplift of the foreland basin. In the Western Canada Sedimentary Basin, the tectonic thrusting and compression occurred in two main episodes, the first during the Late Jurassic to Early Cretaceous, and the second during the Late Cretaceous to early Tertiary. The main stage of dolomitization and mineralization probably occurred during the second episode because: 1) fluid flow was probably more active during the Late Cretaceous to early Tertiary due to a more extensive gravity-driven flow system that was formed by uplift of foreland basin; and 2) the Western Canada Sedimentary Basin reached maximum burial during the Late Cretaceous and early Tertiary, providing an adequate supply of brines in the deeper part of the basin for dolomitization.

The Presqu'ile barrier probably acted as a deeply buried regional porous permeable conduit system. When hot fluids with radiogenic Sr were expelled tectonically from deeply buried sediments into the Presqu'ile barrier, the temperatures in the conduit would increase, thus explaining why the homogenization temperatures of saddle dolomite fluid inclusions exceed the maximum burial temperatures of the Western Canada Sedimentary Basin. As hot fluids moved eastward updip along the Presqu'ile barrier, they would gradually cool, resulting in the eastward decrease in homogenization temperatures and a corresponding increase in δ^{18} O values of CCD and SD.

The radiogenic Sr could have come from deeply buried sediments and/or from the crystalline basement during tectonic thrusting and compression. In support of this, SD in the western downdip part of the Presqu'ile barrier are the most radiogenic. As dolomitizing fluids moved updip eastward along the Presqu'ile barrier, the radiogenic Sr gradually mixed with less radiogenic formation waters. As result, the **TSr/**Sr ratio of the SD decreased eastward along the Presqu'ile barrier.

9.3 ORIGIN OF DISSOLUTION VUGS AND BRECCIAS

Meteoric karst has been inferred to be responsible for extensive solution and brecciation at Pine Point and in many other MVT districts. In many cases, there is no direct evidence to support a meteoric origin for the solutions and the timing of

dissolution is not sufficiently well constrained. This study indicates that dissolution related to the sub-Watt Mountain exposure differs from subsurface dissolution associated with the MVT deposits at Pine Point in at least three aspects:

- 1) dissolution vugs related to meteoric water during the sub-Watt Mountain exposure are small (usually 1 to 2 cm), while vugs that host MVT deposits at Pine Point are much larger, ranging from centimetres to metres in size, and are more extensive;
- 2) the dissolution vugs and breccias related to the sub-Watt Mountain unconformity are commonly filled with green shale, and locally with pendant calcite cements. Dissolution vugs at Pine Point are commonly filled with saddle dolomite, sulphide, and late-stage calcite cements;
- 3) dissolution features resulting from subaerial exposure only occur below the sub-Watt Mountain unconformity, while later-stage vugs and breccias occur continuously across the unconformity.

Therefore, meteoric waters caused only minor dissolution in the upper part of the Presqu'ile barrier during the sub-Watt Mountain unconformity. Although meteoric dissolution could have enhanced porosity and permeability in the barrier and provided conduits for later hydrothermal fluids, the majority of dissolution vugs and breccias were produced by hydrothermal fluids during burial. These results have important implications for mineral exploration:

1) MVT deposits are not always related to a unconformity. Mineralization can occur in any available vugs and/or fractures whatever their origin.

2) Evidence of meteoric-karst for other MVT districts should be critically reexamined. In cases like Pine Point, the influence of subaerial exposure has been over-emphasized and later extensive hydrothermal dissolution of carbonates overlooked.

9.4 TIMING OF MINERALIZATION

One of the unsolved problems is that the age of mineralization is only constrained within broad limits between the Pennsylvanian and early Tertiary by a variety of dating methods. As SD is closely associated with and overlaps with mineralization at Pine Point, the timing of dolomitization can place additional constrains on the timing of mineralization.

The systematic decrease of 87 Sr/ 86 Sr ratios and homogenization temperatures with corresponding increasing δ^{18} O values of saddle dolomites from west to the east suggest that hot, radiogenic fluids were possibly expelled from more deeply buried sediments and the crystalline basement by tectonic thrusting and compression and by a gravity-driven flow system as a result of the uplift of the foreland basin during the Late Cretaceous to early Tertiary.

9.5 CLOSING REMARKS

This study suggests that diagenetic features in a sedimentary basin, such as hydrothermal dissolution, dolomitization, and mineralization, are genetically related

to subsidence and deformation of the basin. Tectonic thrusting and compression, sedimentary loading, and uplift of a foreland basin create hydrodynamic systems that initiated large-scale flow of basinal fluids, which played a key role in dolomitization and mineralization along preferential conduit systems in a sedimentary basin, like the Presqu'ile barrier. In such cases, the diagenetic features must be systematically studied across a basin. If one just restricts a study to a local area, one might miss the whole picture, because one cannot see the forest for the trees. In Chinese, I would put it this way:

REFERENCES

ADAMS. J.E. AND RHODES, G.M., 1960, Dolomitization by seepage refluxion: American Association of Petroleum Geologists Bull., v.44, p.1912-1920.

ALLAN, J.R. AND MATTHEWS, R.K., 1982, Isotope signatures associated with early meteoric diagenesis: Sedimentology, v.29, p.797-817.

ANDERSON, G.M., 1983, Some geochemical aspects of sulphide precipitation in carbonate rocks: in Kisvarsanyi, G., Grant, S.K., Pratt, W.P., and Keonig, J.W. (eds): International conference on Mississippi Valley type lead-zinc deposits, Proceedings volume, Rolla, Missouri, p.61-76.

ANDERSON, G.M. AND MACQUEEN, R.W., 1976, Ore deposit models - 6. Mississippi Valley-type lead-zinc deposits: Geoscience Canada, v.3, p.108-117

ANDERSON, G.M. AND GARVEN, G., 1987, Sulphate-sulphide-carbonate associations in Mississippi Valley-type lead-zinc deposits: Economic Geology, v.82, p.482-488.

ANDERSON, T. F., AND ARTHUR, M.A., 1983, Stable isotopes of oxygen and carbon and their application to sedimentologic and paleoenvironmental problems: in Stable Isotopes in Sedimentary Geology, Soc. Econ. Paleontologists & Mineralogists short course No. 10, p.1-1--1- 151.

ARENE, D., 1991, Regional thermal history of the Pine Point area, Northwest Territories, Canada, from apatite fission-track analysis: Economic Geology, v.86, p.428-435.

AULSTEAD, K.L. AND SPENCER, R.J., 1985, Diagenesis of the Keg River

7

Formation, northeastern Alberta: fluid inclusion evidence: Bull. of Canadian Petroleum Geology, v.33, p.167-183.

AULSTEAD, K.L., SPENCER, R.J., AND KROUSE, H.R., 1988, Fluid inclusion and isotopic evidence on dolomitization, Devonian of Western Canada: Geochim. et Cosmochim. Acta, v.52, p.1027-1035.

BADIOZAMANI, K., 1973, The Dorag dolomitization model - application to the Middle Ordovician of Wisconsin: Jour. of Sedimentary Petrology, v.43, p.965-984.

PALMER, M.V., 1987, Thermal genesis of dissolution caves in the Black Hills, South Dakota: Geological Society of America Bull., v.99, p.729-738.

BAKER, P.A. AND BURNS, S.J., 1985, Occurrence and formation of dolomite in organic-rich continental margin sediments: American Association of Petroleum Geologists Bull., v.69, p.1917-1930.

BANNER, J.L., HANSON, G.N., AND MEYERS, W.J., 1988a, Rare earth element and Nd isotopic variations in regionally extensive dolomites from the Burlington-Keokuk Formation (Mississippian): implications for REE mobility during carbonate diagenesis: Jour. of Sedimentary Petrology, v.58, p.415-432.

BANNER, J.L., HANSON, G.N., AND MEYERS, W.J., 1988b, Water/rock interaction history of regionally extensive dolomites of the Burlington-Keokuk Formation (Mississippian): isotope evidence, in Shukla, V. and Baker, P.A. (eds): Sedimentology and geochemistry of dolostones: Soc. Econ. Paleontologists & Mineralogists Spec. Publ. No. 43, p.97-113.

BEALES, F.W. AND HARDY, J.L., 1980, Criteria for the recognition of diverse

dolomite types with an emphasis on studies on host rocks for Mississippi Valley-type ore deposits: in, D.H. Zenger, J.B. Dunham and R.L. Ethington (eds.), Concepts of models of dolomitization: Soc. Econ. Paleontologists & Mineralogists Spec. Publ. No. 28, p.197-213.

BEALES, F. AND JACKSON, C., 1982, Multiple genetic and diagenetic models help the unravelling of Mississippi Valley-type ore genesis: 11th International Congress on Sedimentology, MacMaster Univ., Hamilton, Ontario, 1982, Abstracts, p.17.

BELYEA, H.R., 1970, Middle Devonian tectonic history of the Tathlina uplift, southern District of Mackenzie and northern Alberta: Canada Geological Survey Paper 70-14, 30p.

BETHKE, C.M., REED, J.D., AND OLTZ, D., 1991, Long-range petroleum migration in the Illinois basin: American Association of Petroleum Geologists Bull., v.75, p.295-945.

BOGACZ, K., DZULYNSKI, S., AND HARANCZYK, C., 1970, Ore-filled hydrothermal karst features in the Triassic rocks of the Cracow-Silesian region: Acta Geologica Polonica, v.20, p.247-265.

BURKE, W.H., DENISON, R.E., HETHERINGTON, E.A., KOEPINCK, R.B., NELSON, H.F., AND OTTO, J.B., 1982, Variation of seawater ⁸⁷Sr/⁸⁶Sr throughout Phanerozoic time: Geology, v.10, p.516-519.

CAMPBELL, C.V. 1987, Stratigraphy and facies of the Upper Elk Point subgroup, northern Alberta, in Krause, F.F. and Burrowes, G. (eds.), Devonian lithofacies and reservoir styles in Alberta: 13th Canadian Soc. Petroleum Geologists Core Conference and Display and Second International Symposium on the Devonian

CAMPBELL, N., 1966, The lead-zinc deposits of Pine Point: Canadian Mining Metall. Bull., v.59, p.953-960.

CLARK, J.P., AND PHILP, R.P., 1989, Geochemical characterization of evaporite and carbonate depositional environments and correlation of associated crude oils in the Black Creek Pasin, Alberta: Bull. of Canadian Petroleum Geology, v.37, p.401-416.

COLLINS, J.F. AND LAKE, J.H., 1989, Sierra reef complex, Middle Devonian, northeastern British Columbia, in Geldsetzer, H.H.J., James, N.P., and Tebbutt, G.E. (eds.): Reefs, Canada and adjacent areas: Canadian Soc. Petroleum Geol. Memoir 13, p.414-421.

CONNOLLY, C.A., WALTER, L.M., BAADSGAARD, H., AND LONGSTAFFE, F.J., 1990a, Origin and evolution of formation waters, Alberta Basin, Western Canada Sedimentary Basin. 1. Chemistry: Applied Geochemistry, v.5, 375-395.

CONNOLLY, C.A., WALTER, L.M., BAADSGAARD, H., AND LONGSTAFFE, F.J., 1990b, Origin and evolution of formation waters, Alberta Basin, Western Canada Sedimentary Basin. 2. Isotope systematics and water mixing: Applied Geochemistry, v.5, 397-413.

CRAIG, H., 1957, Isotopic standards for carbon and oxygen and correction factors for mass-spectrometric analysis of carbon dioxide: Geochim. et Cosmochim. Acta, v.12, p.272-374.

CRAWFORD, M.L., 1981, Phase equilibria in aqueous fluid inclusions: in Hollister, L.S. and Crawford, M.L. (eds.), Short Course in Fluid Inclusions: Application to

Petrology, Mineralogical Asso. of Canada, pp.75-100.

CUMMING, G.L. AND ROBERTSON, D.K., 1969, Isotopic composition of lead from the Pine Point deposits: Economic Geology, v.64, p.731-732.

CUMMING, G., KYLE, J., AND SANGSTER, D., 1990, Pine Point: a case history of lead isotope homogeneity in a Mississippi Valley-type district: Economic Geology, v.85, p.133-144.

DICKSON, J.A.D., 1965, A modified staining technique for carbonates in thin section: Nature, v.205, p.587.

DONOVAN, D.T. AND JONES, E.J.W., 1979, Causes of world wide changes in sea level: Jour. of Geological Society of London, v.136, p.175-186.

DOROBEK, S.L. AND FILBY, R.H., 1988, Origin of dolomites in a downslope biostrome, Jefferson Formation (Devonian), central Idaho: evidence from REE patterns, stable isotopes, and petrography: Bull. of Canadian Petroleum Geology, v.36, p.202-215.

DOUGLAS, R.J.W., 1974, Geology, Trout River, District of MacKenzie: Geological Survey of Canada, map 1371 A, 1:500,000.

DOUGLAS, R.J.W., GABRIELSE, H., WHEELER, J.O., STOTT, D.F., AND BELYEA, H.R., 1970, Geology of western Canada, in Douglas, R.J.W. (ed), Geology and Economic Minerals of Canada, Geological Survey of Canada, Economic Geology Report 1, p.367-488.

DZULYNSKI, S., 1976, Hydrothermal karst and Zn-Pb sulfide ores: Annales de la Societe Geologique de Pologne, v.46, p.217-230.

FAURE, G., 1986, Principles of Isotope Geology, 2nd. edition, John Wiley and Sons, Inc. New York,

FORD, D. AND WILLIAMS, P., 1990, Karst geomorphology and hydrology: Unwin Hyman Ltd., pp.601.

FRIEDMAN, I. AND O'NEIL, J.R., 1977, Composition of stable isotope fractionation factors of geochemical interest, in Data of Geochemistry, 6th ed. (M. Fleischer, etc.), U.S. Geol. Survey, Prof. Paper, 440 kk.

FRITZ, P., 1969, The oxygen and carbon isotopic composition of carbonates from the Pine Point lead-zinc ore deposits: Economic Geology, v.64, p.733-742.

FRITZ, P. AND SMITH, D.C.W., 1970, The isotopic composition of secondary dolomite: Geochim. et Cosmochim. Acta., v.34, p.1161-1173.

FRITZ, P. AND JACKSON, S.A., 1972, Geochemical and isotopic characteristics of Middle Devonian dolomites from Pine Point, northern Canada: in 24th International Geological Congress, Proceedings, Section 6, p.230-243.

GARVEN, G., 1985, The role of regional fluid flow in the genesis of the Pine Point deposits, Western Canadian Sedimentary Basin: Economic Geology, v.80, p.307-324.

GARVEN, G., 1989, A hydrogeological model for the formation of the giant oil sands deposits of the Western Canada Sedimentary Basin: American Jour. of Science, v.289, p.105-166.

GIVEN, R.K. AND LOHMANN, K.C., 1986, Isotopic evidence for the early diagenesis of the reef facies, Permian reef complex of west Texas and New Mexico: Jour. of Sedimentary Petrology, v.56, p.183-193.

GONZALEZ, L.A. AND LOHMANN, K.C., 1985, Carbon and oxygen isotopic composition of Holocene reefal carbonates: Geology, v.13, p.811-814.

GRAF, J.L., 1984, Effects of Mississippi Valley-type mineralization on REE patterns of carbonate rocks and minerals, Viburnum Trend, southeast Missouri: Jour. of Petrology, v.92, p.307-324.

GREGG, J.M. AND SHELTON, K.L., 1989, Minor and trace element distributions in the Bonneterre Dolomite (Cambrian), southeast Missouri: evidence for possible multiple basin fluid sources and pathways during lead-zinc mineralization: Geological Society of America Bull., v.101, p.221-230.

HARDIE, L.A., 1987, Dolomitization: A critical view of some current views: Jour. Sedimentary Petrology, v.57, p.166-183.

HARRJS, L.D., 1971, A Lower Palaeozoic paleoaquifer-the Kingsport Formation and Mascot dolomite of Tennessee and southwest Virginia: Economic Geology, v.66, p.735-743.

HAYNES, F.M. AND KESLER, S.T., 1987, Chemical evolution of brines during Mississippi Valley-type mineralization: evidence from East Tennnessee and Pine Point: Economic Geology, v.82, p.53-71.

HITCHON, B., 1984, Geothermal gradients, hydrodynamics, and hydrocarbon occurrences, Alberta, Canada: Bull. of American Association of Petroleum Geologists, v.68, p.713-743.

HUMPHREY, J.D., 1988, Late Pleistocene mixing zone dolomitization, southeast Barbados, West Indies: Sedimentology, v.35, p.327-348.

Ą

HUMPHREY, J.D. AND QUINN, T.M., 1989, Coastal mixing zone dolomite, forward modeling, and massive dolomitization of platform-margin carbonates: Jour. of Sedimentary Petrology, v.59, p.438-454.

HUMPHRIS, S.E., 1984, The mobility of the rare earth elements in the crust: in P. Henderson (ed.), Rare Earth Element Geochemistry, New York, Elsevier, p.317-342.

HUTCHEON, I. AND ABERCROMBIE, H., 1990, Carbon dioxide in clastic rocks and silicate hydrolysis: Geology, v.18, p.541-544.

JACKSON, S.A. AND BEALES, F.W., 1967, An aspect of sedimentary basin evolution: the concentration of Mississippi Valley-type ores during late stages of diagenesis: Bull. of Canadian Petroleum Geology, v.15, p.383-433.

JONES, R.M.P., 1980, Basinal isostatic adjustment faults and their petroleum significance: Bull. of Canadian Petroleum Geology, v.28, p.211-251.

KAUFMAN, J., MEYERS, W.J., AND HANSON, G.N., 1990, Burial cementation in the Swan Hills Formation (Devonian), Rosevear Field, Alberta, Canada: Jour. of Sedimentary Petrology, v.60, p.918-939.

KESLER, S., STOIBER, R., AND BILLINGS, G., 1972, Direction of flow of mineralizing solutions at Pine Point, NWT: Economic Geology, v.67, p.19-24.

KINSMAN, D.J.J., 1969, Interpretation of Sr²⁺ concentrations in carbonate minerals and rocks: Jour. of Sedimentary Petrology, v.39, p.486-508.

KIRSTE, D., FOWLER, M.G., GOODARZI, F., AND MACQUEEN, R.W., 1989, Optical and compositional characters and paleothermal implications of a diverse suite of natural bitumens from Middle Devonian carbonate rocks, Pine Point, Northwest

Territories: in Current Research, Part G, Geological Survey of Canada, Paper 89-1G, p.51-55.

1

KREBS, W. AND MACQUEEN, R., 1984, Sequence of diagenetic and mineralization events: Pine Point lead-zinc property, NWT, Canada: Bull. of Canadian Petroleum Geology, v.32, p.434-464.

KRETZ, R., 1982, A model for the distribution of trace elements between calcite and dolomite: Geochim. et Cosmochim. Acta., v.46, p.1979-1981.

KROUSE, H.R., VIAU, C.A., ELIUK, L.S., UEDA, A., AND HALAS, S., 1988, Chemical and isotopic evidence of thermochemical sulphate reduction by light hydrocarbon gases in deep carbonate reservoirs: Nature, v.333, p.415-419.

KYLE, J.R., 1981, Geology of Pine Point lead-zinc district, in Wolf, K.H. ed., Handbook of strata-bound and stratiform ore deposits: New York, Elsevier, v.9, p.643-741.

KYLE, J.R., 1983, Economic Aspects of subaerial carbonates, in Scholle, P.A., Bebout, D.G., and Moore, C.H. (eds): Carbonate depositional environments, American Association of Petroleum Geologists Memoir 33, p.73-92.

LAND, L.S., 1973, Holocene meteoric dolomitization of Pleistocene limestones, North Jamaica: Sedimentology, v.20, p.411-424.

LAND, L.S., 1980, The isotopic and trace element geochemistry of dolomite: The state of the art: *in* D.H. Zenger, J.B. Dunham and R.L. Ethington (eds.), Concepts of models of dolomitization: Soc. Econ. Paleontologists & Mineralogists Spec. Publ. No.28, p.87-110.

LAND, L.S., 1983, The application of stable isotopes to studies of the origin of dolomite and to problems of diagenesis of clastic sediments: in Stable Isotopes in Sedimentary Geology, Soc. Econ. Paleontologists & Mineralogists short course No. 10, p.4-1--4-22.

LAND, L.S., 1985, The origin of massive dolomite: Jour. Geol. Educ., v.33, p.112-125.

LAW, J., 1955, Geology of northwestern Alberta and adjacent areas: American Association of Petroleum Geologists Bull.., v.39, p.1927-1975.

LEACH, D.L., PLUMLEE, G.S., HOFSTRA, A.H., LANDIS, G.P., ROWAN, E.L., AND VIETS, J.G., 1991, Origin of late dolomite cement by CO₂-saturated deep basin brines: evidence from the Ozark region, central United States: Geology, v.19, p.348-351.

LEACH, D.L. AND ROWAN, E.L., 1986, Genetic link between Ouachita foldbelt tectonism and the Mississippi Valley-type lead-zinc deposits of the Ozarks: Geology, v.14, p.931-935.

LORENS, R.B., 1981, Sr, Cd, Mn and Co distribution coefficients in calcite as a function of calcite precipitation rate: Geochim. et Cosmochim. Acta, v.45, p.553-561.

MACHEL, H.G., 1987a, Saddle dolomite as a by-product of chemical compaction and thermo-chemical sulfate reduction: Geology, v.15, p.936-940.

MACHEL, H.G., 1987b, Some aspects of diagenetic sulphate-hydrocarbon redox reactions: in J.D. Marshall (ed), Diagenesis of Sedimentary Sequences, Geological Society Special Publication No.36, p.15-28.

MACHEL, H.G., 1988, Fluid flow direction during dolomite formation as deduced from trace element trends, in Shukla, V. and Baker, P.A. (eds), Sedimentology and geochemistry of dolostones: Soc. Econ. Paleontologists & Mineralogists Spec. Publ. No. 43, p.

4

1

MACHEL, H.G., 1990, Bulk solution disequilibrium in aqueous fluids as exemplified by diagenetic carbonates, in Meshri, I.D. and Ortoleva, P.J. (eds.), Prediction of Reservoir Quality Through Chemical Modelling: American Association of Petroleum Geologists Memoir 49, p.71-83.

MACHEL, H.G. AND ANDERSON, J.H., 1989, Pervasive subsurface dolomitization of the Nisku Formation in central Alberta: Jour. of Sedimentary Petrology, v.59, p.891-911.

MACHEL, H.G., AND MOUNTJOY, E.W., 1986, Chemistry and environments of dolomitization--A reappraisal: Earth Science Rev., v.23, p.175-222.

MACHEL, H.G. AND MOUNTJOY, E.W., 1987, General constraints on extensive pervasive dolomitization - and their application to the Devonian carbonates of western Canada: Bull. of Canadian Petroleum Geology, v.35, p.143-158.

MACQUEEN, R.W. AND POWELL, T.G., 1983, Organic geochemistry of the Pine Point lead-zinc ore field and region, Northwest Territories, Canada: Economic Geology, v.78, p.1-25.

MAIKLEM, W.R., 1971, Evaporative drawdown - a mechanism for water-level lowering and diagenesis in the Elk Point Basin: Bull. of Canadian Petroleum Geology, v. 19, p.487-503.

MATTES, B.W. AND MOUNTJOY, E.W., 1980, Burial dolomitization of the

Upper Devonian Miette buildup, Jasper National Park, Alberta, in, D.H. Zenger, J.B. Dunham and R.L. Ethington eds., Concepts of models of dolomitization: Soc. Econ. Paleontologists & Mineralogists Spec. Publ. No. 28, p.259-297.

McCAMIS, J.G., AND L. S. GRIFFITH, 1967, Middle Devonian facies relationships, Zama area, Alberta: Bull. of Canadian Petroleum Geology, v.15, p.434-467.

McINTIRE, W.L., 1963, Trace element partition coefficients- a review of theory and application to geology: Geochim. et Cosmochim. Acta, v.27, p.1209-1264.

McLENNAN, S.M., 1989, Rare earth elements in sedimentary rocks: influence of provenance and sedimentary processes: in B.R. Lipin and G.A. McKay (eds.), Geochemistry and Mineralogy of rare earth elements, Mineralogical Society of America short course, v.21, p.169-200.

McNUTT, R.H., FRAPE, S.K., FRITZ, P., JONES, M.G. AND MacDONALD, I.M., 1990, The ⁸⁷Sr/⁸⁶Sr values of Canadian Shield brines and fracture minerals with application to groundwater mixing, fracture history and geochronology: Geochem. et Cosmochim. Acta, v.54, p.205-215.

MEDFORD, G.A., MAXWELL, R.J., AND ARMSTRONG, R.L., 1984, ⁸⁷Sr/⁸⁶Sr ratio measurements on sulfides, carbonates, fluid inclusions from Pine Point, Northwest Territories, Canada: an ⁸⁷Sr/⁸⁶Sr ratio increase accompanying the mineralizing process: Economic Geology, v.78, p.1375-1378.

MELJER DREES, N.C., 1986, Evaporitic deposits of western Canada: Geological Survey of Canada, Paper 85-20, 118p.

MEIJER DREES, N.C., 1988, The Middle Devonian sub-Watt Mountain

unconformity across the Tathlina uplift; District of Mackenzie and northern Alberta, Canada: in N.J. McMillan, A.F. Embry, and D.J. Glass (eds.), Devonian of the world, Proceedings of the Second International Symposium on the Devonian System, Canadian Society of Petroleum Geologists, Alberta, v.II., p.477-494.

į

MEYERS, W.J. AND LOHMANN, K.C., 1985, Isotope geochemistry of regionally extensive calcite cement zones and marine components in Mississippian limestones, New Mexico: in Schneidermann, N and Harris, P.M. (eds.) Carbonate Cements, Soc. Econ. Paleont. Miner. Spec. Pub 36, p.223-239.

MORROW, D.W., 1982, Diagenesis II. Dolomite--part II: Dolomitization models and ancient dolostones: Geoscience Canada, v.9, p.95-107.

MORROW, D.W., CUMMING, G.L., AULSTEAD, K.L., 1990, The gas-bearing Devonian Manetoe Facies, Yukon and Northwest Territories: Geol. Survey of Canada, Bull 400, 54p.

MORROW, D.W., CUMMING, G.L., AND KOEPNICK, R.B., 1986, Manetoe Facies - a gas-bearing, megacrystalline, Devonian dolomite, Yukon and Northwest Territories, Canada: Bull. of American Association of Petroleum Geologists, v.70, p.702-720.

MORROW, D.W., CUMMING, G.L., AND AULSTEAD, K.L., 1990, The gasbearing Devonian Manetoe Facies, Yukon and Northwest Territories: Geological Survey of Canada Bull. 400.

MOORE, P.F., 1988, Devonian geohistory of the Western Interior of Canada, in N.J. McMillan, A.F. Embry, and D.J. Glass (eds), Devonian of the world, Proceedings of the Second International Symposium on the Devonian System, Canadian Society of Petroleum Geologists, Alberta, v.I., p.67-83.

MOUNTJOY, E.W. AND HALIM-DIHARDJA, M.K., 1991, Multiple phase fracture and fault-controlled burial dolomitization, Upper Devonian Wabamun Group, Alberta: Jour. of Sedimentary Petrology, v.61, p.590-612.

MOUNTJOY, E.W., QING, H., AND MCNUTT, R., in press, Sr isotopic composition of Devonian dolomites, Western Canada: significance regarding sources of dolomitizing fluids: Applied Geochemistry.

MUCCI, A., 1988, Manganese uptake during calcite precipitation from seawater: conditions leading to the formation of a pseudokutnahorite: Geochim. et Cosmochim. Acta, v.52, p.1859-1868.

NORRIS, A.W., 1965, Stratigraphy of Middle Devonian and older Palaeozoic rocks of the Great Slave Lake region, N.W.T.: Canada Geological Survey Mem. 322, 180p.

OHLE, E.L., 1985, Breccias in Mississippi Valley-type deposits: Economic Geology, v.80, p.1736-1752.

OLIVER, J., 1986, Fluids expelled tectonically from orogenic belts: their role in hydrocarbon migration and other geologic phenomena: Geology, v.14, p.99-102.

PACKARD, J.J., PELLIGRIN, G.J., AL-AASM, I.S., SAMSON, I., AND GAGNON, J, 1990, Diagenesis and dolomitization associated with hydrothermal karst in Famennian upper Wabamun ramp sediments, northwestern Alberta: in Bloy, G.R. and Hadley, M.G. (eds.), The development of porosity in carbonate reservoirs: Canadian Society of Petroleum Geologists Continuing Education Short Course, Section 9.

PAQUETTE, J. AND REEDER, R., 1990, New type of compositional zoning in calcite: Insights into crystal-growth mechanisms: Geology, v.18, p.1244-1247.

PAREKH, P.P., MOLLER, P., DULSKI, P., AND BAUSCH, W.M., 1977, Distribution of trace elements between carbonate and noncarbonate phases of limestone: Earth and Planetary Science Letters, v.34, p.39-50.

PALMER, M.R., 1985, Rare earth elements in foraminifera tests: Earth and Planetary Science Letters, v.73, p.285-298.

PATTERSON, R.J. AND KINSMAN, D.J.J., 1982, Formation of diagenetic dolomite in coastal sabkha along Arabian (Persian) Gulf: American Association of Petroleum Geologists Bull., v.66, p.28-43.

PINGITORE, N.E., EASTMAN, M.P., SANDIGE, M., ODEN, K., AND FREIHA, B., 1988 The coprecipitation of manganese(II) with calcite: an experimental study: Marine Chemistry, v.25, p.107-116.

POPP, B.N., ANDERSON, T.F. AND SANDERG, P.A., 1986, Textural, elemental, and isotopic variations among constituents in Middle Devonian limestones, North America: Jour. of Sedimentary Petrology, v.56, p.715-727.

PORTER, J.W., PRICE, R.A., AND MCCROSSAN, R.G., 1982, The Western Canada Sedimentary Basin: Phil. Trans. R. Soc. Lond., v.A305, p.169-192.

POTTER, A.P., CLYNNE, M.A., AND BROWN, D.L., 1978, Freezing point depression of aqueous sodium chloride solutions: Economic Geology, v.73, p.284-285.

POWELL, T.G., 1984, Some aspects of the hydrocarbon geochemistry of a Middle Devonian barrier-reef complex, western Canada, in Palacas, J.G. (ed.), Petroleum geochemistry and source rock potential of carbonate rocks: American Association of Petroleum Geologists Studies in Geology No. 18, p.45-61.

Ž

POWELL, T.G. AND MACQUEEN, R.W. 1984, Precipitation of sulfide ores and organic matter: sulfate reactions at Pine Point, Canada: Science, v.224, p.63-66.

QING, H., AND MOUNTJOY, E., 1989, Multistage dolomitization in Rainbow buildups, Middle Devonian Keg River Formation, Alberta, Canada: Jour. of Sedimentary Petrology, v.59, p.114-126.

QING, H. AND MOUNTJOY, E., 1990, Petrography and diagenesis of Middle Devonian Presqu'ile barrier: implications on formation of dissolution vugs and breccias at Pine Point and adjacent subsurface, District of Mackenzie, in Current Research, Part D, Geological Survey of Canada, Paper 90-1D, p.37-45.

REEDER, R.J. AND PROSKY, J.L., 1986, Compositional sector zoning in dolomite: Jour. of Sedimentary Petrology, v.56, p.237-247.

REEDER, R.J. AND GRAMS, J.C., 1987, Sector zoning in calcite cement crystals: Implications for trace element distribution in carbonates: Geochim. et Cosmochim. Acta, v.51, p.187-194.

RHODES, D., LANTOS, E.A., LANTOS, J.A., WEBB, R.J., AND OWENS, D.C., 1984, Pine Point orebodies and their relationship to the stratigraphy, structure, dolomitization, and karstification of the Middle Devonian barrier complex: Economic Geology., v.79, p.991-1055.

ROEDDER, E., 1968, Temperature, salinity, and origin of the ore-forming fluids at Pine Point, Northwest Territories, Canada, from fluid inclusion studies: Economic Geology, v.63, p.439-450.

ROSS, J.R., 1990, Deep crust and basement structure of Peace River Arch region: constraints on mechanisms of formation: Bull. of Canadian Petroleum Geology,

RUSH, P.F. AND CHAFETZ, H.S., 1990, Fabric-retentive, non-luminescent brachiopods as indicators of original δ^{13} C and δ^{18} O composition: A test: Jour. of Sedimentary Petrology, v.60, p.968-981.

SALLER, A.H., 1984, Petrologic and geochemical constraints on the origin of subsurface dolomite, Enewetak Atoll: an example of dolomitization by normal sea water: Geology, v.12, p.217-220.

SANGSTER, D.F., 1988, Breccia-hosted lead-zinc deposits in carbonate rocks, in James, N.P. and Choquette, P.W. (ed.), Paleokarst, Springer-Verlag, 416p.

SASAKI, A. AND KROUSE, H.R., 1969, Sulfur isotopes and the Pine Point leadzinc mineralization: Economic Geology, v.64, p.718-730.

SASS-GUSTKIEWICZ, M., DZULYNSKI, S., AND RIDGE, J.D., 1982, The emplacement of zinc-lead sulfide ores in the Upper Silesian district - a contribution to the understanding of Mississippi Valley-type deposits: Economic Geology, v.77, p.392-412.

SCHERER, M. AND SEITZ, H., 1980, Rare-earth element distribution in Holocene and Pleistocene corals and their redistribution during diagenesis: Chemical Geology, v.28, p.279-289.

SCHMIDT, V., McILREATH, I.A. AND BUDWILL, A.E., 1985, Middle Devonian cementation reefs encased in evaporites, Rainbow field, Alberta, in Roehl, P.O. and Choquette, P.W. eds., Carbonate petroleum reservoirs: Springer-Verlag Inc., p.141-160

SKALL, H., 1975, The paleoenvironment of the Pine Point lead-zinc district: Economic Geology, v.70, p.22-45.

SPIRAKIS, C.S. AND HEYL, A.V., 1988, Possible effects of thermal degradation of organic matter on carbonate paragenesis and fluorite precipitation in Mississippi Valley-type deposits: Geology, v.16, p.1117-1120.

SPIRAKIS, C.S. AND HEYL, A., 1990, Organic matter as the key to localization of Mississippi Valley-type ores: 8th IAGOD Symposium, Aug., 1990, Ottawa, program with abstracts, p.A36-A37.

TEARE, M., 1990, Sedimentology and diagenesis of Middle Devonian Winnipegosis Reef complexes, Dawson Bay, Manitoba [unpub. M.Sc. Thesis]: McGill University, Montreal, 163p.

VAHRENKAMP, V.C. AND SWART, P., 1990, New distribution coefficient for the incorporation of strontium into dolomite and its implications for the formation of ancient dolomites: Geology, v.18, p.387-391.

VAIL, P.R., MITCHUM, R.M. Jr., AND THOMPSON, S., 1977, Seismic stratigraphy and global changes of sea level: in Payton, C.E. (ed.) Seismic Stratigraphy - Applications to hydrocarbon Exploration, American Association of Petroleum Geologists Memoir 26, p.83-97.

VEIZER, J., 1983, Chemical diagenesis of carbonates: Theory and application of trace element technique, in Stable isotopes in sedimentary geology: Soc. Econ. Paleontologists & Mineralogists short course No. 10, p.3-1--3-100.

VEIZER, J., FRITZ, P., AND JONES, B., 1986, Geochemistry of brachiopods: oxygen and carbon isotopic records of Paleozoic oceans: Geochim. et Cosmochim.

Acta, v.50, p.1679-1696.

WALLS, R.A. AND BURROWES, G., 1985, The role of cementation in the diagenetic history of Devonian reefs: in N. Schneidermann and P.M. Harris (eds.), Carbonate Cements, Soc. Econ. Paleontologists & Mineralogists Spec. Publ. No. 36, p.185-220.

Appendix 1. List of well studied (see Fig. 1 for location; depth in ft.)

a) NWT

```
#1 G-15
                                         #4 D-34
                                         BRIGGS NE TATHLINA LAKE #9
GENERAL
           CRUDE
                    RANVIK REEF
CREEK LOCATION: 60-54-24; 116-17-30
                                         LOCATION:
                                                      60-43-12;
                                                                 117-22-17;
GEOLOGIC TOPS:
                                         GEOLOGIC TOPS:
   Slave P
                                            Slave P
                                                     2185
            653
                                                     2389
   Watt
            805
                                             Watt
                                                     2390
                                            Sul. P.
   Presq
            830
                                            Pine P
                                                     2500
   Pine P
            901
  CORED INTERVALS:
                                             Chin.
                                                     2820
                                           CORED INTERVALS
   879-909; 916-934
                                             2386-2519.
#2 C-19
NWT DESMARAIS LAKE #1
                                         #5 K-48
                                         PLACID WOOD W. TATHLINA K-48
LOCATION:
              60-48-00;
                          116-48-00;
GEOLOGIC TOPS:
                                         LOCATION:
                                                       60-37-36;
                                                                   117-53-40:
                                         GEOLOGIC TOPS:
   Slave P
            1560
   Watt
             ?
                                             Slave P
                                                     2770
             ?
                                             Watt
                                                     2950
   Sul. P.
   Pine P
            1820
                                             Sul. P.
                                                     2957
            2280
                                             Pine P
                                                     3060
   Chin
  CORED INTERVALS
                                             Keg. R.
                                                      3080
   1290-1304; 1563-1573;
                                             Basal B
                                                      3238
2147-2155.
                                           CORED INTERVALS
                                             3033-3093.
#3 K-18
                                          #6 F-60
BRIGGS NE TATHLINA LAKE #2
                                          BRIGGS FEOTUS LAKE #1
                          117-17-57;
                                          LOCATION:
LOCATION: 60-47-35;
                                                        60-55-12;
                                                                    118-31-48;
GEOLOGIC TOPS:
                                          GEOLOGIC TOPS:
   Slave P
                                             Slave P
            1817
                                                      2250
   Watt
            2034
                                             Watt
                                                     2470
   Sul. P.
           2040
                                             Sul. P.
                                                     2476
   Pine P
            2120
                                             Pine P
                                                      2498
  CORED INTERVALS
                                                     2674
                                             Chin.
    2021-2104; 2433-2466.
                                             Basal B
                                                      2728
                                            CORED INTERVALS
                                             2252-2744.
```

#7 B-07 BRIGGS RABBIT LAKE #3 LOCATION: 60-56-06; 118-45-43; GEOLOGIC TOPS: Slave P 2350 Watt ? Sul. P. 2540 Pine P 2569 CORED INTERVALS 2510-2588; 2590-2619.	#10 I-19 BRIGGS TROUT RIVER #3 LOCATION: 60-58-44; 120-01-55; GEOLOGIC TOPS: Horn R. 2930 Watt ? Sul. P. 2998 Pine P 3240 CORED INTERVALS 3459-3534.
#8 O-25 BRIGGS RABBIT LAKE #2 LOCATION: 60-54-53; 118-49-36; GEOLOGIC TOPS: Slave P 2492 Watt 2647 Sul. P. 2659 Pine P 2700 Chin. 2830 CORED INTERVALS 2495-2910.	#11 L-59 UNION PAN AM TRAINOR L-59 LOCATION: 60-28-33; 120-40-50; GEOLOGIC TOPS: Slave P 5662 Watt 5792 Sul. P. 5802 Pine P 5862 KLUA T. 6042 KEG. R. 6060 CHIN. 6285 CORED INTERVALS 5770-5950.
#9 N-06 IMPERIAL REDKNIFE N-06 LOCATION: 60-55-49; 119-16-10; GEOLOGIC TOPS: Slave P	#12 F-51 H.B. CAMERON HILLS F-51 LOCATION: 60-00-15; 117-19-55; GEOLOGIC TOPS: Slave P 4200 Watt 4362 Sul. P. 4378 Muskeg 4472 Keg R. 4787 CORED INTERVALS: 4903-4963

SP TAN

#13 G-48 BRIGGS WEST TATHLINA #1 LOCATION: 60-37-21; 117-53-08; GEOLOGIC TOPS: Slave P 2780 Watt 2950 Sul. P. 2965 Pine P. 3030 Ss CORED INTERVALS: 3158-3163	#16 J-74 CDR CPOG CHEVRON MILLS LAKE LOCATION: 61-13-37; 118-13-47; GEOLOGIC TOPS: Slave P ? Watt ? Sul. P. ? Pine P. ? Basal KR 2096 Chin 2125 CORED INTERVALS: 2090-2152
#14 C-22 PAN AM ANDEX CAMERON C-22 LOCATION: 60-11-11; 117-49-47; GEOLOGIC TOPS: Slave P	#17 O-72 UNION PAIN AM TRAINOR O-72 LOCATION: 60-11-48; 120-13-50; GEOLOGIC TOPS: Slave P 5691 Watt 5925 Sul. P. 5946 Pine P. 6302 Chin 6610 CORED INTERVALS: 5827-5858
#15 K-21 BRIGGS NE RABBIT LAKE #1 LOCATION: 61-00-34; 118-35-09; GEOLOGIC TOPS: Slave P 2404 Watt ? Sul. P. 2595 Pine P. 2607 Ss 2780 CORED INTERVALS: 2605-2634; 2748-2765.	#19 J-26 MURPHY CANADA ALEXANDRA FALL #2 LOCATION: 60-15-30; 116-34-40; GEOLOGIC TOPS: Slave P

#20 NWT ESCAPMENT LAKE #3 LOCATION: 60-15-30; 116-34-40; GEOLOGIC TOPS: Slave P	B02 LOCATION: D-44-C/94-I-10 GEOLOGIC TOPS: Slave P 5895 Watt 6161 Presq 6162 Muskeg 6174 CORED INTERVALS: 5903-5917; 6191-6217.
CORED INTERVALS: 1537-1550.	B03 LOCATION: D-79-K/94-I-15
#21 H.B. CAMERON A-05 LOCATION: 60-04-02; 117-30-27; GEOLOGIC TOPS: Slave P.	GEOLOGIC TOPS: Slave P 6446 Watt 6778 Muskeg 6780 Chin. 7650 CORED INTERVALS: 6656-6697; 6873-6908. B04 LOCATION: C-09-D/94-P-06 GEOLOGIC TOPS: Slave P 7052 Watt 7312 Muskeg 7317 Presq. 7317 CORED INTERVALS: 7431-7454.
B01 LOCATION: D-37-B/94-I-7 GEOLOGIC TOPS:	B05
Slave P 6300 Watt 6655 Muskeg 6660 Chin 7584 CORED INTERVALS: 6417-6466; 6653-6702; 7101-7148.	LOCATION: D-67-K/94-P-09 GEOLOGIC TOPS: Slave P 5622 Watt 6070 Muskeg 6350 Chin. 6489 CORED INTERVALS: 6375-6494.

B06	B10
LOCATION: B-22-B/94-P-10	LOCATION: A-41-J/94-P-09
GEOLOGIC TOPS:	GEOLOGIC TOPS:
Slave P 6158	Slave P 5360
Hi 6446	Watt 6121
Keg R 6611	Muskeg 6270
Chin. 6760	Chin. 6440
CORED INTERVALS:	CORED INTERVALS:
6651-6711.	CORED INTERVALS.
0051-0711.	
D	
B07	B11
LOCATION: D-47-C/94-P-12	LOCATION: A-27-K/94-P-12
GEOLOGIC TOPS:	GEOLOGIC TOPS.
Slave P 6861	Slave P 6587
Watt 7140	W att 6876
Sul. P. 7146	Muskeg 6880
Presq. 7218	Presq. 6926
Chin. 8020	CORED INTERVALS:
CORED INTERVALS:	6615-6675; 6904-6928.
6875-7273	0010 0010, 0111 0720
0010 1215	
B08	B12
LOCATION: B-40-A/94-P-05	LOCATION: C-60-E/94-I-11
GEOLOGIC TOPS:	GEOLOGIC TOPS:
Slave P 6900	Slave P 6233
Watt 7027	Watt 6680
CORED INTERVALS:	Muskeg 6681
6921-7047	Presq. 6682
	Chin. 7630
	CORED INTERVALS:
	6264-6780; 6906-6966
B09	
LOCATION: B-46-A/94-I-16	
GEOLOGIC TOPS:	
Slave P 5184	
Watt 5432	
Presq. 5454	
· •	
Muskeg 5455	
Chin. 6414	
CORED INTERVALS:	
5194-5216: 5900-5926.	

Appendix 2. $\delta^{18}O$ and $\delta^{13}C$ values of the Presqu'ile carbonates.

Туре	Location	Depth (ft)	δ ¹⁸ O ‰ PDB	δ ¹³ C ‰ PDB
SD-PP	PP-N81	OPEN PIT	-7.38	0.42
SD-PP	PP-N81	OPEN PIT	-8.51	0.19
SD-PP	PP-N81	OPEN PIT	-10.39	0.13
SD-PP	PP-N81	OPEN PIT	-10.22	-0.4
SD-PP	PP-G03-19	40	-10.8	1.19
SD-PP	PP-7070	165	-10.52	-0.28
SD-PP	PP-N81-19	321	-10.05	0
SD-SUB1	NWT-D50	1899	-12.3	0.98
SD-SUB2	NWT-072	5852	-16.01	-0.08
SD-SUB2	NWT-072	5856	-15.5	0.08
SD-SUB2	B12	6634	-14.91	0.03
SD-SUB2	B08	6971	-13.23	-1.34
SD-SUB2	B08	6952	-12.89	-0.5
SD-SUB2	B08	7003	-13.87	-3.65
SD-SUB2	B08	7025	-13.06	-1.22
SD-PP	PP-M64	OPEN PIT	-10.42	-0.29
SD-PP	PP-M64	OPEN PIT	-10.27	-0.35
SD-PP	PP-M64	OPEN PIT	-10.47	-0.72
SD-PP	PP-M64	OPEN PIT	-9.57	0.42
SD-PP	PP-M64	OPEN PIT	-9.54	0.72
SD-PP	PP-P24	OPEN PIT	-9.21	0.56
SD-PP	PP-P24	OPEN PIT	-9.4	0.54
SD-PP	PP-P77	OPEN PIT	-10.05	-0.11
SD-PP	PP-T37	OPEN PIT	-8.92	1.52
SD-PP	PP-T37	OPEN PIT	-7.32	1.11
SD-PP	PP-T37	OPEN PIT	-7.36	1.2

Туре	Location	Depth (ft)	δ ¹⁸ O ‰ PDB	δ ¹³ C ‰ PDB
SD-PP	PP-X15	OPEN PIT	-9.59	0.7
SD-PP	PP-X15	OPEN PIT	-8.03	-0.11
SD-PP	PP-X51	OPEN PIT	-8.3	1.27
SD-PP	PP-X51	OPEN PIT	-8.07	1.13
SD-PP	PP-X51	OPEN PIT	-8.32	1.53
SD-PP	PP-X51	OPEN PIT	-7.03	1.24
SD-PP	PP-X53	OPEN PIT	-9.41	1.18
SD-PP	PP-Y53	OPEN PIT	-7.71	1.18
SD-PP	PP-Y53	OPEN PIT	-8.52	1.08
SD-PP	PP-Y53	OPEN PIT	-8.43	1.22
SD-PP	PP-X51	OPEN PIT	-7.77	1.62
SD-PP	PP-X51	OPEN PIT	-8.01	1.69
SD-PP	PP-Y56	OPEN PIT	-8.15	1.45
SD-PP	PP-Y56	OPEN PIT	-8.07	1.61
SD-PP	PP-G03-19	270	-8.05	0.33
SD-PP	PP-5315B	115	-9.01	0.1
SD-PP	PP-M64-6	157	-8.14	0.39
SD-PP	PP-2822	349	-8.88	0.14
SD-PP	PP-2822	253	-10.76	-1.22
SD-PP	PP-2822	282	-11.12	-0.91
SD-PP	PP-2822	275	-10.04	-0.55
SD-PP	PP-2870	221	-8.69	1.32
SD-SUB1	NWT-G15	916	-12.35	-0.2
SD-SUB1	NWT-A77	1545	-10.99	-2.24
SD-SUB1	NWT-C19	1569	-12.78	1.66
SD-SUB1	NWT-K48	3075	-10.57	-0.24
SD-SUB1	NWT-M05	4191	-11.82	-1.29
SD-SUB1	NWT-E33	3229	-12.77	-1.25
SD-SUB1	MWT-A05	4652	-10.56	0.2

				δ ¹³ C ‰ PDB
SD-SUB2	B01	6702	-13.12	-0.53
SD-SUB2	B04	7439	-13.02	-2.59
SD-SUB2	B06	6252	-13.28	-1.53
SD-SUB2	B08	7032	-14.47	-3.38
SD-SUB2	B08	7048	-14.13	-3.45
SD-SUB2	B08	7048	-13.61	-2.31
CCD-PP	PP-N81	OPEN PIT	-9.5	0.66
CCD-PP	PP-N81	OPEN PIT	-10.39	0.35
CCD-PP	PP-N81	OPEN PIT	-9.02	-1.42
CCD-PP	PP-N81	OPEN PIT	-7.85	0.06
CCD-PP	PP-N81	OPEN PIT	-9.32	1.03
CCD-PP	PP-G03-19	135	-9.14	0.76
CCD-SUB1	NWT-D50	1899	-11.12	1.41
CCD-SUB2	NWT-O72	5852	-15.49	-0.6
CCD-SUB2	NWT-O72	5856	-15.35	-1.44
CCD-SUB2	NWT-O72	5877	-14.53	-0.04
CCD-SUB2	B12	6666	-15.84	0.28
CCD-SUB2	B08	6973	-13.36	-1.38
CCD-SUB2	B08	6971	-12.96	-1.52
CCD-SUB2	B08	6952	-12.98	-0.56
CCD-SUB2	B08	7003	-14.44	-3.45
CCD-PP	PP-M64	OPEN PIT	-10.45	-0.77
CCD-PP	PP-X51	OPEN PIT	-8.24	1.29
CCD-PP	PP-X51	OPEN PIT	-7.88	1.4
CCD-PP	PP-T37	OPEN PIT	-7.62	1.55
CCD-PP	PP-T37	OPEN PIT	-8.32	1.34
CCD-PP	PP-Y53	OPEN PIT	-8.52	1.28
CCD-PP	PP-E30	740	-10.59	-0.23
CCD-PP	PP-5135B	115	-8.97	0.3

CCD-PP PP-2162 359 CCD-PP PP-2822 253 CCD-PP PP-2822 269	-10.71 -10.62 -8.48 -9.86	0.31 -0.89 0.05
	-8.48	
CCD_DD		0.05
CCD-F1 11-2022 207	-9.86	3.02
CCD-PP PP-2822 320		-0.34
CCD-PP PP-2813 268	-10.49	-0.5
CCD-PP PP-2813 356	-9.38	-0.53
CCD-PP PP-2813 363	-8.91	0.49
CCD-PP PP-2813 250	-11.19	-0.78
CCD-PP PP-2582 48	-7.89	0.22
CCD-PP PP-3337 80	-7.67	0.16
CCD-PP PP-3316 189	-7.88	-0.37
CCD-PP PP-2870 221	-9.14	-0.11
CCD-PP PP-2729 374	-10.13	-1.2
CCD-PP PP-2729 419	-8.73	-0.21
CCD-PP PP-2729 433	-8.34	0.42
CCD-PP PP-2729 502	-8.24	0.67
CCD-SUB1 NWT-G15 916	-12.01	0.07
CCD-SUB1 NWT-C19 1569	-12.44	1.78
CCD-SUB1 NWT-K48 3075	-12.03	1.18
CCD-SUB2 B06 6252	-10.41	-0.21
CCD-SUB2 B08 7032	-13.96	-3.8
CCD-SUB2 B08 7044	-13.23	-2.24
MCD PP-M64 OPEN PIT	-7.36	0.85
MCD PP-3305 682	-9.43	1.38
MCD PP-2822 534	-5.92	0.65
MCD PP-2822 645	-5.56	1.6
MCD PP-2822 736	-5.53	2.22
MCD PP-2822 835	-6.61	1.95
MCD PP-2813 392	-7.59	1.09

Туре	Location	Depth (ft)	δ ¹⁸ O ‰ PDB	δ ¹³ C ‰ PDB
MCD	PP-2813	472	-7.04	1.26
MCD	PP-2813	530	-5.14	1.78
MCD	PP-2813	575	-5.23	2.53
MCD	PP-2813	642	-5.86	1.42
MCD	PP-2813	679	-3.7	1.47
MCD	PP-2813	751	-4.03	-1.29
MCD	PP-2813	870	-4.06	0.98
MCD	PP-2143	38	-4.98	2.25
MCD	PP-2225	57	-5.49	2.11
MCD	PP-2582	154	-4.89	2.08
MCD	PP-3337	280	-6.59	1.16
MCD	PP-3316	241	-5.57	1.94
MCD	PP-2870	309	-5.99	2.46
MCD	PP-2729	577	-6.35	1.29
FCD	NWT-J26	2370	-2.95	0.27
FCD	NWT-A05	4609	-1.58	0.77
FCD	MWT-C22	3192	-3.84	1.65
A-FCD	PP-W17	OPEN PIT	-6.73	0.92
A-FCD	PP-2822	384	-7.92	0.2
A-FCD	PP-2822	452	-7.14	0.89
BRACH	PP-3305	670	-4.21	1.86
BRACH	PP-3305	670	-3.85	1.84
CRINO	PP-1839	105	-8.02	0.64
CRINO	PP-1839	113	-7.99	-0.62
CRINO	PP-1828	73	-8.02	-0.55
STROM	PP-1828	70	-10.73	-2.33
AMPHI	PP-M64	OPEN PIT	-8.45	-0.48
LCC	PP-N81	OPEN PIT	-9.64	-2.61
LCC	PP-N81	OPEN PIT	-12.81	-6.85

Type	Location	Depth (ft)	δ ¹⁸ O ‰ PDB	δ ¹³ C ‰ PDB
LCC	PP-N81	OPEN PIT	-10.32	0.66
LCC	PP-M64	OPEN PIT	-8.67	0
LCC	PP-Y65	OPEN PIT	-11.42	-3.61
LCC	PP-X15	OPEN PIT	-9.34	0.72
LCC	PP-7070	165	-9.94	0.24
LCC	B08	7009	-16.7	-5.52
LCC	B07	7242	-15.42	-3.43
WCC	PP-X51	OPEN PIT	-10.48	1.37
WCC	PP-P24	OPEN PIT	-8.82	0.15
WCC	PP-P24	OPEN PIT	-11.24	-1.17
WCC	PP-P24	OPEN PIT	-11.78	-1.25
WCC	PP-P24	OPEN PIT	-11.35	-1.15
WCC	PP-165	OPEN PIT	-6.94	-0.1
WCC	PP-165	OPEN PIT	-6.13	0.74
WCC	PP-N81	OPEN PIT	-8.63	-4.01
WCC	PP-N81	OPEN PIT	-9.02	0.12
WCC	PP-N81	OPEN PIT	-8.11	-1.63
WCC	PP-M64	OPEN PIT	-10.78	-1.57
WCC	PP-M64	OPEN PIT	-11.53	-5.54
WCC	PP-M64	OPEN PIT	-11.71	-2.6
WCC	PP-3316	124	-7.55	-1.07
WCC	PP-2870	120	-10.25	0.39
WCC	PP-2870	200	-8.38	0.45
WCC	PP-5315B	115	-9.02	0.04

Appendix 3. 87 Sr/ 86 Sr ratios of the Presqu'ile carbonates and their corresponding δ^{18} O and δ^{13} C values.

Location	Depth	⁸⁷ Sr/ ⁸⁶ Sr	δ ¹⁸ O ‰ PDB	δ ¹³ C ‰ PDB
fine-crystalli	ne dolomite			
NWT-J26	2370	0.70812	-2.95	0.27
NWT-C22	3192	0.70790	-3.84	1.65
NWT-A05	4609	0.70790	-1.58	0.77
PP-2822	452	0.70822	-7.14	0.89
PP-W17	PIT	0.70833	-6.73	0.92
medium-crys	talline dolom	ite		
PP-2822	645	0.70871	-5.56	1.60
PP-2822	736	0.70812	-5.14	1.78
PP-3305	682	0.70846	-9.43	1.38
coarse-crysta	lline dolomite	2		
PP-2822	230	0.70829	-9.86	-0.34
PP-Y53	PIT	0.70816	-8.52	1.28
PP-N81	PIT	0.70850	-9.50	0.66
PP-N81	PIT	0.70866	-9.32	1.03
PP-2822	349	0.70880	-8.88	0.14
B12	6666	0.71055	-15.84	0.28
B08	7025	0.70951	-13.06	-1.22
NWT-072	5852	0.71211	-15.49	-0.60
B08	6973	0.70934	-13.36	-1.38
saddle dolom	iite			
PP-2822	275	0.70847	-10.04	-0.55
PP-Y53	PIT	0.70816	-8.43	1.22
PP-N81	PIT	0.70807	-10.22	-0.40
PP-M64	PIT	0.70831	-10.27	-0.72

Location	Depth	⁸⁷ Sr/ ⁸⁶ Sr	δ ¹⁸ O ‰ PDB	δ ¹³ C ‰ PDB
saddle dolon	nite			
PP-M64	PIT	0.70840	-9.54	0.72
PP-P77	PIT	0.70818	-10.05	-0.11
PP-P77	PIT	0.70818	-9.02	0.12
PP-N81	PIT	0.70821		
NWT-C19	1569	0.70839	-12.78	1.66
NWT-K48	3075	0.70859	-12.03	-0.24
NWT-G15	916	0.70850	-12.35	-0.20
NWT-E33	3229	0.70918	-12.77	-1.25
NWT-O72	5852	0.70895	-16.01	-0.08
B08	6971	0.70955	-13.23	-1.34
B12	6634	0.71060	-14.91	0.03
B08	7048	0.70920	-13.61	-2.31
B04	7439	0.70942	-13.02	-2.59
white calcite	<u> </u>			
PP-2870	120	0.71420	-10.25	0.39
PP-2870	200	0.71428	-8.38	0.45
PP-N81	PIT	0.71360	-8.11	-1.63
PP-M64	PIT	0.71468	-10.78	-1.57
PP-M64	PIT	0.70850	-11.53	-5.54
PP-I65	PIT	0.71282	-6.13	0.74
PP-I65	PIT	0.71388	-6.94	-0.10
late-stage co	oarse-crystalli	ne calcite		
PP-2822	344	0.71612	· ————————————————————————————————————	
PP-Y65	PIT	0.71613	-11.42	-3.61
B08	7009	0.71054	-16.70	-5.52
B07	7242	0.71121	-15.42	-3.43

Appendix 4. Fluid inclusion measurements(°C)

	B01-67	702' sad	dle dolo	omite			B08-69	971' sad	dle dol	omite
	Th	Tm	S	Te			Th	Tm	S	Te
	117	-11.0	15.0	-45.8			204	-18.8	21.8	-46
	153.1	-10.8	14.8	-43.9			170	-18.0	21.2	-51
	166.3	-10.6	14.6	-49.9			158	-18.0	21.2	-51
	188.2	-9.1	13.0	-42.0			164	-17.8	21.0	-43
	176.1		10,0	-44.6			162			
	121						202			
AVG.	153.6	-10.4	14.4	-45.2			204			
A V O.	133.0	-10.4	1.4.4	-45.2			164			
	B06-62	252' sad		omite	av	g.	178.5	-18.2	21.3	-47.8
	Th	Tm	S	Te						
	195	-14.5	18.4	-47.0						
	156	-15.5	19.2	-50.5			C19-15	569' sad	dle dolo	omite
	237	-14.7	18.5	-52.0			Th	Tm	S	Te
	163	-15.1	18.9	-49.0			120	-9.4	13.3	-48.1
	169			-47.0			118	-12.8	16.8	-46.5
		-16.1	19.7	-52.5			119	-9.8	13.8	-39.0
		-15.8	19.5	-51.5			109	-13.7	17.6	-51.0
	151						112	-11.7	15.7	-51.4
	147							-11.9	15.9	-47.1
	162							-15.8	19.5	-51.0
	143						109			
	161						123			
	181						100			
	152					avg.	113.8	-12.2	16.2	-47.7
avg.	168.1	-15.3	19.0	-49.9						
	B08-69	952' sad	dle dola	omite			D50-10	901' sad	ldle dol	omite
	Th	Tm	S	7			Th	701 sau	S	Te
	164	-17.4	20.7	-41			121	-7.6	11.2	-36.0
	157	-18.2	21.3	-40			108	-7.4	11.0	-30.0
	170	-15.5	19.2	-48			113	-6.6	10.0	-44.0
	182	-17.5	20.8	- 6 -51			137	-0.6 -7.5	11.1	-42.0
	151	-18.4	21.5	-52			109	-7.5 -7.6	11.1	-34.0
	161	-18.4	21.5	-52 -52			109	-7.6	11.2	-34.0
	162	-18.6	21.6	-52 -52			101	-7.0	11.2	
	168	-10.0	21.0	-32			101			
							124			
	170						100			
	163					_	179		11.0	00.0
	162					avg.	121.3	-7.4	11.0	-39.0
	162									
	168									
-	162	10.0	21.0	40.0						
avg	164.4	-17.7	21.0	-48.0						

	E30-74	10' sadd	le dolor	nite		M05-4	191' sa	ddla dal	lomito
	Th	Tm	S	Te		Th	Tm	S	
	115.2	-26.1	26.7	-64.3		128.1			Te
	122.6	-33.0	31.2	-59.7			-14.1	18.0	-51.5
	108.2	-29.9	29.1	-58.7		1209	-13.8	17.7	-50.6
	120.7					149.5	-18.0	21.2	-49.7
		-31.9	30.5	-59.4		117.2	-7.9	11.6	-44.8
	114.6	-31.5	30.2	-64.7		122	-13.3	17.3	-48.8
	110.8	-32.6	30.9	-64.8		146.2	-7.0	10.4	-45 5
	112.7	-31.4	30.1	-59.7		144.7			
	124.8	-26.2	26.8	-64.9		147.3			
	114.7	-29.3	28.7	-57.2		132.2			
	125.2	-21.0	23.4	-59.6		122.6			
	110.5	-32.6	30.9	-64.5		116.5			
	110	-30.6	29.6	-64.8		115			
AVG.	115.8	-29.7	29.0	-61.9		131.5			
				0.112		116			
						141			
	F33-33	220' sad	dle dolo	mite		119.3			
	Th	Tm	S	Te	AVG.	128.4	12.2	16.4	40.5
	122.6	-20.5	23.0		AVU.	120.4	-12.3	16.4	-48.5
				-61.4					
	155.4	-21.9	24.0	-58.0					
	141.6					_			
	144.9						851' sa		lomite
	156.2					Th	Tm	S	Te
	139.7		1			122	-12.7	16.7	-32.0
	113.9					154	-11.4	15.4	-31.7
	148.1					152	-11.5	15.5	-27.6
	141.2					151	-7.5	11.1	
	131.6					151			-22.0
AVG.	139.5	-21.2	23.5	-59.6		155			-40.3
						145			
						117			
	G15-9	16' sadd	lle doloi	mite		127			
	Th		S			135			
	115	-21.7	_	-58.2		142			
	113	-21.0		20.2		149			
	113	-23.5		-63.8					
	110	-23.3	23.4			151			
	112			-61.1		165			
		-21.8	23.9	-61.8	avg	143.9	-10.8	14.8	-30.7
	112	-20.3		-60.1					
	111	-20.2		-60.6					
	111	-20.5	23.0	-60.2					
	115								
	116								
	109								
avg	112.5	-21.3	23.5	-60.8					

	Pine P	. pit N8	1, sadd	le dolomite		B08-69	952', qı	uartz	
	Th	Tm	S	Те		Th	Tm	S	Te
	114	-23.4	25.0	-65.1		211	-8.2	12.0	-36
	107	-22.1	24.1	-65.6		165	-7.6	11.2	-27
	101	22.1	~	05.0		186	-6.8	10.2	-33
	102					170	-7. 9	11.6	-29
	107					185	-8.6	12.4	-43
	107					199	-12.3	16.3	-32
	112					17 5 17 5	-10.3	14.3	-34
	103					173	.9.3 12.6	13.2	26
	95					205	-13.6	17.6	-36
	116					205			
	100					206			
	118					165			
	105	22.0	24.5	(5.2		166			
avg	106.4	-22.8	24.5	-65.3		168			
						170			
						172			
						173			
	Pine P	. pit P24	4, saddle	dolomite		189			
			_			176			
	Th	Tm	S	Te		168			
	95	-16.0	19.6		avg.	180.2	-9.4	13.3	-33.8
	88	-15.1	18.9						
	98	-19.6	22.4						
	102								
av	114	99.4	-16.9	20.3		B07-7	242', ca	lcite	
u v	5	<i>)</i>	10.7	20.5		Th	Tm	S	Te
						158	-11.1		-47
	Dine D	nit Y5	1 caddl	e dolomite		157	-10.2	14.2	-47
	I IIIC I	. pit A3	i, saddi	c doloinie		157			
	Th	Tm	S	То			-10.3	14.3	-47
		1 111	3	Те		157	-10.3	14.3	-48 45
	85 91					157	-11.2	15.2	-45 52
	99					155	-12.3	16.3	-52
						155	-11.2	15.2	-46
	94					158	-11.0	15.0	-50
	94					155	-10.6	14.6	-55
	93					157	-11.5	15.5	-53
avg.	92.67					157	-10.6	14.6	-44
						157	-10.0	14.0	-46
					avg	156	-10.9	14.9	-48.4

B08-7009', calcite

	Th	Tm	S	Te
	157	-13.7	17.6	-51
	157	-13.2	17.2	
	169	-13.1	17.1	-47
	162	-13.3	17.3	-48
	160	-15.1	18.9	-50
	130	-11.3	15.3	-49
	151	-12.9	16.9	-46
	166	-12.1	16.1	-48
	168	-14.1	18.0	-48
	176	-13.1	17.1	-49
	170	-13.1	17.1	-44
	170	-12.9	16.9	-48
		-13.6	17.6	-48
		-14.4	18.3	-50
	169			
	153			
	162			
	154			
	160			
	165			
	169			
	170			
avg	161.9	-13.3	17.3	-48.2

M05-4217', calcite

	Th	Tm	S	Te
	115.7	-7.6	11.2	-55.2
	102.4	-10.0	14.0	-49.4
	146.7	-7.4	11.0	-37.9
	140.8			
	135.7			
	97.2			
	85.4			
	118.4			
	112.6			
avg.	117.2	-8.3	12.1	-47.5

Pine P pit N81, calcite

	Th	Tm	S	Te
	71.8	-4.3	6.9	-36.6
	73.2	-4.7	74	-35.6
	87.5	-4 4	70	-34.5
	105.8	-3.9	6.3	-35.7
	93.9	-5.8	8.9	-40.2
	124.5	-5.4	8.4	-36.1
	97.2	-3.6	5.8	-32.1
	106.7	-38	6.1	-39,5
avg.	95.08	-4 5	7.1	-36.3

Appendix 5. Major and trace element concentrations of the Presqu'ile carbonates. Major element concentrations and insoluble residues are reported in percentage and trace element concentrations in ppm.

Locat	Dep	Туре	Ba	Ca %	Fe	К	Mg %	Mn	Na	Sr	IR%
PP-X51	OP	FCD	65	22 35	668	181	13.12	100	345	60	2.8
PP-X51	ОР	FCD	73	21.33	691	163	1291	119	490	55	1.6
PP-2822	482	FCD	114	20.39	592	28	12.98	206	340	126	1.6
PP-2162	614	FCD	182	23.93	152	112	11.41	78	363	119	1.7
NWT-F51	4946	FCD	73	20.99	111	154	12.12	115	354	101	2.7
NWT-C22	3192	FCD	<25	20.1	1032	139	11.43	38	477	80	9.2
NWT-A05	4609	FCD	483	22.86	465	52	11.45	24	454	229	0.9
NWT-J26	2370	FCD		20.27	432	242	11.33	7	282	77	1.2
PP-M64	OP	MCD	438	24.28	401	31	11.6	200	226	55	0.4
PP-2143	38	MCD	106	20.41	275	34	12.9	153	281	50	1.9
PP-2225	57	MCD	161	21.9	422	73	12.3	184	278	36	1.7
PP-2582	154	MCD	145	21.75	204	57	12.84	151	302	46	2.0
PP-3337	280	MCD	106	21.05	365	26	12.94	208	267	36	1.5
PP-3316	241	MCD	46	21.9	1081	26	13.51	234	309	30	1.8
PP-2729	577	MCD	60	21.12	102	19	13.69	127	276	42	1.7
PP-2813	472	MCD	171	21.45	736	27	12.93	238	290	49	1.8
PP-2813	530	MCD	179	21.68	120	16	12.86	171	267	42	1.6

2,0

Locat.	Dep.	Туре	Ba	Ca %	Fe	K	Mg %	Mn	Na	Sr	IR%
PP-2813	575	MCD	194	22 74	174	55	12 74	138	285	55	16
PP-2813	642	MCD	175	21 59	131	84	12 56	96	312	43	29
PP-2813	679	MCD	126	20 49	209	366	11 12	90	355	66	6 1
PP-2813	751	MCD	158	21 53	174	364	12 01	107	391	73	5 7
PP-2813	870	MCD	192	22 69	341	217	13 03	165	295	50	24
PP-2822	384	MCD	59	21 12	110	28	12 97	250	402	40	16
PP-2822	452	MCD	175	24 49	382	104	11 99	218	373	65	07
PP-2822	534	MCD	148	24 07	119	1	12 83	146	179	32	06
PP-2822	645	MCD	156	23 51	129	4	12 6	125	152	48	0 4
PP-2822	736	MCD	114	24 61	227	52	12 09	132	168	48	07
PP-2822	835	MCD	156	22 97	153	18	12 16	126	109	39	07
PP-2870	309	MCD	58	20 19	4256	34	12 34	253	393	48	1 7
PP-3306	330	MCD	240	23 79	215	27	12 07	148	276	50	0 4
PP-3306	346	MCD	240	21.29	270	23	12 81	156	198	51	09
PP-3306	400	MCD	176	21 45		77 2	12 03	182	160	50	24
PP-3306	587	MCD	153	22 43	61	90	11 27	154	225	61	4 5
PP-3306	667	MCD	40	21 37	246	283	11.24	203	186	72	100
PP-3302	701	MCD	171	22 33	178	59	12.27	184	217	57	13
PP-5321	429	MCD	398	22.8		15	12 24	50	269	62	04
PP-5321	460	MCD	702	22.25	226	8	12 69	197	251	56	0 5

Locat	Dep.	Туре	Ba	Ca %	Fe	K	Mg %	Mn	Na	Sr	IR%
PP-5321	493	MCD	146	23 83	340	12	12.28	222	246	32	0.3
PP-2162	391	MCD	156	22.43	330	146	11 4	150	162	43	23
PP-2162	422	MCD	493	24 61	250	15	10 01	207	149	69	05
PP-2162	724	MCD	251	23 34	147	35	11 86	82	345	74	07
PP-2162	765	MCD	267	23 05	162	59	11 4	119	230	58	07
PP-2162	931	MCD	341	23.36	137	29	11 74	125	193	33	0 4
PP-2162	850	MCD	387	24.73	299	39	11.99	153	191	51	06
PP-3305	682	MCD	341	21.89	87	92	11 59	123	151	67	28
PP-M64	OP	CCD	46	21 47	271	6 8	12 85	175	492	47	1 1
PP-N81	OP	CCD	407	22.04	151	129	11 88	264	215	67	1.5
PP-N81	OP	CCD	388	22.9	318	183	11 39	166	213	76	4.0
PP-Y53	OP	CCD	331	24 12	2883	37	12 94	214	440	57	0 4
PP-764	OP	CCD	78	20.32	562	35	13 02	235	419	31	1 4
PP-2582	48	CCD	149	20 49	3451	40	12 84	245	410	35	1 5
PP-2729	374	CCD	76	21 41	26	42	13.21	225	394	41	1.8
PP-2729	419	CCD	7 0	21 3	238	48	13 14	281	436	36	18
PP-2729	433	CCD	69	20.31	2854	41	12 98	348	382	33	19
PP-2729	502	CCD	97	19 94	149	32	13 14	227	371	43	1.9
PP-2813	250	CCD	87	21 78	20	33	12.84	112	403	36	1.6
PP-2813	268	CCD	91	21.39	24	30	12.95	182	350	35	1.1

				=======================================						·	
Locat.	Dep.	Туре	Ba	Ca %	Fe	K	Mg %	Mn	Na	Sr	IR%
PP-2813	356	CCD	99	20 66	5037	34	12 82	268	357	32	1 1
PP-2813	363	CCD	71	20 18	3055	35	12 41	242	438	38	17
PP-2822	253	CCD	120	23 81	38	11	11.37	137	275	44	1 1
PP-2822	269	CCD	125	22 8	33	27	11 98	284	352	40	11
PP-2822	320	CCD	161	23 63	30	23	11 74	226	290	44	09
PP-2822	349	CCD	194	21 69	42	32	13 01	273	385	35	1.4
PP-2822	367	CCD	163	23 93	83	27	11 97	220	259	36	0.5
PP-2870	221	CCD	63	20.43	5907	35	13 1	327	405	36	18
PP-3306	265	CCD	261	24 21	53	142	12 65	172	349	56	1 1
PP-3306	269	CCD	260	23 97	39	32	12 19	206	430	46	0 4
PP-3306	287	CCD	271	23 22	29	24	11 97	229	488	50	0.5
PP-3316	189	CCD	73	20 68	1078	25	13 16	208	329	38	22
PP-3337	80	CCD	109	20 23	6051	30	12 38	348	404	40	16
PP-5321	343	CCD	292	23 24	290	17	12 48	202	441	48	0 7
PP-5321	368	CCD	189	22.37	4230	19	12 44	99	351	51	0.5
PP-5321	371	CCD	219	22 89	1888	25	11 94	85	359	46	07
PP-5321	420	CCD	395	24 62	898	20	12 89	90	322	62	0 4
NWT-072	5852	CCD	577	19 96	106	417	11 72	164	605	67	77
B08	6952	CCD	241	22.06	52	11	12.65	314	303	41	30
B08	6971	CCD	208	20 87	29	18	12 85	334	266	41	3 7

Locat	Dep.	Туре	Ba	Ca %	Fe	K	Mg %	Mn	Na	Sr	IR%
B08	6973	CCD		19.25	34	29	11 99	248	378	39	5.7
B 08	7003	CCD	239	21 23	56	97	12.06	344	168	52	46
B08	7032	CCD	236	22 52	109	276	12 11	305	502	70	4 4
B 08	7044	CCD	275	22 79	80	174	13 09	258	337	47	3.6
B12	6610	CCD	238	22 04	346	277	11.7	228	302	73	3.2
B12	6648	CCD	172	21 88	504	3 86	12 13	190	530	55	5.2
B12	6666	CCD	600	17 47	77	178	10.02	168	631	72	5 3
B12	6689	CCD	252	21 63	83	36	12.33	303	399	64	4.5
B12	6706	CCD	221	21 55	118	167	13.09	181	395	36	2.4
PP-M64	OP	SD	69	23 88	47		10.06	234	381	57	1.5
PP-M64	OP	SD	541	19 2	110	44	12.01	268	565	38	22
PP-N81	OP	SD	627	23 62	5	4	10.61	197	165	53	06
PP-Y53	OP	SD	250	23 93	4239	29	11.74	448	364	52	0 5
PP-2822	275	SD	148	24.95	17	5	11.87	184	334	36	1.0
PP-M64	OP	SD		20.28	1125	242	11 75	221	274	40	07
PP-M64	OP	SD		21.72		15	11.72	145	194	54	06
PP-N81	OP	SD	698	22 24	21	<4	11.25	241	351	82	1.5
NWT-G15	916	SD	54	21 36			11.89	133	418	59	0.5
NWT-A77	1545	SD		21.34	902		12.37	101	245	36	0.6
NWT-E33	3229	SD		21 37			11 29	172	272	50	0 4

,

Locat.	Dep.	Туре	Ba	Ca %	Fe	к	Mg %	Mn	Na	Sr	IR%
NWT-C19	1569	SD		20 66	34		11 58	135	238	39	0.4
NWT-K48	3075	SD		21 34	52	28	11 07	132	137	51	08
NWT-M05	4181	SD		21 82	70		11 19	106	158	64	06
NWT-072	5852	SD		21 70			11.70	45	194	74	06
B04	7439	SD		21 28			12 67	301	276	45	0 4
B01	6702	SD		21 14			11 48	269	329	52	0.4
B08	6952	SD	255	23 08	125	14	12 93	493	386	54	1 8
B08	6971	SD	245	21 83	26	15	13	398	356	41	1.5
B08	7032	SD	241	21 34	45	19	12 64	553	344	49	3.4
B08	7048	SD	305	21 54	38	22	12 66	404	345	44	25
B12	6634	SD	226	22 62	126		12 32	232	371	61	20
B12	6689	SD	221	21 74	21	44	13 08	285	401	35	1 5
B12	6704	SD	169	22 35	505	355	12 7	176	568	48	1 7
B12	6727	SD	219	21 99	30	35	13 04	321	369	38	19
B12	6742	SD	209	22.88	59	25	13 09	222	299	33	1 7
B12	6752	SD	203	22.15	36	20	12 92	209	344	34	18
B12	6762	SD	236	21 6	3 6	25	12 73	261	464	57	16
B12	6772	SD	318	23 92	94	31	11 96	235	390	60	13
PP-165	OP	WCC	39	37 78	2 0	20	0 52	148	206	102	3
PP-165	OP	WCC	<35	33 14	<13	<13	0 49	138	160	90	49

							÷				
Locat.	Dep	1 ypc	Ba	Ca %	Fe	к	Mg %	Mn	Na	Sr	IR%
PP-M64	OP	WCC	<35	36 5	14	14	1.04	214	184	184	3 3
PP-M64	ОР	WCC	<35	22 64	18	18	3.15	141	251	91	17.7
PP-N81	OP	WCC	<35	33 95	<13	<13	1 79	195	263	132	4.8
PP-2870	120	WCC	<35	31.86	17	17	1.65	206	224	114	7.0
PP-2870	200	WCC	<35	36.32	≼ 13	<13	0 65	234	185	123	3.3
PP-5321	230	LS/S	12	38.1	53	7	2096	38	72	132	1.8
PP-2162	270	LS/S	12	38 09	246	7	3001	76	104	243	4.6
PP-2822	242	LS/S	12	36.67	144	113	2000	97	112	192	62
PP-2162	28 6	LS/S	12	38 98	153	7	1373	93	27	110	1.1
PP-2162	326	LS/S	15	40.47	85	7	1092	39	33	113	0.3
PP-2162	354	LS/S	12	36.16	59	7	1172	39	22	106	0.4
PP-1839	105	LS/S	16	38 5	18	7	551	37	35	90	0.2
PP-2162	281	LS/D	12	39.55	99	7	1666	36	26	104	6
PP-2162	283	LS/D	12	37.62	81	7	1786	99	13	207	1.5
PP-2822	246	LS/D	27	36 38	78	7	3801	78	28	104	1 2
PP-2822	239	LS/L	12	37.31	238	84	2555	104	74	194	5.5
PP-5321	228	LS/L	29	34.63	114	7	854	68	20	87	0.5
PP-N81	OP	LS/L	29	36 44	57	7	1209	45	48	156	0.6
PP-3306	484	LS/P	12	31 32	50	39	8109	16	250	370	19.1
PP-3306	532	LS/P	12	34 46	64	20	0 010 8	15	327	87	9.5
PP-3302	528	LS/P	12	26.43	124	144	7960	70	227	97	22 4

Locat.	Dep.	Туре	Ba	Ca %	Fe	K	Mg %	Mn	Na	Sr	IR%
PP-2822	344	LCC	59	37.49	10	7	1582	184	7	120	0.5
PP-2822	450	LCC	24	39.2	37	7	2218	179	12	175	19
PP-2822	390	LCC	42	39	10	7	1283	153	19	368	09
B08	7009	LCC		43 75		80	1098	150	51	217	0 1
PP-N81	OP	LCC		41.49			1301	278		130	10
NWT-M05	4217	LCC		40 81	11		405	53	56	78	1 2
B07	7242	LCC		44.39	15		1423	466	38	153	0 1
PP-Y53	OP	LCC		39 79	12		781	100		50	34
PP-M64	OP	LCC		40 23	15		510	243		59	07
PP-Y65	OP	LCC		37.89	22		1409	281		110	5 7

Appendix 6. REE concentration of Presqu'ile carbonates (ppm).

Sample Locations														_
	La	Ce	Pr	Nd	Sm	Eu	Gd	Тъ	Dy	Но	Er	Tm	Yb	Lu
limestone														
P.P2822-239' Sul. P.	1.98	491	0.63	2.34	0.46	0.11	0.44	0.08	0.42	0.08	0.21	0.03	0.21	0.03
P.P2822-246' Sul. P.	3.73	5.61	0.83	3.41	0.71	0.16	0.72	0.10	0.60	0.12	0.31	0.04	0.22	0.03
fine-crystalline dolomite														
NWT-A05-4609' Muskeg	0.63	1.19	0.13	0.51	0.10	0.02	0.10	0.02	0.10	0.02	0.05	0.00	0.04	0.01
NWT-C22-3192' Muskeg	1.15	2.69	0.35	1.35	0.33	0.06	0.24	0.04	0.30	0.05	0.16	0.02	0.13	0.01
medium-crystalline dol.														
P.P2822-645' Pine P.	2.20	1.00	0.29	1.14	0.23	0.06	0.32	0.06	0.40	0.10	0.30	0.04	0.17	0.03
P.P2813-472' Pine P.	1.10	0.58	0.15	0.61	0.11	0.03	0.17	0.03	0.16	0.04	0.12	0.01	0.07	0.01
P.P2813-473' Pine P.	1.17	0.67	0.16	0.61	0.11	0.03	0.20	0.03	0.20	0.05	0.13	0.02	0.09	0.01
P.P2813-530' Pine P.	1.15	0.61	0.15	0.62	0.12	0.03	0.17	0.03	0.21	0.05	0.14	0.02	0.10	0.01
P.P2813-575' Pine P.	2.32	1.20	0.31	1.20	0.24	0.06	0.29	0.05	0.33	0.09	0.26	0.03	0.15	0.02

														
Sample Locations	La	Ce	Pr	Nd	Sm	Eu	Gd	Тъ	Dy	Но	Er	Tm	Yb	Lu
coarse-crystalline dol.														
P.P2822-320' Sul. P.	0.87	0.84	0.11	0.35	0.08	0.02	0.09	0.02	0.09	0.02	0.04	0.01	0.03	0.00
P.P. pit Y53, Sul. P.	9.70	5.47	0.93	3.10	0.39	0.10	0.61	0.07	0.42	0.09	0.23	0.03	0.13	0.02
B.CB08-7025' Watt M.	1.11	2.93	0.59	2.66	0.75	0.14	0.73	0.16	1.05	0.20	0.58	0.08	0.56	0.07
NWT-072-5852' Slave P.	1.26	2.34	0.32	1.08	0.24	0.05	0.19	0.04	0.20	0.04	0.14	0.02	0.09	0.01
P.P2822-349' Sul. P.	1.02	0.89	0.13	U.46	0.10	0.01	0.10	0.02	0.10	0.02	0.08	0.01	0.06	0.00
saddle dolomite														
P.P2822-275' Sul. P	1.71	1.48	0.25	0.90	0.19	0.06	0.23	0.03	0.24	0.05	0.15	0.02	0.10	0.01
P.P. pit N81, Watt M.	3.32	2.45	0.36	1.26	0.25	9.07	0.27	0.04	0.25	0.05	0.14	0.02	0.11	0.01
P.P. pit M64, Sul. P.	2 16	1.84	0.26	0.95	0.19	0.05	0.21	0.03	0.21	0.04	0.12	0.02	0.09	0.01
P.P. pit M64, Sul. P.	17.94	7.62	1.15	3.79	0.48	0.27	0.61	0.08	0.49	0.11	0.34	0.04	0.17	0.02
P P. pit P77, Sul. P.	2.29	1.50	0.24	0.87	0.18	0.06	0.20	0.04	0.19	0.04	0.13	0.02	0.07	0.01
B.CB12-6634' Sul. P.	3.11	3.61	0.63	2.32	0.43	0.11	0.38	0.05	0.32	0.06	0.14	0.02	0.09	0.01

									 					
Sample Locations	La	Ce	Pr	Nd	Sm	Eu	Gd	Tb	Dy	Но	Er	Tm	Yb	Lu
B.CB08-7047' Sul. P.	0.80	1.05	0.17	0.66	0.13	0.03	0.14	0.02	0.16	0.03	0.09	0.01	0.07	0.01
P.P. pit M64, Sul. P.	4.52	3.68	0.51	1.74	0.30	0.09	0.32	0.05	0.31	0.07	0.19	0.02	0.12	0.02
white calcite														
P.P. pit N81, Watt M.	4.35	2.80	0.42	1.55	0.29	0.07	0.31	0.05	0.25	0.06	0.17	0.02	0.13	0.01
P.P. pit 165, Sul. P.	23.56	17.24	2.89	9.40	1.42	0.41	1.56	0.22	1.25	0.26	0.72	0.08	0.39	0.06
P.P. pit 165, Sul. P.	17.08	11.89	2.07	7.38	1.21	0.37	1.41	0.20	1.12	0.24	0.63	0.07	0.35	0.06
P.P. pit M64, Sul. P.	28.95	14.17	2.18	6.77	0.80	0.40	1.20	0.15	0.83	0.20	0.54	0.06	0.31	0.04
P.P. pit M64, Sul. P.	3.04	2.41	0.34	1.20	0.23	0.07	0.27	0.04	0.24	0.05	0.15	0.02	0.09	0.01
late-stage cx. calcite														
P.P2822-344' Sul. P.	0.97	0.96	0.16	0.64	0.16	0.05	0.22	0.04	0.22	0.04	0.14	0.03	0.10	0.02
P.P2822-344' Sul. P.	1.03	1.04	0.18	0.67	0.15	0.05	0.21	0.04	0.24	0.05	0.14	0.02	0.13	0.02
P.P. pit Y65, Sul. P.	0.61	0.72	0.19	1.01	0.26	0.07	0.34	0.05	0.28	0.06	0.15	0.01	0.06	0.01

Appendix 7. List of figures.

Figure	page
1	Middle Devonian Presqu'ile barrier and location of the wells studied15
2	Simplified regional geological map of the Western Canada Sedimentary Basin during Middle Devonian
3	Schematic cross section of the Western Canada Sedimentary basin26
4	Estimated paleolatitude and surficial wind directions of western North American during the Middle Devonian31
5	Eustatic sea-level changes for the Western Canada Sedimentary Basin during Middle Devonian time
6	Stratigraphy and spatial distribution of different types of dolomites in the Presqu'ile barrier35
7	Diagenetic paragenesis of the Presqu'ile barrier43
8	Submarine cementation, compaction, and stylolitization45
9	Subaerial diagenetic features48
10	Hydrothermal dissolution features52
11	Other diagenetic features55
12	Burial history of the Presqu'ile barrier61
13	A generalized east-west stratigraphic cross section of the Presqu'ile barrier
14	Petrographic features of fine-crystalline dolomite
15	Petrographic features of medium-crystalline dolomite77
16	Hand sample and outcrop sample of coarse-crystalline and saddle dolomites80
17	Thin section and SEM photomicrography of coarse-crystalline dolomite83

Figure	page
18	Petrographic features of saddle dolomite86
19	Cross section of pit N81 (Pine Point)89
20	Cross section of pits W85 and A70 (Pine Point)90
21	Cross section A-A' from subsurface Presqu'ile barrier from NWT91
22	Cross plot of δ^{18} O and δ^{13} C for calcine fossil fragments, late-stage calcites, and white calcites
23	Cross plot of δ^{18} O and δ^{13} C values for various types of dolomites and brachiopod fragments95
24	δ ¹⁸ O and δ ¹³ C profiles of MCD from drill holes 2813 and 2822 from Pine Point area104
25	Cross plot of δ ¹⁸ O and δ ¹³ C values of CCD and SD from different parts of the Presqu'ile barrier
26	Variation of δ ¹⁸ O values of saddle dolomites along the Presqu'ile barrier108
27	Comparison of δ ¹⁸ O and δ ¹³ C of CCD and SD above sub-Watt Mountain unconformity with those below it
28	Variation of ⁸⁷ Sr/ ⁸⁶ Sr ratios through geological time
29	87Sr/86Sr ratios of dolomites associated with the Presqu'ile barrier115
30	87Sr/86Sr ratios of late-stage coarse-crystalline calcite and white calcite118
31	Variation of ⁸⁷ Sr/ ⁸⁶ Sr ratios of saddle dolomite along the Presqu'ile barrier121
32	Cross plot of ⁸⁷ Sr/ ⁸⁶ Sr ratios and δ ¹⁸ O values of various dolomites124
33	Photomicrograph showing two-phase aqueous fluid inclusions129
34	Homogenization temperatures of saddle dolomites from the Presqu'ile barrier131

Figure	page
35	Variation of average homogenization temperatures of fluid inclusions in saddle dolomites along the Presqu'ile barrier132
36	Average homogenization temperature (Th) of saddle dolomites vs their present burial depths
37	Final melting temperatures (Tm) of saddle dolomite fluid inclusion135
38	Initial melting temperatures (Te) of saddle dolomite fluid inclusions136
39	Homogenization temperatures of fluid inclusions in late-stage coarse-crystalline calcites
40	Cross plot of average homogenization temperature of fluid inclusions in late-stage coarse-crystalline ralcites (LCC) and burial depths139
41	Final melting temperatures (Tm) of fluid inclusions in late-stage coarse-crystalline calcites
42	Initial melting temperatures (Te) of fluid inclusions in late-stage coarse-crystalline calcites
43	Fluid inclusion temperatures of quartz143
44	Homogenization temperatures of Presqu'ile saddle dolomites vs calculated burial depths
45	Cross plot of homogenization temperature and δ^{18} O values of saddle dolomite
46	Cross plot of homogenization and final melting temperatures for saddle dolomites and late-stage coarse-crystalline calcites
47	Sr concentration (ppm) of different dolomites
48	Mn concentration (ppm) of different dolomites
49	Average Sr and Mn contents (ppm) of different dolomites157

Figure	page
50	Cross plot of Sr (ppm) and mol % MgCO ₃ for seawater dolomite from Litt ¹ e Bahama Bank
51	Cross plots of Sr (ppm) and mol % MgCO ₃ for dolomites from Presqu'ile barrier
52	Vertical profiles of Sr and Mn of MCD for Pine Point diamond drill holes 2813 and 2822165
53	Vertical profiles of Sr and Mn of CCD166
54	Variation of Sr concentration of saddle dolomite along the Presqu'ile barrier
55	Variation of Mn concentration of saddle dolomite along the Presqu'ile barrier169
56	Schematic fluid flow in a sedimentary basin during tectonic thrusting and compression
57	Schematic cross section and modelled fluid-flow patterns of the Western Canada Sedimentary Basin during the Tertiary180
58	REF patterns of limestones and fine-crystalline dolomite
59	REE patterns of medium-crystalline dolomites
60	REE patterns of coarse-crystalline dolomites
61	REE patterns of saddle dolomites190
62	REE patterns of late-stage coarse crystalline calcite and white calcite192
63	Variations in the isotopic composition of O, Sr, C, and Nd during open-system recrystallization of limestone
64	A cross section of the Watt Mountain Formation, showing saddle dolomite and late-stage calcite in dissolution vugs and fractures209

Appendix 8. List of tables.

Table	page
1.	Estimated maximum burial depths and δ^{18} O values of coarse-crystalline and saddle dolomites of the Presqu'ile barrier106
2.	Estimated maximum burial depths and ⁸⁷ Sr/ ⁸⁶ Sr ratios of coarse-crystalline and saddle dolomites of the Presqu'ile barrier120
3.	Eutectic temperatures for some chloride-salt systems127
4.	Comparison of pressure corrected homogenization temperatures and estimated maximum burial temperatures146
5.	Previously proposed models of dolomitization of the Presqu'ile barrier171
6.	Maximum burial depths, ⁸⁷ Sr/ ⁸⁶ Sr ratios, δ ¹⁸ O values, and pressure corrected homogenization temperature of the Presqu'ile barrier177
7.	Previous interpretations on formation of dissolution vugs204
8.	Inferred timing for Pine Point MVT deposits224